frontiers | Research Topics

Territorial spatial evolution process and its ecological resilience, volume II

Edited by
Xiao Ouyang, Juergen Pilz, Xue-Chao Wang and Salvador García-Ayllón Veintimilla

Published in
Frontiers in Environmental Science

ISSN 1664-8714
ISBN 978-2-8325-6251-2
DOI 10.3389/978-2-8325-6251-2

About Frontiers

Frontiers is more than just an open access publisher of scholarly articles: it is a pioneering approach to the world of academia, radically improving the way scholarly research is managed. The grand vision of Frontiers is a world where all people have an equal opportunity to seek, share and generate knowledge. Frontiers provides immediate and permanent online open access to all its publications, but this alone is not enough to realize our grand goals.

Frontiers journal series

The Frontiers journal series is a multi-tier and interdisciplinary set of open-access, online journals, promising a paradigm shift from the current review, selection and dissemination processes in academic publishing. All Frontiers journals are driven by researchers for researchers; therefore, they constitute a service to the scholarly community. At the same time, the *Frontiers journal series* operates on a revolutionary invention, the tiered publishing system, initially addressing specific communities of scholars, and gradually climbing up to broader public understanding, thus serving the interests of the lay society, too.

Dedication to quality

Each Frontiers article is a landmark of the highest quality, thanks to genuinely collaborative interactions between authors and review editors, who include some of the world's best academicians. Research must be certified by peers before entering a stream of knowledge that may eventually reach the public - and shape society; therefore, Frontiers only applies the most rigorous and unbiased reviews. Frontiers revolutionizes research publishing by freely delivering the most outstanding research, evaluated with no bias from both the academic and social point of view. By applying the most advanced information technologies, Frontiers is catapulting scholarly publishing into a new generation.

What are Frontiers Research Topics?

Frontiers Research Topics are very popular trademarks of the *Frontiers journals series*: they are collections of at least ten articles, all centered on a particular subject. With their unique mix of varied contributions from Original Research to Review Articles, Frontiers Research Topics unify the most influential researchers, the latest key findings and historical advances in a hot research area.

Find out more on how to host your own Frontiers Research Topic or contribute to one as an author by contacting the Frontiers editorial office: frontiersin.org/about/contact

Territorial spatial evolution process and its ecological resilience, volume II

Topic editors

Xiao Ouyang — Hunan University of Finance and Economics, China

Juergen Pilz — University of Klagenfurt, Austria

Xue-Chao Wang — Beijing Normal University, China

Salvador García-Ayllón Veintimilla — Polytechnic University of Cartagena, Spain

Citation

Ouyang, X., Pilz, J., Wang, X.-C., Veintimilla, S. G.-A., eds. (2025). *Territorial spatial evolution process and its ecological resilience, volume II*. Lausanne: Frontiers Media SA. doi: 10.3389/978-2-8325-6251-2

Table of contents

frontiers | Frontiers in Environmental Science

TYPE Editorial
PUBLISHED 10 April 2025
DOI 10.3389/fenvs.2025.1601067

OPEN ACCESS

EDITED AND REVIEWED BY
Alexander Kokhanovsky,
German Research Centre for Geosciences, Germany

*CORRESPONDENCE
Salvador García-Ayllón,
salvador.ayllon@upct.es

RECEIVED 27 March 2025
ACCEPTED 27 March 2025
PUBLISHED 10 April 2025

CITATION
García-Ayllón S and Pilz J (2025) Editorial: Territorial spatial evolution process and its ecological resilience, volume II.
Front. Environ. Sci. 13:1601067.
doi: 10.3389/fenvs.2025.1601067

Editorial: Territorial spatial evolution process and its ecological resilience, volume II

Salvador García-Ayllón[1]* and Jürgen Pilz[2]

[1]Department of Mining and Civil Engineering, Technical University of Cartagena, Cartagena, Spain, [2]Institut für Statistik, Universität Klagenfurt, Klagenfurt, Austria

KEYWORDS

nature based solutions, ecological resilience, land use analysis, territorial diffuse anthropization, resilience-related indicators, ecological restoration policy, environmental management, remote sensing analysis

Editorial on the Research Topic
Territorial spatial evolution process and its ecological resilience, Volume II

1 Introduction

The analysis of anthropic impacts on the environment from a territorial perspective is possibly one of the most important fields of study in the current context of climate change. The evolution of land space demonstrates the shift of land use types from natural and semi-natural land (e.g., forest land and cropland) to built-up land, altering ecosystem cycling patterns and leading to degradation of ecosystem services in terms of regulation, provisioning and support. At the same time, production and living space crowding out ecological space brings high potential threats, such as soil erosion, forest productivity decline and habitat fragmentation. Accordingly, in response to the problems of imbalanced territorial space development, inefficient resource utilization and ecological environment degradation, how to improve the diversity, stability and sustainability of ecosystems is an urgent issue to promote modernization and green development in the new era of territorial space evolution.

Parallel to this phenomenon, there has been an increase in our capacity to monitor the characteristics of land space and its socioecological configuration. At a time when many voices are being raised in defense of climate denialism, it is important that diagnoses are based on methodologically rigorous processes. This Research Topic follows in the footsteps of its previous edition (García-Ayllón and Pilz, 2024) and aims to systematically investigate the evolutionary process of territorial space and ecological resilience to clarify the dynamic trend of ecological resilience under the action of nature and human. The proposed research framework focuses on the establishment of territorial space simulation models for enhancing ecological resilience to encourage the stability and sustainability of ecosystems and promote the modernization of the harmonious coexistence of human beings and nature.

FIGURE 1
Damage suffered in the area surrounding the Albufera Natural Park in Valencia (Spain) during the floods of October 2024, exacerbated by the ongoing territorial anthropization process in the area. Source: NASA Earth Observatory.

2 Overview of the state of the art

There are many ways for this accelerated epoch of the Anthropocene in which we currently find ourselves is expressed. Rising temperatures, increasing frequency of new types of wildfires, the so-called flash floods (Serra-Llobet et al., 2023), persistent droughts (Jodar-Abellan et al., 2019), coastal erosion (Bianco et al., 2020) and loss of soil value (Cao et al., 2024), reduced biodiversity (Ricotta and Szeidl, 2006), sea level rise on the coast (Bianco and García-Ayllón, 2021), etc. The effects that an incorrect transformation of land use can have on the appearance of many of the catastrophic phenomena with which our society lives are numerous that affect the natural ecosystems and even human security (see Figure 1), and sometimes even unsuspected (García-Ayllón et al., 2019). Among all of them, the impact of diffuse territorial anthropization is especially dangerous, a silent phenomenon derived from the processes of transformation of the soil by human beings, whose diversity of causes makes its diagnosis very complex. However, thanks to the important methodological and technological advances in this field we can now be aware of the magnitude of this problem and how its effects are expressed in the environment.

The new methodologies of spatial statistical analysis with GIS tools, technological advances in the field of recognition of land uses and conditions with satellite images through remote sensing or the existence of an ever-growing spatiotemporal cartographic database freely accessible to the entire planetary scientific community, are just some of the many tools that currently allow researchers to obtain more and more analyses and diagnoses sophisticated in this field. Good examples of these advances can be found in the innovative use of InVEST models.

For example, Wei et al. employs the Theil-Sen Median method combined with Mann-Kendall test to analyze the trend changes in habitat quality more accurately, utilizing high temporal resolution land use data to analyze in the area of Beijing from 1980 to 2020 through the habitat quality module of the InVEST model. Another interesting example in this field can be found in Liu et al., that explore the changing characteristics of land use/land cover (LULC), landscape pattern and ecosystem service (ES) and their drivers for regional ecosystem management and sustainable development in the Bohai Rim region of China, using the land use transfer matrix, landscape pattern index and InVEST models. Another interesting variant can be that of Xuan et al., who explore the relationship between ecosystem services and land use transition, using a InVEST model combined with a geographically weighted regression (GWR) model, to examine the impact of land use transition on ecosystem services in the Dongting Lake area in China.

A different but also interesting approach in the methodological advances of this discipline can also be found in the exploration of the multifunctional trade-off and synergy relationship of cultivated land for protecting cultivated land resources. Fang et al. evaluate obtaining very relevant results in this field the three-dimensional functional level of "production-society-ecology" of cultivated land from 2010 to 2020 using the coupling coordination degree model, land system function trade-off degree model, and K-means clustering analysis method to analyze the trade-off and synergy relationship between cultivated land functions in the Yellow River Basin.

In this field we must not forget more traditional, but also very useful, visions such as those derived from advances in the analysis and interpretation of historical cartography. Traditional analyses based solely on historical records may lack precision due to deviations and artistic interpretations found in ancient maps. However, considering the reciprocal compatibility between local geomorphology, undulating terrains, and water bodies allows for accurate reduction of the land use morphology by inferring and validating its geographical features. For example, Wang and Cheng combine historical interpretation and geographical analysis to reconstruct the historical shape of Xuanwu Lake, uncover the intrinsic mechanisms driving spatial changes over time, and analyze the morphological changes and connectivity patterns of its hydrological system.

An approach that is also traditional, but full of new possibilities for improvement, is the socio-ecological analysis of natural spaces as a design tool in the field of strategic planning of the territory. In this field, ecological restoration holds great significance in addressing environmental degradation and rock desertification in karst areas, for example. In these cases, zoning strategy is a fundamental task in understanding the interrelationship between human-environment to foster sustainable development. Liu et al. explore "social-ecological" system and conduct a case study on the karst region in Guangdong Province, China. They performed an evaluation framework using remote sensing computing cloud service platforms, consisting of "development pressure," "sensitivity status," and "resilience potential," showing how regions with high pressure of development are predominantly located in high-density urban areas.

Other approaches with a more numerical focus are also booming thanks to the growth and technological progress of geostatistics in the field of human-land relationship studies at the regional scale. For example, Zhou and Huang adopts an integrative approach to investigate spatiotemporal patterns, influencing factors, and

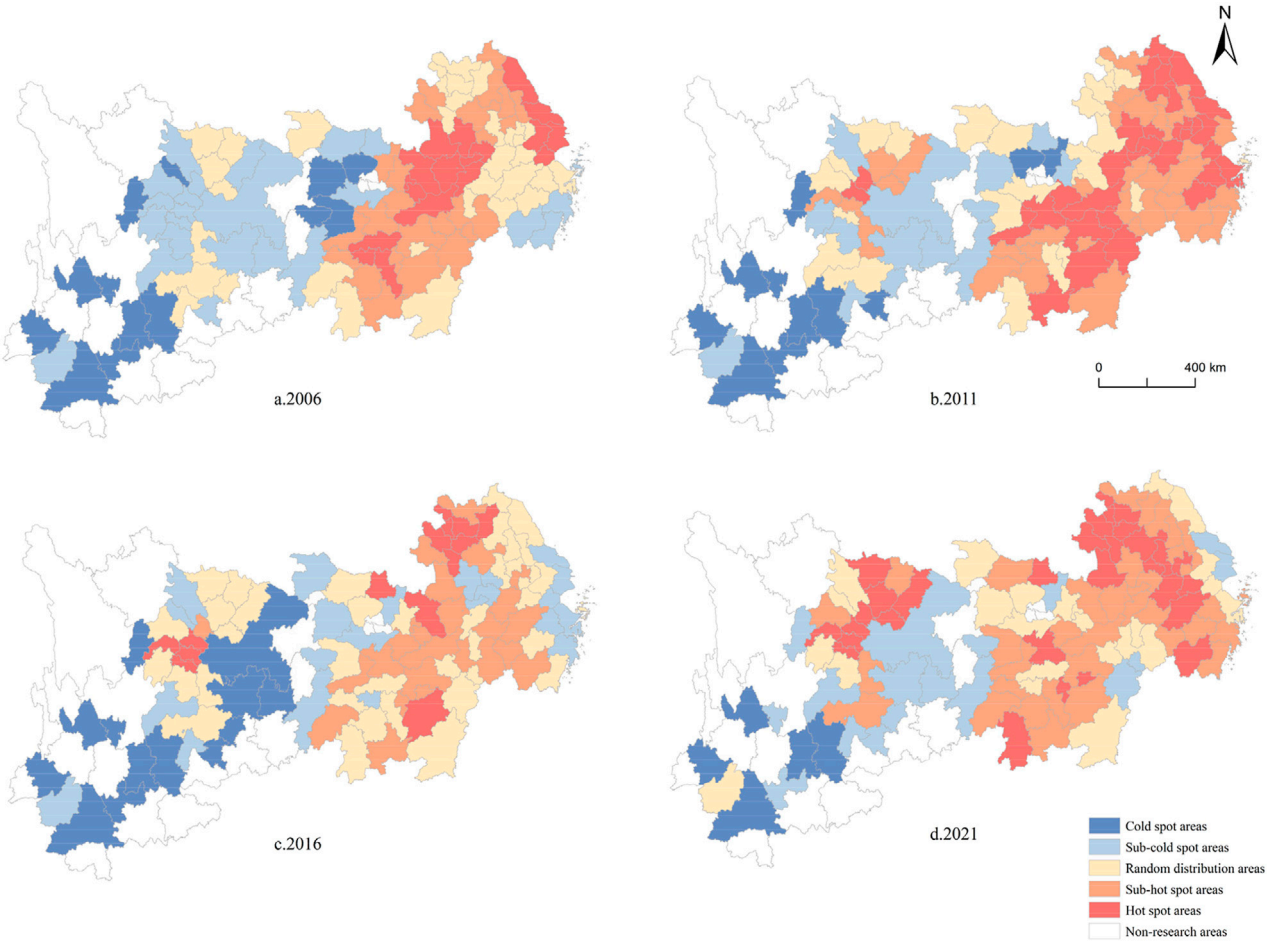

FIGURE 2
Spatial distribution of cold and hot spots of the coupled coordination degree between population urbanization and land urbanization in the Yangtze. Source: Zhou and Huang.

driving mechanisms of the coupling coordination between population urbanization and land urbanization in the Yangtze River Economic Belt (see Figure 2). By combining the coupling coordination degree model, exploratory spatial data analysis (ESDA), and panel data model, they provide new insights into the heterogeneity and spatial dependence of human-land dynamics in this region, revealing regional disparities, spatial clusters, and key influencing factors shaping the coupling coordination, which represents valuable knowledge for sustainable urbanization and regional development policies.

2.1 River economic belt

Liu and Ma employ double fixed-effects models, spatial econometric models, and instrumental variables methods to empirically explore how the digital economy influences environmental pollution, using panel data from 30 provinces in China spanning the years 2011–2022. Their results demonstrate that the digital economy significantly lowers environmental pollution: the primary mechanism is through the government's environmental governance behaviors, which are positively moderated by public environmental concerns, enhancing effectiveness. In addition, the digital economy induces a spatial spillover effect on environmental pollution since this promotion of collaborative management between the government and the public is poised to become a pivotal direction in future environmental governance.

Finally, we have continuous improvements that occur in the field of remote sensing thanks to the generalization of researchers' access to increasingly dense, accurate satellite information with a higher level of coverage throughout the planet. In this field, Wu et al. study fluvial islands, which are vital ecosystemic areas from both morphological and ecological perspectives and consequently have been hotspots of morphodynamic research in large rivers around the world. This study selected 14 representative fluvial islands in the lower reaches of the Yangtze River and explored their spatial-temporal evolution, including their shape and area dynamics during 1945–2016, by interpreting remote sensing images and analyzing the hydrological data. Results indicated that the total area of the 14 fluvial islands showed a growing trend at an average rate of 0.30 km2 yr−1 during the 72 years, providing an important reference for sustainable utilization and management of fluvial islands.

3 Conclusion

Spatial analysis in the field of the correlation between territory and environment is a discipline in continuous growth, in which new variants and new work formulas appear every day. We can conclude, therefore, that the field of territorial analysis of environmental evolution processes is a field of scientific research with a great future due to its continuous progress and improvement. The resilience of territory in the current context of climate change has traditionally been a variable that is difficult to measure. However, methodological and technological improvements in this field, together with progress in access to information (especially in those developing countries currently at greater risk of anthropization), are a fundamental variable in this respect.

Even so, we must continue to deepen this dynamic in a changing world, given that the understanding of the complex correlation between the phenomena of territorial anthropization and its implications in the analysis of behavioral patterns in the environmental and ecological field is also increasingly difficult and sophisticated. There is no alternative to this path in the current context of climate emergency, even more so if the aim is to fight in a convincing and effective way against denialist theories that question this correlation, which is not always evident at first glance. Science is the path, and research is its best tool.

Author contributions

SG-A: Project administration, Formal Analysis, Conceptualization, Writing – review and editing, Writing – original draft. JP: Writing – review and editing, Supervision, Writing – original draft, Validation, Conceptualization, Formal Analysis, Project administration.

Funding

The author(s) declare that no financial support was received for the research and/or publication of this article.

Acknowledgments

We deeply thank all the authors and reviewers who have participated in this Research Topic.

Conflict of interest

The authors declare that the research was conducted in the absence of any commercial or financial relationships that could be construed as a potential conflict of interest.

Generative AI statement

The authors declare that no Generative AI was used in the creation of this manuscript.

Publisher's note

References

Bianco, F., Conti, P., García-Ayllon, S., and Pranzini, E. (2020). An integrated approach to analyze sedimentary stock and coastal erosion in vulnerable areas: resilience assessment of san vicenzo's coast (Italy). *Water* 12 (3), 805. doi:10.3390/w12030805

Bianco, F., and García-Ayllón, S. (2021). Coastal resilience potential as an indicator of social and morphological vulnerability to beach management. *Estuar. Coast. Shelf Sci.* 253, 107290. doi:10.1016/j.ecss.2021.107290

Cao, Y., Hua, L., Peng, D., Liu, Y., Jiang, L., Tang, Q., et al. (2024). Decoupling the effects of air temperature change on soil erosion in Northeast China. *J. Environ. Manag.* 351, 119626. doi:10.1016/j.jenvman.2023.119626

García-Ayllón, S., and Pilz, J. (2024). Editorial: territorial spatial evolution process and its ecological resilience. *Front. Environ. Sci.* 12. doi:10.3389/fenvs.2024.1373672

García-Ayllón, S., Tomás, A., and Ródenas, J. L. (2019). The spatial perspective in post-earthquake evaluation to improve mitigation strategies: geostatistical analysis of the seismic damage applied to a real case study. *Appl. Sci.* 9 (15). doi:10.3390/app9153182

Jodar-Abellan, A., Valdes-Abellan, J., Pla, C., and Gomariz-Castillo, F. (2019). Impact of land use changes on flash flood prediction using a sub-daily SWAT model in five Mediterranean ungauged watersheds (SE Spain). *Sci. Total Environ.* 657, 1578–1591. doi:10.1016/j.scitotenv.2018.12.034

Ricotta, C., and Szeidl, L. (2006). Towards a unifying approach to diversity measures: bridging the gap between the Shannon entropy and Rao's quadratic index. *Theor. Popul. Biol.* 70(3), 237–243. doi:10.1016/j.tpb.2006.06.003

Serra-Llobet, A., Radke, J., and Kondolf, M. (2023). Floods after fires: a history informed hazard planning approach applied to the 2018 debris flows, Montecito, California. *Front. Environ. Sci. Sec. Land Use Dyn.* 11. doi:10.3389/fenvs.2023.1183324

frontiers | Frontiers in Environmental Science

TYPE Original Research
PUBLISHED 16 February 2024
DOI 10.3389/fenvs.2024.1369635

OPEN ACCESS

EDITED BY
Xiao Ouyang,
Hunan University of Finance and Economics, China

REVIEWED BY
Xiaojun Deng,
Zhejiang University of Finance and Economics, China
Yanxu Liu,
Beijing Normal University, China

*CORRESPONDENCE
Wei Lin,
gis_xifan@163.com

RECEIVED 12 January 2024
ACCEPTED 31 January 2024
PUBLISHED 16 February 2024

CITATION
Liu Y, Huang J and Lin W (2024), Zoning strategies for ecological restoration in the karst region of Guangdong province, China: a perspective from the "social-ecological system".
Front. Environ. Sci. 12:1369635.
doi: 10.3389/fenvs.2024.1369635

Zoning strategies for ecological restoration in the karst region of Guangdong province, China: a perspective from the "social-ecological system"

Yang Liu[1], Jiajun Huang[2] and Wei Lin[3]*

[1]Guangdong Duoyuan Geographic Information Service Co., Ltd., Zhaoqing, China, [2]Planning Office of the People's Government of Guanghai Town, Jiangmen, China, [3]College of Forestry and Landscape Architecture, South China Agricultural University, Guangzhou, China

Ecological restoration holds great significance in addressing environmental degradation and rock desertification in karst areas. Zoning strategy is a fundamental task in understanding the interrelationship between human-environment to foster sustainable development. We explore "social-ecological" system and conduct a case study on the karst region in Guangdong Province, China. An evaluation framework consists of "development pressure", "sensitivity status", and "resilience potential" was established. The results show that: regions with high pressure of development are predominantly located in high-density urban areas. The generally distribution of the comprehensive status index exhibits significant spatial heterogeneity. Regions with low sensitivity are found on the eastern and western sides of the study area. The comprehensive resilience values are largely influenced by *per capita* energy-saving and environmental protection expenditures. The restoration zones mainly concentrated in the contiguous regions of the northwestern and southern parts, covering more than half of the total area. The conservation zones are more numerous and primarily situated in the northern and eastern parts. By integrating socio-economic and ecological factors, this study proposes ecological restoration strategies for specific zones. It helps for improve development issues arising from complex interactions between human-environment, facilitating the implementation of restoration practices.

KEYWORDS

social-ecological system, ecological restoration zoning, development pressure, sensitivity status, resilience potential, restoration strategies, karst region of Guangdong province, China

1 Introduction

Increasingly severe degradation and damage to ecosystems are among the current global hot topics (Van der Biest et al., 2020). With the acceleration of China's industrialization and urbanization, high-intensity development and irrational human activities have led to continuous deterioration of the ecological environment, to some extent affecting the economy and the sustainable use of natural resources (Tang et al., 2022; Hu et al., 2023). To address the escalating environmental issues and gradually achieve the goal of

sustainable development, it is crucial to correctly understand and manage the relationship between human activities and ecosystems (Li et al., 2023a). In recent years, the significance of ecological restoration for sustainable development has become increasingly prominent. Actively identifying priority areas for ecological protection and restoration through natural or human interventions to restore degraded ecosystems is a critical strategic task for ecological security and human wellbeing (Peng et al., 2020; Zhao et al., 2023). Scientifically delineating zones enhances the precision and targeting of ecological restoration, serving as an important prerequisite for spatial control of ecological restoration projects and differentiated spatial governance (Yue et al., 2022). Currently, ecological restoration primarily focuses on administrative units or natural watersheds, and zoning methods include research frameworks based on regional dominant functions (Tian et al., 2017; Cai et al., 2020), ecological security pattern construction (Ni et al., 2020; Jiang et al., 2022; Zhang et al., 2023), supply-demand of ecosystem services (Xie et al., 2020; Yue et al., 2022; Hu et al., 2023; Li et al., 2023c), comprehensive indicator systems. Regional context, landscape heterogeneity, human activities, socio-economic are interplay with ecosystem, which needs to be integrated during ecological restoration zoning, the comprehensive indicators not only offer an intuitive depiction of the ecological characteristics and interplay of human activities and economic growth but can also be aligned with the critical objectives of enhancing the level of ecosystem services. The multi-dimensional and multi-functional evaluation underscores the holistic and systematic nature of ecological restoration, demonstrating its effectiveness (Cao et al., 2019; Dan et al., 2020; Li et al., 2023b).

In previous studies, human activities and economic indicators were generally considered as stressors on regional ecological environments, reflecting the conflict within the "social-ecological" system (Wang and Zhong, 2019). However, there is a growing demand for promoting a harmonious coexistence of humans and nature and for reconciling the relationship between ecosystems and socio-economic development (Bai et al., 2019). In recent years, the focus has shifted towards the "social-ecological" system perspective in human-environment research (Vos et al., 2019). Qualitative and quantitative research, which includes aspects such as vulnerability and resilience, marks the beginning of "social-ecological" system research (Liu et al., 2023). While frameworks like DSPIR, PSR, and VSD provide evaluation methods for ecological vulnerability and ecosystem health, they have not offered partitioning schemes for mitigating ecosystem degradation and restoring ecosystem functions and services (Song et al., 2019; Liu et al., 2020). Therefore, to comprehensively address the systemic and holistic issues in both ecosystem protection and social system governance (Ahammad et al., 2023; Wang H. et al., 2023), integrating ecological conservation and restoration into socio-economic development can effectively promote the coordination of human-environment relationships and the sustainable development of the "social-ecological" system (Tedesco et al., 2023). Ecological restoration zoning needs to consider simultaneously the pressure of human activities on the ecosystem, the state of the ecosystem itself, and the resilience potential created by socio-economic development. Based on the results of ecological restoration zoning, appropriate governance approaches and relevant policy recommendations can be proposed.

Karst areas account for about a fifth of the global land area, of which the South China Karst (SCK), is an ecologically fragile area of the largest distribution (Xiong et al., 2023). The SCK is characterized by acute human-environment conflicts, resulting in issues such as frequent soil erosion, the degradation of vegetation cover, and increased poverty. The combined effects of a fragile natural environment and irrational human activities severely hampers socio-economic development, making it imperative to implement ecological protection and restoration (He et al., 2019). The primary task is to delineate comprehensive zoning. Previous land spatial zoning studies in karst areas have not comprehensively considered the spatial variations of desertification and human disturbances (Zhang et al., 2020). Some researchers have established ecological restoration zoning at the basin and grid scales, they have elucidated the inherent characteristics and relationships between various levels of zoning, but precise boundary delineation for implementation was not addressed (Wang and Zhao, 2022; Wang Y. et al., 2023). The key ecological protection and restoration areas from a "social-ecological" system perspective and policy implementation still need to be explored. Therefore, ecological restoration zoning in karst areas should not only consider factors like the degree of ecosystem degradation but should also integrate human activities and the resilience potential of social systems into the framework. Only then can it better contribute to regional sustainable development and improvement of human-environment relationships.

Guangdong's karst region is mainly concentrated in the northern and northwestern parts of the province. It is situated in the upstream of the Pearl River Delta, serving as a critical ecological barrier and freshwater source for the Guangdong-Hong Kong-Macau Greater Bay Area. Compared to the existing research on karst regions in the SCK, the desertification control in Guangdong's karst region is currently limited to statistical analysis and comprehensive zoning strategies are still unclear. There is an urgent need for zoning studies to guide the steady progress of ecological restoration efforts. This paper approaches the issue from the perspective of the "social-ecological system" and proposes the "development pressure-sensitivity state-resilience potential" framework. By constructing comprehensive evaluation indicators for quantitative assessment, the goal is to delineate ecological restoration zones that harmonize ecological conditions with the socio-economic systems. This is expected to provide a reference for differentiated management and restoration strategies of desertification issues in karst areas.

2 Materials and methods

2.1 Study area overview

The selected study area focuses on the concentrated and contiguous regions with prominent desertification issues, which account for over 90% of the total desertification area in Guangdong province. This area includes the following counties and cities: Qingxin District, Yingde City, Yangshan County, Liannan Yao Autonomous County, and Lian-zhou City in Qingyuan City; Lechang City, Ruyuan Yao Autonomous County, Wujiang District, and Wengyuan County in Shaoguan City; and Lianping County in Heyuan City (Figure 1). The study area is

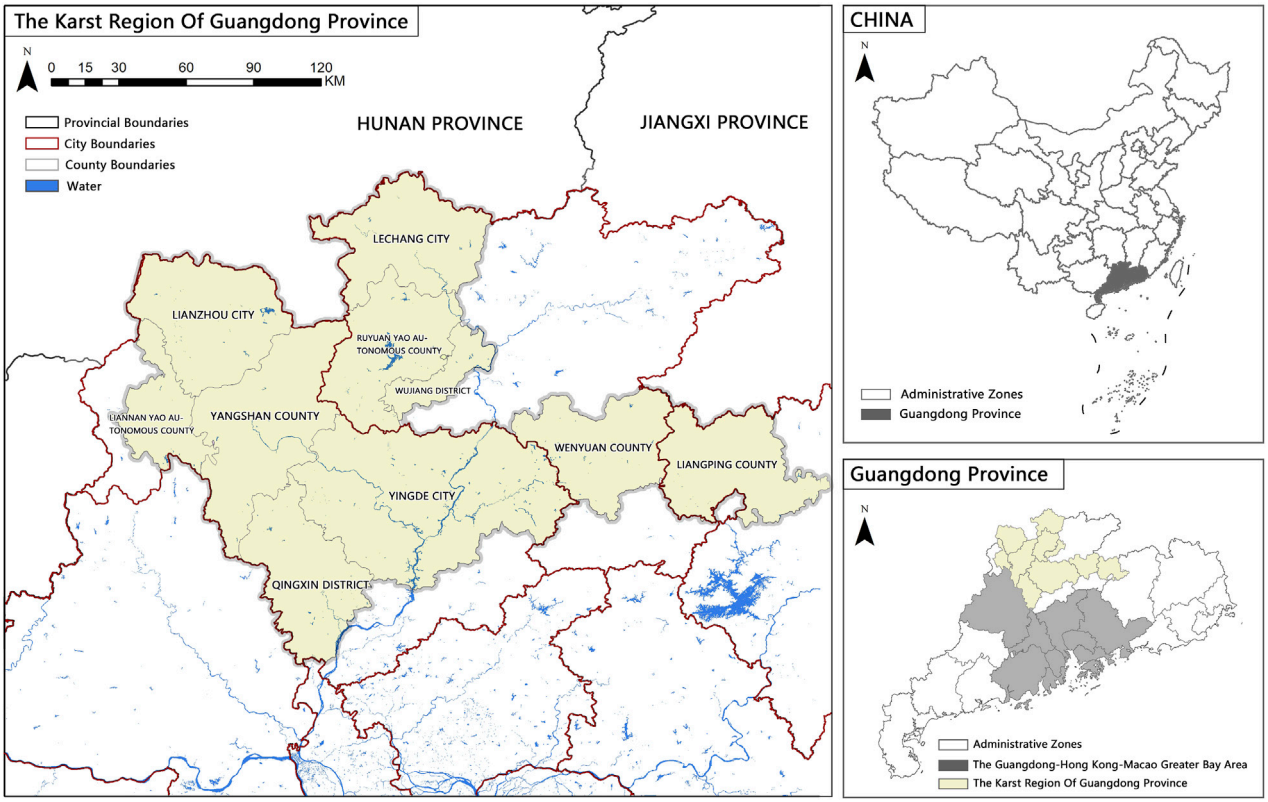

FIGURE 1
Location of the karst region of Guangdong province, China.

located between 112°2′to 114° 56′east longitude and 23°32′to 25°34′north latitude, covering a total area of approximately 25,077.23 square kilometers. The topography of the study area is complex and includes various landforms. It falls within a subtropical monsoon climate zone with abundant rainfall, averaging between 1,200 and 2000 mm annually. According to data from various city statistical year-books, the study area had a permanent population of approximately 3,993,200 people in the year 2020. The population distribution is uneven, with sparsely populated areas in the mountainous regions and dense populations in hilly areas. The overall Gross Domestic Product (GDP) of the region is relatively low, with Wujiang District and Qingxin District ranking first and second, respectively.

2.2 Data sources and initial data processing

The research data mainly include the following: 1. Land use remote sensing monitoring data with a spatial resolution of 1 km for the years 2013 and 2020.2. Normalized Difference Vegetation Index (NDVI) data with a spatial resolution of 1 km for the year 2020.3. Digital Elevation Model (DEM) data with a spatial resolution of 1 km. All three types of data are sourced from the Chinese Academy of Sciences Resource and Environmental Science Data Center. 4. Normalized Difference Rock Index (NDRI) data, calculated using the PIE Engine Studio remote sensing computing cloud service platform, with a spatial resolution of 1 km for the year 2020.5. Meteorological data, obtained from the National Earth System Science Data Center, with a spatial resolution of 1 km, providing monthly rainfall data for the year 2020.6. Soil erodibility data for Guangdong Province, sourced from the High-Performance Computing Platform for Geographic Data and Application Analysis at the Faculty of Geographic Science, Beijing Normal University. The data has been resampled to a spatial resolution of 1 km for the year 2021.7. Socio-economic and population data collected from the official websites of Qingyuan, Shaoguan, and Heyuan governments, statistical yearbooks, and the "Compilation of National Agricultural Product Cost and Income Data." The data is for the year 2020.

All raster data types have been reprojected to a common coordinate system, specifically the National Geodetic Coordinate System, and have been extracted based on the study area's boundaries.

2.3 Research methods

The issue of karst desertification in karst regions arises from the intricate interplay between social and natural factors. It is consequence of the detrimental effects of human activities on the ecosystems, with unreasonable human interventions being the predominant contributing factor. This expansion of urban

TABLE 1 Evaluation indicators.

Dimension	Indicators	Attribute of indicators
Development pressure	Spatial Conflict Comprehensive Index between PLES	-
	Population density	-
	Proportion of built-up land area	-
Sensitivity status	Vegetation coverage	+
	Rock exposure rate	-
	Soil Erosion Modulus	-
Resilience potential	Ecosystem Service Value	+
	Per Capita Energy Conservation and Environmental Protection Expenditure	+
	Proportion of Land Converted to Woodland and Grassland	+

development and the rapid population growth, exerting substantial pressure on the local ecosystems.

The level of sensitivity reflects the degree to which karst regions react to the disruptions caused by socio-economic development and human activities. It signifies how easily and likely karst desertification might occur in response to disturbances. This level can be described using a set of indicators or characteristics, including vegetation cover, soil erosion, and exposed bedrock, which highlight the critical features of karst desertification.

Resilience potential describes the ability of karst regions to self-regulate their ecosystems in response to disturbances and pressures. It also encompasses the capacity of socio-economic factors to facilitate the restoration of ecosystems to their original structure and functional levels. Typically, the government capital investment and human-initiated restoration activities are employed to measure resilience potential. The crucial principle in ecological restoration practices is "giving priority to natural restoration", nature-based solutions can be assessed using ecosystem service values (Fan et al., 2022; Gong et al., 2020).

To scientifically delineate ecological restoration zones for karst desertification, it is crucial to select representative and systematic indicators. In this study, based on the interaction between socio-economic factors and ecosystems, we have established an evaluation framework of "development pressure-sensitivity status-resilience potential" and selected appropriate indicators to create an evaluation system (Table 1).

2.3.1 Development pressure

We selected indicators such as the proportion of built-up land area and population density for characterization. Specifically, a higher proportion of built-up land indicates a greater likelihood of encroachment on arable land and woodland. Population density serves as a reflection of the pressure on the ecosystem, where higher population density implies greater stress on the ecosystem. With the promotion of rapid economic and social development, land use has undergone profound processes of transition, leaving the production–living–ecological spaces (PLES) and landscape pattern reconfigured, thus further affecting regional eco-environmental quality and landscape ecological risk (Chen et al., 2022). Therefore, we also incorporated the Spatial Conflict Comprehensive Index between PLES to reflect the irrational land use in karst areas.

2.3.1.1 Spatial conflict comprehensive index between PLES

Based on the multifunctionality of land, and considering the dominant and secondary functions in space, land use is divided into following categories (Liao et al., 2017; Zhao et al., 2019).

- Living-Production Space (urban land, rural residential areas, and other construction land)
- Production-Ecological Space (paddy fields and dryland)
- Ecological -Production Space (woodland and reservoirs/ponds)
- Ecological Space (grassland, rivers, lakes, tidal flats, wastelands, and bare land)

The conflict in land use spatially can be represented as a comprehensive analysis of system complexity, vulnerability, and stability. This conflict index aims to capture the spatial dynamics and potential tensions resulting from land use activities in karst regions.

$$SCCI = CI + FI - SI \quad (1)$$

In the Eq. 1, SCCI, representing the Spatial Conflict Comprehensive Index between PLES, is accompanied by CI (Spatial Complexity Index), FI (Spatial Fragility Index), and SI (Spatial Stability Index). The detailed methods for computing each of these indices can be found in the cited reference (Liao et al., 2017).

Taking into consideration factors like the study area's extent, zoning units, and spatial resolution, these indices were computed using a 10 km × 10 km window size, resulting in the Spatial Conflict Comprehensive Index (SCCI) with values falling within the [0,1] range. Drawing inspiration from the curve distribution model of Spatial Conflict Index, the index values are classified into the following categories (Feng, 2021): Stable and Controllable [0, 0.4), Essentially Controllable [0.4, 0.6), Essentially Uncontrollable [0.6, 0.8), and Significantly Conflictive [0.8, 1].

2.3.1.2 Population density and proportion of construction land area

Population density (people/km^2) is computed based on 2020 population data for each county. The proportion of construction land area is determined as the ratio of the

combined area occupied by urban, industrial, mining, and residential land to the total administrative area of each county, utilizing land use remote sensing monitoring data from the year 2020.

2.3.1.3 Comprehensive pressure index

The comprehensive pressure index is derived to delineate the spatial distribution characteristics and data variations among the three indicators. Given the substantial numerical differences in population density and the proportion of construction land area among individual counties, we employ a natural logarithm method from statistics to mitigate the sharp fluctuations between assessment units (Dan et al., 2020). All three indicators in the pressure layer share the same directionality, which means that a larger value of the comprehensive pressure index signifies heightened development pressure on the county. The specific formula for calculation is as follows:

$$\boldsymbol{P_i = SCCI_i \times lg\,(POP_i) \times CLP_i} \tag{2}$$

In the Eq. 2, P_i denotes the comprehensive pressure index for the ith county evaluation unit, while $SCCI_i$ corresponds to the Spatial Conflict Comprehensive Index between PLES. POP_i represents the population density, and CLP_i signifies the proportion of construction land area.

2.3.2 Sensitivity status

Sensitivity status provides insights into the responsiveness of ecosystem to human-induced pressures. Among the key characterization factors, vegetation coverage and rock exposure rate are pivotal for accurately assessing the distribution of karst desertification (Wang et al., 2019). Higher vegetation coverage suggests a lower likelihood of karst desertification in the region. Conversely, a higher rate of rock exposure signifies a more severe karst desertification issue. Notably, karst desertification is often accompanied by secondary disasters like soil erosion, which further exacerbate its severity. Soil erosion modulus, a commonly used indicator for assessing soil erosion risk, is inversely related to sensitivity status, meaning lower soil erosion intensity corresponds to lower sensitivity.

2.3.2.1 Vegetation cover

Based on pixel-based binary models, the normalized difference vegetation index (NDVI) is selected to extract vegetation cover. Specific calculation methods can be found in the referenced literature (Wu et al., 2020). The average vegetation cover for each county is calculated using zoning statistics tools.

2.3.2.2 Rock exposure rate

The rock exposure rate (D) is extracted by combining the calculation of the normalized rock index (NDRI) with pixel-based binary models. Specific calculation formulas can be found in the referenced literature (Sun et al., 2022). The average rock exposure rate for each county is calculated using the PIE Engine Studio remote sensing computing cloud service platform and zoning statistics tools.

2.3.2.3 Soil erosion modulus

The Revised universal Soil Loss Equation (RUSLE) model is used to assess soil erosion. The model expression is as follows:

$$\boldsymbol{A = R \times K \times L \times S \times C \times P} \tag{3}$$

In the Eq. 3.

- A represents the soil erosion modulus, measured in "t/(hm^2·a)".
- R is the rainfall erosion factor, measured in "[(MJmm)/(hm^2·a)]".
- K is the soil erodibility factor, measured in "[(thm^2·h)/(MJhm^2·mm)]".
- L and S are terrain factors, with L being the slope length factor and S being the slope steepness factor.
- C is the land cover management factor.
- P is the soil conservation measure factor.

All factors (L, S, C, P) are dimensionless. The rainfall erosion factor R is calculated based on monthly rainfall data following the guidelines in "SL 773–2018 - Guidelines for Estimating Soil Loss from Production and Construction Projects." The soil erodibility factor K is obtained directly from the 2018 Chinese soil erodibility factor dataset, specifically the data for Guangdong Province, and is extracted based on the study area.

The slope length factor (LS) is calculated using the slope length model as proposed by (Liu et al., 2010). The land cover management and soil conservation factors (C, P) are assigned values based on regional similarity and reference from existing research (Zhong et al., 2022).

The study employs the Albers projection as the spatial reference, and the spatial resolution is set at 1 km × 1 km. The calculations for individual factors and erosion modulus are performed using raster calculators.

2.3.2.4 Comprehensive state index

The comprehensive state index is calculated by combining vegetation cover, rock exposure rate, and soil erosion. A natural logarithm method is used to mitigate local fluctuations in the soil erosion index. To account for the differing trends of vegetation cover, rock exposure, and soil erosion on ecosystem status, a negative standardization is applied during calculation. A higher value of the comprehensive state index indicates a higher level of sensitivity. The specific calculation formula is as follows:

$$\boldsymbol{S_i = F_i \times D_i \times \lg(A_i)} \tag{4}$$

In the Eq. 4, Si denotes the comprehensive state index for the ith county evaluation unit, Fi corresponds to the negatively processed vegetation cover data, Di represents the rock exposure rate, and Ai indicates the soil erosion modulus.

2.3.3 Resilience potential

While socio-economic development exerts pressure on ecosystem, it also presents opportunities for ecological restoration. A primary goal of ecological restoration is to preserve and enhance regional ecosystem services (Kong et al., 2019). Ecosystem services value can visually demonstrate the contribution of ecosystems to supporting socio-economic development (He et al., 2019; Bai et al., 2019), reflecting the self-restoration capacity within the "socio-ecological" system and providing a foundation for ecological restoration zoning. Regional economic development, coupled with increased environmental

TABLE 2 Ecosystem Services value of per unit area (CNY).

Ecosystem services	Arable land	Woodland	Grassland	Water	Unused land
Food production	1.105	0.253	0.233	0.655	0.005
Raw material production	0.245	0.580	0.343	0.365	0.015
Water resource production	−1.305	0.300	0.190	5.440	0.010
Atmospheric regulation	0.890	1.908	1.207	1.335	0.065
Climate regulation	0.465	5.708	3.190	2.945	0.050
Waste disposal	0.135	1.673	1.053	4.575	0.205
Hydrological regulation	1.495	3.735	2.337	43.235	0.120
Soil maintenance	0.520	2.323	1.470	1.620	0.075
Nutrient cycling maintenance	0.155	0.178	0.113	0.125	0.005
Biodiversity maintenance	0.170	2.115	1.337	5.210	0.070
Recreation	0.075	0.928	0.590	3.310	0.030

protection efforts, gradually introduces resilience potential for ecosystem recovery and management strategies (Ye et al., 2019). *Per capita* energy-saving and environmental protection expenditure reflects the government's financial commitment to ecological restoration, and the conversion of cropland to forests and grassland is a widely acknowledged ecological engineering measure in the context of desertification control, with the proportion of the area used as an indicator of existing ecological restoration achievements.

2.3.3.1 Ecosystem services value (ESV)

We utilized the Chinese ecosystem service value equivalent table to estimate the ecosystem service values of the primary ecosystem types in the study area. Compared to woodland, arable land and wetland, *etc.*, the ESV of construction land is almost negligible. Therefore, according to the previous studies (Xie et al., 2015; Zhu et al., 2020; Feng et al., 2022), urban, industrial, mining, and residential land were omitted from the computation. The unit standard equivalent was based on major food crops and adjusted to align with the economic development status of the study area. Specific parameters can be found in Table 2.

2.3.3.2 Per capita energy conservation and environmental protection expenditure

We retrieved data on energy conservation and environmental protection expenditures from the statistical yearbooks of each county in the study area. To calculate *per capita* energy conservation and environmental protection expenditure (in thousands of RMB per square kilometer), we divided the total expenditure by the administrative area of each county.

2.3.3.3 Proportion of land converted to woodland and grassland

This metric assesses the extent of land transformation from arable land in 2013 to woodland and grassland areas in 2020.

2.3.3.4 Comprehensive potential index

The comprehensive potential index is derived from the data of the three aforementioned indicators. A higher value of this index indicates a greater level of socio-economic investment in ecological restoration and a higher resilience potential. The specific formula is as follows:

$$\boldsymbol{R_i} = \mathbf{lg}(\boldsymbol{ESV_i}) \times \mathbf{lg}(\boldsymbol{Z_i}) \times \boldsymbol{T_i} \tag{5}$$

In this Eq. 5, R_i signifies the comprehensive potential index of the ith county-level evaluation unit, ESV_i represents the corresponding ecosystem service value, Z_i denotes the per-square-kilometer energy-saving and environmental protection expenditure, and T_i reflects the proportion of converted cropland to woodland and grassland.

2.3.4 Ecological restoration zoning

Considering that the delineation of ecological restoration zones should cater to regional coordinated development and specific governance needs, it is prudent to establish these zones at the county level to ensure a high degree of territorial integrity. To strike a balance between the influence of development pressure, sensitivity status, and resilience potential on the restoration zones, making restoration strategies more precise and well-founded, we employ z-score standardization based on three key indicators: comprehensive pressure, sensitivity status, and resilience potential. By comparing the relative magnitudes of these indicators, we categorize the ecological restoration zones into different types. Z-score standardization facilitates the comparison of multiple datasets on a consistent scale. The specific formula for calculation is as follows:

$$\boldsymbol{y_i} = \frac{\boldsymbol{x_i}\text{-}\boldsymbol{\mu}}{\boldsymbol{\sigma}} \tag{6}$$

In the Eq. 6, y_i represents the z-score standardized value of the ith indicator for a county, x_i is the original value, "μ" denotes the mean of all county-level indicator data for the ith indicator, and "σ" is the standard deviation of all county-level indicator data for the ith indicator.

The comprehensive sensitivity, being more representative of each county's ecosystem status, serves as the primary determinant

TABLE 3 Criteria for karst desertification ecological restoration zones.

Type	Zone name	Criteria for division	Basis for division
Restoration (Sensitive status >0, poor ecosystem status)	Priority Restoration Zone	Pressure >0, Resilience <0	Human activities lead to increased development pressure and reduced levels of societal investment in ecological restoration
	Autonomous Restoration Zone	Pressure <0, Resilience >0	Human activities lead to lower development pressure and higher ecological restoration potential
	Coordinated Restoration Zone	Pressure <0, Resilience <0	Human activities lead to lower development pressure and reduced societal investment in ecological restoration
Protection (Sensitive status <0, good ecosystem status)	Autonomous Conservation Zone	Pressure >0, Resilience >0	Human activities impose significant development pressure, and they are complemented by a substantial commitment to ecological restoration
	Priority Conservation Zone	Pressure >0, Resilience <0	Intensive human activities create significant development pressure, accompanied by a relatively limited commitment to ecological restoration efforts within society
	Coordinated Conservation Zone	Pressure <0, Resilience <0	Human activities lead to less development pressure, and there is a comparatively lower level of societal investment in ecological restoration

Note: Sensitive status refers to the sensitivity of the ecosystem to human activities. Pressure represents the impact of human activities on development, while resilience represents the potential for ecological restoration.

for zone classification. Because of a negative standardization is applied during sensitivity calculation, the standardized comprehensive status index higher than 0 means relatively poorer ecological status and high sensitivity, classifying them as restoration zones. Conversely, those with values smaller than 0 are categorized as conservation zones. Further distinction in the urgency of restoration or conservation is made by considering the development pressure and resilience potential indicators. Those with standardized result of comprehensive resilience potential higher than 0 means more resilient, which are designated as autonomous zones, signifying a greater level of socio-economic investment for restoration or conservation. In contrast, areas where with resilience potential values smaller than 0 and development pressure values higher than 0 means less resilient and ongoing expansion of human activities and more socioeconomic pressure on ecosystem, which are identified as priority zones. Both the standardized comprehensive pressure and resilience potential results are small than 0 means the lower level of socioeconomic growth and ecological restoration investment, which is classified as coordination zones (Table 3).

3 Results

3.1 Development pressure index

There are significant spatial variations in both population density and urban development extent in the study area. Regions characterized by low population density, with approximately 100 people per square kilometer, are primarily found in minority autonomous counties. In contrast, areas with high population density and substantial urban development are predominantly situated in Wujiang District and Qingxin District, corresponding to the urban centers of Shaoguan and Qingyuan. In Wujiang District, the population density reaches 554.83 people per square kilometer, with a construction land pro-portion of 6.86%, significantly higher than in most other counties, which remains largely below 3%. This highlights the intense nature of urban development in these areas. The Spatial Conflict Comprehensive Index, applied across all counties, consistently falls within the range from “stable and controllable” to “basically controllable.” Yingde City, Lechang City, Wujiang District, and Wengyuan County exhibit relatively higher values. This is primarily due to the dense and fragmented distribution of production and living spaces within these regions, signifying a heightened degree of land development and utilization. In contrast, counties characterized by lower conflict levels are primarily concentrated within minority autonomous regions, where ecological spaces exhibit a broader and more dispersed pattern. The comprehensive evaluation of development pressure (Table 4) across the study area is notably influenced by population density. Regions facing increased pressure from human activities are mainly concentrated within urban areas, showing a discernible southeast-to-northwest gradient. Wujiang District, situated within the high-value zone, serves as a prominent example. Meanwhile, medium-value areas encompass Qingxin District, Yingde City, and Wengyuan County, primarily distributed in the eastern sector. Conversely, substantial low-value areas are identified in the western part of the study area, including counties such as Lianzhou, Liannan Yao Autonomous County, Yangshan County, Ruyuan Yao Autonomous County, and Lechang City (Figure 2).

3.2 Sensitivity status index

Significant variations are observed among the sensitivity status indicators within the study area. Notably, the implementation of the national land greening project has had a substantial impact on vegetation cover. Lianping County and Liannan Yao Autonomous County stand out with vegetation cover exceeding 85%. Conversely, Wujiang District, Qingxin District, and Yingde City exhibit relatively lower vegetation cover, all falling below the 80% mark. The distribution of exposed bedrock rates follows a contrasting pattern, with higher values predominantly found in Wujiang District and Yingde City, both ex-ceeding 43%. In contrast, Yangshan

TABLE 4 Development pressure index evaluation.

County/ District	Spatial conflict comprehensive index between PLES	Population density (people/km^2)	Proportion of construction land area (%)	Comprehensive development pressure index
Wujiang District	0.43	554.82	6.86	0.081
Wengyuan County	0.43	148.05	3.24	0.030
Ruyuan Yao Autonomous County	0.34	81.69	1.31	0.009
Lechang City	0.43	158.12	1.94	0.018
Lianping County	0.38	125.37	1.69	0.013
Qingxin District	0.40	262.40	3.13	0.030
Yangshan County	0.38	110.38	0.62	0.005
Liannan Yao Autonomous County	0.30	110.62	0.61	0.004
Yingde City	0.48	167.05	3.11	0.033
Lianzhou City	0.39	140.96	1.42	0.012

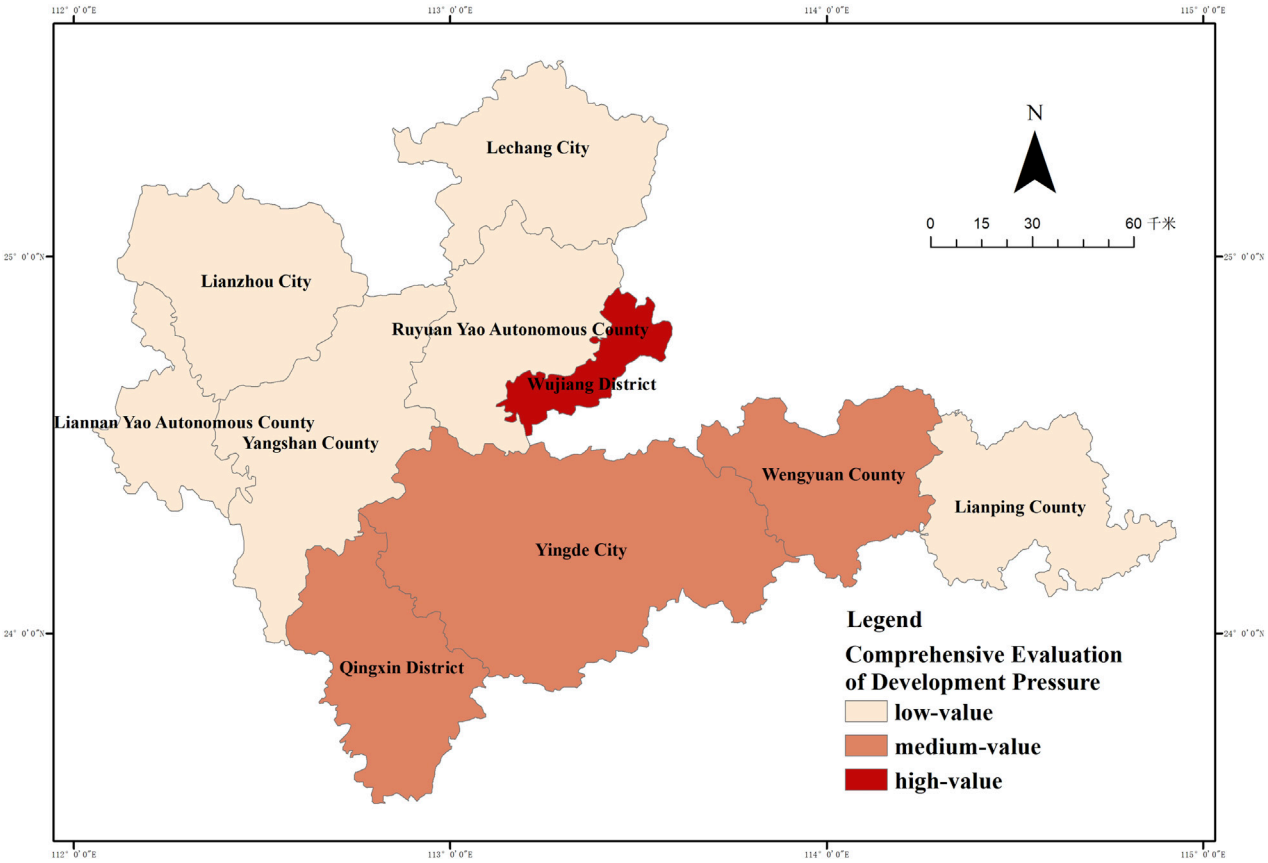

FIGURE 2
Comprehensive evaluation of development pressure.

TABLE 5 Sensitivity status index evaluation.

County/District	Vegetation cover (%)	Rock exposure rate (%)	Soil erosion modulus (%)	Comprehensive sensitivity status index
Wujiang District	78.61	43.69	116.65	0.193
Wengyuan County	82.73	41.21	525.02	0.194
Ruyuan Yao Autonomous County	83.16	40.66	480.21	0.184
Lechang City	82.55	40.85	456.36	0.190
Lianping County	87.57	39.29	573.05	0.135
Qingxin District	78.45	41.43	526.45	0.243
Yangshan County	81.32	39.71	1,035.51	0.224
Liannan Yao Autonomous County	85.51	37.95	347.43	0.140
Yingde City	79.56	43.83	1,452.87	0.283
Lianzhou City	80.61	40.52	594.57	0.218

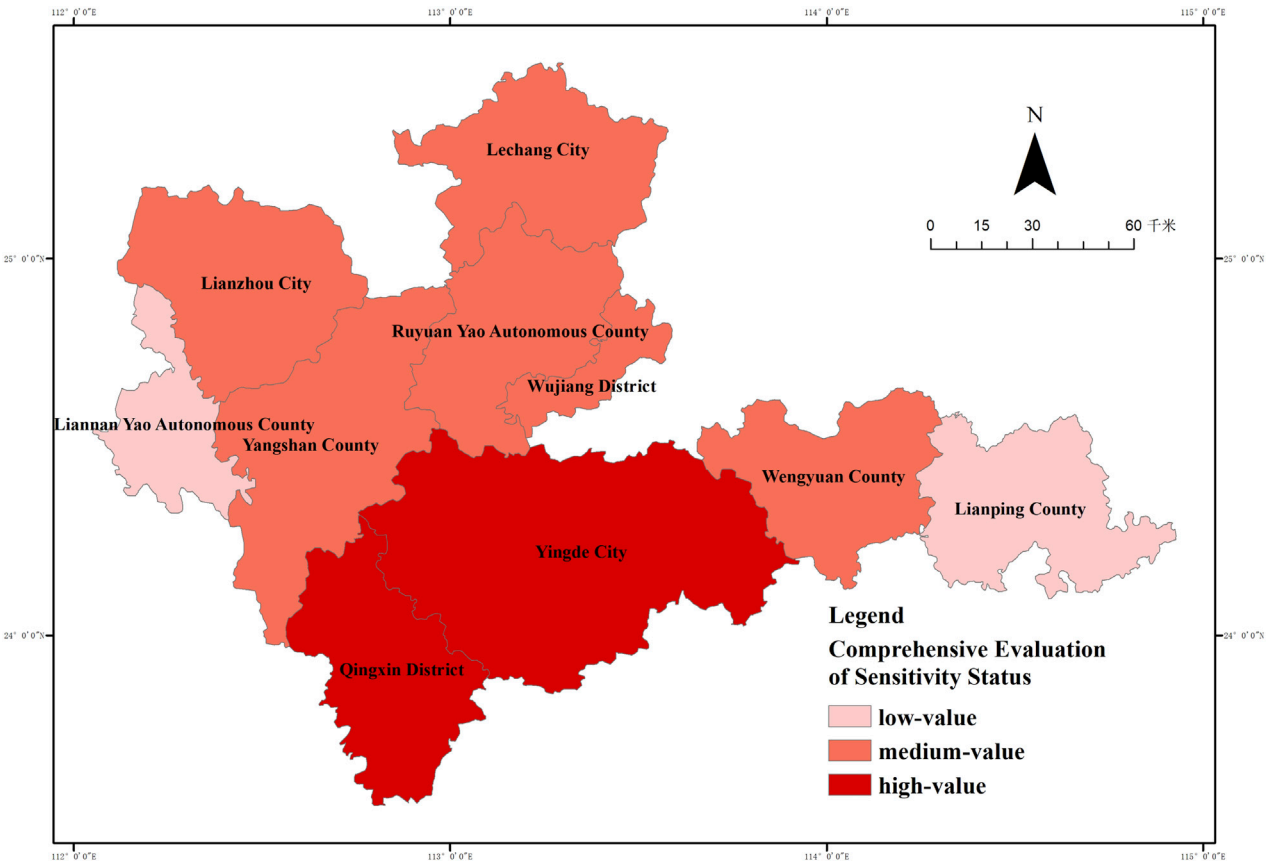

FIGURE 3
Comprehensive evaluation of sensitivity status.

County, Lianping County, and Liannan Yao Autonomous County show relatively lower rates of exposed bedrock. Soil erosion levels are notably high in Yangshan County and Yingde City, attributed to the typical impact of karst desertification. On the other hand, areas with lower erosion levels primarily include Liannan Yao Autonomous County and Wujiang District. This is influenced by effective vegetation cover management and soil conservation practices. The comprehensive state index (Table 5)

TABLE 6 Resilience potential index evaluation.

County/ District	ESV(CNY)	Per capita energy conservation and environmental protection expenditure (thousands of RMB per square kilometer)	Proportion of land converted to woodland and Grassland (%)	Comprehensive resilience potential index
Wujiang District	$1.73*10^{13}$	2.12	6.35	0.274
Wengyuan County	$5.60*10^{13}$	12.41	6.89	1.037
Ruyuan Yao Autonomous County	$6.73*10^{13}$	4.23	4.01	0.347
Lechang City	$6.13*10^{13}$	13.25	7.30	1.129
Lianping County	$6.00*10^{13}$	4.05	5.17	0.433
Qingxin District	$6.31*10^{13}$	2.63	6.21	0.360
Yangshan County	$8.82*10^{13}$	1.23	7.05	0.088
Liannan Yao Autonomous County	$3.55*10^{13}$	3.26	4.50	0.313
Yingde City	$1.43*10^{14}$	3.17	7.72	0.547
Lianzhou City	$6.69*10^{13}$	0.82	7.85	−0.095

reflects significant spatial disparities throughout the study area, with higher values concentrated in the central region and lower values along the eastern and western sides. Counties with lower index values are less numerous and encompass Lianping County and Liannan Yao Autonomous County. Conversely, Qingxin District and Yingde City stand out with higher index values, with Qingxin District having the least vegetation cover compared to other counties. Yingde City exhibits the highest levels of exposed bedrock and soil erosion in the study area, resulting in the highest overall sensitivity (Figure 3).

3.3 Resilience potential index

Owing to substantial variations in county sizes, the distribution pattern of ESV across the study area exhibits a higher value in the central regions and lower values along the periphery. The highest ESV is observed in Yingde City, which is also the largest area county-level administrative in Guangdong Province. Counties with relatively lower ESV include Wujiang District and Liannan Yao Autonomous County. As a whole, the study area demonstrates relatively lower per-unit area expenditures in energy conservation and environmental protection. The majority of counties have per-unit expenditures below 4,000 yuan per square kilometer. The highest expenditures are found in Lechang City and Wengyuan County, while the lowest can be seen in Lianzhou City at just 0.82 yuan per square kilometer. From 2013 to 2020, the study area achieved a total afforestation area of 1,663 square kilometers. Areas with a relatively high afforestation rate include Lechang City, Lianzhou City, and Yingde City, while counties with smaller afforestation areas con-sist of Liannan Yao Autonomous County, Ruyuan Yao Autonomous County, and Lianping County. The overall comprehensive resilience potential (Table 6) in the study area is significantly influenced by per-unit area expenditures in energy conservation and environmental protection. There are notable disparities in the overall levels: Lechang City and Wengyuan County fall into the high-value category, with per-unit expenditures in energy conservation and environmental protection significantly surpassing those in Lianzhou City and Yangshan County, which belong to the low-value category. The remaining counties are generally classified as mid-value (Figure 4).

3.4 Zoning results and ecological restoration strategies

Based on the z-score standardized results, the study area is classified into Restoration Zones and Conservation Zones (Figure 5). Notably, the Restoration Zones cover more than half of the total area and are primarily situated in the northwestern and southern parts of the study area, with these regions bordering each other. The Conservation Zones consist of six counties in total, primarily located in the northern, western, and eastern parts of the study area. All three zone—Autonomous Restoration, Coordinated Restoration, and Coordinated Conservation—encompass more than 20% of the total area (Table 7).

3.4.1 Priority restoration zone

Qingxin District, situated within Qingyuan City, is under substantial development pressure due to human activities. Pressure is influenced by low vegetation cover, high rock exposure rates, and soil erosion, resulting in a less favorable ecological system status. Furthermore, *per capita* energy expenditure and reforestation areas show limited resilience potential. To reverse the adverse ecological conditions, this region should increase in-vestments in ecological restoration,

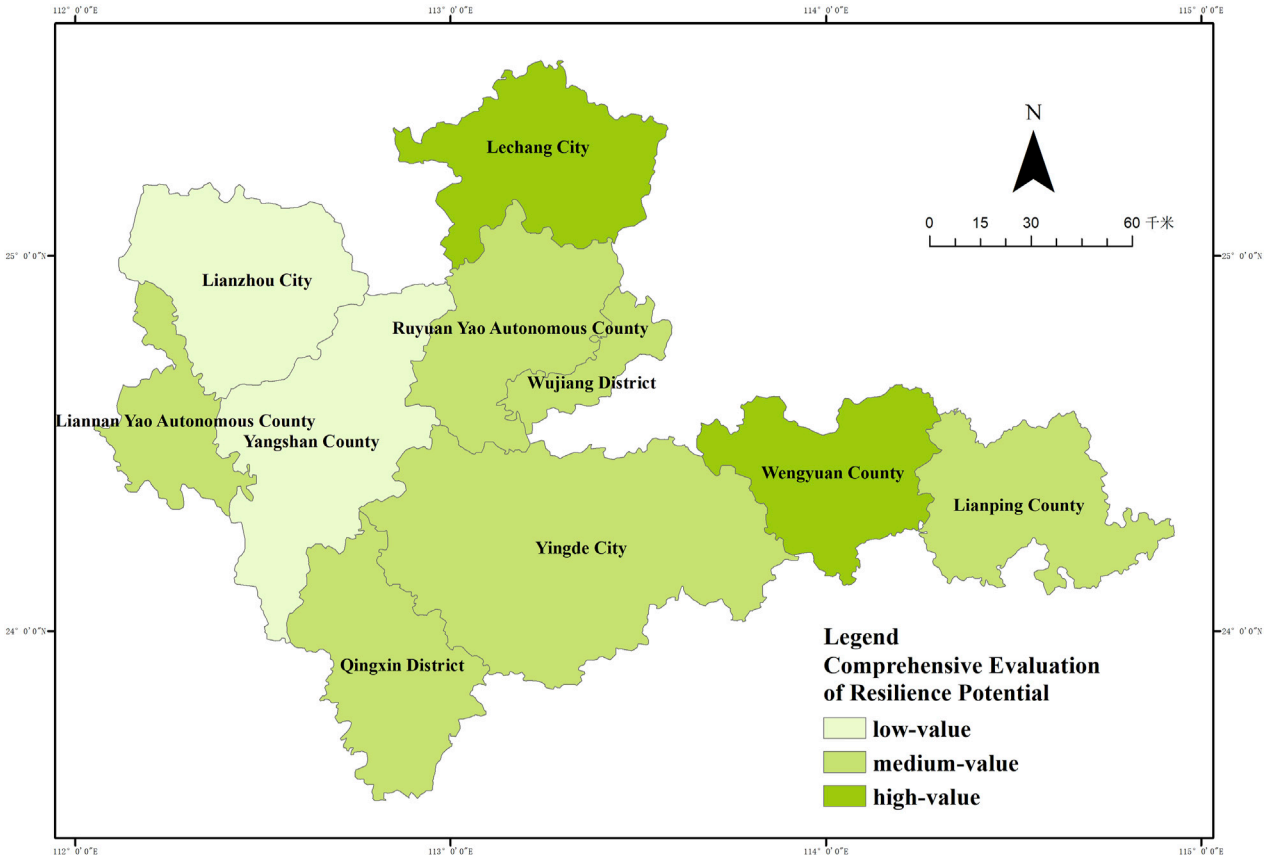

FIGURE 4
Comprehensive evaluation of resilience potential.

implement ecological protection and restoration policies, and prioritize actions aimed at preventing ecosystem degradation from inappropriate human activities. The goal is to transform the excessive pressure exerted on the ecosystem by human development into resilience potential. Continuously advance the greening of territorial space, develop distinctive forestry products, and focus on the development model of undergrowth economy, including “medicine, fungi, tea, livestock, and forest tourism."

3.4.2 Autonomous restoration zone

Corresponding to Yingde City, this area experiences low pressure and exhibits high resilience potential. The primary focus here is on alleviating conflicts within the PLES, strengthening the advantages of ecosystem service values, and enhancing the self-restorative capacity of the ecosystem. Due to the relatively high rock exposure rates and severe soil erosion, additional efforts should be made to enhance water source conservation forests, ecological public welfare forest construction. With the engineering measures and reforestation, promote comprehensive mining reclamation. This will help prevent soil erosion caused by inappropriate human activities. Additionally, implementing ecological compensation policies and creating a “those who undertake the restoration stand to gain the benefits " market mechanism can encourage the involvement of social capital in the entire ecological restoration process.

3.4.3 Coordinated restoration zone

This zone includes Lianzhou City and Yangshan County, characterized by low human activity pressure and limited resilience potential. The main focus is to increase environmental governance investments, thereby facilitating effective ecological restoration. Due to the low investment in energy conservation and environmental protection funds, it is crucial to make effective use of financial support from higher-level governments and rein-force lateral collaborative governance in the region. In order to the effective restoration of damaged ecosystems, this zone can also collaborate with the Guangdong Nanling National Park construction, integrating ecological elements such as mountains, water, and forests in the restoration of natural resources, by preventing and managing soil erosion, it aims to maintain the ecological barrier integrity of the surrounding mountains. This is achieved through a combination of afforestation, greening initiatives, and forest regeneration, thereby promoting the continuous advancement of desertification control efforts.

3.4.4 Autonomous conservation zone

This category comprises Lechang City and Wengyuan County, regions with a well-established ecological foundation, a high development pressure, and strong resilience potential. The primary objective is to consolidate the existing ecological

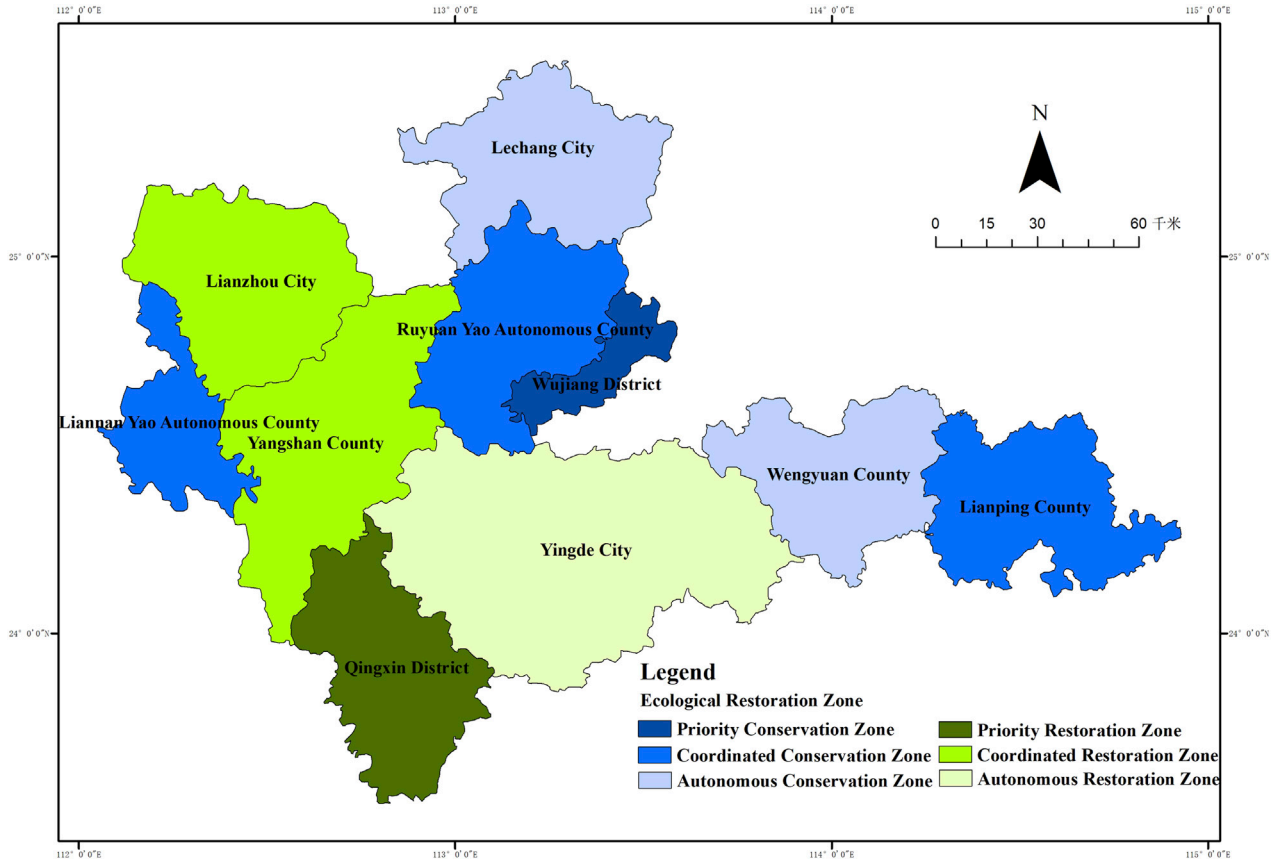

FIGURE 5
Ecological restoration zone.

TABLE 7 Karst desertification ecological restoration zone results.

Zone name	County/District	Area (km^2)	Proportion (%)
Priority Restoration Zone	Qingxin District	2 351.75	9.38
Autonomous Restoration Zone	Yingde City	5 634.95	22.47
Coordinated Restoration Zone	Lianzhou City, Yangshan County	6 006.05	23.95
Autonomous Conservation Zone	Wengyuan County, Lechang City	4 598.44	18.34
Coordinated Conservation Zone	Ruyuan Yao Autonomous County, Lianping County, Liannan Yao Autonomous County	5 810.33	23.17
Priority Conservation Zone	Wujiang District	675.71	2.69

foundation, implement water source conservation forests, and precisely enhance forest quality. Innovative measures for desertification control should be introduced, with continued investment in energy conservation and environmental protection, ensuring the protection of the eco-system's services. Simultaneously, single human intervention measures should be avoid-ed, with further regulation of human development activities and the optimization layout of the PLES, resulting in an improved pattern of production and living. Implementing ecological restoration measures on historically abandoned industrial sites to enhance the ecological quality of the land, while also creating opportunities for local green economic growth.

3.4.5 Coordinated conservation zone

This zone encompasses Ruyuan Yao Autonomous County, Lianping County, and Liannan Yao Autonomous County, with low development pressure and resilience potential. This area has high vegetation cover and should implement afforestation and greening initiatives. By promoting regional economic development while enhancing ecological protection efforts, it aims to advance the construction of the Wanshanchaowang National Desert Park and the Xijing Ancient Road National Desert Park. Leveraging its excellent ecological foundation, the zone should develop leisure tourism industries and actively promote the development of high-value specialty industries. This approach explores the efficient transformation path for the value realization of ecological product, promoting ecological restoration through ecological industrialization.

3.4.6 Priority conservation zone

The corresponding administrative region is Wujiang District, which is the most densely populated built-up area in the study. It experiences significant development pressure and possesses limited resilience potential. The primary objective is to prevent excessive damage to the ecological foundation, balancing ecological and economic benefits. This area should engage in strategic urban planning within the limits of its resource and environmental carrying capacity, thereby avoiding new issues related to desertification and human-induced soil erosion. Additionally, it should increase investments in environmental protection to improve small watershed soil and water erosion control efforts. Gradually expanding forest coverage and enhancing forest quality, and creating a new pattern for ecological construction.

4 Discussion

4.1 Framework for zoning, restoration goals, and stakeholders based on the "social-ecological" system

The study area, situated in a karst region characterized by prominent human-environment conflicts and ecological sensitivity, underscores the intricate interplay between social-ecological system. Unreasonable human activities have led to the degradation of ecosystem functions, impeding local socio-economic development (Ye et al., 2019). If this feedback loop remains unchecked, it may cause the "social-ecological" system to deteriorate further (Wang Z. et al., 2023), leading to a vicious cycle of "vegetation destruction" and "land reclamation equals poverty." Therefore, there is an urgent need for governance strategies based on a "social-ecological" system analysis framework. Desertification is "negative" feedback resulting from human interference with the ecosystem, leading to the unsustainability of the "social-ecological" system. Therefore, the ultimate goal of ecological restoration zoning is to start from sustainability, coupling multiple objectives within the "social-ecological" system, integrating social, economic, and ecological elements (Polyakov et al., 2023) and processes to formulate ecological restoration zoning decision-making and implementation strategies.

In the context of promote harmonious coexistence between human and environment, ecological restoration should primarily prioritize maintaining regional ecological security, promoting continuous improvement in ecosystem diversity and stability, and achieving synergy between conservation and development. By delineating the interactive processes of the "social-ecological" system, conducting a comprehensive analysis of existing ecological issues, and assessing the relationship between socio-economic system and ecosystem, this study proposes restoration strategies and recommendation measures for each zone. Based on the zoning results, the contiguous regions of the northwestern and southern parts of the study area require more comprehensive engineering and greening measures, the benefits from rocky desertification treatment and reforestation/afforestation will promote the synergistic effect of "social-ecological" system. The conservation zones are primarily situated in the northern and eastern parts of the study area, ecological and economic benefits can be brought from giving priority to natural restoration, ecological industry and reasonable PLES layout also contribute to the "social-ecological" system.

Domestic and international trends in ecological restoration zoning research and practical cases reveals an evolving focus (Smith et al., 2022; Zhou et al., 2022; Reader et al., 2023). Ecological restoration in Karst region entails a comprehensive approach, acknowledging the intricate inter-connections and interdependencies among forest, mountain, and water elements. This holistic perspective reflects the core concept of "integral protection, systematic restoration, and comprehensive management" (Suding et al., 2015). Furthermore, it is crucial to recognize that government bodies, corporate investors, and the stakeholder are central participants in the ecological restoration process (Toma and Buisson, 2022). Their varying perspectives and requirements will directly impact the effectiveness of restoration planning and project implementation. The application of multi-agent modeling to support decision analysis encourages the collective involvement of multiple stakeholders. This approach acknowledges that the success of ecological restoration in karst regions necessitates the active collaboration of various stakeholders and underscores the importance of harmonizing their differing interests and needs for the collective benefit of the human and environment.

4.2 Research advantages and limitations

In the context of a transition towards more harmonious human-environment relationships within the realm of ecological restoration, this study takes a "social-ecological" system approach. It constructs an evaluation index that comprises "development pressure," "sensitivity status," and "resilience potential." The study performs quantitative assessments and integrated zoning, using the karst-concentrated areas of Guangdong Province as an illustrative example. This research addresses previous inadequacies by providing a more comprehensive perspective. It considers ecological issues and human disturbances while integrating the restorative capacity created by the ecosystem's resilience potential and socio-economic development. The integrated index allows for the portrayal of societal pressures on ecological systems, the sensitive characteristics of the ecosystem, and the "social-ecological" system's resilience potential. This enhances our overall understanding of how to resolve human-environment conflicts in ecologically vulnerable areas. This study departs from the practice of assigning weights to indicator factors, which can be subjective. Instead, it employs a standardization method to compare the results of different indicator combinations. This approach is more objective and uses a concise set of critical indicators to reflect regional disparities, making it more operationally feasible. The ultimate goal of the zoning method is to facilitate the implementation of zoning results and ecological restoration. The research framework of this study is clear, easily quantifiable, and holds promise for practical applications.

Compared to studies based on grid or watershed units, this research primarily focuses on reflecting the "social-ecological" system characteristics of various administrative units within a region. This approach provides differentiated governance

measures for regional coordinated development. Subsequent steps may involve further refining data granularity and analyzing the spatial heterogeneity characteristics within the units to identify key ecological restoration areas and provide precise strategies (Sun et al., 2022). It is important to note that the sample selection for evaluation units in this study did not include several counties with dispersed distribution of desertification. Future research could encompass a comprehensive analysis of desertification restoration in Guangdong Province and even the karst regions of southern China. Due to data availability and computational constraints, this study did not account for the temporal changes in the "social-ecological" system characteristics. Therefore, it is crucial to explore the relationship between "social-ecological" systems in ecologically fragile karst areas, considering their multi-scale and cross-temporal dimensions in the future.

5 Conclusion

Ecological restoration zoning involves various socio-economic and ecological factors, making it challenging to accurately identify the ecological restoration zones and propose targeted strategies. In the context of shifting towards coordinated human-environment relationships, this study constructs a comprehensive evaluation framework based on the perspective of "socio-ecological" system. This approach represents a preliminary exploration of the complex interplay between socio-economic and ecological factors, offering a more integrated understanding of the multi-target and multi-stakeholder trends in ecological restoration. Moreover, it provides valuable insights for guiding the treatment of karst desertification and ecological restoration.

The spatial distribution of these indicators shows significant characteristics. Development pressure is strongly influenced by population density, with areas experiencing higher human activity pressure primarily concentrated in urban areas, with the most prominent in Wujiang District. Sensitivity status is predominantly determined by soil erosion levels and vegetation coverage. Qinxin District County and Yingde City exhibit the most severe environmental issues. The overall level of resilience potential varies significantly and is mainly influenced by *per capita* energy conservation and environmental protection expenditures.

Based on the characteristics of development pressure, sensitivity status, and resilience potential, the study area is recognized to two main categories of restoration units, corresponding "socio-ecological" system restoration strategies were proposed. Restoration-type units should utilize the ecological resilience and focus on reversing poor ecosystem status preventing further ecosystem degradation due to inappropriate human activities. Participation of inter-regional, multi-stakeholder of restoration mechanisms are yet to be established. Conservation -type units should aim to regulate human activities further and promote the rational layout of PLES. These zones should actively explore paths for realizing ecological product value while intensifying ecological protection.

Data availability statement

The original contributions presented in the study are included in the article/Supplementary material, further inquiries can be directed to the corresponding author.

Author contributions

YL: Conceptualization, Project administration, Validation, Writing–original draft. JH: Formal Analysis, Methodology, Software, Visualization, Writing–original draft. WL: Conceptualization, Data curation, Formal Analysis, Funding acquisition, Investigation, Methodology, Project administration, Resources, Software, Supervision, Validation, Visualization, Writing–original draft, Writing–review and editing.

Funding

The author(s) declare that no financial support was received for the research, authorship, and/or publication of this article.

Conflict of interest

Author YL is employed by Guangdong Duoyuan Geographic Information Service Co., Ltd.

The remaining authors declare that the research was conducted in the absence of any commercial or financial relationships that could be construed as a potential conflict of interest.

Publisher's note

References

Ahammad, R., Kamal Hossain, M., Sobhan, I., Hasan, R., Biswas, S. R., and Mukul, S. A. (2023). Social-ecological and institutional factors affecting forest and landscape restoration in the chittagong hill tracts of Bangladesh. *Land Use Policy* 125 (February), 106478. doi:10.1016/j.landusepol.2022.106478

Bai, Z., Zhou, W., Wang, J., Zhao, Z., Cao, Y., and Zhou, Y. (2019). Overall protection, systematic restoration and comprehensive management of land space. *China Land Sci.* 33 (2), 1–11. doi:10.11994/zgtdkx.20190218.090442

Cai, H., Chen, Yi, Zha, D., Zeng, Y., Shao, H., and Hong, T. (2020). Principle and method for ecological restoration zoning of territorial space based on the dominant function. *China Land Sci.* 36 (15), 261–270+325. doi:10.11975/j.issn.1002-6819.2020.15.032

Cao, Yu, Wang, J., and Li, G. (2019). Ecological restoration for territorial space: basic concepts and foundations. *China Land Sci.* 33 (7), 1–10. doi:10.11994/zgtdkx.20190625.083700

Chen, Z., Liu, Y., and Tu, S. (2022). Comprehensive eco-environmental effects caused by land use transition from the perspective of production–living–ecological spaces in a typical region: a case study of the guangxi Zhuang autonomous region, China. *Land* 11 (12), 2160. doi:10.3390/land11122160

Dan, Y., Peng, J., Zhang, Z., Xu, Z., Qi, M., and Dong, J. (2020). Territorially ecological restoration zoning based on the framework of degradation pressures, upply state and restoration potential: a case study in the Pearl River Delta region. *Acta Ecol. Sin.* 40 (23), 8451–8460. doi:10.5846/stxb202004240982

Feng, Q., Zhou, Z., Quan, C., and Zhu, C. (2022). Spatial-temporal evolution research of ecosystem service value in ecologically vulnerable karst regions under the perspective of poverty alleviation relocation. *Acta Ecol. Sin.* 42 (7). doi:10.5846/stxb202103260798

Fan, Y., Zhou, Y., and Han, Bo (2022). Ecological restoration zoning of agricultural land of the sunan district from the perspective of national land and space governance. *Trans. Chin. Soc. Agric. Eng.* 38 (1), 287–296. doi:10.11975/j.issn.1002-6819.2022.01.032

Feng, Y. (2021). *Construction land optimization of mountain-basin system based on suitability and ecological-production-living spaces conflict——a case study of huishui county in guizhou province*. Master Dissertation. Guiyang, China: Guizhou Normal University. doi:10.27048/d.cnki.ggzsu.2021.000674

Gong, Q., Zhang, H., Ye, Y., and Yuan, S. (2020). Planning strategy of land and space ecological restoration under the framework of man-land system coupling: take the Guangdong-Hong Kong-Macao greater Bay area as an example. *Geogr. Res.* 39 (9), 2176–2188. doi:10.11821/dlyj020200413

He, X., Wang, L., Ke, B., Yue, Y., Wang, K., Cao, J., et al. (2019). Progress on ecological conservation and restoration for China Karst. *Acta Ecol. Sin.* 39 (18). doi:10.5846/stxb201812292842

Hu, M., Zhang, H., Tang, J., and Yan, S. (2023). Zoning and optimization strategies of land spatial ecological restoration in liangjiang new area of chongqing based on the supply–demand relationship of ecosystem services. *Land* 12 (6), 1255. doi:10.3390/land12061255

Jiang, H., Peng, J., Zhao, Y., Xu, D., and Dong, J. (2022). Zoning for ecosystem restoration based on ecological network in mountainous region. *Ecol. Indic.* 142 (September), 109138. doi:10.1016/j.ecolind.2022.109138

Kong, L., Zheng, H., and Ouyang, Z. (2019). Ecological protection and restoration of forest, wetland, grassland and cropland based on the perspective of ecosystem services: a case study in Dongting Lake Watershed. *Acta Ecol. Sin.* 39 (23). doi:10.5846/stxb201905301137

Li, X. H., Zhang, X., Yao, L., Li, Y., and Yue, L. (2023a). Spatial-temporal evolution characteristics of social - ecological system resilience in hexi region. *J. Arid Land Resour. Environ.* 37 (7), 38–47. doi:10.13448/j.cnki.jalre.2023.159

Li, Z., Jiang, C., Cheng, Li, and Gu, S. (2023b). Ecological restoration and protection of national land space in coal resource-based cities from the perspective of ecological security pattern: a case study in huaibei city, China. *Land* 12 (2), 442. doi:10.3390/land12020442

Li, Z., Ma, L., Chen, X., Wang, X., and Bai, J. (2023c). Zoning and management of ecological restoration from the perspective of ecosystem service supply and demand: a case study of yuzhong county in longzhong loess hilly region, China. *Land* 12 (5), 992. doi:10.3390/land12050992

Liao, L., Dai, W., Chen, J., Huang, W., Jiang, F., and Hu, Q. (2017). Spatial conflict between ecological-production-living spaces on pingtan island during rapid urbanization. *Resour. Sci.* 39 (10), 1823–1833. doi:10.18402/resci.2017.10.03

Liu, F., Dai, E., and Yin, J. (2023). A review of social–ecological system research and geographical applications. *Sustainability* 15 (8), 6930. doi:10.3390/su15086930

Liu, Y., Fu, B., Wang, S., Zhao, W., and Li, Y. (2020). Research progress of human-earth system dynamics based on spatial resilience theory. *ACTA Geogr. SIN.* 75 (5), 891–903. doi:10.11821/dlxb202005001

Ni, Q.-lin, Hou, H.-ping, Zhong-yi, D., Yi-bo, Li, and Jin-rong, Li (2020). Ecological remediation zoning of territory based on the ecological security pattern recognition: taking Jiawang district of Xuzhou city as an example. *J. Nat. Resour.* 35 (1), 204. doi:10.31497/zrzyxb.20200117

Peng, J., Li, B., Dong, J., Liu, Y., Lv, D., Du, Y., et al. (2020). Basic logic of territorial ecological restoration. *China Land Sci.* 34 (5), 18–26. doi:10.11994/zgtdkx.20200427.124442

Polyakov, M., Dempster, F., Park, G., and Pannell, D. J. (2023). Joining the dots versus growing the blobs: evaluating spatial targeting strategies for ecological restoration. *Ecol. Econ.* 204 (February), 107671. doi:10.1016/j.ecolecon.2022.107671

Reader, M. O., Eppinga, M. B., Jan de Boer, H., Damm, A., Petchey, O. L., and Santos, M. J. (2023). Biodiversity mediates relationships between anthropogenic drivers and ecosystem services across global mountain, island and Delta systems. *Glob. Environ. Change* 78 (January), 102612. doi:10.1016/j.gloenvcha.2022.102612

Smith, L. M., Erin, M., Reschke, J. J. B., Harvey, J. E., and Kevin Summers, J. (2022). A conceptual approach to characterizing ecological suitability: informing socio-ecological measures for restoration effectiveness. *Ecol. Indic.* 143 (October), 109385. doi:10.1016/j.ecolind.2022.109385

Song, S., Wang, S., Fu, B., Chen, H., Liu, Y., and Zhao, W. (2019). Study on adaptive governance of social-ecological system: progress and prospect. *ACTA Geogr. SIN.* 74 (11), 2401–2410. doi:10.11821/dlxb201911015

Suding, K., Higgs, E., Palmer, M., Baird Callicott, J., Anderson, C. B., Baker, M., et al. (2015). Committing to ecological restoration. *Science* 348 (6235), 638–640. doi:10.1126/science.aaa4216

Sun, R., Jin, X., Han, Bo, Liang, X., Zhang, X., and Zhou, Y. (2022). Does scale matter? Analysis and measurement of ecosystem service supply and demand status based on ecological unit. *Environ. Impact Assess. Rev.* 95 (July), 106785. doi:10.1016/j.eiar.2022.106785

Sun, Y., Zhou, Z., Zhao, Y., Fang, M., and Wu, Y. (2022). Evolution and distribution pattern of land use and rocky desertificaiton in karst mountainous area. *Res. Soil Water Conservation* 29 (1), 311–318. doi:10.13869/j.cnki.rswc.2022.01.034

Tang, F., Wang, Li, Guo, Y., Fu, M., Huang, Ni, Duan, W., et al. (2022). Spatio-temporal variation and coupling coordination relationship between urbanisation and habitat quality in the grand canal, China. *Land Use Policy* 117 (June), 106119. doi:10.1016/j.landusepol.2022.106119

Tedesco, A. M., López-Cubillos, S., Chazdon, R., Rhodes, J. R., Archibald, C. L., Pérez-Hämmerle, K.-V., et al. (2023). Beyond ecology: ecosystem restoration as a process for social-ecological transformation. *Trends Ecol. Evol.* 38 (7), 643–653. doi:10.1016/j.tree.2023.02.007

Tian, M., Gao, J., Song, G., Zou, C., and Zheng, H. (2017). Zoning for ecological remediation by dominant ecological function and ecological degradation degree. *J. Ecol. Rural Environ.* 33 (1), 7–14. doi:10.11934/j.issn.1673-4831.2017.01.002

Toma, T. S. P., and Buisson, E. (2022). Taking cultural landscapes into account: implications for scaling up ecological restoration. *Land Use Policy* 120 (September), 106233. doi:10.1016/j.landusepol.2022.106233

Van der Biest, K., Meire, P., Schellekens, T., D'hondt, B., Bonte, D., Vanagt, T., et al. (2020). Aligning biodiversity conservation and ecosystem services in spatial planning: focus on ecosystem processes. *Sci. Total Environ.* 712 (April), 136350. doi:10.1016/j.scitotenv.2019.136350

Vos, A. de, Biggs, R., and Preiser, R. (2019). Methods for understanding social-ecological systems: a review of place-based studies. *Ecol. Soc.* 24 (4), art16. doi:10.5751/ES-11236-240416

Wang, H., Zhang, D., Ting, H., Zhao, Y., Wang, Z., and Wu, J. (2023). Social-ecological systems: research trends, theme evolution, and regional practices. *Acta Ecol. Sin.* 43 (15), 6499–6513. doi:10.5846/stxb202208212395

Wang, J., and Zhong, L. (2019). Application of ecosystem service theory for ecological protection and restoration of mountain-river-forest-field-lake-grassland. *Acta Ecol. Sin.* 39 (23). doi:10.5846/stxb201905291110

Wang, M., Wang, S., Bai, X., Li, S., Li, H., Cao, Y., et al. (2019). Evolution characteristics of karst rocky desertification in typical small watershed and the key characterization factor and driving factor. *ACTA Ecol. SIN.* 39 (16), 6083–6097. doi:10.5846/stxb201902170278

Wang, P., and Zhao, W. (2022). Ecological restoration zoning of territorial space in typical karst region: a case study of Maotiao River Basin in Guizhou. *J. Nat. Resour.* 37 (9), 2403. doi:10.31497/zrzyxb.20220914

Wang, Y., Hu, Y., Gao, M., and Niu, S. (2023). Land-space ecological restoration zoning of karst rocky desertification areas in guangxi from multi-dimensional perspectives. *Trans. Chin. Soc. Agric. Eng.* 39 (1), 223–231. doi:10.11975/j.issn.1002-6819.202210065

Wang, Z., Fu, B., Wu, X., Li, Y., Wang, S., and Lu, N. (2023). Escaping social–ecological traps through ecological restoration and socioeconomic development in China's loess plateau. *People Nat.* 5 (4), 1364–1379. doi:10.1002/pan3.10513

Wu, Y., Zhou, Z., Zhao, X., Dan, Y., and Huang, D. (2020). Spatiotemporal variation of vegetation coverage in plateau mountainous areas based on remote sensing cloud computing platform: a case study of guizhou province. *CARSOLOGICA Sin.* 39 (2), 196–205. doi:10.11932/karst2020y16

Xie, G., Zhang, C., Zhang, L., Chen, W., and Li, S. (2015). Improvement of the evaluation method for ecosystem service value based on per unit area. *J. Nat. Resour.* 30 (8), 1243–1254. doi:10.11849/zrzyxb.2015.08.001

Xie, Y.-chu, Zhang, S.-xin, Lin, B., Zhao, Y.-jun, and Bao-qing, Hu (2020). Spatial zoning for land ecological consolidation in Guangxi based on the ecosystem services supply and demand. *J. Nat. Resour.* 35 (1), 217. doi:10.31497/zrzyxb.20200118

Xiong, K., Cheng, He, Mingsheng, Z., and Junbing, Pu (2023). A new advance on the improvement of forest ecosystem functions in the karst desertification control. *Forests* 14 (10), 2115. doi:10.3390/f14102115

Ye, Y., Lin, Y., Liu, S., and Luo, M. (2019). Social-ecological system (SES) analysis framework for application in ecological restoration engineering of mountains-rivers-forests-farmlands-lakes-grasslands: utilizing the source area of Qiantang River in Zhejiang Province as an example. *Acta Ecol. Sin.* 39 (23). doi:10.5846/stxb201905301139

Yue, W., Hou, Li, Xia, H., Wei, J., and Lu, Y. (2022). Territorially ecological restoration zoning and optimization strategy in guyuan city of ningxia, China: based on the balance of ecosystem service supply and demand. *Chin. J. Appl. Ecol.* 33 (1), 149–158. doi:10.13287/j.1001-9332.202112.024

Zhang, X., Qi, X., Yue, Y., Wang, K., Zhang, X., and Liu, D. (2020). Natural regionalization for rocky desertification treatment in karst peak-cluster depression regions. *Acta Ecol. Sin.* 40 (16), 5490–5501. doi:10.5846/stxb201910092093

Zhang, X., Wang, Z., Liu, Y., Shi, J., and Du, H. (2023). Ecological security assessment and territory spatial restoration and management of inland river basin—based on the perspective of production–living–ecological space. *Land* 12 (8), 1612. doi:10.3390/land12081612

Zhao, Xu, Tang, F., Zhang, P., Hu, B., and Xu, L. (2019). Dynamic simulation and characteristic analysis of county production-living-ecological spatial conflicts based on CLUE-S model. *Acta Ecol. Sin.* 39 (16). doi:10.5846/stxb201901070059

Zhao, Y., Luo, J., Li, T., Chen, J., Yi, Mi, and Wang, K. (2023). A framework to identify priority areas for restoration: integrating human demand and ecosystem services in dongting lake eco-economic zone, China. *Land* 12 (5), 965. doi:10.3390/land12050965

Zhong, X., Zhang, Su, Wu, R., Jing, Y., Men, L., and Zhou, T. (2022). Analysis of dynamic changes and driving forces of soil erosion in tuojiang river basin. *Res. Soil Water Conservation* 29 (2), 43–49+56. doi:10.13869/j.cnki.rswc.2022.02.003

Zhou, L., Zhang, H., Bi, G., Su, K., Wang, Li, Chen, H., et al. (2022). Multiscale perspective research on the evolution characteristics of the ecosystem services supply-demand relationship in the chongqing section of the three gorges reservoir area. *Ecol. Indic.* 142 (September), 109227. doi:10.1016/j.ecolind.2022.109227

Zhu, C., Zhou, Z., Wu, Y., Tan, W., Ma, G., and An, D. (2020). Spatial coupling between ecosystem services and economy based on grid in rocky desertification area. *Bull. Soil Water Conservation* 40 (3), 189–194+325. doi:10.13961/j.cnki.stbctb.2020.03.027

frontiers | Frontiers in Environmental Science

TYPE Original Research
PUBLISHED 20 March 2024
DOI 10.3389/fenvs.2024.1388854

OPEN ACCESS

EDITED BY
Xiao Ouyang,
Hunan University of Finance and Economics, China

REVIEWED BY
Kaijian Xu,
Hefei University of Technology, China
Cathy Wang,
Xi'an Jiaotong University, China

*CORRESPONDENCE
Chao Gao,
chgao@nju.edu.cn

RECEIVED 20 February 2024
ACCEPTED 08 March 2024
PUBLISHED 20 March 2024

CITATION
Wu J, Fan M, Zhang H, Shaukat M, Best JL, Li N and Gao C (2024), Decadal evolution of fluvial islands and its controlling factors along the lower Yangtze River.
Front. Environ. Sci. 12:1388854.
doi: 10.3389/fenvs.2024.1388854

Decadal evolution of fluvial islands and its controlling factors along the lower Yangtze River

Jingtao Wu[1], Manman Fan[1], Huan Zhang[2], Muhammad Shaukat[3], James L. Best[4], Na Li[5] and Chao Gao[6]*

[1]School of Geography and Planning, Huaiyin Normal University, Huaian, China, [2]School of Marine Science and Engineering, Nanjing Normal University, Nanjing, China, [3]Department of Agricultural Sciences, Allama Iqbal Open University, Islamabad, Pakistan, [4]Departments of Geology, Geography and GIS, Mechanical Science and Engineering and Ven Te Chow Hydrosystems Laboratory, University of Illinois at Urbana-Champaign, Urbana, IL, United States, [5]School of Environmental Science and Engineering, Yancheng Institute of Technology, Yancheng, China, [6]School of Geography and Ocean Science, Nanjing University, Nanjing, China

Fluvial islands are vital from both morphological and ecological perspectives and consequently have been hotspots of morphodynamic research in large rivers around the world. This study selected 14 representative fluvial islands in the lower reaches of the Yangtze River and explored their spatial-temporal evolution, including their shape and area dynamics during 1945–2016, by interpreting remote sensing images and analyzing the hydrological data. Results indicated that the total area of the 14 fluvial islands showed a growing trend at an average rate of 0.30 km^2 yr^{-1} during the 72 years. The island Fenghuangzhou experienced the largest change in area, while Xiaohuangzhou (XHZ) had the smallest change in area. Sediment discharge and flooding were assumed to be the primary natural factors controlling the island dynamics. Furthermore, dam construction and bank reinforcement also played a critical role in preventing shoreline collapse, improving channel conditions, and promoting the stability of fluvial islands. From 1976 to 2016, the maximum erosion occurred on the left XHZ, while the maximum accretion was found on the Qingjiezhou island. Almost the entire river section experienced an accretion process on the right bank, which was assumed to be caused by the construction of erosion control structures. Besides, the dynamics of the fluvial islands along the lower Yangtze River appears to follow the erosion processes of the river bank. Our findings can provide an important reference for sustainable utilization and management of fluvial islands.

KEYWORDS

fluvial island, decadal evolution, controlling factors, remote sensing, Yangtze River

1 Introduction

Fluvial islands are formed and shaped by both sediment deposition and erosion (Baubinienė et al., 2015). Although fluvial islands are generally unstable and transient over various periods, they provide significant ecological functions such as maintaining well-defined banks and persisting long enough to allow the establishment of persistent vegetation (Osterkamp, 1998; Gurnell and Petts, 2002; Wyrick and Klingeman, 2011; Carling et al., 2014). Thus, fluvial islands are generally considered as indicators of both hydrological and biotic capacities, as well as health, of fluvial systems (Knighton and

Nanson, 1993; Hooke and Yorke, 2011; Picco et al., 2014; Sun et al., 2018). Therefore, improving the understanding of the evolution of fluvial islands and their controls is a prerequisite to identifying strategies for sustainable utilization and management of fluvial islands, which is crucial for ensuring the long-term ecological health and resilience of fluvial islands.

Numerous researchers have studied the formation and sedimentary processes associated with transient fluvial islands (Zanoni et al., 2008; Wang and Xu, 2018; Zheng et al., 2019; Leli et al., 2020; Lou et al., 2022; do Amaral et al., 2023). Previous studies have examined various processes of fluvial islands, such as their migration and erosion, and found that these processes have an impact on banks, island bodies, and river channels (Promma et al., 2007; Wintenberger et al., 2015; Sudra et al., 2023). For example, Zanoni et al. (2008) examined the long-term evolution of island in a braided river and analyzed the effects of river flow regime and sediment delivery. Baubinienė et al. (2015) evaluated the changes of island number, area and location under the conditions of climate induced changes of river flow. Hoagland et al. (2024) modeled island evolution using the Lorenzo-Trueba and Mariotti model, which can simulate long-term changes in island system. Also, there are some studies that have been carried out on the channel evolution and maintenance and groundwater and surface water interactions of fluvial islands (Nelson and Sommers, 1983; McCabe et al., 2009; Roquero et al., 2015). The rationale for focusing on fluvial islands is that these islands are essential components of the riparian corridor, which strongly influences the geomorphic adjustment of rivers and floodplains (Singer and Aalto, 2009; Ollero et al., 2015; Bandyopadhyay et al., 2023). However, limited attention has been paid to the evolution of fluvial islands whose shape and size change appreciably with different fluvial processes, especially over decadal timescales.

The evolution of fluvial islands is affected by multiple natural factors of island development (Osterkamp, 1998; Gautier and Grivel, 2006) and anthropogenic factors such as engineering projects (Gao B. et al., 2013; Raška et al., 2017; Best, 2019). For example, Grove et al. (2013) found that floods exerted important influences on the morphological evolution of the fluvial system. Hudson et al. (2019) reported that sedimentary deposition directly prompted the formation of fluvial islands. Shi et al. (2018) showed that the key natural factor that influences island formation in the lower Yangtze River was sediment discharge. In addition, Gao C. et al. (2013) stated that there were no significant relationships between changes in the island area and natural factors, such as annual runoff and precipitation, and speculated that the construction of many large reservoirs could be the primary factor of change. The knowledge about the island dynamics and their driving factors allows the prediction of further fluvial process and the potential influence on the river regime. The present study is an attempt to contribute to the knowledge about fluvial islands based on a case study of the lower reaches in the Yangtze River.

This study reports on the island evolution in the Yangtze River, which is the third longest river in the world and the longest river in Asia, with its lower reaches being the most prosperous and populous area in China (Wu et al., 2020). Some fluvial islands are well-developed in the Anhui section of the lower Yangtze River and are vital for the stability of the Yangtze River. However, the sizes and shapes of these islands have changed rapidly due to rapid economic development since the launch of China's reform and opening-up policies (Bai and Li, 2009; Sun et al., 2018). In particular, the construction of Three Gorges Dam (TGD), which is currently the largest hydroelectric complex in the world (Lou et al., 2018), affects the hydrological regime and dozens of fluvial islands in the lower reaches of the Yangtze River (Li et al., 2011; Xu et al., 2013; Chen et al., 2022). Therefore, the present study selected 14 fluvial islands in the lower reach of the Yangtze River due to their substantial size, well-defined shapes, and relatively stable morphological changes. This study investigated the evolution of fluvial islands and aimed to: 1) quantitatively document the morphological evolution of fluvial islands and 2) explore the possible driving factors that affect the evolution of fluvial islands.

2 Materials and methods

2.1 Study area

The Anhui section of the Yangtze River (Figure 1) lies in the south-central region of Anhui Province, China (29°34′–31°53N and 115°52′–118°50E), which is within the transition zone between a temperate and subtropical monsoon climate. The study area is 416 km long along the lower Yangtze River, in which fluvial islands were identified. The study period covers four decades and is subdivided into five time periods: 1976, 1986, 1996, 2006, and 2016. During the past 40 years, great changes have taken place in the lower Yangtze River, as it has adjusted to a variety of human impacts, especially the reduction of sediment discharge and channel engineering caused by dams, revetments, and meander bend cutoffs (Zhang et al., 2008; Luo et al., 2012; Liu et al., 2013; Chen et al., 2014; Yang et al., 2018).

The shape of islands has been divided previously into several categories: straight, micro-bend, and goose head branches (Chinese Academy of Sciences, 1985). The general characteristics and names of the 14 islands in the Anhui region (Figure 1) selected for the study are summarized in Table 1.

2.2 Data acquisition

2.2.1 Aerial photographs and Landsat data

Multi-decadal Landsat data and scanned copies of aerial photographs were used to investigate the spatial-temporal evolution of these 14 fluvial islands. Aerial photographs taken in 1945 at a scale of 1:250,000, were obtained from the U.S. Army Map Service, Series L500 (https://www.utexas.edu/). Landsat MSS (Multispectral Scanner), Landsat TM (Thematic Mapper), and ETM+ (Enhanced Thematic Mapper) data from December 1976, 1986, 1996, 2006, and 2016, were acquired at 10-year intervals (Table 2), with cloud-free images being selected to enhance the clarity and richness of the image information. Furthermore, to minimize the effect of the water stage on interpreting the change in the size and shape of the fluvial islands, all Landsat images used were captured during the dry season of November and December

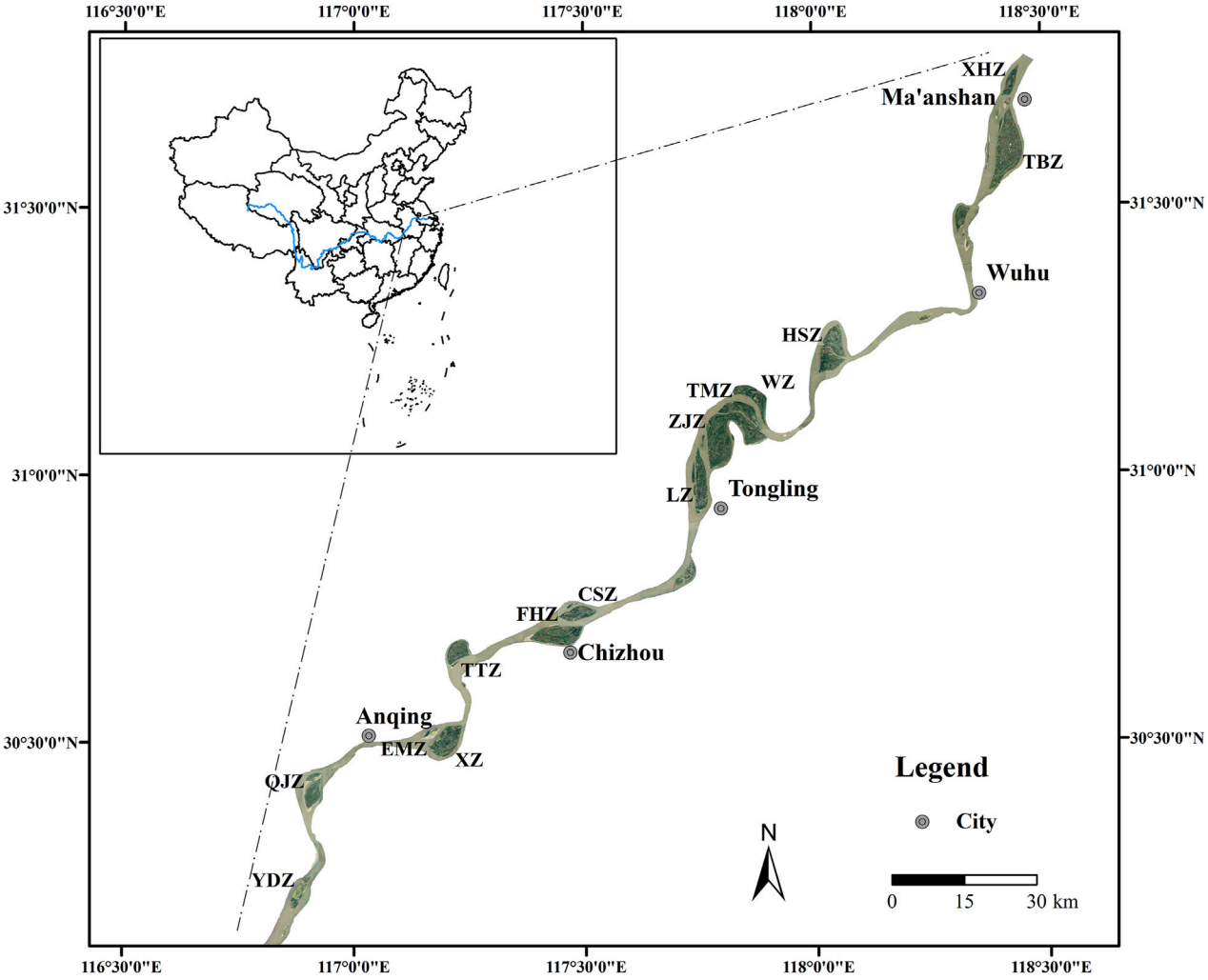

FIGURE 1
The Location of the study area and map of the fluvial islands in the study area, as derived from Landsat7/ETM+, acquired in December 2016.

when the discharge was considered constant within the channel in the study area. The Landsat dataset was acquired from the Geospatial Data Cloud (http://www.gscloud.cn).

2.2.2 Hydrological data

The annual runoff and sediment discharge data from 1950 to 2016 for the Datong hydrological station were obtained from the Changjiang Water Resources Committee (CWRC) (http://www.cjw.gov.cn/). Statistics indicate that from 1950 to 2016, the average annual runoff was 8,960 × 10^8 m^3, and from 1950 to 2016, the average annual sediment discharge, average annual sediment concentration, and average sediment delivery were 3.63 × 10^8 t, 0.414 kg m^{-3}, and 216 t km^{-2}, respectively. The maximum runoff of 13,590 × 10^8 m^3 and minimum runoff of 6,671 × 10^8 m^3 were recorded in 1954 and 2011, respectively. The highest sediment discharge was recorded at 6.78 × 10^8 t in 1964, while the lowest sediment discharge was measured at 0.72 × 10^8 t in 2011. In this study, the runoff and sediment discharge data at Datong Station from 1950 to 2016 were used to analyze the evolution of the islands and evaluate the uncertainties associated with changes in the area of the fluvial islands, as inferred from the interpretation of the remote sensing data.

2.3 Methods

2.3.1 Pre-processing of aerial and image photographs

Multiperiod Landsat data and scanned copies of aerial photographs were used to perform a spatial-temporal analysis of the fluvial islands over approximately a 72-year time series. Only permanent islands were selected in the study area (Figure 1). The aerial photographs were mosaiced and vectorized, and the bank lines were digitalized in ArcGIS 10.2 (ESRI Inc., United States).

To assess the variations in the land area of the fluvial island, a geometric correction process was applied to each satellite image. This involved transforming the images from the Universal Transverse Mercator (UTM) projection to the Albers Equal Area

TABLE 1 Summary of the typical fluvial islands in the Anhui section of the lower Yangtze River.

Island name	Area (km^2)	Approx. date of initial formation (year/AD)
Yudaizhou (YDZ)	12.5	–
Qingjiezhou (QJZ)	16	1851–1874
Emaozhou (EMZ)	2.8	–
Xinzhou (XZ)	40	618–907
Tietongzhou (TTZ)	18.5	~1400
Fenghuangzhou (FHZ)	28	960–1279
Changshengzhou (CSZ)	16	~1600
Laozhou (LZ)	26.5	1876–1911
Zhangjiazhou (ZJZ)	70	1600–1690
Tiemaozhou (TMZ)	18.8	~1966
Wuzhou (WZ)	17.3	–
Heishazhou (HSZ)	20	960–1279
Taibaizhou (TBZ)	59.5	~1368
Xiaohuangzhou (XHZ)	9.5	~1890

Note: "–" represents no data.

TABLE 2 Information about the Landsat images in the study.

Satellite/Sensor	Center latitude (°)	Center longitude (°)	Date	Resolution (m)
Landsat2/MSS	31.73	117.32	1976/12/17	80
Landsat2/MSS	30.25	118.33	1976/11/28	80
Landsat5/TM	30.3	116.89	1986/12/25	30
Landsat5/TM	31.72	117.33	1986/12/25	30
Landsat5/TM	31.75	118.83	1986/12/18	30
Landsat5/TM	30.31	116.85	1996/12/25	30
Landsat5/TM	31.73	117.37	1996/12/25	30
Landsat5/TM	31.73	118.92	1996/12/18	30
Landsat7/TM	30.31	116.83	2006/12/21	30
Landsat7/TM	31.76	117.21	2006/12/21	30
Landsat7/TM	31.77	118.75	2006/12/30	30
Landsat7/ETM+	30.3	116.89	2016/12/24	30
Landsat7/ETM+	31.74	117.28	2016/12/24	30
Landsat7/ETM+	31.74	118.82	2016/12/17	30

Conic projection, ensuring a uniform and accurate representation of the island's topography for comparative analysis. To correct the resolution discrepancies between TM and MSS images, we employed a combination of band synthesis, region of interest (ROI) subsets, and resampling tools in ArcGIS 10.2. Using the near-infrared bands available in both TM and ETM+, we can effectively differentiate between water bodies and vegetation cover. Additionally, to ensure accuracy, we refine the image correction process by selecting the ground control point (GCP) using ENVI 5.1 (ITT Visual Information Solutions Inc., United States).

2.3.2 Methodology for extracting the change of fluvial islands

Using a suite of remote sensing image processing techniques, the morphology and area of the selected fluvial islands were delineated for the period from 1945 to 2016. To elucidate the trends in area

change, the following equation was applied to compute anomalies for both individual island areas and the aggregate total area (see Eq. (1)).

$$\Delta A_{ij} = A_{ij} - \overline{A_j} \quad (1)$$

where the term j refers to a specific fluvial island, i denotes a particular year, ΔA_{ij} represents the area change of a specific fluvial island j in the year i, A_{ij} is the area of a specific fluvial island j in the year i, and $\overline{A_j}$ is the mean area of the fluvial island j over 72 years.

Historical aerial photographs and remote sensing imagery from the years 1945, 1976, 1986, 1996, and 2016 were utilized to delineate the boundaries of the fluvial islands in the lower Yangtze River. All images were scanned at a resolution of 600 dpi and geo-rectified using ArcGIS 10.2. During the image rectification process, each photograph was resampled at a resolution of 0.5 m to ensure consistency across all images. Rectification resulted in a root mean square error of <5 m for all images.

Individual image frames and mapping tables were mosaicked in ENVI to obtain georeferenced images that cover the entire study area. The image stitching process is influenced by two sources of errors: distortion errors between adjacent frames and inherent errors of the orthoimages. When GCPs are combined in areas that overlap between adjacent frames, distortion caused by topographical variations is minimized, thereby reducing these errors to a minimum.

2.3.3 Quantitative analysis of bank erosion and deposition

The shoreline of the Yangtze River in Anhui Province, which stretches a straight-line distance of 250 km, was systematically divided into segments with equal intervals of 1 km. Cross sections were defined as perpendicular to the trend surface along the river segment. For this length, a 1 km interval is considered sufficient to characterize the morphological changes of the river channel within the study area. The displacement of both banks for each segment was determined using the methodology proposed by Kummu et al. (2008). Using GIS overlay analysis, the banklines of two periods were compared to quantify the displacement of each segment. Subsequently, the intersection points of the terminal lines of each end-member with the riverbank lines were calculated and their coordinates were compared to determine the variations in the riverbank line locations.

3 Results

3.1 Spatial-temporal variations of fluvial islands

3.1.1 Changes in the shape of fluvial islands

Remote sensing imagery and aerial photographs were used to extract the morphological characteristics of typical fluvial islands from different periods (Figure 2). As illustrated in Figure 2, the overall morphology of the fluvial islands appears relatively stable in the past 72 years. However, due to fluvial erosion and sediment deposition, some islands exhibit significant local changes. Specifically, HSZ and WZ have undergone erosion, while TMZ, FHZ, and YDZ have experienced significant sediment deposition. In the northern HSZ island, a diminutive island emerged around 1945. This island underwent a modest decrease in its expanse by approximately 1996 and ultimately integrated with the principal island by the year 2006. Concurrently, since 1966, a new island has been gradually accumulating at the northern edge of ZJZ, maturing into the more stable TMZ. Furthermore, WZ Island has been observed to exhibit convergence with the riverbank, while LZ and ZJZ have become morphologically stable.

3.1.2 Changes in the area of fluvial islands

The total area of the 14 selected fluvial islands experienced an expansion, growing from 373.3 km^2 in 1945 to 394.9 km^2 in 2016 (Figure 3A). Prior to 1986, the aggregate area of the islands witnessed a steady rise, with an average annual expansion of 0.32 km^2 yr^{-1}. In contrast, the period between 1986 and 1996 saw a swift decline in the total area, with an erosion rate of 1.5 km^2 yr^{-1}. Subsequently, post-1996, the total area resumed an upward trend at an average annual rate of 0.73 km^2 yr^{-1}.

During the last 72 years, the average areas of individual islands can be ranked as follows: ZJZ > TBZ > HSZ > LZ > XZ > FHZ > WZ > CSZ > TTZ > TMZ > QJZ > XHZ > YDZ > EMZ (Figures 3B, C) with the areas of the 14 islands varying significantly before the 2000s and then remaining relatively stable after that. Specifically, the island ZJZ is the main island of Tongling City and the largest of the 14 islands, with an average area of 69.1 km^2 and erosion that occurred during 1945–2016 (Figure 3B). The EMZ has the smallest area, with an average annual area of 3.5 km^2 (Figure 3C). TBZ and XHZ were also observed to show similar tendencies, with an increase from 1945 (42.6 km^2 and 8.8 km^2, respectively) to 1986 (61.9 km^2 and 10.9 km^2, respectively) and then a substantial decrease from 1986 to 2006, followed by a slight growth of 0.2 km^2 and 0.51 km^2 from 2006 to 2016.

3.2 Trends in the evolution of fluvial islands

In order to explore the dynamics of the fluvial islands, the trends in the total area of the islands and the area of individual island were calculated. The data presented in Figure 4 indicate that the total area of the fluvial islands increased more rapidly between 1945 and 1986 and then slowed from 1986 to 2016. The total area of the fluvial islands demonstrated a general trend of expansion, with an annual average area of 386.3 km^2 during the 72-year period, and with a steady average annual growth of 0.3 km^2 yr^{-1}.

The annual average area change during the 72-year period was shown in Figures 5A, B. Most fluvial islands increased in area during 1945–2016, except for EMZ, HSZ, WZ, and ZJZ. The rate of increase in the island area varied significantly during the different periods. The FHZ, TMZ, and QJZ islands kept increasing in area from 1945 to 2016, with average growth rates of 0.29 km^2 yr^{-1}, 0.26 km^2 yr^{-1}, and 0.13 km^2 yr^{-1}, respectively. The island FHZ stand out as the fastest-growing, whereas ZJZ faced the most significant area reduction with an annual loss of 0.20 km^2 yr^{-1}. The area of XZ island initially expanded from 1945 to 1996, and then declined from 1996 to 2016. The island XHZ had the slightest area change with a minuscule decrease at a rate of 0.007 km^2 yr^{-1}. The island with a

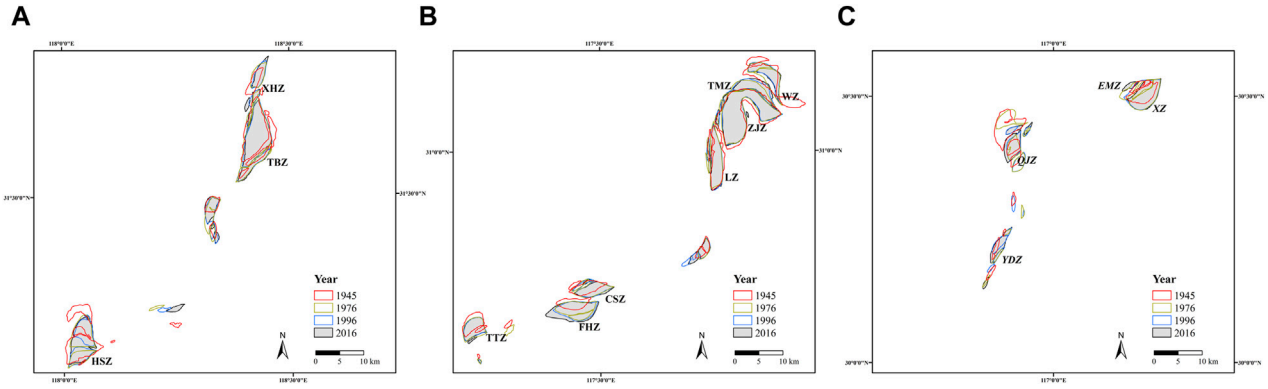

FIGURE 2
Area changes of the 14 fluvial islands in 1945, 1976, 1996, and 2016. The changes of islands HSZ, TBZ and XHZ were shown in **(A)**, TTZ, FHZ, CSZ, LZ, ZJZ, TMZ, and WZ in **(B)** and YDZ, QJZ, XZ, and EMZ in **(C)**.

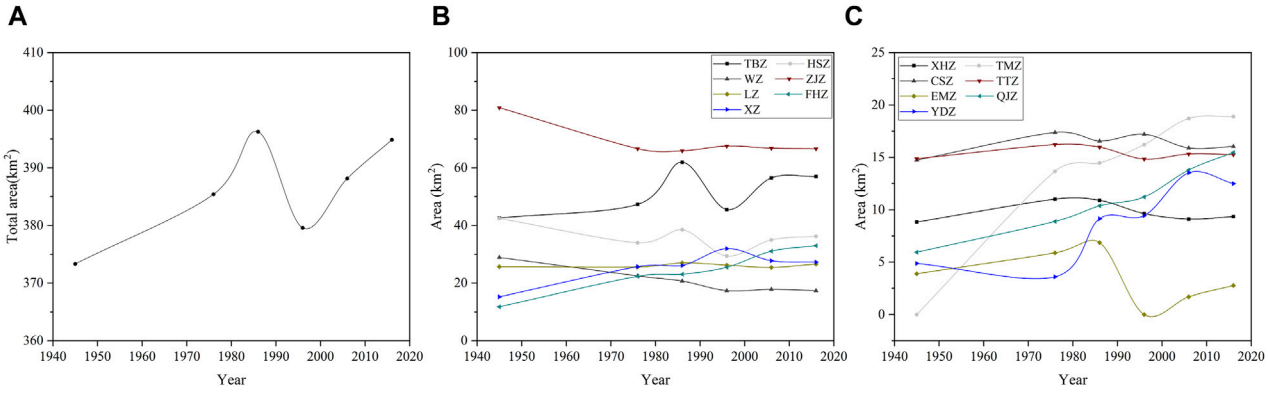

FIGURE 3
Changes in total area of the fluvial islands (km^2) **(A)**, and change in area of the individual island during 1945–2016 **(B, C)**.

change in area change tending toward zero suggested a trend toward stability. The areas of islands WZ and ZJZ demonstrated a descending trend, which decreased faster from 1945 to 1996, but then increased at a relatively slower speed from 1996 to 2016.

3.3 Spatial pattern of bank erosion and deposition

Both the left and right banks of the lower Yangtze River experienced erosion and deposition during 1976–2016 (Figure 6). Specifically, the left bank of the lower Yangtze River has exhibited more accretion rather than erosion during the last 40 years. During this period, the maximum accretion occurred on the island QJZ and maximum erosion on the left bank of island XHZ. On the right bank, almost the full reach exhibited accretion.

Figure 7 demonstrates a considerable movement of the bank lines resulting from accretion, indicating the movement of the banks in the river and the erosion, which depicts the movement of the banks in the land during 1976–2016. The bank line of 1976 is taken as reference, and the bank movement distances were calculated from the difference between the bank line of 1976 and the bank line of 2016 in ArcGIS. From the bank movement analysis during 1976–2016, the estimated maximum movement distances of erosion and deposition were approximately 3,500 m and 1,000 m, respectively, on the left bank, while the corresponding distances for the right bank were approximately 2,000 m and 800 m, respectively. Furthermore, the fluvial islands with an area larger than 20 km^2, such as the islands ZJZ, HSZ and LZ (Figure 7), were generally stable, and the island change rates were close to 0 over time. However, the islands with an area of less than 20 km^2, such as the islands YDZ and QJZ, were unstable during 1976–2016, with an area change rate of more than 0.15 km^2 yr^{-1}.

4 Discussion

4.1 Decadal evolution of fluvial islands

By comparing Landsat MSS, TM, and ETM + images from 1945 to 2016, changes in the shapes of islands in the lower Yangtze River were clearly visible. The spatial pattern of the morphologic changes varied between the different islands due to differences in their erosion and deposition processes. Overall, the total areas of

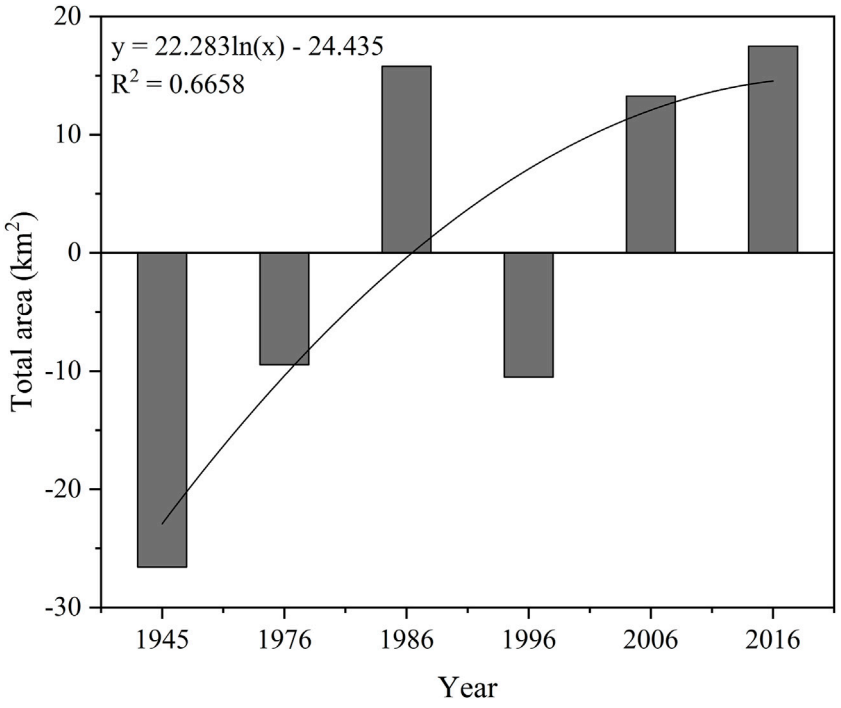

FIGURE 4
Trend in total area changes of the fluvial islands in the Anhui section of the Yangtze River from 1945 to 2016.

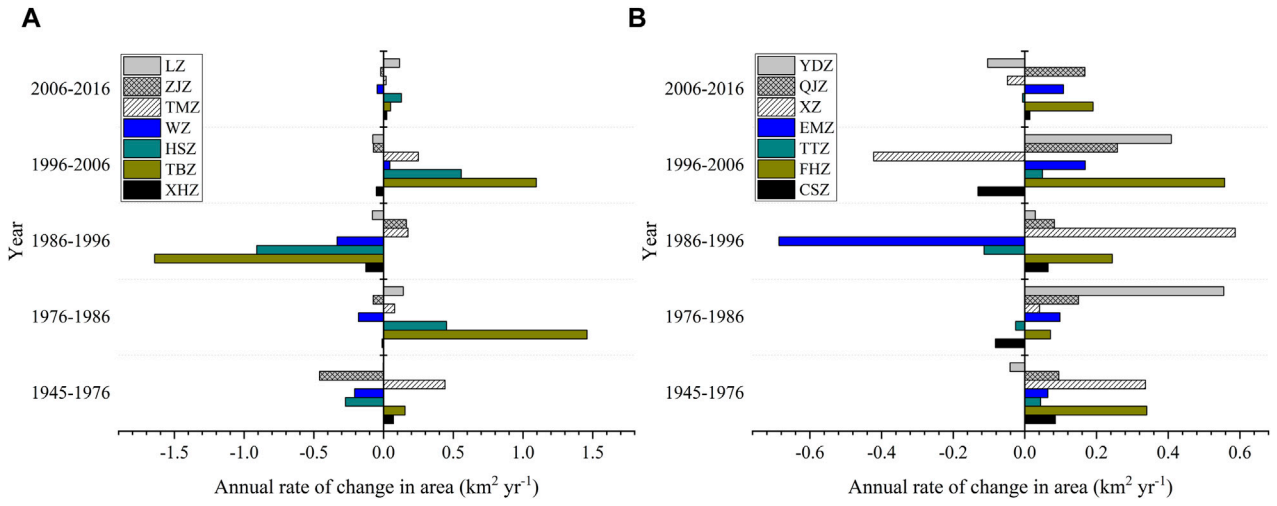

FIGURE 5
Annual area changes for islands LZ, ZJZ, TMZ, WZ, HSZ, TBZ and XHZ **(A)** and annual area changes for islands YDZ, QJZ, XZ, EMZ, TTZ, FHZ and CSZ **(B)**.

these fluvial islands increased from 1945 to 2016. Smaller islands, such as XHZ and YDZ, have undergone notable morphological transformations, characterized by erosion at the island's head and accretion at the tail, leading to a downstream extension of the island body. This conforms with the fact that the island head is typically subjected to erosion due to the impact of larger water flows, followed by a decrease in hydrodynamics as the water divides, resulting in sediment accumulation at the island's tail (Hooke and Yorke, 2011). Mapping from the four images also indicated that the positions of the fluvial islands had shifted slightly during that development, with a general pattern of erosion on the left margin and sedimentation on the right. Previous studies have speculated that the changes on the left margin of fluvial islands are due to waves generated by vessels that navigate the left channel, which intensify erosion. On the contrary, the right margin has shown a more stable development with a higher degree of soil maturation (Zheng et al., 2018).

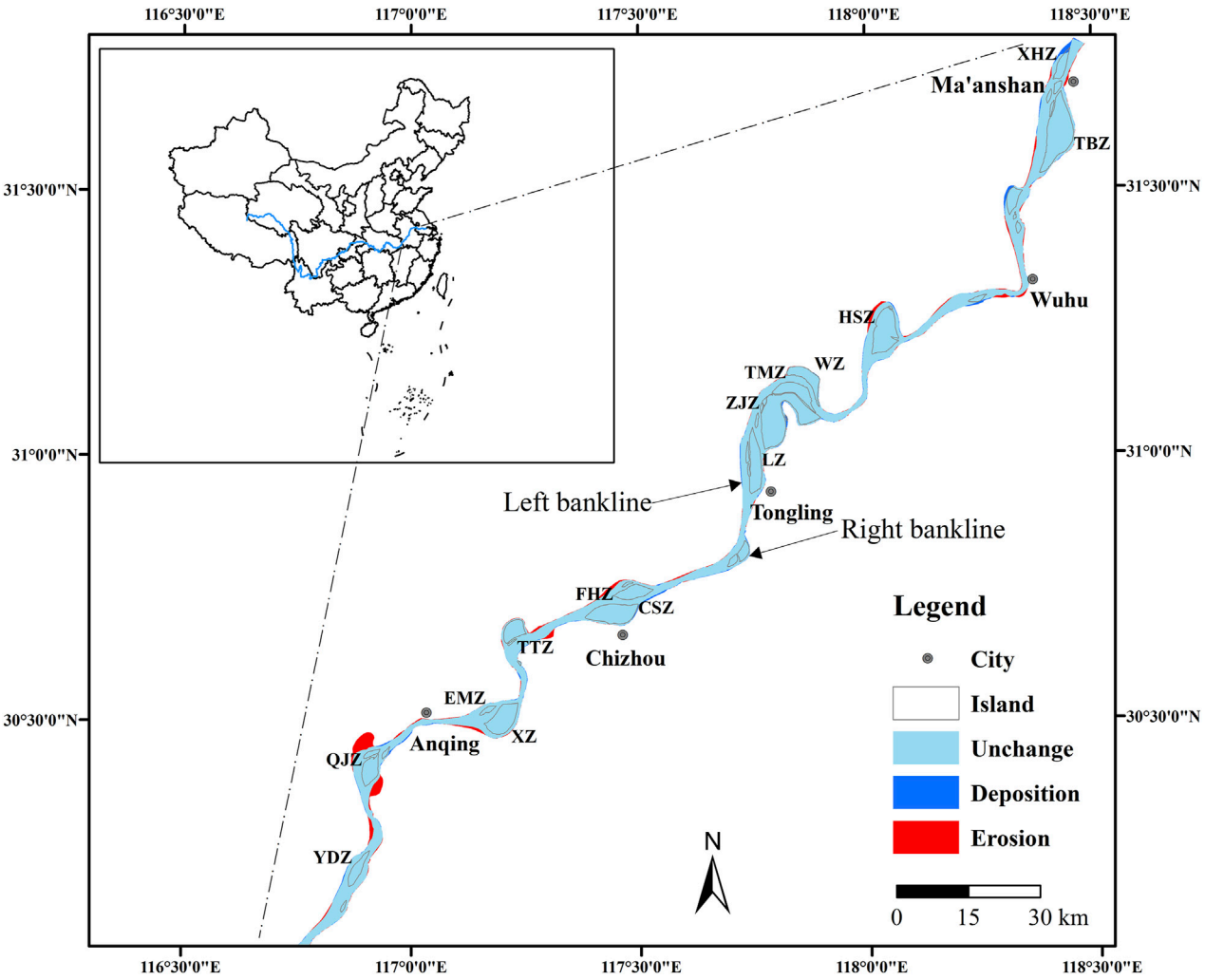

FIGURE 6
Spatial patterns of bank erosion and deposition along the lower Yangtze River between 1976 and 2016.

The larger fluvial islands, such as ZJZ and TBZ, which covered the largest area among all the fluvial islands, showed slight changes in their shapes during the past 72 years. The island ZJZ, located near the central area of Tongling City, stretches approximately 11.8 km in length and reaches a maximum width of 2.7 km (Figure 1). In this section of the Yangtze River, a relatively straight braided channel has formed, with the left channel serving as the main channel, contributing up to 95% of the water and 96% of the sediment to the main channel. The flow velocities along the course of TBZ and ZJZ are nearly identical, averaging about 46,000 $m^3 s^{-1}$ (Gao, 2012). The island TBZ, located to the south of Maanshan City in the middle part of the lower Yangtze River, runs southwest to northeast. The island TBZ has a length of 17.6 km and a maximum width of 5.6 km (Figure 1), which was formed by sediment erosion and deposition with its current contour having taken form during the Song Dynasty (Shi et al., 2017). The Yangtze River exhibits a straight two-channel anabranching form. Since 1860, the river has been bifurcated by TBZ into a left and right channel, with the left channel being the main one. This channel contributes a significant proportion of the water and sediment to the main channel, with the water and sediment contributions reaching up to 89% and 92%, respectively (Liu et al., 2016).

4.2 Factors controlling the dynamics of fluvial islands

4.2.1 Natural factors

As presented in Figure 8, the annual runoff at Datong Station did not show an obvious trend, except that the annual runoff for the years 1954 and 1998 was much higher than that in other years. However, the annual sediment discharge experienced a notable decline post-1986 (Figure 8), which had a significant impact on the sedimentary input and the total area of fluvial islands (Figure 3A), thereby affecting the formation and stability of the fluvial islands. This trend suggests that there was an insufficient sediment supply to support the expansion of the islands. Previous studies have found that natural factors such as runoff and sediment discharge play an important role in the evolution of fluvial islands or deltas in large rivers (Baki and Gan, 2012; Ve et al., 2021; Quang

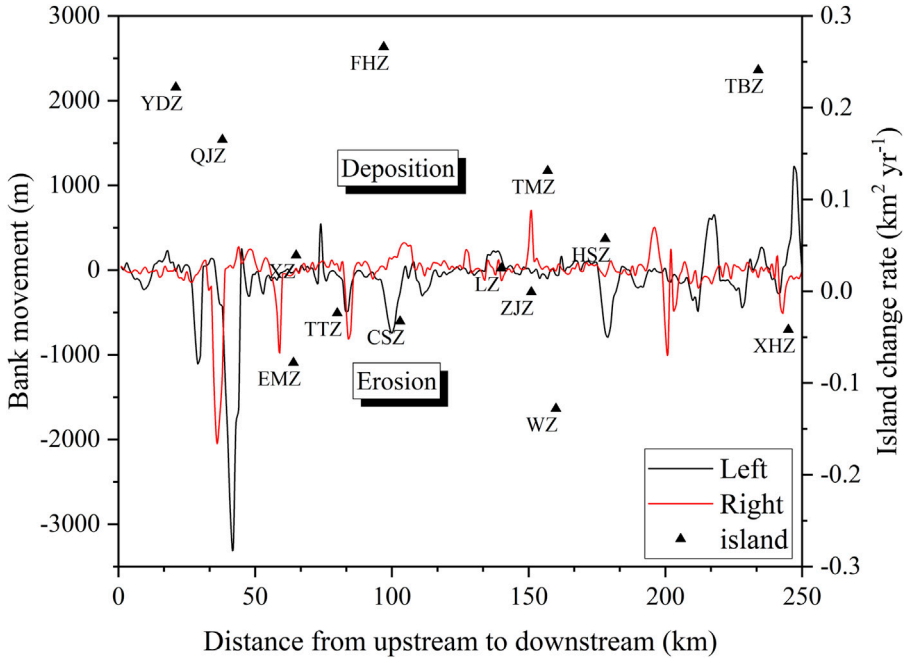

FIGURE 7
Bank movement along the lower Yangtze River for both the left and the right banks, and the island change rate between 1976 and 2016.

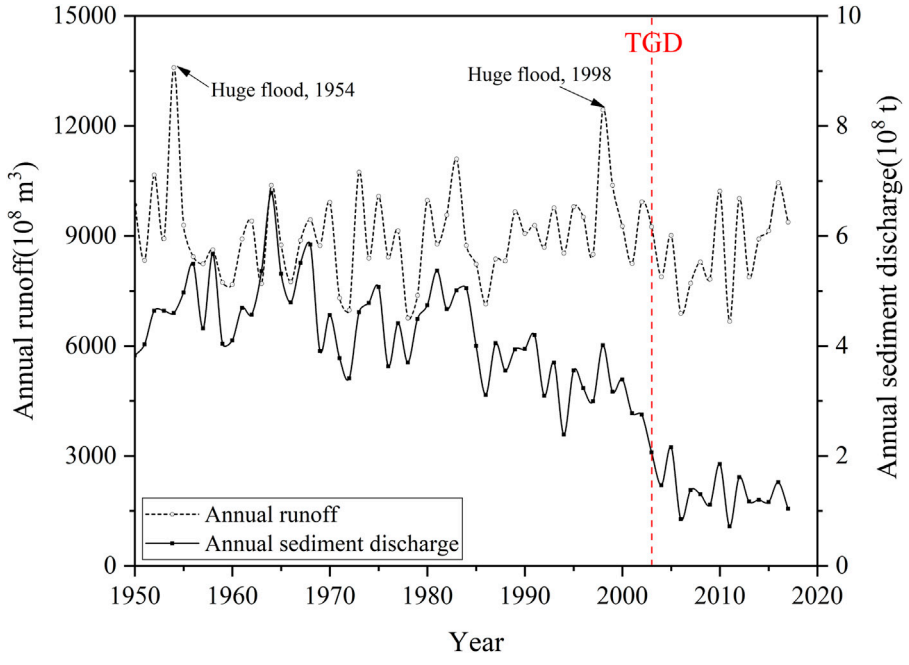

FIGURE 8
Annual runoff and sediment discharge of Datong hydrological station from 1950 to 2016.

et al., 2023). The annual migration rate of high sediment concentration rivers is higher than that of low sediment concentration rivers, due to the rapid growth and migration of the bars that force bank erosion (Constantine et al., 2014). The average annual sediment discharge was 3.63×10^8 t and decreased drastically after the construction of the TGD. The area of the 14 islands tended to decrease with the decrease in sediment content, while increasing the sediment content. This coincides with the findings of Li et al. (2019), and similar phenomena have been observed in the channel bars in the middle Yangtze River. River

sediment discharge is usually considered one of the major factors controlling island dynamics (Moretto et al., 2014). In this study, it is inferred that sediment discharge is the primary factor responsible for the observed reduction in the area of the fluvial islands.

Flooding is also considered a significant factor that causes morphological changes in fluvial islands (Asaeda and Rashid, 2012). Within the time span from 1945 to 2016, there were two historic crests. The data presented in Figure 8 also show that annual runoff and sediment discharge reached a relatively high level, while the total area of the fluvial islands decreased to the lowest in 1954 and 1998. In 1954, a huge flood occurred with the water stage reaching 16.6 m and a maximum flow of 92,600 $m^3 s^{-1}$ at Datong Station. In 1998, another catastrophic flood occurred with a maximum flow of 81,000 $m^3 s^{-1}$ (CWRC). The flood in 1998 reduced the total area to its lowest area after 1950. Bertoldi et al. (2009) also observed similar phenomena in their study of the Tagliamento River, a braided river where water flow and sediment transport are largely uncontrolled, with extreme floods being a major cause of erosion on fluvial islands. Annual runoff also influences the flow velocity along the fluvial islands, with the river segments of the study area exhibiting relatively stable flow velocities. It was observed that narrower stretches of the river exhibit higher velocities compared to wider ones and that velocities are higher upstream than downstream. Consequently, fluvial islands situated in regions with higher velocities, such as EMZ and HSZ, experienced more erosion (Moretto et al., 2012).

The evolution of fluvial islands is the result of long-term interactions between river boundaries and sediment transport (Shi et al., 2017). In this case, the evolution of fluvial islands in the lower reaches will be affected by riverbank erosion and deposition. The left bank shows more deposition than erosion, while almost all sections of the right bank show deposition. This may be due to the fact that a large number of shore protection projects effectively prevent shore erosion. The area with the largest erosion distance on both banks happens to be along with the merging of fluvial islands, and a similar island merging phenomenon also occurs in the Zhen-Yang reach of the Yangtze River (Yang, 2020). Fluvial islands with large morphological changes are found around the bank with evident displacement, suggesting that the evolution of fluvial islands in the Anhui section of the Yangtze River may be closely related to the erosion and deposition process on both banks of the Yangtze River. Comparing this study with the findings of Baki and Gan (2012) and Hudson et al. (2019), we suggest that the riverbank migration plays an important role in the island dynamics. Specifically, in this study area, the narrowing of the river channel will hinder the development of fluvial islands, while the widening of the river channel will promote the silting and growth of fluvial islands. Further investigations should be carried out to detail this point in the future.

The evolution of fluvial islands is also influenced by other natural factors, such as precipitation, vegetation cover, and vegetation types (Baubinienė et al., 2015). In the present study, the area changes of ZJZ and TBZ are relatively minor, and they are situated under similar hydro-sedimentary conditions. However, they have experienced different erosion and deposition processes, which is hypothesized to be due to the overflow of water from the lakes within the fluvial islands during the rainy season, leading to the loss of soil and shallow banks after the river scavenging. Furthermore, the higher the vegetation coverage and the richer the vegetation types, the less soil erosion on the island. Among them, trees are superior to shrubs and grasses, mixed forests are better than single-species forests, and the dense reeds along the outer edge of the island also serve as natural flood barriers. Short shrubs and trees that grow in the floodplain can also play a good role in stabilizing the embankment (Corenblit et al., 2015). In a study on channel bar morphodynamics in the middle Yangtze River, Wang et al. (2018) reported that the bars with high vegetation coverage tend to be stable during floods, while the bars with less vegetation are prone erosion. It can be seen that the vegetation can enhance the anti-erosion ability and thus promote the stability of fluvial islands.

4.2.2 Human factors

With the development of the social economy, anthropogenic influences play an increasingly significant role in the evolution of fluvial islands (Luan et al., 2018; Yang et al., 2018). Due to overexploitation and unreasonable land use, bank collapse often occurs. The evolution of the fluvial islands within the lower Yangtze River is also related to anthropogenic engineering and planning. The construction of the dams, the submerged banks, bank reinforcements, as well as guard works, have been significant factors in preventing shoreline collapse, improving the channel conditions, and stabilizing the branching pattern. These projects have weakened the scouring in the channel and protected the river channels and dikes along the two banks (Hudson et al., 2019).

In the lower reaches of the Yangtze River, the significant reduction in sediment discharge and external material input, which are necessary for the development of islands, is closely related to the construction of the TGD (Shi et al., 2017). As reported by Chen et al. (2016), the construction of over 50,000 reservoirs in the Yangtze River basin since the 1950s has had a minimal effect on the annual runoff, yet the seasonal fluctuations in dam storage could influence the monthly distribution of runoff. The completion of the TGD has been associated with a notable reduction in the annual volume of sediment transport, serving as a compelling indicator of the significant impact of human activities on sediment dynamics (Zhao et al., 2017). Typically, the increasing runoff correlates with the increasing scouring, leading to a decrease in the area of fluvial islands due to erosion. However, since 2006, the total area of these islands has paradoxically expanded along with the annual runoff (Figures 3, 8). This trend could be attributed to the government's initiatives to reinforce the embankment system along the Anhui section of the Yangtze River, which has mitigated island erosion and facilitated ongoing sediment deposition.

Previous studies have revealed that ongoing enhancement of embankment systems has been instrumental in mitigating erosion and submersion of fluvial islands by river waters, fostering their stable development and progressive accretion, which in turn has led to a gradual expansion of their surface areas (Hudson et al., 2019). Following the completion of the TGD, both the individual and cumulative areas of the fluvial islands exhibited a slow growth. This indicates that the significant decrease in sediment supply from upstream, has hindered the expansion of these islands due to the construction of the TGD (Li et al., 2016). Additionally, the dam has exacerbated the scouring effects during periods of high water,

further eroding the islands and impeding their sedimentation and expansion. This process has also been observed to induce changes in the morphology of the fluvial islands (Luan et al., 2018).

Human activities such as sand mining, reforestation, and water regulation projects have a profound impact on the development of fluvial islands (Gurnell et al., 2005). Since the end of the last century, the evolution of these islands in the Lower Yangtze River has been notably influenced by human interventions. Practices such as riverbed dredging have incised the riverbed, leading to deeper and narrower channels, which in turn affect the morphological development of the fluvial islands (Lou et al., 2018). Previous studies have demonstrated that the fluctuation in the area of the fluvial islands of Yangtze River is a direct result of changes in the hydrological and sedimentary regimes. Sand and gravel extraction can fragment the riverbed, fostering vegetation growth and accelerating the amalgamation of fluvial islands (Moretto et al., 2012). Afforestation efforts on these islands, coupled with increased vegetation cover, have a stabilizing effect on the riverbanks and the islands, thus influencing the dynamics of sediment transport. This intervention limits erosion and channel migration, leading to channel incision and enhanced stability of the fluvial islands. These anthropogenic influences indirectly modify the distribution of water flow and can even alter the main distributaries, thereby affecting the conditions of exogenous material for the formation of fluvial islands.

Furthermore, the formation and evolution of fluvial islands not only influence their morphology, area, and direction of their development, but also profoundly influence their geochemical characteristics and regional variations. The age of island formation is correlated with the degree of soil development and the extent of soil utilization, which, in turn, markedly affects the accumulation and migration patterns of the physicochemical properties and elements of the soil (including the major and trace elements). This inevitably impacts their geochemical characteristics and regional differences. In contrast, variations in land use and soil properties also indirectly reflect the surface processes within the watershed, to some extent affecting the stability of the morphology of the fluvial islands. The interplay between these factors and their implications for the morphology and geochemistry of fluvial islands remains an area that is ready for further investigation.

5 Conclusion

This study analyzed the spatiotemporal evolution of fluvial islands and their influencing factors during 1945–2016 in the lower Yangtze River, based on historical aerial photographs and Landsat MSS, TM, and ETM + data. During the past 72 years, the total area of the 14 fluvial islands showed a general increase at an average rate of 0.30 km^2 yr^{-1}. The island FHZ experienced the largest change in area, while XHZ had the smallest change in area. Sediment discharge and flooding were assumed to be the most significant natural factors controlling island dynamics. Additionally, the construction of dams and bank reinforcement also played a critical role in preventing shoreline collapse, improving channel conditions, and promoting the stability of the fluvial islands. From 1976 to 2016, the maximum accretion occurred on the island QJZ and the maximum erosion occurred on the left bank of island XHZ. On the right bank, almost the full reach exhibited accretion, which could be due to the erosion control structures that were built. The dynamics of the fluvial islands along the lower Yangtze River seems to follow the river bank erosion processes. The results of this study can provide an important reference for decision-making of sustainable island utilization and management. Further work is still necessary to quantify the relationship between island evolution and riverbank movement.

Data availability statement

The original contributions presented in the study are included in the article/Supplementary material, further inquiries can be directed to the corresponding author.

Author contributions

JW: Conceptualization, Data curation, Formal Analysis, Funding acquisition, Writing–original draft. MF: Formal Analysis, Funding acquisition, Writing–original draft. HZ: Writing–review and editing. MS: Writing–review and editing. JB: Conceptualization, Methodology, Writing–review and editing. NL: Writing–review and editing. CG: Conceptualization, Funding acquisition, Methodology, Supervision, Writing–review and editing.

Funding

The author(s) declare that financial support was received for the research, authorship, and/or publication of this article. This research was supported by the National Natural Science Foundation of China (Grant No: 41877002 and 42101062) and the Natural Science Foundation of the Jiangsu Higher Education Institutions of China (Grant No: 22KJB170008).

Conflict of interest

The authors declare that the research was conducted in the absence of any commercial or financial relationships that could be construed as a potential conflict of interest.

Publisher's note

References

Asaeda, T., and Rashid, M. H. (2012). The impacts of sediment released from dams on downstream sediment bar vegetation. *J. Hydrol.* 430, 25–38. doi:10.1016/j.jhydrol.2012.01.040

Baki, A. B. M., and Gan, T. Y. (2012). Riverbank migration and island dynamics of the braided Jamuna River of the Ganges-Brahmaputra basin using multi-temporal Landsat images. *Quatern. Int.* 263, 148–161. doi:10.1016/j.quaint.2012.03.016

Bandyopadhyay, S., Kar, N. S., Dasgupta, S., Mukherjee, D., and Das, A. (2023). Island area changes in the sundarban region of the abandoned western ganga–brahmaputra–meghna delta, India and Bangladesh. *Geomorphology* 422, 108482. doi:10.1016/j.geomorph.2022.108482

Baubinienė, A., Satkunas, J., and Taminskas, J. (2015). Formation of fluvial islands and its determining factors, case study of the River Neris, the Baltic Sea basin. *Geomorphology* 231, 343–352. doi:10.1016/j.geomorph.2014.12.025

Bertoldi, W., Gurnell, A. M., Surian, N., Tockner, K., Ziliani, L., Zolezzi, G., et al. (2009). Understanding reference processes: linkages between river flows, sediment dynamics and vegetated landforms along the Tagliamento River, Italy. *Italy. River Res. Appl.* 25, 501–516. doi:10.1002/rra.1233

Best, J. (2019). Anthropogenic stresses on the world's big rivers. *Nat. Geosci.* 12, 7–21. doi:10.1038/s41561-018-0262-x

Carling, P., Jansen, J., and Meshkova, L. (2014). Multichannel rivers: their definition and classification. *Earth Surf. Proc. Land.* 39 (1), 26–37. doi:10.1002/esp.3419

Chen, J., Finlayson, B. L., Wei, T., Sun, Q., Webber, M., Li, M., et al. (2016). Changes in monthly flows in the Yangtze River, China-with special reference to the three Gorges dam. *J. Hydrol.* 536, 293–301. doi:10.1016/j.jhydrol.2016.03.008

Chen, J., Wu, X., Finlayson, B. L., Webber, M., Wei, T., Li, M., et al. (2014). Variability and trend in the hydrology of the Yangtze River, China: annual precipitation and runoff. *J. Hydrol.* 513, 403–412. doi:10.1016/j.jhydrol.2014.03.044

Chen, Z., Xu, K., and Watanabe, M. (2022). "Dynamic hydrology and geomorphology of the Yangtze River," in *Large rivers: geomorphology manage*. Second Edition (Wiley), 687–703. doi:10.1002/9781119412632.ch23

Chinese Academy of Sciences (1985). *Chinese natural geography" committee. General introduction to Chinese natural geography*. Beijing, China: Chinese Academy of Sciences Press. (in Chinese).

Constantine, J. A., Dunne, T., Ahmed, J., Legleiter, C., and Lazarus, E. D. (2014). Sediment supply as a driver of river meandering and floodplain evolution in the Amazon Basin. *Nat. Geosci.* 7, 899–903. doi:10.1038/ngeo2282

Corenblit, D., Davies, N. S., Steiger, J., Gibling, M. R., and Bornette, G. (2015). Considering river structure and stability in the light of evolution: feedbacks between riparian vegetation and hydrogeomorphology. *Earth Surf. Proc. Land.* 40 (2), 189–207. doi:10.1002/esp.3643

do Amaral, D. D., de Fátima Rossetti, D., Gurgel, E. S. C., and Pereira, J. L. G. (2023). Phytophysiognomy in the east of the Marajó island (mouth of the Amazon River) from the perspective of geological history in the Late Quaternary. *Catena* 220, 106711. doi:10.1016/j.catena.2022.106711

Gao, B., Yang, D., and Yang, H. (2013a). Impact of the three Gorges dam on flow regime in the middle and lower Yangtze River. *Quatern. Int.* 304, 43–50. doi:10.1016/j.quaint.2012.11.023

Gao, C. (2012). Study on channel islands in Ma-Wu-tong section of Yangtze River based on MSS/TM/ETM remote sensing image. *Remote Sens. Technol. Appl.* 27 (1), 135–141. doi:10.11873/j.issn.1004-0323.2012.1.135

Gao, C., Chen, S., and Yu, J. (2013b). River islands' change and impacting factors in the lower reaches of the Yangtze River based on remote sensing. *Quatern. Int.* 304, 13–21. doi:10.1016/j.quaint.2013.03.001

Gautier, E., and Grivel, S. (2006). "Multi-scale analysis of island formation and development in the Middle Loire River, France," in Proceedings of symposium (Dundee, United Kingdom: Sediment dynamics and the hydromorphology of fluvial systems), 179–187. AIAHS Pub. 306.

Grove, J. R., Croke, J. C., and Thompson, C. J. (2013). Quantifying different riverbank erosion processes during an extreme flood event. *Earth Surf. Proc. Land.* 38 (12), 1393–1406. doi:10.1002/esp.3386

Gurnell, A., Tockner, K., Edwards, P., and Petts, G. (2005). Effects of deposited wood on biocomplexity of river corridors. *Front. Ecol. Environ.* 3 (7), 377–382. doi:10.1890/1540-9295(2005)003[0377:EODWOB]2.0.CO;2

Gurnell, A. M., and Petts, G. E. (2002). Island-dominated landscapes of large floodplain rivers, a European perspective. *Freshw. Biol.* 47 (4), 581–600. doi:10.1046/j.1365-2427.2002.00923.x

Hoagland, S. W., Irish, J. L., and Weiss, R. (2024). Morphodynamic and modeling insights from global sensitivity analysis of a barrier island evolution model. *Geomorphology* 451, 109087. doi:10.1016/j.geomorph.2024.109087

Hooke, J. M., and Yorke, L. (2011). Channel bar dynamics on multi-decadal timescales in an active meandering river. *Earth Surf. Proc. Land.* 36 (14), 1910–1928. doi:10.1002/esp.2214

Hudson, P. F., van der Hout, E., and Verdaasdonk, M. (2019). (Re) Development of fluvial islands along the lower Mississippi River over five decades, 1965–2015. *Geomorphology* 331, 78–91. doi:10.1016/j.geomorph.2018.11.005

Knighton, A. D., and Nanson, G. C. (1993). Anastomosis and the continuum of channel pattern. *Earth Surf. Proc. Land.* 18 (7), 613–625. doi:10.1002/esp.3290180705

Kummu, M., Lu, X. X., Rasphone, A., Sarkkula, J., and Koponen, J. (2008). Riverbank changes along the Mekong River: remote sensing detection in the Vientiane-Nong Khai area. *Quatern. Int.* 186 (1), 100–112. doi:10.1016/j.quaint.2007.10.015

Leli, I. T., Stevaux, J. C., and Assine, M. L. (2020). Origin, evolution, and sedimentary records of islands in large anabranching tropical rivers: the case of the Upper Paraná River, Brazil. *Geomorphology* 358, 107118. doi:10.1016/j.geomorph.2020.107118

Li, D. F., Lu, X. X., Chen, L., and Wasson, R. J. (2019). Downstream geomorphic impact of the three Gorges dam: with special reference to the channel bars in the middle Yangtze River. *Earth Sur. Process. Landforms* 44 (13), 2660–2670. doi:10.1002/esp.4691

Li, Q., Yu, M., Lu, G., Cai, T., Bai, X., and Xia, Z. (2011). Impacts of the gezhouba and three Gorges reservoirs on the sediment regime in the Yangtze River, China. *J. Hydrol.* 403 (3–4), 224–233. doi:10.1016/j.jhydrol.2011.03.043

Li, X., Liu, J. P., and Tian, B. (2016). Evolution of the Jiuduansha wetland and the impact of navigation works in the Yangtze Estuary, China. *Geomorphology* 253, 328–339. doi:10.1016/j.geomorph.2015.10.031

Liu, J., Zang, C., Tian, S., Liu, J., Yang, H., Jia, S., et al. (2013). Water conservancy projects in China: achievements, challenges and way forward. *Glob. Environ. Chang.* 23 (3), 633–643. doi:10.1016/j.gloenvcha.2013.02.002

Liu, X., Huang, H. Q., and Nanson, G. C. (2016). The morphometric variation of islands in the middle and lower Yangtze River: a variational analytical explanation. *Geomorphology* 261, 273–281. doi:10.1016/j.geomorph.2016.03.004

Lou, Y., Dai, Z., Lu, X., and Li, D. (2022). Anthropogenic pressures induced hydromorphodynamic changes of riverine islands in the upper Jingjiang reach along the Changjiang (Yangtze) river. *Catena* 217, 106488. doi:10.1016/j.catena.2022.106488

Lou, Y., Mei, X., Dai, Z., Wang, J., and Wei, W. (2018). Evolution of the mid-channel bars in the middle and lower reaches of the Changjiang (Yangtze) River from 1989 to 2014 based on the Landsat satellite images: impact of the Three Gorges Dam. *Environ. Earth Sci.* 77 (10), 394. doi:10.1007/s12665-018-7576-2

Luan, H. L., Ding, P. X., Wang, Z. B., Yang, S. L., and Lu, J. Y. (2018). Morphodynamic impacts of large-scale engineering projects in the Yangtze River delta. *Coast. Eng.* 141, 1–11. doi:10.1016/j.coastaleng.2018.08.013

Luo, X. X., Yang, S. L., and Zhang, J. (2012). The impact of the Three Gorges Dam on the downstream distribution and texture of sediments along the middle and lower Yangtze River (Changjiang) and its estuary, and subsequent sediment dispersal in the East China Sea. *Geomorphology* 179, 126–140. doi:10.1016/j.geomorph.2012.05.034

McCabe, R. M., MacCready, P., and Hickey, B. M. (2009). Ebb-tide dynamics and spreading of a large river plume. *J. Phys. Oceanogr.* 39 (11), 2839–2856. doi:10.1175/2009JPO4061.1

Moretto, J., Rigon, E., Mao, L., Picco, L., Delai, F., and Lenzi, M. A. (2012). Medium- and short-term channel and island evolution in a disturbed gravel bed river (Brenta River, Italy). *J. Agr. Eng.* 43 (4), 27–7. doi:10.4081/jae.2012.e27

Moretto, J., Rigon, E. L. L. F., Mao, L., Picco, L., Delai, F., and Lenzi, M. A. (2014). Channel adjustments and island dynamics in the Brenta River (Italy) over the last 30 years. *River Res. Appl.* 30 (6), 719–732. doi:10.1002/rra.2676

Nelson, D. W., and Sommers, L. E. (1983). Total carbon, organic carbon, and organic matter. *Methods soil analysis* 9, 539–579. doi:10.2134/agronmonogr9.2.2ed.c29

Ollero, A., Ibisate, A., Granado, D., and Asua, R. R. D. (2015). "Channel responses to global change and local impacts: perspectives and tools for floodplain management, Ebro river and Tributaries, NE Spain," in *Geomorphic approaches to integrated floodplain management of lowland fluvial systems in North America and Europe* (New York, NY: Springer), 27–52. doi:10.1007/978-1-4939-2380-9_3

Osterkamp, W. R. (1998). Processes of fluvial island formation, with examples from plum creek, Colorado and snake river, Idaho. *Wetlands* 18 (4), 530–545. doi:10.1007/BF03161670

Picco, L., Mao, L., Rainato, R., and Lenzi, M. A. (2014). Medium-term fluvial island evolution in a disturbed gravel-bed river (Piave River, Northeastern Italian Alps). *Geogr. Ann. A* 96 (1), 83–97. doi:10.1111/geoa.12034

Promma, K., Zheng, C., and Asnachinda, P. (2007). Groundwater and surface-water interactions in a confined alluvial aquifer between two rivers: effects of groundwater flow dynamics on high iron anomaly. *Hydrogeol. J.* 15 (3), 495–513. doi:10.1007/s10040-006-0110-8

Quang, N. H., Thang, H. N., An, N. V., and Luan, N. T. (2023). Delta lobe development in response to changing fluvial sediment supply by the second largest river in Vietnam. *Catena* 231, 107314. doi:10.1016/j.catena.2023.107314

Raška, P., Dolejš, M., and Hofmanová, M. (2017). Effects of damming on long-term development of fluvial islands, Elbe River (N Czechia). *River Res. Appl.* 33 (4), 471–482. doi:10.1002/rra.3104

Roquero, E., Silva, P. G., Goy, J. L., Zazo, C., and Massana, J. (2015). Soil evolution indices in fluvial terrace chronosequences from central Spain (Tagus and Duero fluvial basins). *Quatern. Int.* 376, 101–113. doi:10.1016/j.quaint.2014.11.036

Shi, H., Cao, Y., Dong, C., Xia, C., and Li, C. (2018). The Spatio-Temporal Evolution of river island based on Landsat Satellite Imagery, hydrodynamic numerical simulation and observed data. *Remote Sens.* 10 (12), 2046. doi:10.3390/rs10122046

Shi, H., Gao, C., Dong, C., Xia, C., and Xu, G. (2017). Variation of river islands around a large city along the Yangtze River from satellite remote sensing images. *Sensors* 17 (10), 2213. doi:10.3390/s17102213

Singer, M. B., and Aalto, R. (2009). Floodplain development in an engineered setting. *Earth Surf. Proc. Land.* 34 (2), 291–304. doi:10.1002/esp.1725

Sudra, P., Demarchi, L., Wierzbicki, G., and Chormański, J. (2023). A comparative assessment of multi-source generation of Digital Elevation Models for fluvial landscapes characterization and monitoring. *Remote Sens.* 15 (7), 1949. doi:10.3390/rs15071949

Sun, J., Ding, L., Li, J., Qian, H., Huang, M., and Xu, N. (2018). Monitoring temporal change of river islands in the Yangtze River by remotely sensed data. *Water* 10 (10), 1484. doi:10.3390/w10101484

Ve, N. D., Fan, D., Van Vuong, B., and Lan, T. D. (2021). Sediment budget and morphological change in the Red River Delta under increasing human interferences. *Mar. Geol.* 431, 106379. doi:10.1016/j.margeo.2020.106379

Wang, B., and Xu, Y. J. (2018). Dynamics of 30 large channel bars in the Lower Mississippi River in response to river engineering from 1985 to 2015. *Geomorphology* 300, 31–44. doi:10.1016/j.geomorph.2017.09.041

Wang, Z. Y., Li, H., and Cai, X. B. (2018). Remotely sensed analysis of channel bar morphodynamics in the middle Yangtze River in response to a major monsoon flood in 2002. *Remote Sens.* 10 (8), 1165. doi:10.3390/rs10081165

Wintenberger, C. L., Rodrigues, S., Bréhéret, J. G., and Villar, M. (2015). Fluvial islands: first stage of development from nonmigrating (forced) bars and woody-vegetation interactions. *Geomorphology* 246, 305–320. doi:10.1016/j.geomorph.2015.06.026

Wu, J., Margenot, A. J., Wei, X., Fan, M., Zhang, H., Best, J. L., et al. (2020). Source apportionment of soil heavy metals in fluvial islands, Anhui section of the lower Yangtze River: comparison of APCS–MLR and PMF. *J. Soil Sediment.* 20, 3380–3393. doi:10.1007/s11368-020-02639-7

Wyrick, J. R., and Klingeman, P. C. (2011). Proposed fluvial island classification scheme and its use for river restoration. *River Res. Appl.* 27 (7), 814–825. doi:10.1002/rra.1395

Xu, X., Tan, Y., and Yang, G. (2013). Environmental impact assessments of the three Gorges project in China: issues and interventions. *Earth-Sci. Rev.* 124, 115–125. doi:10.1016/j.earscirev.2013.05.007

Yang, H. F., Yang, S. L., Xu, K. H., Milliman, J. D., Wang, H., Yang, Z., et al. (2018). Human impacts on sediment in the Yangtze River: a review and new perspectives. *Glob. Planet. Change* 162, 8–17. doi:10.1016/j.gloplacha.2018.01.001

Yang, X. (2020). Evolution processes of the sandbanks in the Zhenjiang-Yangzhou reach of the Yangtze River and their driving forces (from 1570 to 1971). *Acta Geogr. Sin.* 78 (12), 1512–1522. (in Chinese). doi:10.11821/dlxb202007013

Zanoni, L., Gurnell, A., Drake, N., and Surian, N. (2008). Island dynamics in a braided river from analysis of historical maps and air photographs. *River Res. Appl.* 24 (8), 1141–1159. doi:10.1002/rra.1086

Zhang, Q., Chen, G., Su, B., Disse, M., Jiang, T., and Xu, C. Y. (2008). Periodicity of sediment load and runoff in the Yangtze River basin and possible impacts of climatic changes and human activities/Périodicité de la charge sédimentaire et de l'écoulement dans le bassin du Fleuve Yangtze et impacts possibles des changements climatiques et des activités humaines. *Hydrol. Sci. J.* 53 (2), 457–465. doi:10.1623/hysj.53.2.457

Zhao, Y., Zou, X., Liu, Q., Yao, Y., Li, Y., Wu, X., et al. (2017). Assessing natural and anthropogenic influences on water discharge and sediment load in the Yangtze River, China. *Sci. Total Environ.* 607, 920–932. doi:10.1016/j.scitotenv.2017.07.002

Zheng, S., Edmonds, D. A., Wu, B., and Han, S. (2019). Backwater controls on the evolution and avulsion of the qingshuigou channel on the yellow river delta. *Geomorphology* 333, 137–151. doi:10.1016/j.geomorph.2019.02.032

Zheng, S., Xu, Y. J., Cheng, H., Wang, B., Xu, W., and Wu, S. (2018). Riverbed erosion of the final 565 kilometers of the Yangtze River (Changjiang) following construction of the three Gorges dam. *Sci. Rep.* 8 (1), 11917. doi:10.1038/s41598-018-30441-6

frontiers | Frontiers in Environmental Science

TYPE Original Research
PUBLISHED 20 June 2024
DOI 10.3389/fenvs.2024.1412047

OPEN ACCESS

EDITED BY
Xiao Ouyang,
Hunan University of Finance and Economics, China

REVIEWED BY
Hua Lu,
Jiangxi University of Finance and Economics, China
Qianli Chen,
Xinjiang Agricultural University, China
Yan Wang,
Zhengzhou University of Aeronautics, China

*CORRESPONDENCE
Yixin Huang,
tory.huangyx@gmail.com

RECEIVED 04 April 2024
ACCEPTED 28 May 2024
PUBLISHED 20 June 2024

CITATION
Zhou L and Huang Y (2024), Spatiotemporal dynamics and determinants of human-land relationships in urbanization: a Yangtze River Economic Belt case study.
Front. Environ. Sci. 12:1412047.
doi: 10.3389/fenvs.2024.1412047

Spatiotemporal dynamics and determinants of human-land relationships in urbanization: a Yangtze River Economic Belt case study

Laiyou Zhou and Yixin Huang*

School of Economics and Management, Xinyu University, Xinyu, China

Introduction: The importance of harmonious human-land dynamics and the practical value of investigating the interplay between demographic urbanization and land development.

Methods: The study area (110 prefecture-level cities within the Yangtze River Economic Belt) and the integrative methodology employed (coupled coordination model, exploratory spatial data analysis, and fixed effects model).

Results: The main findings, including the progression in the coupled coordination level, the spatial gradient, and the factors influencing the coupled coordination level.

Discussion: Recommendations for surmounting institutional and policy impediments, fostering resource exchange, and facilitating the integrated evolution of human-land dynamics within the region.

KEYWORDS

population urbanization, land urbanization, coupled coordination degree, spatiotemporal dynamics, Yangtze River Economic Belt

1 Introduction

Since the reform and opening up period, China has experienced the most extensive and rapid urbanization process in recorded global history (Wen and Wang, 2019). Chinese urbanization has progressed in tandem with industrial acceleration, unfolding in three distinct phases: industrial, land, and population urbanization (Sun et al., 2023). The urbanization rate of the permanent resident population surged from 17.92% in 1978 to 64.72% in 2021, reflecting an average annual increase of 1.09 percentage points. This urbanization, while significantly bolstering China's economic and societal development and noticeably improving living standards, has simultaneously precipitated challenges to the harmonious human-land nexus, including unregulated urban spatial growth, rural depopulation, and environmental degradation. Notably, despite limited land resources, numerous cities have encountered issues of suboptimal land utilization and, in some cases, egregious mismanagement of land resources (Yao et al., 2013). The 14th Five-Year Plan for National Economic and Social Development of the People's Republic of China, alongside the Long-Range Objectives Through the Year 2035, promotes the establishment of a well-organized, collaboratively specialized, and functionally comprehensive urban spatial configuration. Nonetheless, the contentious nature of the negative repercussions of

urbanization strategies casts doubt on whether these objectives can be fulfilled, with implications regarding the success of China's modernization endeavors (Lu and Chen, 2015).

The concerted progression of human-land interactions is at the heart of the implementation of the urbanization strategy in China. This issue has attracted keen interest within scholarly circles in recent years, resulting in a wealth of research findings. Scholars have predominantly examined this topic from several vantage points.

A primary area of inquiry is the construction of indicators. Prevailing studies have employed methodologies such as the entropy method, analytical hierarchy process, and principal component analysis to devise robust systems for evaluating indicators. These systems are designed to encapsulate the multifaceted nature of population and land urbanization. For instance, population urbanization is typically quantified through factors such as demographic composition, employment distribution, generational makeup, and educational attainment (Yang et al., 2021), or simply use the proportion of urban population, the size of urban population, and the number of employees in secondary and tertiary industries to measure changes in the urban population quantity (Chen et al., 2009). On the other hand, land urbanization measurements rely on parameters such as the extent of land use, intensity of land investment, and efficiency of land output (Lü et al., 2016), other scholars also use land structure, land use scale, land investment, and land output to measure (Shan et al., 2021). This article builds upon a robust foundation of existing studies, wherein constructing multidimensional indicators has proven to comprehensively enhance the measurement of urbanization levels, as well as the synchronized development of human-environment interactions. Nonetheless, the selection of indicators remains largely subjective, leading to redundancy among them and a lack of objective benchmarks. Consequently, the outcomes of tested models are often overly optimistic, failing to accurately depict the dynamics between population and land urbanization (Wei et al., 2013). Additionally, the scale of research varies, encompassing national, regional, provincial and municipal levels (Yang et al., 2013; Lin and Fan, 2015; Wu et al., 2018; Li et al., 2020). From the perspective of research content and methods, there are many studies on the interactive relationship between population urbanization and land urbanization. The research topics include determining the degree of coordinated development, analyzing regional and size differences, and formulating optimization strategies, resulting in a series of rich research findings (Deng et al., 2021; Xu et al., 2022; Zhang et al., 2021). In terms of research methods, quantitative methods are commonly used, such as coupling coordination models, the Cobb-Douglas model, and quantile regression models (Han and Li, 2020; Feng et al., 2019; Xu et al., 2020). In the context of the Yangtze River Economic Belt, numerous studies have investigated the interplay between urbanization and other factors, adopting lenses such as urbanization with the ecological environment, the population-land-economy nexus, and the shift toward nonagricultural industrialization (Deng et al., 2019; Huang and Yang, 2021; Yang et al., 2021). For instance, Liu Huan employed the entropy method, the development level evaluation model, and the balanced development model to assess the coordination between population and land urbanization by analyzing spatiotemporal distribution patterns from 2006 to 2013 (Liu et al., 2016). Similarly, Chen Xicai investigated the spatial dynamics and foundational mechanisms of urbanization within the belt region and forecasted the coordination level for 2021 (Chen et al., 2021). However, existing research has not sufficiently examined the determinants influencing the degree of coordination.

Existing research primarily focuses on human-land relationship studies at the national or provincial levels, with relatively less attention paid to the coordinated development of population urbanization and land urbanization across different regions and time periods at the regional scale. Investigating the human-land relationship in different regions during various development stages holds significant importance for China's regional development. Moreover, related studies often directly explore the coordination relationship between population urbanization and land urbanization without clarifying the factors influencing their coordination degree. In light of this, based on the panel data of population and construction land in the Yangtze River Economic Belt from 2006 to 2021, this study employs a single dimension to measure the development levels of population urbanization and land urbanization, unlike previous scholars who constructed indicators using multiple dimensions, to avoid the subjectivity of indicator selection affecting the objectivity of the results.

This study adopts an integrative approach to investigate the spatiotemporal patterns, influencing factors, and driving mechanisms of the coupling coordination between population urbanization and land urbanization in the Yangtze River Economic Belt. By combining the coupling coordination degree model, exploratory spatial data analysis (ESDA), and panel data model, we provide new insights into the heterogeneity and spatial dependence of human-land dynamics in this region. Our findings reveal regional disparities, spatial clusters, and key influencing factors shaping the coupling coordination, offering valuable implications for sustainable urbanization and regional development policies.

Guided by the theory of human-land relationship, this study expands its connotation and application boundaries by incorporating population and land into the urbanization analytical framework. The quantitative analysis of the spatiotemporal matching relationship between population urbanization and land urbanization, and the examination of human-land imbalance manifestations and mechanisms, provide theoretical support for high-quality new urbanization development. Focusing on the Yangtze River Economic Belt as a typical region, this study offers new perspectives for regional sustainable development, making significant contributions to both theoretical innovation and practical guidance.

2 Research area, data sources, and research methods

2.1 Research area

The Yangtze River Economic Belt, established by the State Council and relying on the golden waterway of the Yangtze River, is a new economic support zone in China characterized mainly by its urban agglomerations (Fang et al., 2015). Notably, the Belt is predominantly characterized by its extensive urban

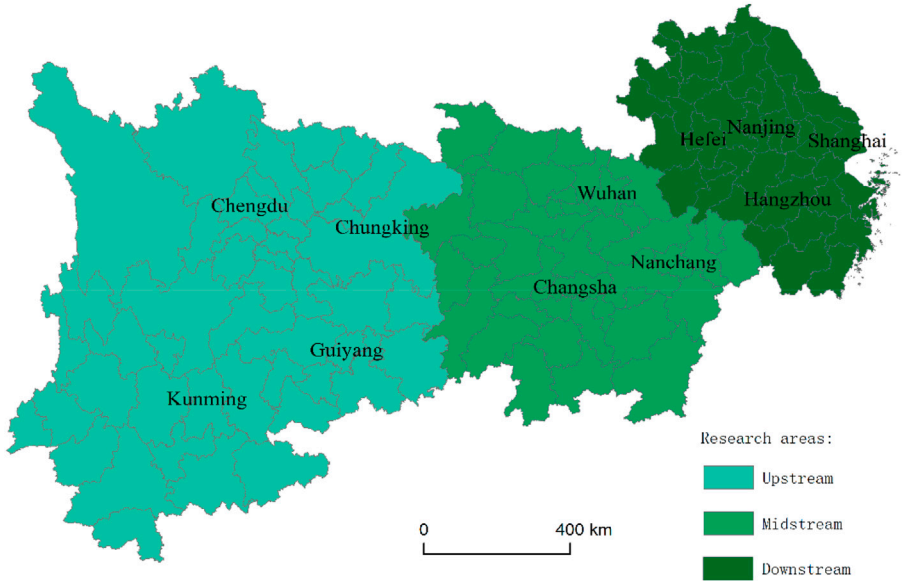

FIGURE 1
Regional division of the Yangtze River Economic Belt.

clusters. It extends from Shanghai in the east to Yunnan in the west, spanning 9 provinces and 2 municipalities, which together consist of 130 administrative divisions at the prefecture level or higher. Encompassing an area close to 2.05 million km^2, it forms a significant part of China's geographical and economic landscape. Geographically, the Yangtze River Economic Belt is segmented into three distinct sections: the upper, middle, and lower reaches (as depicted in Figure 1). The upper reaches include Chongqing, Sichuan, Guizhou, and Yunnan, which form the most upstream section. The middle reaches, which lie between the upper and lower sections, include the provinces of Hunan, Hubei, and Jiangxi. Finally, the lower reaches, which are nearest to the East China Sea, comprise the bustling metropolis of Shanghai, along with Zhejiang, Jiangsu, and Anhui provinces.

The Yangtze River Economic Belt is not only a focal area of urbanization and development but also plays a crucial role in China's environmental and sustainable growth strategies. With a varied landscape that includes large metropolitan areas, important industrial regions, and diverse ecosystems, research on this area has the potential to yield insights into urban development, economic reform, and environmental policies. In 2022, the Yangtze River Economic Belt had a population of 608 million, representing 43.08% of China's total population. Of this total, the urban populace amounted to 393 million, constituting 42.73% of the country's urban inhabitants. The average urbanization rate in the region was 64.92%, marginally surpassing the national average by 0.25%. The importance of the Yangtze River Economic Belt was officially recognized by the State Council in 2014 with the issuance of the "Guiding Opinions of the State Council on Promoting the Development of the Yangtze River Economic Belt by Relying on the Golden Waterway," elevating the region to a significant national strategic status. The development trajectory was further defined in 2016 when the Political Bureau of the CPC Central Committee approved the Outline for the Development Plan of the Yangtze River Economic Belt, establishing a framework for a national strategy to advance the region's growth. Moreover, at the 20th National Congress of the Communist Party of China in 2022, General Secretary Xi Jinping underscored the importance of propelling the Yangtze River Economic Belt's development, with an emphasis on a people-centric approach to urbanization and the promotion of coordinated regional development. The role of the Yangtze River Economic Belt as a principal area of new urbanization in China and a pivotal engine for economic expansion has been a focal point of government policy. According to Fang et al. (2015), the success of urbanization in the Yangtze River Economic Belt is intrinsically tied to the overall success and security of China's urbanization strategy.

The Yangtze River Economic Belt is a crucial economic development corridor in China, covering 11 provinces and cities, accounting for 21% of the country's land area, and more than 40% of its population and economic output. The Yangtze River Economic Belt plays a pivotal role in China's regional development and urbanization process. However, the region exhibits unbalanced internal development, with significant disparities in resource endowments, economic foundations, and urbanization levels among the upper, middle, and lower reaches. Rapid urbanization has led to prominent conflicts between human activities and land resources in the Yangtze River Economic Belt.

Focusing on the Yangtze River Economic Belt allows for a better understanding of the internal spatial heterogeneity and the coupling relationship between population and land urbanization at different

development stages. It also helps to analyze the causes of human-land relationship imbalances and provide decision-making references for achieving sustainable regional development. Despite limitations in data availability, the Yangtze River Economic Belt's representativeness and importance justify its selection as the study area. The findings from this region can provide valuable insights into regional development dynamics in China, and the analytical framework and methods employed can be extended to other regions.

In summary, the Yangtze River Economic Belt is selected as the research area due to its critical role in China's regional development, its internal spatial heterogeneity, and the prominent human-land conflicts it faces. This study aims to provide targeted references for formulating place-based policies and achieving sustainable regional development by investigating the coupling relationship between population and land urbanization and the causes of human-land relationship imbalances in the Yangtze River Economic Belt.

2.2 Data sources

To elucidate the spatiotemporal dynamics of human-land interactions and the factors influencing them, this study focuses on prefecture-level cities within the Yangtze River Economic Belt to discern the underlying trends. The Belt comprises 130 administrative entities at the prefecture level or higher. However, the absence of essential data in certain localities necessitates sample selection based on data availability. Consequently, this paper examines a subset of 110 prefecture-level cities from the Belt. To ensure the reliability of the data, which is essential for deriving accurate conclusions, the primary sources of data are the "China Statistical Yearbook" and the "China City Statistical Yearbook," spanning the years 2007–2022. These data are supplemented with data from provincial and municipal statistical yearbooks, as well as statistical bulletins from the respective cities over the same period. In instances of missing data for certain years, interpolation methods are employed to estimate the missing values.

2.3 Research methods

2.3.1 Coupled coordination degree model

A coupled coordination degree model is developed to investigate the nexus between population and land urbanization within the Yangtze River Economic Belt. The ratio of the urban population to the total population serves as a metric for population urbanization, and the ratio of developed land area to the total territorial extent of the administrative region quantifies the level of land urbanization. The coupling degree between population urbanization and land urbanization is computed using Eq. 1. Subsequently, this metric is integrated with a comprehensive coordination index, calculated with Eq. 2, to determine the overall coupled coordination degree, as outlined in Eq. 3. With the available data, these equations can be precisely formulated.

2.3.1.1 Coupling degree (C)

The coupling degree (C) quantifies the interplay between population urbanization and land urbanization for city "i" during the study periods t_1 and t_2.

TABLE 1 Classification Criteria for the coupled coordination degree of population urbanization and land urbanization.

Degree of coupled coordination	Type of coupled coordination
0.0 ≤ D < 0.2	Severe imbalance
0.2 ≤ D < 0.4	On the verge of imbalance
0.4 ≤ D < 0.6	Moderate coordination
0.6 ≤ D < 0.8	Good coordination
0.8 ≤ D < 1	High-level coordination

$$C_i = 2 \times \left[\frac{U_i \times L_i}{(U_i \times L_i)^2} \right]^{\frac{1}{2}} \quad (1)$$

where "C_i" represents the coupling degree for city "i," "U_i" is the standardized value of the population urbanization index for city "i," and "L_i" is the standardized value of the land urbanization index for city "i".

2.3.1.2 Comprehensive coordination index (T)

The comprehensive coordination index (T) reflects the degree of harmony between population urbanization (U) and land urbanization (L), representing the integrated state of urbanization concerning both demographic and spatial factors.

$$T_i = aU_i + bL_i \quad (2)$$

2.3.1.3 Coupled coordination degree (D)

The coupled coordination degree (D) reflects the overall congruence between the processes of population urbanization and land urbanization. The coupling degree (C) is combined with the comprehensive coordination index (T) to reflect the extent of synchronization between the two facets of urbanization.

$$D = \sqrt{C \times T} \quad (3)$$

In this equation, "a" and "b" denote the weights attributed to population urbanization and land urbanization, respectively, indicating their relative significance in terms of the urbanization dynamic. For the purposes of this analysis, the weights are deemed equivalent and are assigned a value of 0.5, underscoring the equal importance of both population and land urbanization in the city's urbanization trajectory.

Leveraging insights from prior research (Wang and Wen, 2019), Table 1 delineates the classification of the coupled coordination degree into five distinct categories.

2.3.2 Exploratory spatial data analysis

Exploratory spatial data analysis (ESDA) comprises a suite of methods and techniques for analyzing spatial data. These tools are utilized to characterize the spatial distributions of various phenomena, elucidate the distribution characteristics of entities, propose mechanisms of spatial interactions, identify patterns of spatial connectivity, and provide statistical approaches to quantify spatial heterogeneity.

In ESDA, global and local spatial autocorrelation methods are pivotal. This study employs these methods within the ArcGIS 10.8 software environment to capture the spatial heterogeneity and development patterns of the human-land relationships in the Yangtze River Economic Belt. Global spatial autocorrelation methods are used to assess the degree of population–land coordination across a region, and local Moran's I is frequently applied to determine spatial associations at finer scales. The corresponding formula is as follows:

$$I = \frac{n\sum_{i=1}^{n}\sum_{j=1}^{n}\omega_{ij}(x_i-\bar{x})\left(x_j-\bar{x}\right)}{\sum_{i=1}^{n}\sum_{j=1}^{n}\omega_{ij}\sum_{i=1}^{n}(x_i-\bar{x})^2} \quad (4)$$

In the Eq. 4 presented, I denotes the global Moran's I index. The number of regions being studied is represented by n, and ω_{ij} constitutes the spatial weight matrix between regions i and j. The observed values for cities i and j are given by x_i and x_j, respectively. A positive value of I > 0 signifies the spatial clustering of similar values, indicative of positive spatial autocorrelation. Conversely, a negative value of I < 0 suggests a clustering of dissimilar values, reflecting negative spatial autocorrelation. The index I typically varies between −1 and 1, with values approaching 1 signifying pronounced clustering and those nearing −1 indicating greater dispersion.

The global Moran's I quantifies the average similarity of features within the study area; however, it does not differentiate between clusters of high-value and low-value features. To account for spatial heterogeneity among the study subjects, the Getis-Ord Gi* statistic is utilized to identify the spatial clusters of features. The Eq. 5 for this calculation is as follows:

$$G_i^* = \frac{\sum_{j-1}^{n}\omega_{ij}x_{ij}}{\sum_{j-1}^{n}x_{ij}} \quad (5)$$

2.3.3 Panel data model

This study employs a panel data framework for construction of an analytical model. The canonical form of the panel data model is presented below as Eq. 6:

$$y_{it} = \alpha_{it} + \sum_{k=1}^{K}\beta_{kit}x_{kit} + \mu_{it} \quad (6)$$

where y_{it} is the dependent variable and x_{it} is the vector of independent variables for the i^{th} sample at time t, with i ranging from 1 to N and t ranging from 1 to T. The term α_{it} denotes the intercept, k signifies the number of independent variables, β_{it} represents the coefficients to be estimated for the respective independent variables, and μ_{it} is the random error component.

By integrating the coupling coordination degree model, exploratory spatial data analysis (ESDA), and panel data model, we gain an in-depth understanding of the spatiotemporal evolution, spatial patterns, and potential driving mechanisms of the coupling coordination between population urbanization and land urbanization in the Yangtze River Economic Belt. The coupling coordination degree model quantifies the synchronization and interaction between the two urbanization processes; ESDA reveals the spatial patterns and clusters of coupling coordination; and the panel data model identifies key influencing factors and their explanatory power.

The integration of these three complementary methods provides a comprehensive framework for analyzing the complex interactions between population urbanization and land urbanization in the Yangtze River Economic Belt. The findings contribute to a better understanding of the coordination between population and land urbanization processes and provide empirical evidence to support sustainable urban planning and policy-making in this region.

3 Results

3.1 Temporal dynamics of the coordination of population and land urbanization

Between 2006 and 2021, the Yangtze River Economic Belt experienced changes in both population and land urbanization levels, as well as the degree of coupled coordination, as depicted in Figure 2. A time-series analysis revealed that the urbanization index of the region notably improved during this period. Specifically, the average population urbanization index increased from 0.42 to 0.61, and the average land urbanization index increased slightly from 0.07 to 0.08. The corresponding annual average growth rates were 2.58% for population urbanization and 0.76% for land urbanization. These figures demonstrate more rapid advancement in population urbanization than in land urbanization.

In the temporal analysis, there was a consistent enhancement in the coupled coordination level of population and land urbanization within the Yangtze River Economic Belt. The coordination indices for the years 2006, 2011, 2016, and 2021 were 0.1, 0.76, 0.74, and 0.88, respectively, demonstrating a significant upward trajectory, with an average annual growth rate of 15.75%. This indicates a shift from predominantly low-value to high-value areas. A detailed examination of the coupled coordination degree from 2006 to 2021, as shown in Figure 3, revealed a marked decrease in the number of cities experiencing severe imbalance, which plummeted from 72 prefecture-level cities in 2006 to only 3 in 2010 and eventually to none by 2021. Conversely, the number of cities on the brink of imbalance, as well as those achieving moderate and good coordination, initially increased, then decreased, and ultimately stabilized between 2017 and 2021. Cities with high-level coordination significantly increased from none in 2006 to 8 in 2012, surging to 78 by 2021, a trend concurrent with China's deepening industrialization, increased urbanization, and swift economic structural transformation. In conclusion, the interactive coupled coordination level has demonstrated sustained growth alongside advancements in population and land urbanization.

With the deepening of industrialization and urbanization in China and the accelerating economic structural transformation, cities that were severely imbalanced in the early stages of development have seen significant improvements. This is highly correlated with a series of policies and institutional reforms implemented by the Chinese government aimed at promoting more balanced and sustainable urbanization, including the "New-Type Urbanization Plan (2014–2020)" and the "Yangtze River Economic Belt Development Plan." These policies emphasize the coordination of population growth and land development,

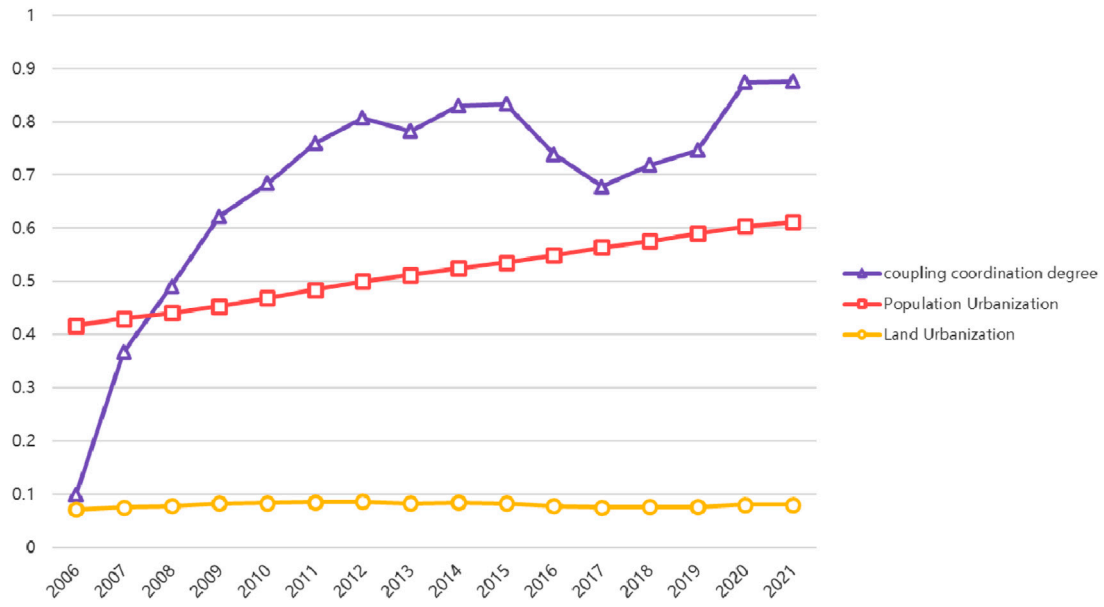

FIGURE 2
Changes in the coupling degree and coordination degree between population urbanization and land urbanization in the Yangtze River Economic Belt.

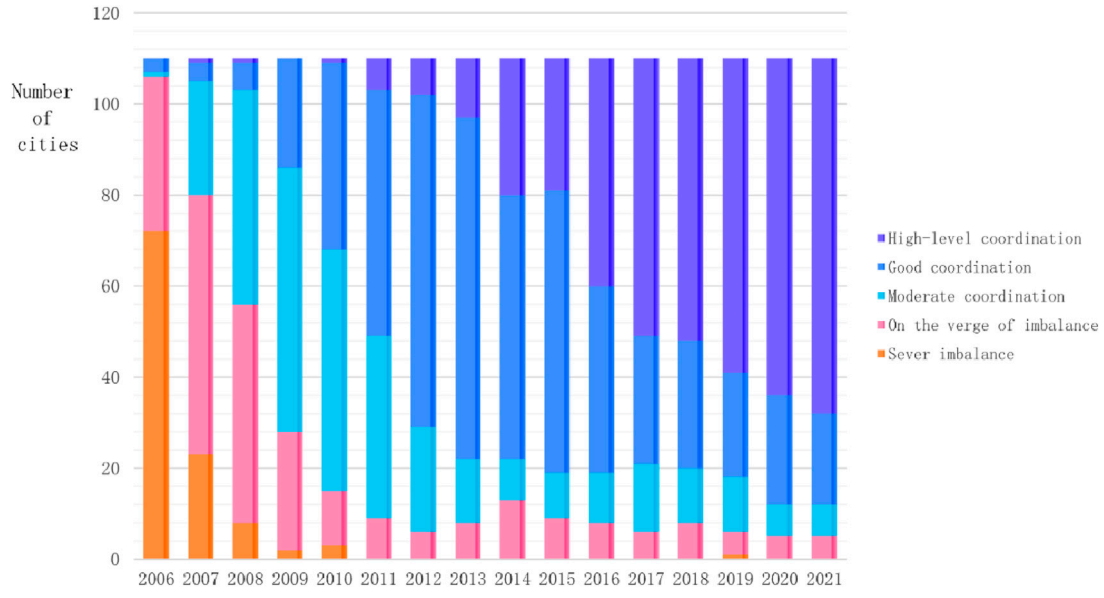

FIGURE 3
Proportions of coupled coordination types from 2006 to 2021.

encouraging local governments to optimize land use planning, improve public service provision, and strengthen environmental protection, thereby promoting the coordination of population and land urbanization.

China's rapid urbanization process is primarily driven by large-scale rural-urban migration. As migrant workers move to cities in search of better employment opportunities and living conditions, the demand for urban land and housing continues to increase. The formation of urban agglomerations, such as the Yangtze River Delta and the Chengdu-Chongqing urban agglomerations, further promotes the efficient allocation of land resources and the coordination of population growth and land development. Simultaneously, the Yangtze River Economic Belt itself has undergone massive investments in transportation infrastructure, such as high-speed railways and highways, enhancing internal connectivity within the region and reducing transaction costs.

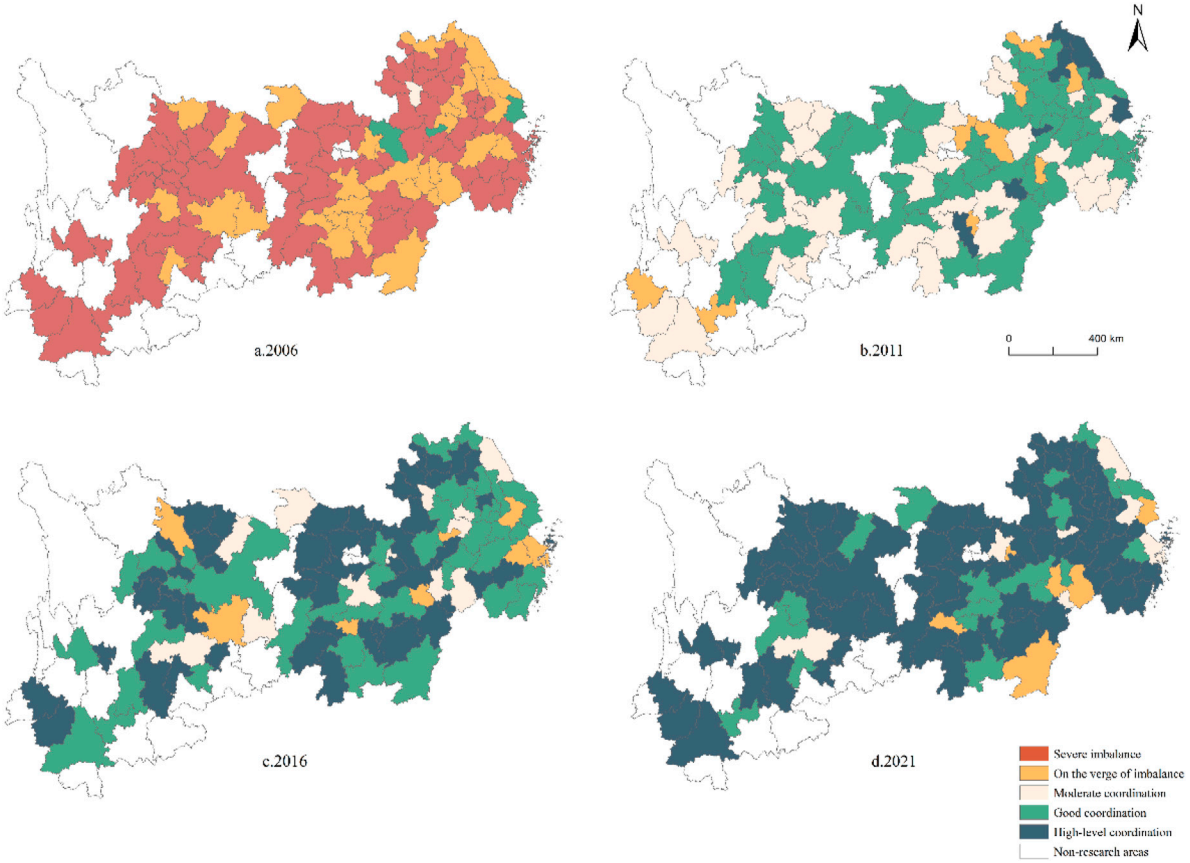

FIGURE 4
Spatial differentiation pattern of the coupled coordination degree between population urbanization and land urbanization.

This facilitates the flow of population, goods, and information, promoting the integration of urban systems and contributing to the coordinated development of population and land urbanization. Moreover, the development of land markets and the increased role of market mechanisms in land allocation have promoted the coordination of population and land urbanization. Rising urban land prices incentivize local governments and developers to optimize land use, promoting compact and intensive development patterns, thereby improving land use efficiency and better aligning with population growth patterns.

3.2 Spatial pattern of the coordination degree between population urbanization and land urbanization

To elucidate the spatial pattern of the coordination of population and land urbanization within the Yangtze River Economic Belt from 2006 to 2021, the years 2006, 2011, 2016, and 2021 were selected as key reference years. Using ArcGIS 10.8 software and referring to the coupled coordination degree classifications in Table 1, spatial distribution maps were constructed for the coordination degree of each prefecture-level city, as depicted in Figure 4.

Spatial analysis revealed a year-over-year increase in the coupled coordination degree among prefecture-level cities within the Yangtze River Economic Belt.

3.2.1 Regions of good and high-level coordination

The areas characterized by good and high-level coordination predominantly lie in the middle and lower reaches of the Yangtze River Economic Belt, encompassing Shanghai, Zhejiang, and Jiangsu, as well as certain provincial capitals. These regions boast a robust industrial base and a fruitful employment landscape, fostering tight economic integration and a high capacity to draw rural populations into urban settings. The combination of population concentration and the expansion of urban construction land has accelerated the pace of land urbanization, resulting in a synergistic interplay between population and land dynamics.

3.2.2 Regions at the brink of imbalance and with moderate coordination

Initially, in 2006 and 2011, the regions on the verge of imbalance and those exhibiting moderate coordination comprised approximately half of the study area. However, by 2016 and 2021, such regions were limited to sporadic distributions across several provinces throughout the upper, middle, and lower reaches of the Yangtze River basin.

TABLE 2 Global Moran's I index and test results of the coupled coordination degree of cities in the Yangtze River economic belt.

Year	2006	2007	2008	2009	2010	2011	2012	2013	2014	2015	2016	2017	2018	2019	2020	2021
Moran's I	0.140	0.350	0.316	0.307	0.339	0.269	0.241	0.208	0.149	0.120	0.158	0.108	0.139	0.137	0.141	0.141
Z Score	2.719	6.415	5.791	5.634	6.207	4.965	4.459	3.862	2.797	2.291	2.976	2.065	2.632	2.59	2.668	2.656
p-value	0.007	0.000	0.000	0.000	0.000	0.000	0.000	0.000	0.005	0.022	0.003	0.039	0.008	0.001	0.008	0.008

3.2.3 Severely imbalanced regions

Over the study period from 2006 to 2022, the highest incidence of severe imbalance occurred in 2006, with 72 cities representing 65.45% of the sample. Since 2011, following the adoption of comprehensive national policies and the recurrent promotion of the Yangtze River Economic Belt as a pivotal national development initiative, no prefecture-level cities within the belt have experienced a severe imbalance in the coupled coordination of population urbanization and land urbanization.

Overall, disparities between regions exhibiting high and low levels of coupled coordination are progressively diminishing. This trend may reflect the efficacy of targeted policy interventions alongside the inherent dynamics of economic advancement, contributing to a more uniform and synchronized urbanization process throughout the Yangtze River Economic Belt.

3.3 Spatial correlation analysis of the coupled coordination between population and land urbanization

3.3.1 Global spatial autocorrelation

The global Moran's I index was employed to assess the spatial clustering tendencies of the degree of coupled coordination between population urbanization and land urbanization, as presented in Table 2. The analysis revealed that from 2006 to 2010, there was a progressive intensification of spatial autocorrelation in the coupled coordination degree, with Moran's I increasing from 0.14 in 2006 to 0.339 in 2010. This trend was followed by a consistent decline post-2011. The temporal pattern of the global Moran's I index during the study period exhibited a fluctuating trend, and the *p*-value was statistically significant at the 5% level, indicating a consistent normal distribution. A positive value of the global Moran's I index, greater than zero, confirms a significant positive spatial correlation, implying that the coupled coordination degree of a given city is not only influenced by but also influences that of neighboring cities.

3.3.2 Analysis of spatial hot spots and cold spots

A detailed examination of the local spatial heterogeneity in the coupled coordination degree of population and land urbanization within the Yangtze River Economic Belt was conducted. The Getis-Ord Gi* index was calculated for the constituent cities for 2006, 2011, 2016, and 2021. By applying the natural breaks (Jenks) classification method, the indices were organized in ascending order into categories of cold spots, subcold spots, areas with a random distribution, subhot spots, and hot spots. This classification facilitated the development of spatial distribution maps depicting these hot spots and cold spots, as illustrated in Figure 5.

The analysis revealed a consistent spatial transition from hot spots to cold spots across the east–west axis of the Yangtze River Economic Belt for the years 2006, 2011, 2016, and 2021, with pronounced spatial differences in the degree of coupled coordination between population and land urbanization. Initially, in 2006, hot spots and subhot spots were predominantly located in the central and lower reaches of the Belt, encompassing specific cities. Over time, cities such as Xiangyang, Yichang, Jingmen,

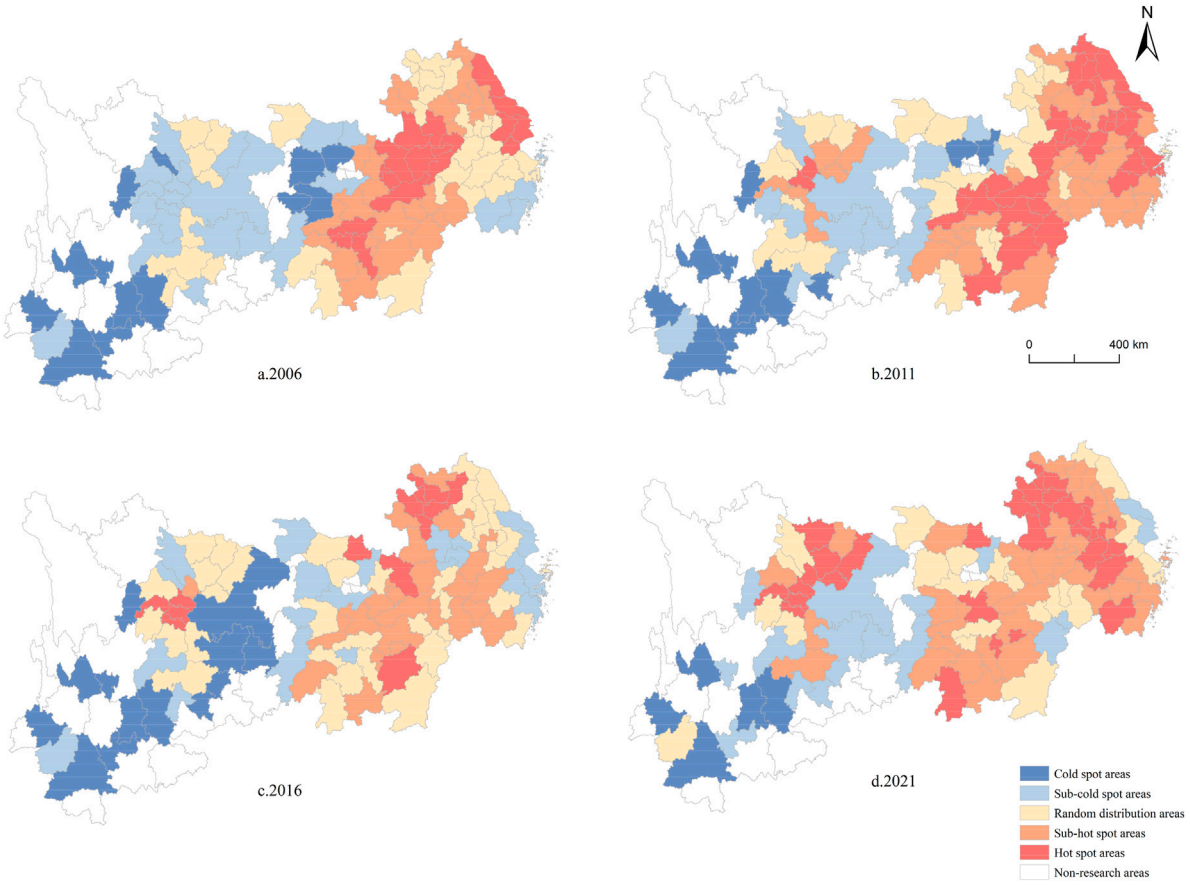

FIGURE 5
Spatial distribution of cold and hot spots of the coupled coordination degree between population urbanization and land urbanization in the Yangtze River Economic Belt.

Jingzhou, and Suizhou in Hubei Province and the majority of cities in Sichuan Province emerged as hot spots and subhot spots. Conversely, cold spots and subcold spots were mainly situated in the upper reaches, particularly in most cities of Yunnan Province, as well as Anshun, Zunyi, and Tongren in Guizhou Province and Ya'an in Sichuan Province. Chongqing consistently ranked as a cold or subcold zone, while certain cities in Sichuan and Guizhou exhibited a trend of evolving from subcold spots to hot or subhot spots. This dynamic culminated in a spatial distribution pattern typified by prominent hotspots juxtaposed with smaller cold spots.

The enhanced coordination between demographic and land urbanization manifests in urban planning and management through several key aspects. Firstly, urban planners can leverage the increased coordination to develop more integrated land use and transportation plans, strategically locating residential areas, employment centers, and public amenities along transit corridors. This optimizes the spatial distribution of urban functions, reduces commuting times and traffic congestion, and promotes compact and efficient urban forms. Secondly, the enhanced coordination allows urban managers to better align the provision of infrastructure and public services with the changing demographic and spatial patterns of urbanization. By anticipating and responding to the evolving needs of urban residents, managers can ensure the timely and efficient delivery of essential services, improving the quality of life in cities. Thirdly, the shift towards greater coordination necessitates more collaborative and participatory planning processes that engage diverse stakeholders. Urban planners can facilitate multi-stakeholder dialogues and partnerships to co-create and implement shared visions for sustainable urban development, fostering a sense of ownership and social cohesion.

4 Factors influencing the coordinated development of population urbanization and land urbanization

4.1 Selection of influencing factors

Drawing upon the studies of Zhang et al. (2019) and Zhang and Duan (2021) and Chen and Yu. (2023) and considering data accessibility, critical variables such as economic development level, fixed asset investment, educational expenditure, and governmental actions were identified as determinants of the coupled coordination degree of population and land urbanization in the Yangtze River Economic Belt (refer to Table 3). To neutralize the effect of differing units of measurement, all variables were converted into logarithmic form. The rationale for selecting these variables was based on the following premises.

TABLE 3 Factors influencing the coupled coordination degree.

Variable type	Variable Name	Variable Description	Unit
Dependent variable	Coupled coordination degree	Results calculated from the coupled coordination model between population urbanization and land urbanization	Dimensionless
Explanatory variables	Economic development level	Per capita GDP	Yuan/person
	Fixed asset investment	Per capita fixed asset investment	Yuan/person
	Educational input	Per capita fiscal education expenditure	Yuan/person
	Government management	Proportion of fiscal expenditure in GDP	%

4.1.1 Economic development as an urbanization driver

The level of economic development constitutes the foundation of urbanization. As it advances, the expansion of cities accelerates, fostering land development and utilization. Concurrently, this growth engenders an increase in employment opportunities and remuneration, thereby stimulating population urbanization, as indicated by *per capita* GDP. As an indicator of economic development, higher *per capita* GDP implies better job opportunities, infrastructure, and public services in urban areas, which can attract more population inflow and promote population urbanization. Meanwhile, economic growth also stimulates the demand for urban land expansion, driving land urbanization.

4.1.2 Impact of fixed-asset investment

Investment in fixed assets bolsters urban infrastructure, propels the expansion of urban construction land, and refines the configuration of urban functional zones. Its integral role in urbanization is captured by the *per capita* fixed-asset investment indicator. Increased investment in fixed assets, such as infrastructure and real estate, directly contributes to land urbanization by expanding the built-up area. It also indirectly promotes population urbanization by improving urban living conditions and attracting population inflow.

4.1.3 Role of educational investment

Educational investment supplies the human capital essential for urban development, catalyzing the concentration of innovative forces in urban areas. By enhancing the populace's educational quality and propelling technological progress, this type of investment bridges the urban–rural divide and is quantified by *per capita* fiscal educational spending. Higher education expenditure indicates better educational resources and human capital development in urban areas, which can attract more population inflow and enhance the quality of urbanization. This factor mainly influences population urbanization.

4.1.4 Influence of governmental action

Governmental action is pivotal in urbanization, with active policy direction shaping the resource distribution across urban centers. The efficacy of local governmental management markedly influences this process, as reflected by the share of local fiscal spending in GDP. A higher ratio of this factor suggests a stronger role of the government in urban development. Government expenditure on public services, infrastructure, and urban planning can guide and regulate the processes of population urbanization and land urbanization, promoting their coordinated development.

However, these four influencing factors exhibit an interrelated and mutually reinforcing relationship. Firstly, the level of economic development, as measured by *per capita* GDP, is closely linked to fixed asset investment. Economic growth can stimulate investment in infrastructure and real estate, which in turn supports further economic development, creating a virtuous cycle. Secondly, fiscal education expenditure and local fiscal expenditure are both tied to government policies and budget allocation. They respectively reflect the government's priorities in terms of human capital development and urban development. Lastly, economic development and government expenditure are also interconnected. Government investment in public services and infrastructure can create a conducive environment for economic growth, while economic growth can generate more fiscal resources to support government expenditure.

4.2 Analysis of results

When investigating the impact of factors such as economic development level, fixed asset investment, educational input, and government management on the coupling coordination degree of population and land urbanization, endogeneity issues may affect the reliability of the results. Endogeneity problems mainly stem from two aspects: omitted variables and measurement errors. First, the model may omit some important variables that simultaneously influence the coupling coordination degree of population and land urbanization and the explanatory variables in the model, leading to the correlation between explanatory variables and the error term. For instance, factors such as the geographical location and resource endowment of a city may concurrently affect the coupling coordination degree of population and land urbanization and the level of economic development, but these factors are difficult to accurately measure and incorporate into the model. Second, there may be measurement errors in the explanatory variables (e.g., economic development level, fixed asset investment, educational input, and government management), causing the measurement errors to be correlated with other variables, thus leading to endogeneity issues.

To mitigate the endogeneity problems, this study employs a fixed-effects model for analysis. The fixed-effects model introduces individual and time effects, which to a certain extent controls for the

TABLE 4 Analysis results of factors influencing the coupled coordination degree between population and land urbanization in the Yangtze River Economic Belt.

Explanatory variable	Entire Region	Upper reaches	Middle reaches	Lower reaches
Constant	−1.312***(0.305)	−1.443***(0.304)	−1.530*(0.895)	−0.278 (1.195)
Per capita GDP	0.130***(0.0287)	0.123***(0.0292)	0.196**(0.0819)	0.0936 (0.104)
Per capita fixed-asset investment	0.259***(0.0269)	0.449***(0.0390)	0.217***(0.0766)	0.0483 (0.0698)
Per capita fiscal education expenditure	0.120***(0.0229)	0.116***(0.0226)	−0.107 (0.0865)	0.468***(0.0877)
Proportion of local fiscal expenditure in GDP	0.331***(0.0464)	0.440***(0.0769)	0.846***(0.138)	0.182***(0.0675)
R^2	0.573	0.681	0.528	0.562
Sample size	1760	528	576	656

Note: * * *, ** *, * represent significance levels of 1%, 5% and 10%, respectively, and the robust standard error is in brackets.

omitted variables that do not change over time and individual heterogeneity, thereby alleviating the impact of endogeneity issues. Furthermore, we determine the applicability of the fixed-effects model through the F-test and Hausman test.

The model's computed outcomes reveal that the R-squared (R^2) values for the entire Yangtze River Economic Belt, as well as its upper, middle, and lower reaches, are 0.573, 0.681, 0.528, and 0.562, respectively. These figures indicate that the models possess relatively strong explanatory capabilities (refer to Table 4).

The regression analysis indicates that government administration is the dominant factor influencing the degree of coupled coordination, exerting a significant positive impact that is statistically significant at the 1% level. Specifically, a 1% increase in the ratio of local fiscal expenditure to GDP results in a 0.331% increase in the degree of coupled coordination. Within the Yangtze River Economic Belt, government management has emerged as the crucial element affecting the degree of coordination. Regional bias in governmental decision-making influences the resource distribution among cities. Following the 2006 national strategy to advance the development of the central region, an economic network centered on the five-way linkage of Wuhan, Yueyang, Changsha, Nanchang, and Jiujiang emerged. In August 2012, the State Council's "Several Opinions on Vigorously Implementing the Promotion of the Central Region's Rise" advocated for strategic cooperation among the Wuhan, Changsha-Zhuzhou-Xiangtan, and Poyang Lake city clusters, aiming to foster the integrated evolution of the central Yangtze River's urban conglomerates. By September 2021, Hubei, Hunan, and Jiangxi provinces launched the "General Concept of Strategic Cooperation in the Middle Reaches of the Yangtze River," creating a structured promotion mechanism with distinct decision-making, coordination, and execution layers. National and provincial governments have placed considerable emphasis on the growth of central cities along the Yangtze River's midsection, enhancing the urbanization of both the population and land in this region. The data analysis in Table 3 reveals that the influence of local governments on the degree of coupled coordination is most pronounced in the central region, with the upper reaches following and the lowest impact in the lower reaches. This variation is attributed to the more stringent urban construction land indicators in the lower reaches, where government land development strategies for individual cities differ markedly from those in the central and western regions, with a trend toward fine-scale management.

A comprehensive analysis revealed that fixed asset investment ranks as the second-most-crucial factor following government management, surpassing the 1% significance threshold. An increase of one percentage point in *per capita* fixed asset investment correlates with a 0.259% increase in the coupled coordination degree. Specifically, the regression coefficients for the upper and middle reaches are 0.449 and 0.217, respectively, both exceeding the 1% significance level. However, the effect in the lower reaches was not statistically significant. These findings underscore the growing influence of fixed-asset investment on population and land urbanization, which is intimately linked to escalating urban construction investments across the Yangtze River Economic Belt. When considering aggregate fixed-asset investment, the sequence is as follows: lower reaches > middle reaches > upper reaches. This suggests that the influence of fixed-asset investment on the coupled coordination degree is characterized by diminishing marginal returns.

The economic development level is a significant determinant of the degree of coupled coordination. Regression analyses indicate that economic development exerts a positive effect on this degree, confirmed by surpassing the 1% significance level. Specifically, a 1% increase in *per capita* GDP is associated with a 0.13% increase in the degree of coupled coordination. Regionally, the influence of economic development is more pronounced in the middle reaches than in the upper reaches, although it is negligible in the lower reaches. The middle reaches benefit from locational factors such as enhanced openness and a higher capacity for absorbing industrial shifts than that in the lower reaches, fueling industrial structure evolution and deepening the synergy between population and land urbanization. The negligible influence in the lower reaches may stem from the elevated costs of urban residential land, which heighten the expense of rural–urban migration. This 'crowding out' effect is particularly marked in more economically advanced cities, as it impedes labor mobility (Wang et al., 2017).

Overall, the influence of educational investment on the degree of coupled coordination is the least pronounced, manifesting significant effects only in the lower reaches of the Yangtze River Economic Belt. Here, a 1% increase in educational investment corresponds to a 0.468%

TABLE 5 Robustness test by variable substitution.

Explanatory variable	Entire Region
Constant	−2.642***(0.5038)
Per capita disposable income	0.265***(0.0473)
Per capita fixed-asset investment	0.1825***(0.0314)
Per capita fiscal education expenditure	0.1437***(0.0237)
Proportion of local fiscal expenditure in GDP	0.3199***(0.0471)
R2	0.5593
Sample size	1760

Note: * * *, ** *, * represent significance levels of 1%, 5% and 10%, respectively, and the robust standard error is in brackets.

increase in the degree of coupled coordination. In contrast, such investment yields no substantial impact in the upper reaches and demonstrates no correlation in the middle reaches. This disparity can be attributed to the advanced economy and superior infrastructure in the lower reaches, which have historically attracted substantial talent inflows, whereas the middle and upper reaches have only recently experienced more pronounced talent outflows. Consequently, in the upper reaches, human capital fails to translate into tangible benefits from educational investment, exacerbating the industrial and technological divide between the more developed lower reaches and the upper reaches.

4.3 Robustness tests

To ensure the robustness of the regression results, this study conducts robustness tests by replacing variables and changing the study period.

4.3.1 Variable substitution

Following the approach of Li and Cui (2022), this study replaces GDP *per capita* with *per capita* disposable income for robustness testing. The analysis results are presented in Table 5. The test results indicate that the conclusions are consistent with those before the variable substitution, suggesting that the conclusions of this study are robust.

4.3.2 Changing the study period

The impact of the coupling coordination degree of population and land urbanization may vary at different stages of development. Taking 2012 as the time dividing point, the period from 2006 to 2012 is considered the first stage of the coupling coordination development of population and land urbanization, while the period from 2013 to 2021 is the second stage (Sun, 2018). The analysis results are presented in Table 6.

The regression analysis using the fixed-effects model reveals that in the first stage, the development of economic development level, fixed asset investment, educational input, and government management in the Yangtze River Economic Belt still plays a significant positive role in the overall coordinated development of population and land urbanization. In the second stage, economic development level, fixed asset investment, and educational input have a significant positive impact on the coupling coordination degree of population and land urbanization, while the influence of government management loses its significance. This may be due to government policies during this period, such as the "New-type Urbanization Plan (2014–2020)" and the "Yangtze River Economic Belt Development Plan," which emphasize local autonomy, potentially weakening the role of government management. Moreover, after the 18th National Congress of the Communist Party of China, General Secretary Xi Jinping repeatedly emphasized the need to accelerate the transformation of the economic development model and the implementation of an innovation-driven development strategy. This has led to economic growth in the second stage relying more on the service industry and innovation-driven factors, and less on government-led investment and infrastructure construction, which may diminish the impact of government management on urbanization. The robustness test by changing the study period demonstrates that the conclusions of this study remain robust.

5 Conclusion

The novelty of this study lies in its focus on 110 prefecture-level cities in the Yangtze River Economic Belt as the research area and its comprehensive and integrative approach to analyzing the coupling coordination between population urbanization and land urbanization in the Yangtze River Economic Belt. Compared to previous studies, we utilize multiple complementary methods, including the coupling

TABLE 6 Robustness test by changing the study period.

Explanatory variable	2006–2012	2013–2021
Constant	−1.135 (0.7892)	−1.329***(0.2281)
Per capita GDP	0.189***(0.0682)	0.0668***(0.0213)
Per capita fixed-asset investment	0.207***(0.06395)	0.1272***(0.0303)
Per capita fiscal education expenditure	0.457***(0.06851)	0.0504***(0.01582)
Proportion of local fiscal expenditure in GDP	0.222***(0.07292)	−0.1040 (0.0659)
R2	0.6236	0.0984
Sample size	770	990

Note: * * *, ** *, * represent significance levels of 1%, 5% and 10%, respectively, and the robust standard error is in brackets.

coordination degree model, exploratory spatial data analysis (ESDA) techniques, and panel data models, which allow us to reveal the complexity of human-land dynamics from various perspectives. Our study not only uncovers the spatio-temporal patterns and regional disparities of coupling coordination but also identifies the key influencing factors and their relative importance, providing new insights into the driving mechanisms of human-land dynamics in the Yangtze River Economic Belt. The major findings are summarized below.

1. Temporally, the Yangtze River Economic Belt has consistently demonstrated ascending trajectories in population and land urbanization, as well as a concurrent rise in their coupled coordination degree since 2011. The prevalence of severely imbalanced regions was effectively mitigated within the study period. In recent years, the numbers of cities at risk of imbalance, moderately coordinated cities, and well-coordinated cities have stabilized, with an annual increase in highly coordinated cities signaling a shift from low-to high-value coordination areas. Spatially, areas with higher coupled coordination values tend to be clustered in the economically advanced middle and lower reaches of the Yangtze basin, while lower-value areas are predominantly located in the upper reaches. Notably, the disparity in coupled coordination levels across regions is decreasing, exhibiting a distinct pattern of higher values in the east and lower values in the west.
2. The Moran's I index, applied to assess the spatial correlation of the coupled coordination degree between population and land urbanization within the Yangtze River Economic Belt, displays a wave-like pattern, indicative of spatial clustering tendencies. The coupled coordination hot spots are predominantly located in the middle and lower reaches of the belt region; in contrast, cold spots are observed in the upper reaches, specifically in Yunnan and Guizhou, reflecting a spatial pattern characterized by expansive hot spots and confined cold spots.
3. The synergistic progression of population and land urbanization in the Yangtze River Economic Belt can be attributed to the combined influence of various elements, such as governmental regulation, fixed-asset investment, the level of economic development, and investment in education. Among these factors, governmental management has emerged as the foremost driver, and fixed-asset investment exerts a considerable positive effect on coordination; conversely, economic development status and educational investment exert somewhat lesser impacts on the coupling of population and land urbanization.

The selection of 110 prefecture-level cities in the Yangtze River Economic Belt as the research area allows for a granular and localized analysis of the coupling coordination between population urbanization and land urbanization. This regional perspective complements existing studies that have primarily focused on national or provincial levels, providing a more nuanced understanding of the spatial heterogeneity and local variations in human-land interactions during rapid urbanization and economic development.

The integration of multiple complementary methods, including the coupling coordination degree model, ESDA techniques, and panel data models, strengthens the robustness and comprehensiveness of our analysis. These methods enable us to quantify the synchronization and interaction between population urbanization and land urbanization, uncover spatial patterns and clusters, and identify key influencing factors shaping the coupling coordination.

The findings have significant implications for formulating targeted, place-based policies to promote sustainable urbanization and coordinated regional development in the Yangtze River Economic Belt. By identifying regional disparities, spatial clusters, and key influencing factors, our research provides valuable insights for policymakers and urban planners to address imbalances in human-land dynamics and develop effective strategies tailored to the specific needs and characteristics of different cities and regions.

Moreover, our study highlights the value of adopting a comprehensive and integrative approach to analyze human-land dynamics, serving as a useful reference for future related research. The combination of multiple complementary methods demonstrates the importance of considering the multidimensional nature and spatial heterogeneity of human-land interactions, as well as investigating the underlying driving mechanisms from various perspectives.

6 Implications

The strategic vision for the Yangtze River Economic Belt involves harmonizing human and land development to diminish regional imbalances and foster unified progress. Accordingly, the following recommendations are proposed.

6.1 Optimize spatial planning and industrial layout

The government should strengthen the top-level design and spatial planning of the Yangtze River Economic Belt, optimizing the spatial distribution of industries based on local resource endowments and comparative advantages. High-polluting and resource-intensive industries should be gradually phased out or upgraded, while eco-friendly and knowledge-intensive industries should be prioritized. The Yangtze River Delta region should focus on developing high-end manufacturing and modern service industries, while the central and western Yangtze River Economic Belt should leverage their ecological advantages to develop green industries such as ecotourism, organic agriculture, and renewable energy. At the same time, policymakers should prioritize the development of compact, mixed-use urban areas that efficiently utilize land resources while providing accessible employment opportunities and public services. This can be achieved by promoting transit-oriented development, encouraging the growth of knowledge-intensive industries, and revitalizing underutilized urban spaces. By optimizing spatial planning and industrial layout, cities can foster more sustainable and inclusive urbanization patterns that align with the coordinated development of population and land.

6.2 Promote regional coordination and cooperation

To address the regional disparities in the human-land relationship, it is crucial to establish effective coordination mechanisms and platforms for cross-regional cooperation. The government should set

up a high-level coordination committee for the Yangtze River Economic Belt to harmonize regional development strategies, major policies, and key projects. Regional coordination can help mitigate the negative externalities of rapid urbanization, such as urban sprawl, environmental degradation, and social inequalities. Local governments should establish collaborative mechanisms to address cross-jurisdictional issues, such as regional infrastructure planning, environmental protection, and resource sharing. By fostering regional cooperation, policymakers can promote a more integrated and harmonious development pattern that benefits both urban and rural areas. A regional cooperation fund could be established to support joint projects and facilitate resource sharing among regions. The coordination and cooperation should cover various aspects, including infrastructure connectivity, environmental protection, industrial collaboration, and public service provision.

6.3 Improve ecological compensation and green finance mechanisms

To incentivize the protection and sustainable use of natural resources, it is essential to establish a well-functioning ecological compensation mechanism in the Yangtze River Economic Belt. The central government should increase transfer payments to the ecologically fragile areas in the upper reaches of the Yangtze River, compensating them for the ecological services they provide. The compensation funds should be used to support ecological restoration, green infrastructure development, and livelihood improvement for local communities. Additionally, green finance instruments such as green bonds, green credit, and environmental taxes should be leveraged to channel more financial resources into eco-friendly industries and projects.

6.4 Enhance human capital and technological innovation

Investing in human capital and technological innovation is key to improving the human-land relationship in the Yangtze River Economic Belt. The government should increase funding for education, vocational training, and research institutions, particularly in the less-developed central and western regions. Policies should be introduced to attract and retain talent, such as providing housing subsidies, research grants, and entrepreneurship support. Universities and research institutes should be encouraged to collaborate with local industries to promote technology transfer and application. Building a robust regional innovation system is crucial for the Yangtze River Economic Belt to achieve sustainable and high-quality development.

6.5 Foster inclusive and sustainable urbanization

Urbanization has been a major driver of the human-land relationship change in the Yangtze River Economic Belt. To promote inclusive and sustainable urbanization, the government should prioritize the development of small and medium-sized cities, as well as the integration of urban and rural areas. More resources should be allocated to improve public services and infrastructure in rural areas, such as healthcare, education, and transportation. The rural land transfer system should be reformed to protect farmers' land rights while facilitating efficient land use. Moreover, adopting green building standards, promoting sustainable transportation, and preserving urban green spaces can contribute to the creation of livable, low-carbon cities. By fostering inclusive and sustainable urbanization, cities can achieve a more balanced and harmonious development that enhances the wellbeing of both people and the environment.

In conclusion, promoting the coordinated development of the human-land relationship in the Yangtze River Economic Belt requires a holistic and integrated approach that balances economic growth, social equity, and environmental sustainability. The proposed policy recommendations, including optimizing spatial planning, enhancing regional coordination, improving ecological compensation, investing in human capital and innovation, and fostering sustainable urbanization, provide a roadmap for achieving this goal. The successful implementation of these policies calls for concerted efforts from the central government, local authorities, enterprises, and the public. By adopting a more sustainable and inclusive development model, the Yangtze River Economic Belt can become a role model for other regions in China and beyond in terms of harmonizing the human-land relationship and achieving high-quality development.

The coupling relationship between population urbanization and land urbanization is the result of multiple driving factors. This paper adopts analytical methods such as the coupling coordination degree model, exploratory spatial data analysis, and fixed-effects model to analyze the spatiotemporal characteristics and influencing factors of the coordinated development of population urbanization and land urbanization in 110 prefecture-level cities in the Yangtze River Economic Belt. This has important reference significance for optimizing the resource layout of the Yangtze River Economic Belt. Although it can generally reflect the overall spatial pattern and development stage characteristics of population urbanization and land urbanization in the Yangtze River Economic Belt, the coupling relationship between the two is very complex, and the formation and transformation of the coupling state is also subject to the joint action of multiple factors. It should be pointed out that: (1) for the Yangtze River Economic Belt, research on multi-scale and multi-level structures of microscopic subjects is an important direction for future research; (2) the coordinated development level of the Yangtze River Economic Belt shows significant spatial heterogeneity. How to construct differentiated policies for the coordinated development of population urbanization and land urbanization is the direction that needs to be studied next.

Data availability statement

The original contributions presented in the study are included in the article/Supplementary material, further inquiries can be directed to the corresponding author.

Author contributions

LZ: Writing–review and editing. YH: Conceptualization, Data curation, Formal Analysis, Investigation, Methodology, Project administration, Resources, Software, Supervision, Validation, Visualization, Writing–original draft, Writing–review and editing.

Funding

The author(s) declare that financial support was received for the research, authorship, and/or publication of this article. This study was supported by Science and Technology Project of Jiangxi Education Department (No. GJJ2202223) and Humanities and Social Science Project of Jiangxi Province (No. JJ23225).

Conflict of interest

The authors declare that the research was conducted in the absence of any commercial or financial relationships that could be construed as a potential conflict of interest.

The reviewer HL declared a past co-authorship with the author to the handling editor.

Publisher's note

References

Chen, M. X., Lu, D. D., and Zhang, H. (2009). Comprehensive evaluation and the driving factors of China's urbanization. *Acta Geogr. Sin.* 64, 387–398. doi:10.11821/xb200904001

Chen, S. J., and Yu, D. Y. (2023). Spatio-temporal coupling characteristics and influencing factors of the man-land relationship in the urbanization process of Yangtze River Delta urban agglomeration. *World Reg. Stud.*

Chen, X. C., Peng, Y. M., Wang, X. L., Xu, Y., Wang, T., and Pan, Y. (2021). Spatial characteristics and formation mechanism of coordination degree of population and land urbanization in the Yangtze economic belt. *Soil Water Conserv. Res.* 28, 375–379. doi:10.13869/j.cnki.rswc.2021.05.043

Deng, H. D., Zhang, K. E., Wang, F., and Dang, A. (2021). Compact or disperse evolution patterns and coupling of urban land expansion and population distribution evolution of major cities in China, 1998-2018. *Habitat Int.* 108 (34), 102324. doi:10.1016/j.habitatint.2021.102324

Deng, Z. B., Zong, S. W., Su, C. W., and Chen, Z. (2019). Study on the coupled and coordinated development of ecological civilization construction and new urbanization in the Yangtze River economic belt and its driving factors. *Econ. Geogr.* 39, 78–86. doi:10.15957/j.cnki.jjdl.2019.10.011

Fang, C. L., Zhou, C. H., and Wang, Z. B. (2015). Strategic issues and graded gradient development focus of sustainable development of urban agglomerations in the Yangtze economic belt. *Prog. Geogr. Sci.* 34, 1398–1408. doi:10.18306/dlkxjz.2015.11.007

Feng, W. L., Liu, Y. S., and Qu, L. L. (2019). Effect of land-centered urbanization on rural development: a regional analysis in China. *Land Use Policy* 2019, 104072. doi:10.1016/j.landusepol.2019.104072

Han, H. L., and Li, H. (2020). Coupling coordination evaluation between population and land urbanization in Ha-Chang urban agglomeration. *Sustainability* 12, 357. doi:10.3390/su12010357

Huang, L., and Yang, P. (2021). Spatio-temporal characteristics and driving factors of the coordinated development of non-agriculturalization of population-land-industry in the Yangtze River economic belt. *China Agric. Resour. Zoning* 42, 182–192. doi:10.7621/cjarrp.1005-9121.20210821

Li, X. M., and Cui, L. (2022). Coupling and influencing factors of digital logistics, regional economy and carbon environmental governance: an empirical test based on panel data of 30 provinces in China. *China Bus. Mark.* 36, 11–22. doi:10.14089/j.cnki.cn11-3664/f.2022.02.002

Li, Z. L., Kuang, W. H., and Zhao, D. D. (2020). Coupling mechanism of population urbanization and land use in the Beijing-Tianjin-Hebei urban agglomeration. *Econ. Geogr.* 40, 67–75. doi:10.15957/j.cnki.jjdl.2020.08.009

Lin, A. W., and Fan, X. (2015). Analysis of the coordinated development of population urbanization and land urbanization in Hubei Province. *Reg. Res. Dev.* 34, 14–18.

Liu, H., Deng, H. B., and Li, X. F. (2016). Study on the spatio-temporal differences of the coordinated development of population urbanization and land urbanization in the Yangtze River economic belt. *China Popul. Resour. Environ.* 26, 160.

Lu, D. D., and Chen, M. X. (2015). Several understandings on the "national new urbanization plan (2014-2020)" compilation background. *Acta Geogr. Sin.* 70, 179–185. doi:10.11821/dlxb201502001

Lü, T. G., Wu, C. F., Li, H. Y., You, H., and Cai, X. (2016). The coordination and its optimization about population and land of urbanization: a case study of Nanchang city. *Sci. Geogr. Sin.* 36, 239–246. doi:10.13249/j.cnki.sgs.2016.02.010

Shan, L., Jiang, Y. H., Liu, C. C., Wang, Y. F., Zhang, G. H., and Cui, X. F. (2021). Exploring the multi-dimensional coordination relationship between population urbanization and land urbanization based on the MDCE model: a case study of the Yangtze River Economic Belt, China. *PloS one* 6, e0253898. doi:10.1371/journal.pone.0253898

Sun, J. W. (2018). On the development and innovation of regional coordinated development strategy in the new era. *J. Chin. Acad. Gov.*, 109–114+151. doi:10.14063/j.cnki.1008-9314.20180808.005

Sun, J. W., Xi, Q. M., and Yi, S. C. (2023) *New urbanization and regional coordinated development*. Beijing: China Renmin University Press.

Wang, X. F., and Wen, Y. P. (2019). Study on the evolution and coordination of the spatial pattern of population urbanization and land urbanization in Hunan province. *J. Nat. Sci. Hunan Norm. Univ.* 42, 34–43. doi:10.7612/j.issn.2096-5281.2019.05.005

Wang, X. Y., Yang, X. P., and Zhang, X. M. (2017). Evaluation of urbanization efficiency and its influencing factors based on DEA-Tobit two-step method: from the perspective of coordinated development between population urbanization and land urbanization. *Ecol. Econ.* 33, 29–34.

Wei, Y., Xiu, C. L., and Sun, P. J. (2013). Analysis of the urbanization driving mechanism in China since the 21st century. *Geogr. Res.* 32, 1679–1687. doi:10.11821/dlyj201309010

Wen, Y. P., and Wang, X. F. (2019). Study on the coupling and coordination relationship between industrial structure and ecological environment from the perspective of urbanization in the urban agglomeration of the middle reaches of the Yangtze river. *J. Cent. China Norm. Univ.* 53, 263–271. doi:10.19603/j.cnki.1000-1190.2019.02.015

Wu, Y. F., Liu, Y. S., and Li, Y. R. (2018). Spatio-temporal coupling characteristics and driving mechanisms of population and land urbanization in China. *Acta Geogr. Sin.* 73, 1865–1879. doi:10.11821/dlxb201810004

Xu, F., Wang, Z. Q., Chi, G. Q., and Zhang, Z. (2020). The impacts of population and agglomeration development on land use intensity: new evidence behind urbanization in China. *Land Use Policy* 95, 104639. doi:10.1016/j.landusepol.2020.104639

Xu, G., Zheng, M. C., Wang, Y. X., and Li, J. (2022). The urbanization of population and land in China: temporal trend disparities, size, effect and comparisons of measurements. *China Land Sci.* 36, 80–90. doi:10.11994/zgtdkx.20220513.183256

Yang, L. X., Yuan, S. F., and Wang, X. C. (2013). Study on the spatial differences of the coordinated development of population urbanization and land urbanization: taking 69 counties and cities in Zhejiang province as an example. *China Land Sci.* 27, 18–22+30. doi:10.13708/j.cnki.cn11-2640.2013.11.004

Yang, Y., Tang, X. L., Jia, Y. Y., and Zhan, Q. Q. (2021). Spatio-temporal coupling and coordination of population-land-economic urbanization in the Yangtze river basin and analysis of driving factors. *World Geogr. Res.* 30, 978–990. doi:10.3969/j.issn.1004-9479.2021.05.2020120

Yao, S. M., Zhang, Y. H., Lu, D. D., and Yu, C. (2013). Several key issues of China's new urbanization: an interpretation of premier Li Keqiang's new ideas. *Urban Obs.*, 5–13. doi:10.3969/j.issn.1674-7178.2013.05.001

Zhang, L. X., and Duan, W. K. (2021). Urban land urbanization patterns and influencing factors under the background of economic transition: a case study of cities in the Yangtze River economic belt. *J. China Agric. Univ.* 26, 206–215. doi:10.11841/j.issn.1007-4333.2021.09.22

Zhang, S. L., Zheng, H. Q., Zhou, H. Y., Shao, Q., and Wu, Q. (2021). Sustainable land urbanization, urban amenities, and population urbanization: evidence from city-level data in China. *Soc. Sci. Q.* 4, 1686–1698. doi:10.1111/ssqu.13003

Zhang, X. J., Xu, W. X., and Liu, C. J. (2019). Research on spatial-temporal differentiation and influencing mechanism of "economy-land-population-society" urbanization coupling coordination in Guangdong-Hong Kong-Macao greater bay area. *Explor. Econ. Probl.*, 54–64.

frontiers | Frontiers in Environmental Science

TYPE Original Research
PUBLISHED 03 July 2024
DOI 10.3389/fenvs.2024.1435714

OPEN ACCESS

EDITED BY
Xiao Ouyang,
Hunan University of Finance and Economics, China

REVIEWED BY
Bo Liu,
Hunan Agricultural University, China
Peng Cao,
Henan University of Technology, China

*CORRESPONDENCE
Fanglin Ma,
2858463007@qq.com

RECEIVED 20 May 2024
ACCEPTED 12 June 2024
PUBLISHED 03 July 2024

CITATION
Liu K and Ma F (2024), The impact of the digital economy on environmental pollution: a perspective on collaborative governance between government and Public.
Front. Environ. Sci. 12:1435714.
doi: 10.3389/fenvs.2024.1435714

The impact of the digital economy on environmental pollution: a perspective on collaborative governance between government and Public

Kai Liu[1,2] and Fanglin Ma[3]*

[1]College of Finance and Statistics, Hunan University, Changsha, China, [2]The Dalla Lana School of Public Health, University of Toronto, Toronto, ON, Canada, [3]School of Mathematics and Statistics, Hunan Normal University, Changsha, China

The rapid development of the digital economy is driving transformative changes in a multifaceted collaborative environmental governance system. From the perspective of collaborative governance between government and the public, this study employs double fixed-effects models, spatial econometric models, and instrumental variables methods to empirically explore how the digital economy influences environmental pollution, using panel data from 30 provinces in China spanning 2011 to 2022. The results demonstrate that the digital economy significantly lowers environmental pollution. The primary mechanism is through the government's environmental governance behaviors, which are positively moderated by public environmental concerns, enhancing effectiveness. Additionally, the digital economy induces a spatial spillover effect on environmental pollution. This promotion of collaborative management between the government and the public is poised to become a pivotal direction in future environmental governance.

KEYWORDS

digital economy, environmental pollution, environmental governance, coordinated governance, spatial spillover

1 Introduction

As one of the world's largest energy consumers and carbon emitters, improving environmental pollution in China holds significant importance for the global environment. Yet, China's environmental challenges are extremely severe. To tackle this, it's crucial to actively embrace the new development concept, focus on building and enhancing an ecological civilization system, and unwaveringly pursue a green, circular, and low-carbon economic growth path.

The digital economy, which involves economic activities created by connecting individuals, organizations, and information systems via digital technology, is rapidly evolving (Carlsson, 2004; Sturgeon, 2021; Zhen et al., 2021; Zou and Deng, 2022). The influence of the digital economy on environmental pollution is a key focus among scholars. The digital economy reduces environmental pollution by fostering technological innovation and refining industrial structures (Zhang et al., 2023). It also enhances the integration of the real economy with industry using production factors such as knowledge, information, and IT, playing a vital role in boosting production efficiency (Pan et al., 2022), reducing carbon

emissions (Xie et al., 2024), and advancing green transformations (Liu and Zhao, 2024). Technologies like artificial intelligence, big data, and industrial robots are reshaping industrial chains (Moyer and Hughes, 2012)and enhancing green total factor productivity (Chen et al., 2023; Wang et al., 2024), thus driving high-quality development (Wang et al., 2024). From this perspective, studying the impact of the digital economy on environmental pollution and the underlying mechanisms behind it is of significant importance for achieving green and sustainable development.

However, the synergistic mechanisms between government environmental governance and social public participation have not received adequate attention, presenting an opportunity to expand this area of research. The use of big data platforms and Internet technology can enhance the informatization of government environmental oversight, the scientific basis of environmental protection decisions, and deepen social participation (Wei and Zhang, 2023). These advancements improve the government's capacity to manage the environment and further reduce environmental pollution levels. Notably, a diverse and shared environmental governance model is emerging in China, where the government leads and public participation supports. Public involvement acts as an informal environmental regulation (Tan and Eguavoen, 2017), compelling local governments to focus on environmental protection and increase invest-ments in environmental pollution control (Ge et al., 2021), which contributes to environmental improvement (Wang et al., 2023).

This study investigates how the development of digital economy impacts regional environmental pollution governance through collaborative efforts between the government and the public. The findings indicate that the digital economy significantly reduces environmental pollution levels. This reduction prompts local governments to increase investments in environmental pollution control, enhance their focus on environmental governance, and enforce environmental protection penalties, thereby improving regional environmental quality. These conclusions remain robust after various analyses, including the instrumental variable method and substituting explanatory variables. Public environmental concern also positively moderates the relationship between the digital economy and environmental pollution, indicating that the digital economy enhances environmental governance effectiveness through increased government and public interaction and participation.

The potential marginal contribution of this paper is twofold: Firstly, we use the co-management by multiple environmental stakeholders as the entry point, positioning the digital economy, governmental environmental governance, public environmental concern, and environmental pollution prevention within the same analytical framework to systematically assess the governance effects of the digital economy on environmental pollution. This encourages us to consider the synergistic effects of government environmental governance and social public participation, offering a fresh perspective for deeply understanding how the digital economy contributes to green development. Secondly, this paper delves into the specific transmission mechanisms through the interaction between local governments and the public, aiming to explore the long-term mechanisms of environmental governance facilitated by collaborative efforts between the government and the public.

The structure of the paper is as follows: Section 1 introduces the study. Section 2 reviews relevant literature and presents theoretical analyses. Section 3 outlines the research design, including variable selection, data sources, and model construction. Section 4 analyzes empirical results, covering baseline regression outcomes, impact mechanisms, moderating effects, and tests for spatial effects. Section 5 conducts robustness tests, utilizing approaches like the instrumental variables method, substitution of explanatory variables, and heterogeneity analysis. Finally, Section 6 offers conclusions and policy recommendations.

2 Theoretical mechanism and research hypothesis

2.1 The development of digital economy can reduce environmental pollution

The rapid advancement and widespread adoption of digital information technologies—such as the Internet, big data, and artificial intelligence—not only inject new momentum into economic development but also facilitate the restructuring of the environmental governance system encompassing government, businesses, and society. This restructuring supports the economy's transition to green and low-carbon operations. Specifically, within enterprises, the innovative breakthroughs in digital technology serve as a key driver for eco-friendly economic practices. As primary agents of pollution control, businesses utilize digital technologies to gather information and consolidate resources, enabling informed production decisions and enhancing operational efficiency (Zhang Rongwu et al., 2022). Moreover, the digital economy enhances knowledge dissemination efficiency in electronic equipment, communication networks, and information processing, encouraging enterprises to adopt green production models. This undoubtedly fosters technological innovation and industrial upgrading, ultimately contributing to both pollution reduction and green development (Xu et al., 2023).

In terms of governmental environmental governance, digital technology facilitates the development and application of ecological and environmental data, effectively collecting, integrating, and sharing critical information like pollution levels and environmental carrying capacity. This data supports dynamic assessments and supervision of governmental environmental efforts, improving pollution perception and early warning capabilities (Fang et al., 2024), and enhancing the precision and effectiveness of environmental supervision. This provides a robust data foundation for crafting environmental policies and refining the ecological regulation framework, thereby elevating the government's role in environmental management (Shin and Choi, 2015).

Regarding public supervision and participation, the digital economy simplifies ac-cess to environmental information and raises public environmental awareness by enhancing public service platforms and fostering information exchange between the government and the community. The public can engage in environmental oversight through avenues such as social media, ensuring adherence to environmental regulations and governance policies, and supervising pollution activities and enforcement. This transformation of environmental consciousness into action facilitates collaborative governance of environmental pollution by both government and the public (Yang et al., 2020).

In conclusion, the development of digital economy impacts environmental pollution by promoting green production in

enterprises, refining governmental environmental regulatory frameworks, and enhancing social and public oversight. Based on these insights, this paper proposes the following research hypothesis:

Hypothesis 1: The development of digital economy will reduce environmental pollutant emissions, i.e., digital economic development contributes to effective environmental pollution management.

2.2 Government and Public synergy mechanism

2.2.1 Government environmental governance mechanism

Reducing environmental pollution is a systematic project requiring the participation and synergy of multiple actors, including the government, enterprises, and the public. From the perspective of interactive synergy between the government and the public, analyzing the impact of the digital economy on the environmental governance behaviors of local governments can deepen our understanding of China's environmental pollution governance model.

Firstly, the digital economy enables the government to efficiently collect, integrate, and share environmental data, scientifically assess government environmental governance performance, and enhance the accuracy and effectiveness of environmental supervision, thus boosting the government's regulatory capacity (Zhao Shuliang et al., 2023). Additionally, the government can use digital technology to expand communication channels for knowledge diffusion, support environmental regulation, and improve policy formulation and implementation, which also increases government transparency (Peng et al., 2023), and improves environmental governance (Ahlers and Shen, 2018).

Secondly, investment in environmental pollution management reflects the commitment and effort of local governments in environmental governance. The digital economy drives local governments to increase their investments in environmental governance through digitized knowledge, information, technology, and other production factors, thereby elevating the level of ecological and environmental governance (Su et al., 2018; Zhu and Li, 2020).

Thirdly, the digital economy aids the development and utilization of environmental data and information, reducing information asymmetry between various government departments, businesses, and the public. This breaks down data barriers, forms a comprehensive ecological and environmental data system, and improves the transparency of local government environmental protection (Ahlers and Shen, 2018). The digital economy also enhances government environmental supervision and law enforcement capabilities, enabling the government to impose penalties on non-compliant businesses (Wu et al., 2024), strengthen the investigation and handling of environmental violations and penalties (Li Mingxian et al., 2023; Liu et al., 2024), and deter environmental non-compliance by businesses, which in turn reduces environmental pollution emissions.

Based on the above analysis, the following hypothesis is proposed:

Hypothesis 2: The digital economy affects environmental pollution governance through the pathways of government environmental governance attention, environmental pollution governance investment, and environmental protection administrative enforcement efforts.

2.2.2 Regulatory effect of Public environmental concern

Social public participation, supplementing environmental regulation, supervises and influences local government environmental governance behaviors. With the rapid advancement of digital technology, the public can share social resources and create public service platforms using the Internet and big data. This platform model enables the public to easily access environmental information, express their opinions, and voice their dissatisfaction with pollution issues and demand for environmental quality improvement (Tan and Eguavoen, 2017). The theory of government responsiveness suggests that government environmental governance behaviors are influenced by and respond to regional public opinion, aligning environmental policies with public preferences (Arantes, 2023). In response to public environmental demands, the government reduces Environmental pollution by increasing attention to environmental governance, boosting investment in pollution control, and imposing administrative penalties for environmental protection (Sun et al., 2023; Liu et al., 2024).

On the other hand, under the Chinese environmental governance model, public satisfaction with environmental governance is a crucial metric for assessing local government performance. The digital economy promotes public environmental demands, participation, and supervision, compelling higher-level governments to motivate and oversee lower-level government environmental policies and behaviors, which assists in reducing local environmental pollution (Niu et al., 2024). As the primary responder, local governments attend to public environmental demands and actively respond through their governance practices, adjusting their environmental policy preferences, which undoubtedly enhances the environmental governance performance of local governments. The digital economy influences local government environmental policy adjustments and governance behaviors by elevating public environmental concerns and transforming public demands into active participation in environmental protection activities (Arantes, 2023).

The above logical mechanism is summarized as follows: The digital economy contributes to the interaction between the government and the public, influences public environmental awareness and behavior, and guides the public to pay attention to and participate in the process of environmental governance, thus fostering a governance system that is scientific in decision-making, refined in supervision, and convenient in service. By influencing local government environmental governance behaviors, public environmental demands compel local governments to enhance their focus on environmental governance, increase investments in environmental pollution control and enforcement, and ultimately aid in regional environmental pollution control.

As a result, the following hypothesis is derived:

Hypothesis 3: Public environmental concern positively moderates the relationship between the digital economy and environmental pollution, enhancing the impact of digital economy on government environmental regulation.

TABLE 1 Comprehensive Evaluation Indicator System for the development of digital economy.

Primary indicator	Secondary indicator	Description of indicator	Unit
Digital infrastructure	Internet penetration	Number of internet broadband access ports	Ten thousand units
		Number of internet broadband subscribers	Ten thousand households
		Number of internet domains	Ten thousand units
	Mobile phone penetration	Mobile phone base station density	Units per square kilometer
		Mobile phone penetration rate	Devices per 100 people
	Breadth of information transmission	Length of long-distance optical cables per area	Kilometers per square kilometer
Digital industrialization	Software and IT services	Revenue from software business as a percentage of GDP	%
		Number of employees in IT and software services	Ten thousand people
	Level of electronic information manufacturing	Revenue from electronic information manufacturing as a percentage of GDP	%
		Total volume of telecommunications business as a percentage of GDP	%
		Per capita telecommunications business volume	Yuan per person
	Development level of postal and telecommunications	Total postal services per capita	Yuan per person
		Per capita postal business volume	Ten thousand items
		Corporate e-commerce transaction volume	Hundred million yuan
Industrial digitization	Enterprise digital development	Proportion of enterprises engaged in E-commerce transaction	%
		Number of computers per 100 people in enterprises	Units
		Number of websites per 100 enterprises	Units
	Digital inclusive finance	Digital inclusive finance index	—
Digital innovation capacity	R&D level in enterprises	Full-Time equivalent R&D personnel in large-scale industrial enterprises	Person-year
		R&D expenditure in industrial enterprises above a designated size	Ten thousand yuan
		Number of R&D projects in large-scale industrial enterprises	Projects
	Technological innovation capacity	Total amount of technology contracts	Ten thousand yuan
		Number of patent applications granted	Items

2.3 Spatial spillover effects

The spatial spillover effect of the digital economy and environmental pollution is a crucial prerequisite for spatial measurement research. The spatial spillover effect of the digital economy has been extensively studied (Li Guangqin et al., 2023; Hou et al., 2023; Xu, 2024), with scholars exploring its impacts on rural revitalization (Li Guangqin et al., 2023) and industrial green innovation (Li Mingxian et al., 2023).

Conversely, the spatial spillover effect of environmental factors has also garnered significant attention (Liu et al., 2020; Zhang Maomao et al., 2022; Zhao Feng et al., 2023). This includes research on water pollution (Liu, et al., 2020), the interplay between urbanization and environmental pollution (Zhao Feng et al., 2023), the relationship between industrial agglomeration and environmental pollution (Zhang Maomao et al., 2022), and the mismatch of land resources contributing to environmental issues (Wan and Shi, 2022). Given that both the digital economy and environmental pollution exert influences on surrounding areas, it is conceivable that the digital economy might also impact environmental pollution in neighboring regions through spatial spillovers.

Thus, the following hypothesis is proposed:

Hypothesis 4: The digital economy will exert spatial spillover effects on environmental pollution.

3 Research design

3.1 Variable selection

3.1.1 Explained variable

Environmental pollution level (Pol). The entropy weighting method is used to calculate a comprehensive environmental pollution index for regional industrial wastewater, sulfur dioxide

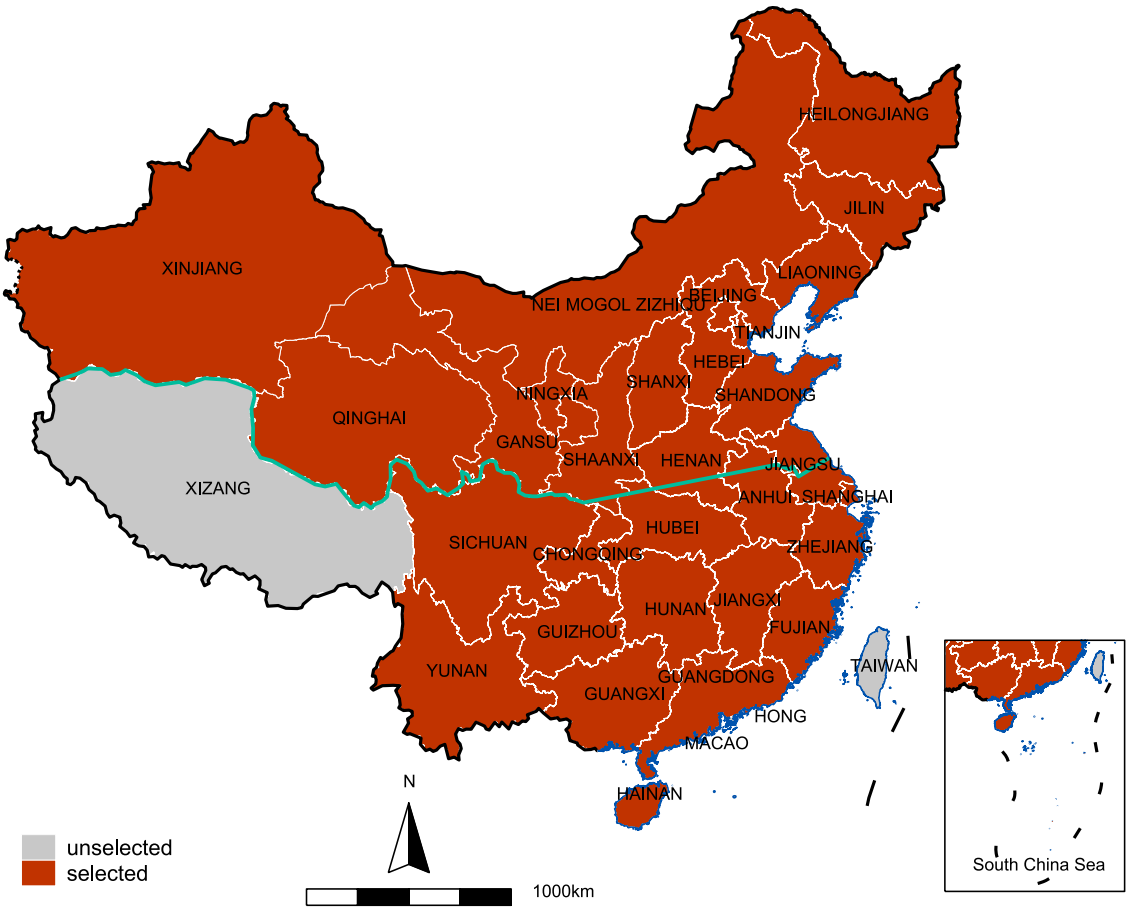

FIGURE 1
Selected provincial samples.

emissions, and solid waste emissions as a measure of the level of environmental pollution in each region.

3.1.2 Main explanatory variable

The explanatory variable in this paper is the digital economy (Dtf). Currently, defining the connotation of the digital economy is challenging, with many scholars understanding it as the sum of economic activities based on modern information technology (Carlsson, 2004; Sturgeon, 2021; Zhen et al., 2021; Zou and Deng, 2022). In this paper, we build on the work of Wang et al. (2021) to construct a digital economy development index using the entropy weight method. We select indicators from four dimensions: digital infrastructure, digital industrialization, industrial digitization, and digital innovation capability. The specific indicators are presented in Table 1.

3.1.3 Mechanistic variables

This study identifies three core mechanistic variables to dissect the behavioral patterns of local governments in environmental governance. First, the degree of pre-existing attention to environmental governance (en) is quantified by analyzing the frequency of environmental and haze-related terms in the annual work reports of provincial governments. Secondly, the financial commitment to environmental pollution control (ei) is gauged by the total provincial investment in this area. Finally, the post-action intensity of enforcing environmental regulations (ez) is measured through the tally of environmental administrative penalty cases. These variables are designed to provide a comprehensive evaluation of the government's dedication and efficacy in environmental protection.

3.1.4 Moderating variable

The moderating variable, public environmental concern (pf), is represented by the Baidu haze search index. This choice is primarily due to Baidu's status as the largest Chinese search engine, which offers extensive coverage and high data availability, allowing for detailed regional analysis based on search frequency and trends. Haze, as an environmental issue, tends to register a higher level of public awareness compared to other issues like environmental pollution, making it an ideal measure of environmental concern.

TABLE 2 Descriptive statistics.

Variable type	Variable name	Variable symbol	Mean	Standard deviation	Minimum	Maximum
dependent variable	environmental pollution Level	Pol	0.795	0.564	0.164	3.643
independent variable	the digital economy	Dtf	0.114	0.102	0.014	0.599
mechanistic variables	government environmental governance attention	en	0.345	0.311	0.017	1.773
	environmental pollution control investment	ei	5.414	2.978	2.108	21.132
	government environmental enforcement effort	ez	0.839	0.647	0.256	3.605
moderating variable	public environmental awareness	pf	0.311	0.368	0.002	2.031
control variables	financial freedom	ff	0.491	0.188	0.151	0.931
	financial development level	fin	0.041	0.013	0.020	0.085
	infrastructure	inf	0.004	0.003	0.001	0.013
	healthcare level	sin	39.064	9.856	16	75
	technology input	tec	111.379	60.476	16.635	324.157
	education level	edu	277.555	85.769	108.2	561.3
	elderly dependency ratio	old	38.553	7.367	19.3	56.7
	child dependency ratio	chi	22.986	6.208	9.9	36.4

3.1.5 Control variables

In a bid to thoroughly examine the digital economy's influence on environmental pollution, this study introduces various control variables: fiscal freedom (ff), gauged by the ratio of fiscal revenue to fiscal expenditures; financial development level (fin), defined by the urban financial employment per 10,000 people; infrastructure (inf), assessed through the ratio of highway kilometers to developed area; medical care level (sin), measured by the number of practicing assistant physicians per 10,000 people; science and technology investment (tec), represented by the ratio of industrial enterprises' R&D expenditures to regional GDP; education level (edu), based on the average higher education enrollment per 10,000 population; old-age burden (old), using the elderly dependency ratio; and parenting burden (chi), determined by the child dependency ratio.

3.2 Model Setting

Based on the results of the Hausman test (test value of 39.472, p-value of 0), the fixed effect model is deemed appropriate. Given that the data are panel data, and drawing on the methodology of Zhang et al. (2023), a double fixed-effect model is employed to analyze the impact of the digital economy on environmental pollution. The specific model (1) is presented as follows.

$$Pol_{i,t} = \alpha_0 + \alpha_1 Dtf_{i,t} + \alpha_2 Z_{i,t} + \mu_i + \delta_t + \varepsilon_{i,t} \quad (1)$$

In Eq. 1, Poli,t represents the level of environmental pollution in province i during period t; Dtfi,t denotes the level of the digital economy in province i during the same period; the vector Zi,t includes a series of control variables for environmental pollution; μi symbolizes the individual fixed effect, while δt controls for the time fixed effect; εi,t is the random disturbance term.

Secondly, to explore the mechanisms through which the digital economy impacts environmental pollution, a transmission effect model is introduced as depicted in Eqs 2, 3. Here, itvi,t represents a series of mechanism variables through which the digital economy influences environmental pollution.

$$Itv_{it} = \beta_0 + \beta_1 Dtf_{i,t} + \beta_2 Z_{i,t} + \mu_i + \delta_t + \varepsilon_{i,t} \quad (2)$$

$$Plo_{i,t} = \gamma_0 + \gamma_1 itv_{i,t} + \gamma_2 Z_{i,t} + \mu_i + \delta_t + \varepsilon_{i,t} \quad (3)$$

Thirdly, to assess the moderating effect of public environmental concern on the mechanism variables, this effect is captured in Eq. 4.

$$Itv_{i,t} = \eta_0 + \eta_1 Dtf_{i,t} + \eta_2 Dtf_{i,t} * \mathrm{p}f + \eta_3 Z_{i,t} + \mu_i + \delta_t + \varepsilon_{i,t} \quad (4)$$

Additionally, the explanatory variables and the cross-multiplication term of each control variable with the spatial weight matrix are integrated into Eq. 1 to construct the Spatial Durbin Model (SDM), as detailed in Eq. 5. Here, φ2 represents the spatial spillover coefficient, and W is the spatial weight matrix.

$$Pol_{i,t} = \varphi_0 + \varphi_1 Dtgf_{i,t} + \varphi_2 WDtf_{i,t} + \varphi_3 Z_{i,t} + \varphi_4 WZ_{i,t} + \mu_i + \delta_t + \varepsilon_{i,t} \quad (5)$$

3.3 Data sources and descriptive statistics

Drawing on the approach of Zhang et al. (2023), 30 provinces in China (excluding Tibet, Taiwan, Hong Kong, and Macau) are selected as the research sample, covering the period from 2011 to 2022. The

TABLE 3 Main results.

Variable	Pol				
	(1)	(2)	(3)	(4)	(5)
Dtf	−1.087***	−1.078***	−1.254***	−1.442***	−1.328***
	(0.270)	(0.274)	(0.262)	(0.265)	(0.264)
ff		−0.987***	−0.926***	−0.984***	−0.849***
		(0.302)	0.287	(0.282)	(0.277)
fin		−2.995***	−3.107***	−5.709***	−5.948***
		(1.515)	(1.445)	(1.495)	(1.465)
inf			9.429	6.381	9.960
			(11.584)	(11.329)	(11.259)
sin			−0.011***	−0.010***	−0.008***
			(0.002)	(0.002)	(0.002)
tec				−0.001***	−0.002***
				(0.001)	(0.001)
edu				−0.002***	−0.002***
				(0.001)	(0.001)
old					−0.025***
					(0.006)
chi					0.017***
					(0.010)
_cons	0.400***	1.346***	1.970***	3.082***	3.299***
	(0.078)	(0.243)	(0.253)	(0.336)	(0.343)
region effects	yes	yes	yes	yes	yes
time effects	yes	yes	yes	yes	yes
N	360	360	360	360	360
adj R^2	0.880	0.917	0.925	0.931	0.934

Note: *, **, *** indicates significant at the 10%, 5%, 1% level, the brackets are robust standard.

selected provinces are shown in Figure 1. The data for the dependent variables are sourced from the China Environmental Yearbook. Composite indicators for the dependent variables are derived from the digital finance Index of Peking University, the China Statistical Yearbook, and the respective statistical yearbooks of each province. The data for the control variables are also obtained from the China Statistical Yearbook and the provincial statistical yearbooks. Descriptive statistics for each variable are presented in Table 2.

4 Empirical analysis

4.1 Benchmark regression

Table 3 illustrates the results of a regression analysis on the impact of the digital economy on environmental pollution. As control variables were incrementally added to the regression model, the estimated coefficient for the core explanatory variable, the digital economy index (Dtf), consistently showed a significant negative effect. This strongly supports the hypothesis that the digital economy significantly mitigates or reduces environmental pollution, confirming Hypothesis 1.

Among the control variables, fiscal freedom's impact on environmental pollution is also negative, suggesting that increased fiscal freedom provides local governments with more resources to combat environmental pollution. Financial development negatively correlates with environmental pollution; higher financial development levels likely channel more funds towards sustainable practices, thereby reducing pollution levels. However, the influence of infrastructure development on environmental pollution was found to be statistically insignificant. Medical care levels also negatively affect environmental pollution, implying that higher levels of healthcare lead to greater public awareness and concern for health, which in turn discourages environmental pollution. The impact of investments in

TABLE 4 Mechanism analysis.

Variable	en	Pol	ei	Pol	ez	Pol
	(6)	(7)	(8)	(9)	(10)	(11)
	2.413***		4.294***		2.083***	
Dtf	(0.082)		(0.991)		(0.321)	
		−0.541***				
en		(0.093)				
				−0.109***		
ei				(0.014)		
						−1.161***
ez						(0.281)
_cons	−0.768***		18.610***	5.211***	1.296***	3.002***
	(0.107)		(1.287)	(0.423)	(0.417)	(0.363)
control variables	yes	yes	yes	yes	yes	yes
region effects	yes	yes	yes	yes	yes	yes
time effects	yes	yes	yes	yes	yes	yes
N	360	360	360	360	360	360
adj R2	0.979	0.936	0.967	0.941	0.926	0.929

science and technology on environmental pollution is also negative, reinforcing the idea that technological advancements drive energy efficiency and pollution reduction. Similarly, higher education levels correlate with reduced environmental pollution, as they foster more expertise in pollution prevention and control. The old-age dependency ratio negatively affects environmental pollution. Elderly populations, being more health-sensitive, tend to reside in areas with better environmental conditions, thus places with higher elderly care levels experience lower pollution. In contrast, the child dependency ratio has a positive impact on environmental pollution. In regions with higher fertility rates, which typically have more outdated production methods, environmental pollution is more severe.

4.2 Mechanism analysis

Hypothesis 2 asserts that the development of the digital economy impacts the level of environmental pollution through pathways such as increased government focus on environmental governance, greater investment in pollution control, and more stringent environmental administrative law enforcement. This section provides an empirical examination of these mechanisms, with regression outcomes detailed in Table 4. Results from columns (7), (9), and (11) reveal that the digital economy substantially enhances government attention to environmental governance, boosts investment in environmental pollution control, and strengthens environmental administrative law enforcement. Furthermore, data from columns (6), (8), and (10) indicate that public environmental concern, environmental regulation level, green innovation level, and industrial structure significantly diminish environmental pollution levels. Consequently, the digital economy mitigates environmental pollution through mechanisms that influence government attention, investment in pollution control, and the enforcement of environmental laws, thus confirming Hypothesis 2.

TABLE 5 Test of moderating effect of public environmental concern.

Variable	pf	en	ei	ez
	(12)	(13)	(14)	(15)
Dtf	3.019***	0.754***	9.407***	4.586***
	0.138	0.143	2.129	0.681
Dtf* pf		0.730***	2.251***	1.102***
		0.056	0.832	0.266
control variables	yes	yes	yes	yes
region effects	yes	yes	yes	yes
time effects	yes	yes	yes	yes
N	360	360	360	360
adj R2	0.958	0.986	0.967	0.931

4.3 Analysis of the regulatory effects of public environmental concerns

Hypothesis 3 posits that public environmental concern positively moderates the relationship between the digital economy and environmental pollution, enhancing the impact of digital economy on government environmental regulation.

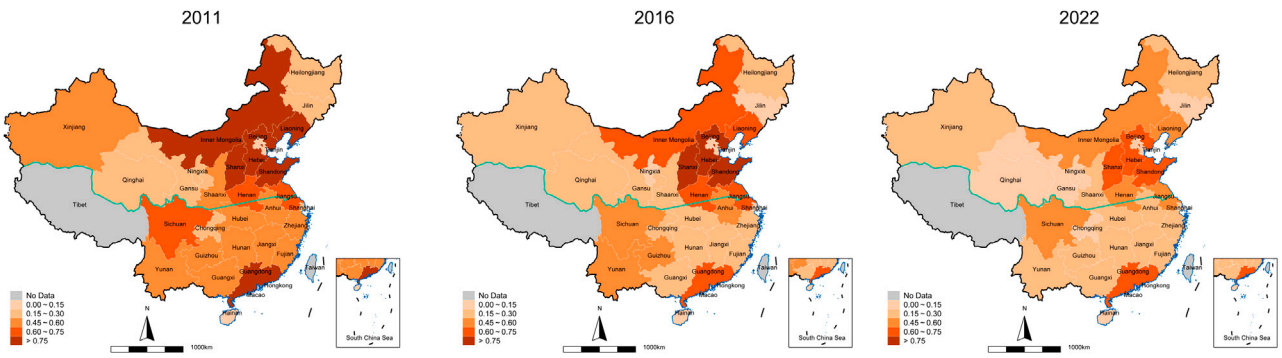

FIGURE 2
Spatial Distribution Map of Environmental pollution.

Table 5, column (12), demonstrates that the impact of the digital economy on public environmental concern is significantly positive at the 1% level, indicating that the digital economy boosts public environmental awareness. Columns (13), (14), and (15) show that after incorporating the interaction term between the digital economy and public environmental concern, the digital economy positively affects local government attention to environmental protection, investment in environmental pollution control, and environmental law enforcement efforts, all significant at least at the 10% level.

Moreover, the interaction term between the digital economy and public environmental concern is significantly positive, highlighting that the digital economy promotes government attention to environmental protection, environmental pollution control investment, and law enforcement efforts by increasing public awareness. In essence, the development of digital economy enhances environmental quality by fostering the synergy of public environmental concerns and prompting local governments to intensify their environmental governance efforts. This process is indicative of China's evolving pattern of diverse and collaborative environmental governance, driven by the government with widespread public involvement, which plays a pivotal role in controlling environmental pollution and outlines the future trajectory of environmental governance. Hypothesis 3 is validated.

4.4 Spatial spillover effect test

Hypothesis 4 believes that the digital economy will have a spatial spillover effect on environmental pollution. This part examines the spatial spillover effect of the digital economy. It is mainly divided into three parts: comparative analysis of spatial distribution maps, spatial autocorrelation test, and spatial econometric regression. The specific process is as follows:

4.4.1 Comparative analysis of spatial distribution maps

Figure 2 shows the spatial distribution of the environmental pollution in 2011, 2016, and 2022. Overall, from 2011 to 2022, the environmental pollution showed a downward trend, indicating that the environmental pollution in China is improving. The provinces with a relatively high degree of environmental pollution are concentrated in the northern part of China, such as Inner Mongolia, Shanxi, and Hebei. The environmental pollution in the eastern coastal provinces is relatively low. The environmental pollution of each province shows certain characteristics of spatial agglomeration.

Figure 3 shows the spatial distribution of the digital economy of various provinces in China in 2011, 2016, and 2022. It can be seen that the level of China's digital economy has achieved relatively large development from 2011 to 2022. Moreover, the development level of the digital economy in northern provinces is lower than that in the south. The development level of the digital economy in southeastern coastal provinces is relatively high, and there is also a certain degree of spatial agglomeration in the development level of the digital economy in space. By comparing Figure 2, it can be found that the environmental pollution of Inner Mongolia, Shanxi, Hebei and other provinces is at a relatively high position in the whole country, and the development level of the digital economy is at a relatively low position in the whole country. The environmental pollution of coastal provinces is at a relatively low level in the whole country, and the development level of the digital economy is at a relatively high position in the whole country. There is a certain correspondence in the spatial distribution between the two. In the following text, the spatial autocorrelation level of the environmental pollution and the development of the digital economy will be further tested.

4.4.2 Spatial autocorrelation test

The premise of the spatial econometric model is the existence of spatial correlation among the study variables. The Moran's Index is used to test the spatial autocorrelation between the digital economy and environmental pollution from 2011 to 2022. Table 6 presents the Moran indices for both digital economy and environmental pollution levels using a geographical distance matrix. The results show significant spatial autocorrelation at the 1% level for the period studied, justifying further spatial econometric regression.

4.4.3 Spatial econometric regressions

The outcomes from spatial measurement regressions are reported in columns (16) to (19) of Table 7, utilizing four different spatial weight matrices: neighborhood distance,

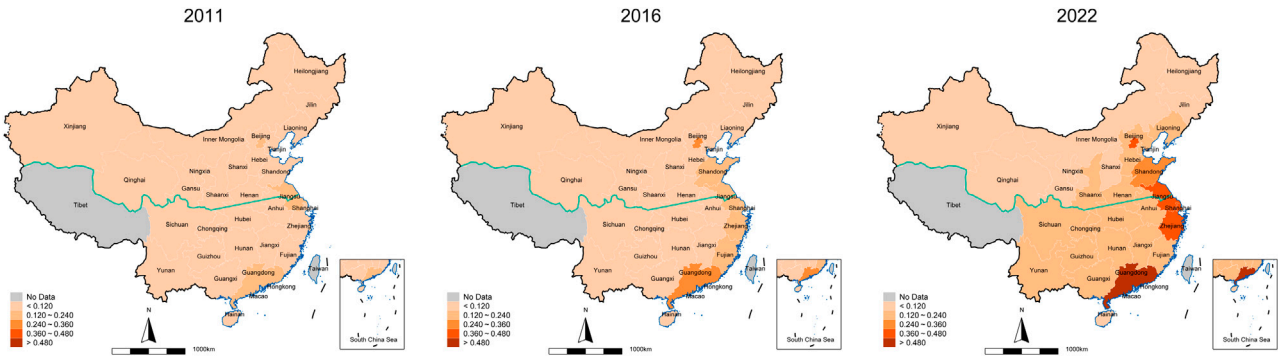

FIGURE 3
Spatial Distribution Map of the Digital economy.

TABLE 6 Results of spatial autocorrelation test.

year	Dtf			Pol		
	Moran's I	Z	p	Moran's I	Z	p
2011	0.097	1.239	0.215	0.349	3.697	0.000
2012	0.195	2.110	0.035	0.347	3.687	0.000
2013	0.188	2.040	0.041	0.184	2.138	0.032
2014	0.185	2.018	0.044	0.195	2.240	0.025
2015	0.196	2.114	0.035	0.195	2.253	0.024
2016	0.212	2.258	0.024	0.183	2.152	0.031
2017	0.220	2.330	0.020	0.182	2.106	0.035
2018	0.195	2.117	0.034	0.176	2.016	0.044
2019	0.211	2.266	0.023	0.145	1.763	0.078
2020	0.194	2.123	0.034	0.138	1.692	0.091
2021	0.186	2.054	0.040	0.125	1.546	0.122
2022	0.162	1.840	0.066	0.106	1.380	0.168

geographic distance, economic distance, and an economic-geographic nested matrix. The results across these matrices are consistent. However, the analysis focuses on the economic-geographic nested matrix shown in column (19), which combines both economic and geographic factors. Note that the spatial econometric model is uniquely characterized, particularly in column (19), rows 3 and 4, which highlight the regression coefficients for the digital economy and its interaction with the spatial weights. The significance of these coefficients primarily indicates whether the digital economy directly influences environmental pollution. However, the actual existence and extent of its spatial impacts require further analysis using spatial econometric modeling techniques, such as partial differentiation; the actual values of the coefficients themselves are less critical here. Detailed examination of the direct and spillover effects is required through partial differentiation, presented in rows 6 and 7 of column (19).

As evident from the third row of column 19, the direct impact of the digital economy on environmental pollution is negative, indicating that the growth of the digital economy within a region is likely to reduce its environmental pollution. Similarly, the fourth row reveals a negative coefficient for the interaction term between the digital economy and the spatial weight matrix. This suggests that while the digital economy may decrease environmental pollution within a region, it can concurrently mitigate pollution in surrounding areas as well. This may stem from the demonstrative effect of the digital economy, where as it prompts an increase in environmental regulatory efforts by local governments, neighboring governments may also face pressure from performance evaluation and public attention, leading to enhanced environmental pollution management. Consequently, when the digital economy reduces environmental pollution in a given region, it tends to have a similar effect in neighboring areas. Thus, Hypothesis 4 is confirmed.

5 Robustness test

5.1 Instrumental variable methods

Drawing on the methodology of Nunn and Qian (2014) and Zhang et al. (2023), we use historical data on post and telecommunications from provinces in 1984 as a basis, combined with the number of Internet users in the country from 2011 to 2022, to construct an instrumental variable. This approach is chosen because the development of the digital economy is closely related to local infrastructure such as postal and telecommunication services, thus satisfying the requirement for correlation between the instrumental variable and the explanatory variables. Additionally, the impact of postal and telecommunication infrastructure on environmental pollution has become negligible over time, meeting the exogeneity requirement of the instrumental variable. Please refer to Table 8 for the relevant regression results.

The results from Table 8 confirm that the digital economy continues to have a significant negative impact on environmental pollution, even after addressing the endogeneity issue.

TABLE 7 Spatial spillover effect test.

Spatial matrix types	Adjacent Distance	Geographic ditance	Economic distance	Economic Geographical nestng
Variable	(16)	(17)	(18)	(19)
Dtf	−0.797***	−0.801***	−0.812***	−0.814***
	(0.267)	(0.270)	(0.271)	(0.274)
W×Dtf	−0.189***	−0.191***	−0.193***	−0.195***
	(0.062)	(0.063)	(0.065)	(0.064)
control variables	yes	yes	yes	yes
direct effect	−0.785***	−0.793***	−0.795***	−0.801***
	(0.273)	(0.276)	(0.277)	(0.279)
spillover effect	−0.093**	−0.095**	−0.096***	−0.098***
	(0.363)	(0.367)	(0.369)	(0.372)
spatial rho	0.144**	0.147***	0.148***	0.150***
	(0.070)	(0.073)	(0.074)	(0.079)
variance sigma^2	0.019***	0.019***	0.019***	0.019***
	(0.001)	(0.001)	(0.001)	(0.001)
N	360	360	360	360
adj R^2	0.860	0.862	0.870	0.873

TABLE 8 Robustness check of instrumental variable method.

Variable	Instrumental variable	
	(20)	(21)
Dtf	−0.776***	−1.323***
	(0.332)	(0.317)
region fixed effect	yes	yes
year fixed effect	yes	yes
control variables	no	yes
LM	212.445	216.559
	[0.000]	[0.000]
F	457.848	466.513
	{16.380}	{16.380}
period number	12	12
N	360	360
adj R^2	0.741	0.945

Note:***, **, * denote significance levels at 1%, 5%, and 10%, respectively; figures in parentheses represent robust standard errors, values in square brackets are *p*-values, and numbers in curly braces are the critical values from the Stock-Yogo weak identification test at the 10% level.

Furthermore, the instrumental variables cleared the LM test with F-values exceeding 10, affirming their statistical validity and appropriateness. These findings robustly support a deeper exploration of the interplay between the digital economy and environmental pollution.

5.2 Replace explained variables

We substituted the main explained variable for its subcomponents sulfur dioxide emissions, water pollutants, and solid pollutant discharge to verify the robustness of our

TABLE 9 Regression with substitute dependent variables.

Variable	Sulfur dioxide emissions	Wastewater discharge	Solid pollutant emissions
	(22)	(23)	(24)
Dtf	−0.602***	−0.75***	−1.63***
	(0.575)	(0.292)	(0.556)
control variables	yes	yes	yes
region effects	yes	yes	yes
time effects	yes	yes	yes
N	360	360	360
adj R2	0.976	0.944	0.919

regression analysis. The modified regression outcomes, presented in Table 9, demonstrate that the results remain robust even after this substitution. This further solidifies the reliability of our regression findings.

5.3 Heterogeneity analysis

At present, various regions in China are at different stages of industrialization and economic development levels, which leads to differences in both environmental pollution and the development of the digital economy. Therefore, in accordance with China's regional planning standards, specifically as shown in Figure 4, it is necessary to analyze the sub-samples from the three regions in order to better understand these differences. The regression results are presented in Table 10.

Table 10 reveals that the impact of the digital economy on environmental pollution is negative across eastern, central, and western regions. However, the most substantial negative impact is observed in the western region, followed by the central and the least in the eastern region. This trend may be attributed to the high level of environmental pollution and the relatively undeveloped the digital economy in the western region, resulting in the largest marginal utility of the digital economy interventions on environmental pollution. In contrast, the digital economy in the eastern region, being more developed and shows a diminishing marginal effect due to lower levels of environmental pollution. Despite this, the development of digital economy remains crucial in the eastern region, which possesses more experience in reducing environmental pollution through digital means. Therefore, the central and western regions could benefit significantly from adopting the eastern region's strategies.

6 Conclusion and policy implications

This study constructs a digital economy development indicator system for 30 provinces spanning from 2011 to 2022, taking into account both government environmental governance and public environmental concerns as the starting points. Utilizing fixed-effect models, spatial econometric models, and an instrumental variable system, it examines the mechanisms of how digital economy development contributes to environmental pollution control. The key findings are as follows: 1) The development of the digital economy significantly reduces environmental pollution, promoting regional green transformation and development. 2) This reduction in environmental pollution is achieved through the government's pre-event focus on environmental governance, in-event investment in pollution control, and post-event enforcement efforts. 3) Public environmental concern positively moderates the relationship between the digital economy and environmental pollution, enhancing the impact of the digital economy on government environmental regulations. 4) The impact of the digital economy on environmental pollution exhibits a spatial spillover effect, where the development of the digital economy reduces pollution in a given region while also lowering pollution levels in surrounding areas.

According to the conclusion, the following suggestions are made:

(1) Vigorously promote the development of the Dtf and improve relevant policies and safeguard systems. Promote the Dtf: strengthen the construction of infrastructure such as 5G and big data, promote the digital transformation of industry, develop new business forms such as platform economy, innovate the application of technology, improve data management and laws and policies, optimize the business environment, train digital talents, narrow the digital divide, and build a healthy and sustainable Dtf ecology.
(2) Give full play to the guiding role of the Dtf in green development through government environmental governance. We will strengthen local governments' attention to environmental governance and enhance their environmental supervision capabilities. We will increase investment in Pol control and improve the government's ability to improve the ecological environment. Strengthen government environmental law enforcement and administrative penalties through information and technology, so as to promote Pol reduction.

FIGURE 4
Regional division of eastern, central and western regions.

TABLE 10 Regional heterogeneity.

Variable	Eastern region	Central region	Western region
	(25)	(26)	(27)
Dif	−0.440***	−1.673***	−4.310***
	(0.153)	(0.639)	(1.977)
control variables	yes	yes	yes
region effects	yes	yes	yes
time efects	yes	yes	yes
the number of regions	11	8	11
N	132	96	132
adjR2	0.976	0.989	0.924

(3) Improve the construction of government public service platforms and improve the channels for the public to express environmental demands. The Dtf will guide the public to pay attention to and participate in environmental governance. With the help of digital technologies and platforms, local governments and social forces are encouraged to interact and cooperate in Pol control, and a collaborative environmental governance system with government supervision as the leading role and public participation as the auxiliary role is better established, so as to improve the public's participation in and supervision of government environmental governance, and thus strengthen the effect of Pol control.

(4) To harness the positive spatial spillover effects of the digital economy on environmental pollution, we should enhance inter-regional communication and cooperation. Through regular dialogues, information sharing, personnel training, and exchange programs, we can facilitate the transfer of technology and expertise from advanced regions to less-developed ones. Additionally, leveraging the technological advantages of the digital economy, we should promote green digital technologies, optimize industrial layouts, and strengthen environmental oversight, ultimately achieving the coordinated development of the digital economy and environmental protection.

Data availability statement

Publicly available datasets were analyzed in this study. This data can be found here: https://idf.pku.edu.cn/yjcg/zsbg/index.htm.

Author contributions

KL: Conceptualization, Software, Writing–original draft. FM: Data curation, Methodology, Writing–review and editing.

Funding

The author(s) declare that no financial support was received for the research, authorship, and/or publication of this article.

Conflict of interest

The authors declare that the research was conducted in the absence of any commercial or financial relationships that could be construed as a potential conflict of interest.

Publisher's note

All claims expressed in this article are solely those of the authors and do not necessarily represent those of their affiliated organizations, or those of the publisher, the editors and the reviewers. Any product that may be evaluated in this article, or claim that may be made by its manufacturer, is not guaranteed or endorsed by the publisher.

References

Ahlers, A. L., and Shen, Y. (2018). Breathe easy? Local nuances of authoritarian environmentalism in China's battle against air pollution. *China Q.* 234 (8), 299–319. doi:10.1017/s0305741017001370

Arantes, V. (2023). DING, iza. 2022. The performative state: public scrutiny and environmental governance in China. Ithaca: cornell university press. *China Perspect.* 132, 75–76. doi:10.4000/chinaperspectives.14719

Carlsson, Bo (2004). The Digital Economy: what is new and what is not? *Struct. Change Econ. Dyn.* 15 (3), 245–264. doi:10.1016/j.strueco.2004.02.001

Chen, H., Ma, Z., Xiao, H., Li, J., and Chen, W. (2023). The impact of digital economy empowerment on green total factor productivity in forestry. *Forests* 14 (1729), 1729. doi:10.3390/f14091729

Fang, J., Zhao, L., and Li, S. (2024). Exploring open government data ecosystems across data, information, and business. *Gov. Inf. Q.* 41 (2), 101934. doi:10.1016/j.giq.2024.101934

Ge, T., Xionglei, H., and Li, J. (2021). Effects of public participation on environmental governance in China: a spatial Durbin econometric analysis. *J. Clean. Prod.* 321, 129042. doi:10.1016/j.jclepro.2021.129042

Hou, L., Tian, C., Xiang, R., Wang, C., and Gai, M. (2023). Research on the impact mechanism and spatial spillover effect of digital economy on rural revitalization: an empirical study based on China's provinces. *Sustainability* 15 (15), 11607. doi:10.3390/su151511607

Li, G., Li, X., and Huo, L. (2023a). Digital economy, spatial spillover and industrial green innovation efficiency: empirical evidence from China. *Heliyon* 9, e12875. doi:10.1016/j.heliyon.2023.e12875

Li, M., Zou, S., and Jing, P. (2023b). Spatial spillover effect of water environment pollution control in basins—based on environmental regulations. *Water* 15 (21), 3745. doi:10.3390/w15213745

Liu, J., and Zhao, Q. (2024). Mechanism testing of the empowerment of green transformation and upgrading of industry by the digital economy in China. *Front. Environ. Sci.* 11. doi:10.3389/fenvs.2023.1292795

Liu, X., Deng, L., Dong, X., and Li, Q. (2024). Dual environmental regulations and corporate environmental violations. *Finance Res. Lett.* 62 (8), 105230. doi:10.1016/j.frl.2024.105230

Liu, X., Sun, T., and Feng, Q. (2020). Dynamic spatial spillover effect of urbanization on environmental pollution in China considering the inertia characteristics of environmental pollution. *Sustain. Cities Soc.* 53, 101903. doi:10.1016/j.scs.2019.101903

Moyer, J. D., and Hughes, B. B. (2012). ICTs: do they contribute to increased carbon emissions? *Technol. Forecast. Soc. Change* 79 (5), 919–931. doi:10.1016/j.techfore.2011.12.005

Niu, X., Ma, Z., Ma, W., Yang, J., and Mao, T. (2024). The spatial spillover effects and equity of carbon emissions of digital economy in China. *Journal of Cleaner Production* 434, 139885. doi:10.1016/j.jclepro.2023.139885

Nunn, N., and Qian, N. (2014). US food aid and civil conflict. *Am. Econ. Rev.* 104 (6), 1630–1666. doi:10.1257/aer.104.6.1630

Pan, W., Xie, T., Wang, Z., and Ma, L. (2022). Digital economy: an innovation driver for total factor productivity. *J. Bus. Res.* 139, 303–311. doi:10.1016/j.jbusres.2021.09.061

Peng, M., Peng, S., Jin, Y., and Wang, S. (2023). Government environmental information disclosure and corporate carbon performance. *Front. Environ. Sci.* 11, 1204970. doi:10.3389/fenvs.2023.1204970

Shin, D.-H., and Choi, M. J. (2015). Ecological views of big data: perspectives and issues. *Telematics Inf.* 32 (2), 311–320. doi:10.1016/j.tele.2014.09.006

Sturgeon, T. (2021). Upgrading strategies for the digital economy. *Glob. Strategy J.* 11 (1), 34–57. doi:10.1002/gsj.1364

Su, P., Lin, D. G., and Qian, C. (2018). Study on air pollution and control investment from the perspective of the environmental theory model: a case study in China, 2005-2014. *Sustainability* 10 (7), 2181. doi:10.3390/su10072181

Sun, J., Hu, J., Wang, H., Shi, Y., Wei, Z., and Cao, T. (2023). The government's environmental attention and the sustainability of environmental protection expenditure: evidence from China. *Sustainability* 15 (11163), 11163. doi:10.3390/su151411163

Tan, J., and Eguavoen, I. (2017). Digital environmental governance in China: information disclosure, pollution control, and environmental activism in the yellow river delta. *Water Altern. - Interdiscip. J. Water Polit. Dev.* 10 (1), 910–929.

Wan, Q., and Shi, D. (2022). Smarter and cleaner: the digital economy and environmental pollution. *China and World Econ.* 30 (6), 59–85. doi:10.1111/cwe.12446

Wang, J., Zhu, J., and Luo, X. (2021). Measurement of China's digital economy development level and evolution (in Chinese). *Quantitative Econ. Tech. Econ. Res.* 38, 26–42. doi:10.13653/j.cnki.jqte.2021.07.002

Wang, L., Liu, B., He, Y., Dong, Z., and Wang, S. (2023). Have public environmental appeals inspired green total factor productivity? empirical evidence from Baidu Environmental Search Index. *Environ. Sci. Pollut. Res.* 30 (11), 30237–30252. doi:10.1007/s11356-022-23993-8

Wang, S., Zheng, Y., and Yang, H. (2024). Digital economy and green total factor productivity in China. *PloS one* 19 (3), e0299716. doi:10.1371/journal.pone.0299716

Wei, J., and Zhang, X. (2023). The role of big data in promoting green development: based on the quasi-natural experiment of the big data experimental zone. *Int. J. Environ. Res. public health* 20 (5), 4097. doi:10.3390/ijerph20054097

Wu, Y., Hu, J., Irfan, M., and Hu, M. (2024). Vertical decentralization, environmental regulation, and enterprise pollution: An evolutionary game analysis. *J. Environ. Manage.* 349, 119449. doi:10.1016/j.jenvman.2023.119449

Xie, B., Liu, R., and Dwivedi, R. (2024). Digital economy, structural deviation, and regional carbon emissions. *J. Clean. Prod.* 434, 139890. doi:10.1016/j.jclepro.2023.139890

Xu, J. (2024). Spatial spillover and threshold effects of digital rural development on agricultural circular economy growth. *Front. Sustain. Food Syst.* 8 (24). doi:10.3389/fsufs.2024.1337637

Xu, Q., Li, X., Dong, Y., and Guo, F. (2023). Digitization and green innovation: how does digitization affect enterprises' green technology innovation? *J. Environ. Plan. Manag.*, 0964–0568. doi:10.1080/09640568.2023.2285729

Yang, J., Li, X., and Huang, S. (2020). Impacts on environmental quality and required environmental regulation adjustments: a perspective of directed technical change driven by big data(Article). *J. Clean. Prod.* 275, 124–126. doi:10.1016/j.jclepro.2020.124126

Zhang, M., Tan, S., Pan, Z., Daoqing, H., Zhang, X., and Chen, Z. (2022a). The spatial spillover effect and nonlinear relationship analysis between land resource misallocation and environmental pollution: evidence from China. *J. Environ. Manag.* 321, 115873. doi:10.1016/j.jenvman.2022.115873

Zhang, R., Fu, W., and Yingxu, K. (2022b). Can digital economy promote energy conservation and emission reduction in heavily polluting enterprises? Empirical evidence from China. *Int. J. Environ. Res. public health* 19 (16), 9812. doi:10.3390/ijerph19169812

Zhang, X., Zhong, J., and Wang, H. (2023). Does the development of digital economy affect environmental pollution? *Sustainability* 15 (2), 9162. doi:10.3390/su15129162

Zhao, F., Yi, S., and Zhang, J. (2023a). Does industrial agglomeration and environmental pollution have a spatial spillover effect? taking panel data of resource-based cities in China as an example. *Environ. Sci. Pollut. Res. Int.* 30 (31), 76829–76841. doi:10.1007/s11356-023-27852-y

Zhao, S., Shuliang, Z., Linjiao, T., Arkorful, V. E., and Hui, H. (2023b). Impacts of digital government on regional eco-innovation: moderating role of dual environmental regulations. *Technol. Forecast. Soc. Change* 196, 122842. doi:10.1016/j.techfore.2023.122842

Zhen, Z., Yousaf, Z., Radulescu, M., and Yasir, M. (2021). Nexus of digital organizational culture, capabilities, organizational readiness, and innovation: investigation of SMEs operating in the digital economy. *Sustainability* 13, 720. doi:10.3390/su13020720

Zhu, X., and Li, B. (2020). Convergence of efficiency of environmental pollution control investment in the coastal areas of China. *J. Coast. Res.* 105, 171–175. doi:10.2112/jcr-si105-036.1

Zou, J., and Deng, X. (2022). To inhibit or to promote: how does the digital economy affect urban migrant integration in China? *Technol. Forecast. Soc. Change* 179, 121647. doi:10.1016/j.techfore.2022.121647

frontiers | Frontiers in Environmental Science

TYPE Original Research
PUBLISHED 23 July 2024
DOI 10.3389/fenvs.2024.1422989

OPEN ACCESS

EDITED BY
Xue-Chao Wang,
Beijing Normal University, China

REVIEWED BY
Siyun Chen,
Hunan University of Finance and Economics, China
Guoen Wei,
Nanchang University, China
Peng Cao,
Henan University of Technology, China

*CORRESPONDENCE
Lei Zhigang,
13077341678@163.com

RECEIVED 25 April 2024
ACCEPTED 01 July 2024
PUBLISHED 23 July 2024

CITATION
Xuan S, Qimeng N and Zhigang L (2024), Impacts of the land use transition on ecosystem services in the Dongting Lake area.
Front. Environ. Sci. 12:1422989.
doi: 10.3389/fenvs.2024.1422989

Impacts of the land use transition on ecosystem services in the Dongting Lake area

Shi Xuan[1], Ning Qimeng[2] and Lei Zhigang[3]*

[1]Songlin College of Architecture and Art, University of South China, Hengyang, China, [2]School of Architecture and Urban Planning, Hunan City University, Yiyang, China, [3]Department of National Spatial Planning Data, The Third Surveying and Mapping Institute of Hunan Province, Changsha, China

Urbanization-induced land use transitions (LUTs) result in a decline in ecosystem services, which has implications for regional ecological security. In order to explore the relationship between ecosystem services and land use transition, this paper utilizes the InVEST model, a geographically weighted regression (GWR) model, to examine the impact of land use transition on ecosystem services in the Dongting Lake area (DLA). The results showed that 1) with the change in urbanization development, the average values of land use transition intensity (LUI) in 2000, 2010, and 2020 are 237.99, 235.82, and 238.92, respectively. Land use dynamics (LUD) show a tendency to increase and then decrease, with average values of 5.58 and 5.62 for the periods 2000–2010 and 2010–2020, respectively, and the transformation of land use shows obvious spatio-temporal heterogeneity. 2) Habitat quality and carbon sequestration showed a downward trend. In contrast, food supply followed an upward trend; soil conservation (SC) and water yield (WY) services initially increased and decreased later. The overall spatial changes in habitat quality and carbon sequestration appear to be insignificant. Food supply shows significant differences in the plains compared to other areas, while soil conservation and water yield service show significant changes in places other than the DLA. 3) From 2000 to 2020, land use transition dynamics, population density, GDP density, night lighting, and transition intensity had mainly negative effects on ecosystem services. Only the Normalized Vegetation Index (NDVI) showed a positive effect on ecosystem services. The results of the research will provide valuable references for the development and implementation of spatial ecological restoration planning and land use policies in the national territory.

KEYWORDS

ecosystem service, Dongting Lake area, land use transitions, InVEST model, geographically weighted regression

1 Introduction

Since the 21st century, with growing urbanization and industrialization (Wang et al., 2023a), the large-scale growth of building land has led to noticeable shifts in land use, in which natural and semi-natural habitat classes have shifted toward artificial habitat classes (Griggs et al., 2013). In addition, current research has identified habitat fragmentation, soil quality deterioration, and increasing environmental contamination as direct effects of human overexploitation (Banks-Leite et al., 2020). These repercussions are predominantly driven by land use transition (LUT), which considerably alters the balance between the supply and demand of ecosystem services (ESs) (Xiang et al., 2022), leading to changes in

their providing ecosystem functions (Keyes et al., 2021). Therefore, disclosing the impacts on ESs in the process of LUT is vital for the creation and implementation of ecological restoration planning and land use regulations in the territorial area (Feng et al., 2023).

LUT is the result of the interaction between social and natural factors (Zhou et al., 2020) and plays an important role in regulating socioeconomic development and ecological restoration (Cao et al., 2021a). The meaning of change, its effects, and other facets have been the subject of several academic studies. Explicit and implicit LUT modes are distinguishable among them based on their respective connotations (Shi et al., 2021). Implicit LUT, on the other hand, primarily refers to changes in land use functions (Zou et al., 2024), including various land attributes in terms of property rights (Wen et al., 2020), inputs, outputs, production, etc. Among them, explicit LUT refers to changes in land use structure (i.e., quantitative and spatial structure) (de Groot, 2006; Burton et al., 2009). In terms of effect, LUT has caused changes in the land use structure, which has led to the reduction in ecological land, thus causing ecological environment damage (Yang et al., 2018). Among them are ESs, which people rely on for direct or indirect environmental benefits. Research has demonstrated that ESs are key components of ecological security (Liu et al., 2023). Natural variables like temperature and rainfall and socioeconomic factors like population growth, construction site expansion, and economic development all have an impact on ESs (Ouyang et al., 2022). Of these, land use change has a major impact on ESs (Xu et al., 2019). Prior research has mostly examined how changes in land use structure affect ESs without taking into account how these changes affect ESs themselves during the LUT process (Bai et al., 2020). Furthermore, research on the effects of changing land use on ESs (Hasan et al., 2020) is primarily conducted at the administrative division level (Liu, 1996; Chen et al., 2019; Song et al., 2022). This limits the ability to suggest relevant planning for the area and makes it challenging to characterize the phenomenon's local changes.

The Dongting Lake Ecological Reserve is an important part of the Yangtze River basin (Liu et al., 2023) and an important area for ecological restoration and food supply in China. The process of urbanization has precipitated a significant shift in land utilization within the locality, exerting a profound impact on the ESs of the area. Hence, this study focuses on the Dongting Lake area (DLA) as the subject of investigation, elucidating the transition in land use and ESs at the grid scale from 2000 to 2020 through a multi-dimensional assessment. It aims to delve into the mechanism by which land use transition impacts ESs, employing a geographically weighted regression (GWR) model. This endeavor seeks to address the following scientific inquiries: 1) What patterns characterize the changes in ESs during the process of land use transition? 2) What is the relationship between land use transition (LUT) and ESs? The ultimate objective is to furnish theoretical underpinnings for the high-quality development of land space in the DLA (Li et al., 2023).

2 Methods

2.1 Overview of the study area

DLA (28°30′N-29°40′N, 113°10′E–114°40′E) is the second largest freshwater lake in China (Song et al., 2022). It is located in the northern part of Hunan Province and the southern part of Hubei Province, serving as an essential storage lake and ecological security function area in the Yangtze River basin (Liu et al., 2022). The region is predominantly characterized by plains, which can be categorized into four main types: lake water bodies and shoals, plains surrounding the lake, hills and low mountains adjacent to the lake, and valley plains and hills (Zhao et al., 2023). The current investigation centered on a subset comprising 19 counties (cities and districts) from the three prefecture-level cities, namely, Yueyang, Yiyang, and Changde, within the DLA (Jiang and Zeng, 2024). These areas encompassed Yueyang city, Linxiang city, Yueyang County, Huarong County, Miluo City, Xiangyin County, Yiyang city, Yuanjiang city, Nan County (including the Datong Lake area), Changde city, Hanshou County, Anxiang County, Li County, Jin city, and Linli County (Jie et al., 2023). As shown in Figure 1, the total area spans approximately 25,800 km^2, constituting 12.18% of Hunan Province. As of the end of 2020, the resident population numbered approximately 10,705,800, accounting for approximately 16.11% of the province. The GDP amounted to 710.44 billion yuan, representing roughly 17% of the province.

In terms of land use, we reclassified land cover into six categories. Of these, forest land accounted for the largest share of 46% of the total area in 2020, followed by cropland at 37%, grassland and unused land both at 2%, watershed at 11%, and built-up land at 3%. There was a shift in land use between 2000 and 2020, mainly for cropland—from 38% of the total area to 37%—and built-up land—from 2% to 3%. The 46% coverage of forested land around Dongting Lake underscores the substantial forest resources in the area, reflecting not only its biodiversity but also its contribution to water yield (WY) and soil conservation (SC), which are pivotal for maintaining the ecological balance of the lake region. The 37% allocation to cultivated areas highlights the significance of agriculture in the Dongting Lake vicinity, particularly in the production of staple crops such as rice, which is vital for local and neighboring food supplies. Moreover, the 11% designated as watershed areas signifies the abundant water resources surrounding Dongting Lake, crucial for sustaining crop growth and ecological equilibrium. Prudent conservation and management of these land resources, including preserving forest cover and wetland ecosystems, as well as enhancing agricultural productivity and sustainability, are essential for maintaining the ecological balance and food security in the Dongting Lake region, ensuring a healthy and stable environmental landscape within the area.

2.2 Materials

2.2.1 Data sources

The data mainly include land use data, food supply, carbon density, night light data, and others, as shown in Table 1.

2.3 Methods

2.3.1 Land use transition intensity

Land use transition intensity (LUI) is a significant metric of the land use function (Yang et al., 2020). From a socio-economic

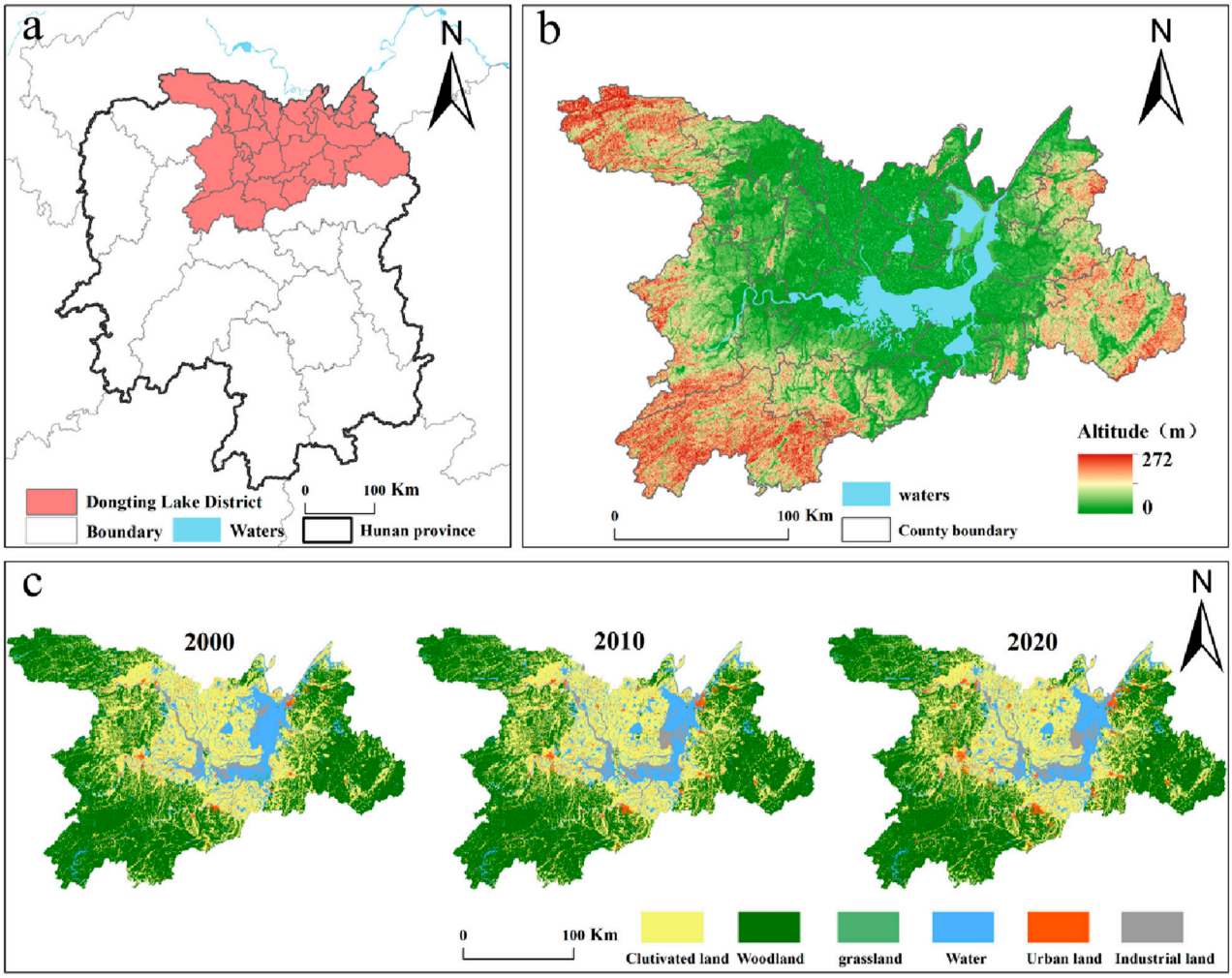

FIGURE 1
Geographic location and land use classification of the Dongting Lake ecological and economic zone. Location of the region **(A)**, digital elevation model **(B)**, and class of land use **(C)**.

standpoint, LUI can indicate varied degrees of land transitions, development, and exploitation. The study will treat each land raster as a sampling point, generating a 1 km × 1 km grid and calculating the LUI of each grid independently, as depicted in Figure 3. Each land use type can be defined as the ability of different land use types to provide products and services for human beings (Kleijn et al., 2009). Their contribution to LUI is consistent with their weights. Therefore, using the grid, LUI can be calculated using the following formula:

$$LUI = \sum_{i=1}^{n} (B_i/B) \times C_i \quad (1)$$

In this formula, B represents the total land area, n is the number of land use types (n = 6 in this study), B_i is the area of each land use type, and C_i is the value of the degree of exploitation of the land use type (Yang et al., 2020). LUI can be classified into four categories, with each land use type within each category having the same value. Specifically, the value of industrial, urban, and rural–urban land, collectively known as build-up land, is defined as "4." Farmland is assigned a value of "3" due to its socio-economic and natural attributes. The Chinese government reinforces the protection of farmland, grassland, and woodland resources, owing to their ecological functions (Yang et al., 2018), which are assigned a value of 2. Bare land is valued at "1" as it has yet to be developed for socio-economic activities.

2.3.2 Land use dynamics model

Land use dynamics (LUD) serves to depict the rate and trajectory of land transition and reflects its overall characteristics within a region over time (El-Naggar et al., 2022). Similarly, this study utilizes the grid as the fundamental unit for LUD calculation. The specific equations are provided below (Li et al., 2021):

$$LUD = \frac{\sum_{i=1}^{n} B_{i\to j}}{B} \times \frac{1}{t_b\text{-}t_a} \times 100\% \quad (2)$$

Here, B is the total land area, n is the number of land use types (n = 6 in this study), and $\Delta B_{i\to j}$ is the area where land use type i is

TABLE 1 Data sources.

Data name	Description of the data	Source of data
Nighttime lighting data	The nighttime light data (NTL) is sourced from the Defense Meteorological Satellite Program Operational Line Scan System (DMSP/OLS), offering a spatial resolution of 1 km × 1 km. Population density datasets for the years 2000, 2010, and 2020 are accessible under the Creative Commons Attribution 4.0 International License, also with a spatial resolution of 1 km × 1 km (Wang et al., 2023b)	Data are provided by the Institute of Geographic Sciences and Natural Resources (IGSNRR), the Centre for Environmental Sciences and Data, Chinese Academy of Sciences (CAS), accessible at https://www.resdc.cn
Population density	The population density datasets for 2000, 2010, and 2020 are accessible under the Creative Commons Attribution 4.0 International License at a spatial resolution of 1 km × 1 km (Wang et al., 2023a)	Taken from ORNL LandScan Viewer—Oak Ridge National Laboratory (landscan.ornl.gov)
GDP intensity	Gross domestic product (GDP), as an essential and comprehensive statistical indicator in the accounting system, shows the rate of economic development in China. It is an indicator that measures the results of productive activities in resident units. The spatial resolution of GDP data for 2000, 2010, and 2020 is 1 km × 1 km	Retrieved from the Center for Resource and Environmental Sciences and Data, Institute of Geographic Sciences and Natural Resources, Chinese Academy of Sciences, available at https://www.resdc.cn
Food supply	The study focused on major food types, including cereals, sugar crops, oil crops, meat, milk, and fruits	Data was sourced from the China Statistical Yearbook (2001–2021) and China Rural Statistical Yearbook (2001–2021), and information on the caloric composition of various foods was obtained from the U.S. agricultural databases and related studies (Cao et al., 2021b)
Habitat quality	Land use data were primarily used for the habitat quality calculations derived from the inVEST Habitat Quality Module	Habitat quality-related parameter settings are taken from the existing literature (Wentland et al., 2020)
Carbon density data	Primarily utilized as references for carbon density data across different carbon pools	Data were mainly obtained from the literature (Wang et al., 2018; Zhou et al., 2020; Buckley Biggs, 2022))
Water yield services data	Derivation of the inVEST water production module	Precipitation data are sourced from the annual spatial precipitation interpolation dataset of China since 2000, available at http://www.resdc.cn/data.aspx?DATAID=229. Potential evapotranspiration data are obtained from World Climate, accessible at https://www.worldclim.org/data/worldclim21.html. Watershed and sub-basin boundary data are derived from the Chinese watershed and river network extraction dataset based on DEM, retrievable from http://www.resdc.cn/DOI/doi.aspx?DOIid=44
Soil data	The soil data resolution is 1000 m, and the terrain ASTER GDEM data resolution is 30 m	National Cryosphere Desert Data Centre can be accessed at https://www.ncdc.ac.cn, while the Geospatial Data Cloud is available at http://www.gscloud.cn
LULC	Spatial resolution of 30 m (2000–2020)	The dataset was provided by the ESA CCI Land Cover Project (https://www.esa-landcover-cci.org/)

transformed into land use type j (Buckley Biggs, 2022). The difference between t_b and t_a represents the time of the study. Broadly speaking, the larger the LUD, the faster and larger the land use transition. The trend will also be more pronounced, and *vice versa*.

2.3.3 Methods for quantifying ecosystem services

Ecosystem services can be classified into four main types: provisioning services (providing food and water), regulating services (controlling floods and diseases), cultural services (offering spiritual, entertainment, and cultural benefits), and supporting services (maintaining nutrient cycling that sustains life on earth) (MA et al., 2017; Ning and Ouyang, 2023).

In this study, we selected carbon sequestration, water yield services, food production, habitat quality, and soil conservation. Carbon sequestration and soil conservation fall under regulating services; water yield services and food production belong to provisioning services; and habitat quality is classified as a supporting service (Yu et al., 2024). Specific quantification was done using the InVEST model (Wei et al., 2021), and the corresponding equations are shown in Table 2.

Since the five ESs of carbon sequestration, water yield services, food production, habitat quality, and soil conservation have different units, a standardized method was used to standardize the ESs to [0,1]. Then all the values were added to obtain the total ESs (TES).

2.3.4 Geographically weighted regression

The GWR model is a classic approach for analyzing spatial heterogeneity. It effectively captures the influence of geographical location on the relationship between dependent and independent variables. Compared to other models, GWR offers higher accuracy. Additionally, the ecosystem service observation data in this paper exhibit spatial correlation. Therefore, incorporating temporal attributes into the GWR model allows for the exploration of the spatio-temporal driving mechanisms underlying the explanatory power of the independent variable on the dependent variable. The specific formula of the GWR model is presented below:

$$Y_{ij} = \beta_0(\mu_i, v_i, t_i) + \sum_{k=1}^{p} \beta_k(\mu_i, v_i, t_i) X_{ik} + \varepsilon_i \quad (3)$$

where Y_{ij} represents the ecosystem services in grid ij, a normalized means of five categories of ecosystem services; (μ_i, v_i, t_i) represents the spatial and temporal coordinates of sampling point i; $\beta_0(\mu_i, v_i, t_i)$ is the regression constant for

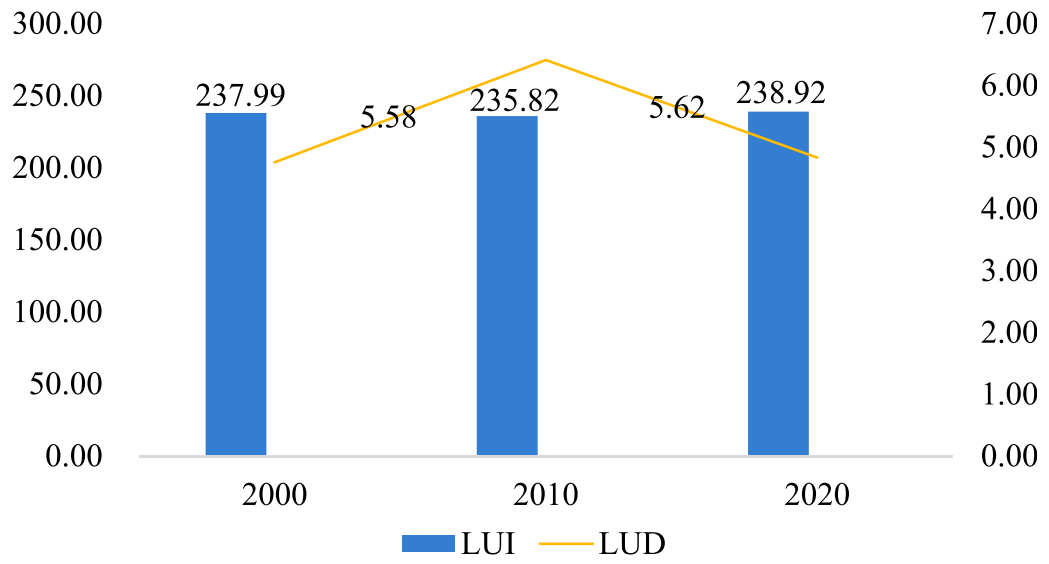

FIGURE 2
Intensity of land use transition and motivation, 2000–2020.

sampling point i; $\beta_k(\mu_i, v_i, t_i)$ represents the kth regression parameter for sample point i; X_{ik} is the driving factor k for sampling point i; and ε_i is the residual term of the model.

3 Results

3.1 Characteristics of spatial and temporal changes in LUT

Overall, the LUI exhibited slight fluctuations, with average values of 237.99, 235.82, and 238.92 in 2000, 2010, and 2020, respectively. The average annual growth rate of the LUI from 2000 to 2010 was −0.22, and from 2010 to 2020, it was 0.31. In contrast, LUD demonstrated a trend of initially increasing and then decreasing, with average values of 5.58 and 5.62 for the periods 2000–2010 and 2010–2020, respectively. Spatially, high-value areas in 2000–2010 were predominantly situated around the lake area and in urban expansion zones, while those in 2010–2020 were dispersed across urban, rural, and urban expansion areas (see Figure 2). The concentration of high-value areas of land use transition intensity in 2000, 2010, and 2020 was observed in the DLA, indicating favorable topography and optimal utilization of land resources in the region (see Figures 3D–F).

From 2000 to 2010, the high-value area of LUD for land use transition motivation was primarily concentrated in the eastern coastal area at the northern end of DLA and in urban construction areas around the region. Conversely, from 2010 to 2020, the high-value area of LUD for land use transition motivation was mainly concentrated in the suburbs of cities and urban and rural areas, particularly in the townships around cities, with a significant range of land use changes. The motivation for change slowed down around the lake area during this period (see Figures 3A–C).

3.2 Characteristics of spatial and temporal changes in ESs

The temporal and spatial variations over the period 2000–2020 for different ESs are discussed in this section. As shown in Table 3 and Figure 4, the mean value of WY increased from 490.18 mm in 2000 to 902.01 mm in 2010. High-value areas are distributed in the southeastern and southern hilly areas; low-value areas are spread in the waters of the Dongting Lake basin. The mean value of WY increased from 902.01 mm in 2010 to 690.10 mm in 2020. High-value areas are sporadically scattered; low-value areas are still distributed in the waters of the Dongting Lake Basin. The average value of CS decreased from 2289.35 t/hm^2 in 2000 to 2255.01 t/hm^2 in 2010, and the high-value areas are distributed in the hilly areas and the Dongting Lake Basin, while the low-value areas are distributed in the plains. The average value of CS in 2010 decreased from 2255.01 t/hm^2 to 2247.46 t/hm^2 in 2020. High values are still distributed in the hilly mountainous areas and the Dongting Lake basin; low values are distributed in the built-up areas and part of the waters of the Dongting Lake. The average value of SC in 2000 increased from 1088.32 t/ha^2/ha^2 to 1822.64 t/ha^2/ha^2 in 2010. High values are distributed in the mountainous areas at the edges of the study area; low values are distributed in the Dongting Lake basin. The mean value of SC increased from 1088.32 t/ha^2 in 2000 to 1822.64 t/ha^2/in 2010. High-value areas were distributed in the marginal mountains of the study area; low-value areas were distributed in the watershed of Dongting Lake. The mean value of SC decreased from 1822.64 t/ha^2 in 2010 to 626.29 t/ha^2 in 2020. High-value areas were distributed in the marginal mountains; low-value areas were distributed in the watershed of Dongting Lake. The mean value of HQ decreased from 0.71 in 2000 to 0.697 in 2010. High-value areas are distributed in the marginal mountains of the study area and in the Dongting Lake Basin; low-value areas are

TABLE 2 Formulas and descriptions of ecosystem service calculations.

ES	Calculation formula	Description
Carbon sequestration (CS)	$CS = C_{above} + C_{below} + C_{soil} + C_{dead}$	CS represents the total sequestered carbon supply (t/ha), C_{above} denotes the above-ground biochar, C_{below} signifies the below-ground biochar, C_{soil} stands for the organic carbon in the soil, and C_{dead} represents the dead organic carbon. These four carbon pools were obtained from the results of a literature review (Terrado et al., 2016; Wang et al., 2018; Qi et al., 2023)
Water yield services (WY)	$Y_{x,j} = (1 - \frac{AET_{x,j}}{P_x}) \times P_x$	$Y_{x,j}$ represents the annual water yield in pixel x in land use type j; $AET_{x,j}$ denotes the actual annual evapotranspiration in pixel x in land use type j, which was estimated based on the reference evapotranspiration data, land use data, and related parameter data. P_x signifies the annual precipitation in pixel x, compiled using precipitation data from the study area. Parameter data for estimating water yield, such as biophysical tables and tensor constants, were obtained through a literature review (Cong et al., 2020; Sancho Santos et al., 2021)
Food supply (FS)	$P_i = \sum_{k=1}^{k}\sum_{c=1}^{c} A_{cki} \times P_{cki}$. Food availability in a given area c can be calculated using the following formula: $P_{cki} = \frac{P_i}{\sum_{k=1}^{k}\sum_{c=1}^{c} A_{cki}} = \frac{\sum_{c=1}^{c} Y_c \times E_c}{\sum_{k=1}^{k}\sum_{c=1}^{c} A_{cki}}$	P_i is the total food energy produced in the area (kJ), A_{cki} is the area occupied by food C in the area I in the land use type K (HM^2), and P_{cki} represents the supply per unit area of the corresponding food c. Y_c here for a given area is the yield of the different food types c (kg), and E_c is the calorie content of the different foods (kJ/kg)
Habitat quality (HQ)	$Q_{xj} = H_j[1 - (\frac{D_{xj}^z}{D_{xj}^z + k^z})]$. Here, the Q_{XJ} series is the habitat quality of the grid x in the habitat type j, k is a semi-saturation constant, H_j the suitability of the habitat for the habitat type j, and the Q_{XJ} series is the degree of disturbance of the habitat type j on the grid x such that the Q_{XJ}'s series $= \sum_{r=1}^{R}\sum_{y=1}^{Y_r} (w_r / \sum_{r=1}^{R} w_r) r_y i_{rxy} \beta_x S_{jr}$ $i_{rxy} = 1 - (\frac{d_{xy}}{d_{r\max}})$	R is the threat factor, y is the number of image elements of the grid layer cells of the threat factor r, Y_r is the total number of cells occupied by the threat factor, and w_r is the weight of the threat factor r taking values in the range of [0,1]. r_y is the value of the threat factor of the grid Y (0 or 1), i_{rxy} is the degree of disturbance of the grid threat factor r on the habitat grid, S_{jr} is the sensitivity of the habitat type j to the threat factor r, and β_x is the availability of the grid x taking values in the range [0,1]. Degree of disturbance i_{rxy} d_{xy} is the linear distance between grids x and y, and $d_{r\max}$ is the maximum working distance r of the threat factor (Sancho Santos et al., 2021)
Soil conservation (SC)	$R = \sum_i^{12} 1.735 \times 10^{[(1.5 \times \log_{10}\frac{p_i^2}{p}) - 0.8188]} K = \left\{0.2 + 0.3\exp[0.256SAN(1 - \frac{SIL}{100})]\right\} \times (\frac{SIL}{CLA+SIL})^{0.3} \times (1 - \frac{0.25C}{C + \exp(3.72 - 2.95C)}) \times (1 - \frac{0.7(1-SAN)}{(1-SAN) + \exp[2.29(1-SAN)] - 5.51})$	R is the rainfall erosion rate, MJ•mm/(ha•hr•yr); p_i is the monthly precipitation (mm/month); and p is the annual precipitation (mm/year). K is the erodibility of the soil using the Erosion Productivity Impact Calculator (EPIC) model (Williams et al., 1984), where SAN, SIL, CLA, and C stand for the proportions of organic matter, sand, silt, and clay in the soil, respectively

10.3389/fenvs.2024.1422989

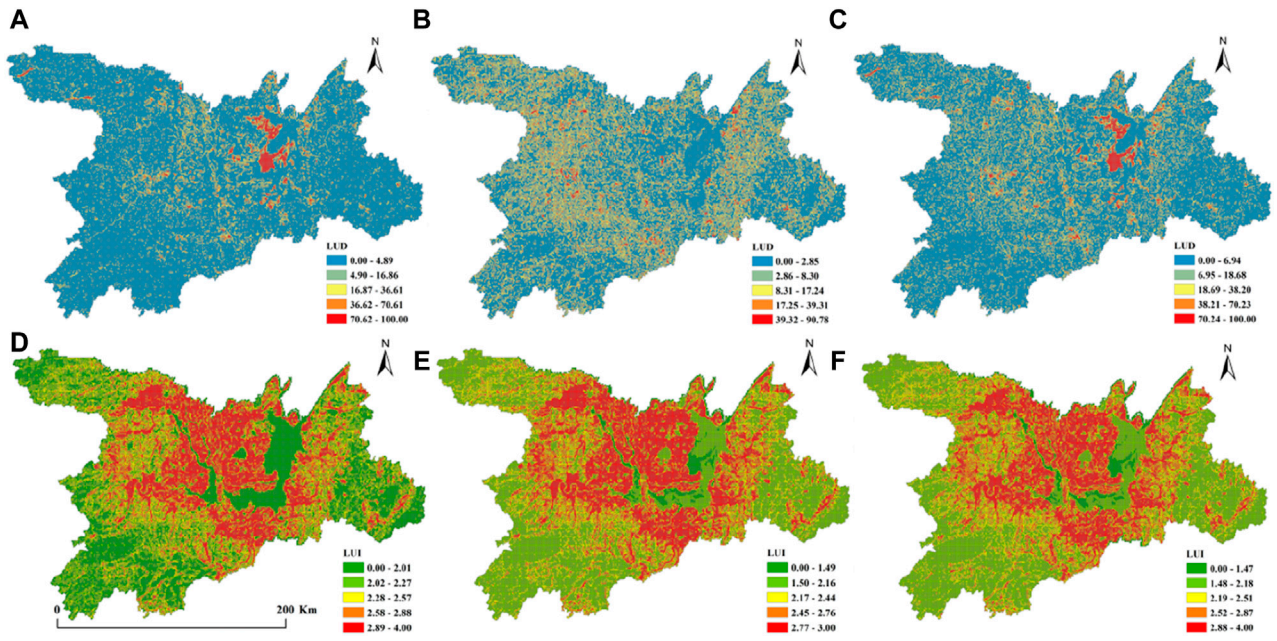

FIGURE 3
Intensity of land use transition and dynamics of motivation. **(A)** LUD during 2000-2010; **(B)** LUD during 2010-2020; **(C)** LUD during 2000-2020; **(D)** LUI 2000; **(E)** LUI 2010; **(F)** LUI 2020.

distributed in the urban areas. The mean value of HQ decreased from 0.697 in 2010 to 0.695 in 2020. High-value areas are still distributed in the marginal mountains and the Dongting Lake basin; low-value areas are still distributed in the urban areas. The average value of FS increased from 4740855.49 KJ in 2000 to 6024647.79 KJ in 2010. High-value areas were distributed in the plains and hills of the Dongting Lake basin; low-value areas were distributed in the marginal mountains of the study area and the Dongting Lake Basin. The average value of FS in 2010 increased from 60246447.79 KJ to 7036502.47 KJ in 2020. High-value areas are still distributed in the Dongting Lake Basin. The high-value areas are still distributed in the plains and hills of the Dongting Lake Basin; the low-value areas are still distributed in the mountains at the edge of the study area and in the Dongting Lake Basin.

3.3 Spatial and temporal correlation between LUT and ESs

The regression parameters of TES between and socio-economics are less variable than those between natural ecological factors (Figures 5, 6). The regression coefficients of NDVI ranged from −0.097836 to 0.208317, with the largest changes in regression coefficients and significant spatial heterogeneity. During the period of 2000–2010, 85% of the grids consisted of negative coefficient spaces, whereas the positive coefficient spaces were distributed in the southwest of Dongting Lake; between 2010 and 2020, the proportion of negative coefficient spaces decreased significantly, while positive coefficient spaces were distributed in the east coast, the western basin, and the southern edge of the study area.

The regression coefficients of LUD ranged from −0.001908 to 0.000521. The magnitude of the change in the regression coefficients varied slightly, indicating weaker spatial heterogeneity. During 2000–2010, 60% of the grids exhibited negative coefficients, with relatively positive coefficient spaces mainly distributed in the southern part of Dongting Lake, the southwestern edge, and the northwestern part of the study area. However, from 2010 to 2020, the positive coefficient spaces varied significantly, with a substantial increase in the proportion of negative coefficient spaces. Positive coefficient spaces were primarily distributed in the southwestern and northeastern parts of the study area.

Additionally, the regression coefficients of LUI ranged from −0.000593 to 0.000370, showing small variations and weak spatial heterogeneity. Positive coefficients during the period 2000–2010 were predominantly observed in the southern and eastern parts of Dongting Lake, as well as the western and northeastern fringes of the study area. Conversely, for the period 2010–2020, high-value areas were primarily concentrated in the northeastern and southwestern parts of the study area, as well as in the southern basin of Dongting Lake.

The socio-economic data encompass population density, GDP density, and nighttime light data. The regression coefficients of the nighttime light data ranged from −0.002690 to 0.002625. Spatially, during the period from 2000 to 2010, high values were primarily concentrated in the eastern, southern, and northern regions of Dongting Lake, as well as the southern part of the western watershed and the northern edge of the study area. Conversely, in the period from 2010 to 2020, high values shifted to the northern, southeastern, and southwestern parts of Dongting Lake, along with the northwestern and western edges of the study area. For GDP density, the regression coefficients ranged from −0.000008 to 0.000024. During the period 2000–2010, high values were dispersed in the southern part of the study area, while during 2010–2020, they were primarily located toward the northwestern

TABLE 3 Changes in ecosystem services, 2000–2020.

Type of ESs	2000	2010	2020	2000–2010	2010–2020
WY	490.726	902.007	690.102	41.128	−21.191
CS	2,289.954	2,255.008	2,247.457	−3.494	−0.755
SC	1,088.317	1,822.635	929.607	73.432	−89.303
HQ	0.711	0.698	0.695	−0.001	−0.001
FS	4,740,855.284	6,024,647.791	7,036,502.467	128,379.251	101,185.468

The unit of WY is mm; the unit of C is t/hm^2; the unit of SC is t/ha^2; the unit of FS is KJ; rate of change is provided in the last two columns.

part of Dongting Lake. The regression coefficients of population density ranged from −0.000008 to 0.000011. During the period 2000–2010, high-value areas were mainly distributed in the northwestern part of the study area and the western part of the Dongting Lake basin, whereas during 2010–2020, they shifted to the western and northwestern parts of the study area, as well as the southern part.

4 Discussion

4.1 Impacts of LUT on ESs

The structure of ecosystems (e.g., cropland and woodland) and processes (e.g., habitat quality) in the process of land-use transition are influenced by human-social factors, which aim to maximize human benefits by transforming natural ecosystems (Long and CHEN, 2021). Concurrently, the process of land use transition affects socio-economic characteristics correspondingly, as evidenced by the growth of night-time lighting data, population density, and GDP density, following the expansion of urban construction land (Song, 2017). As depicted in Figure 4, habitat quality and carbon sequestration exhibit a downward trend, while food supply trends upward; soil conservation and water yield services initially increase and then decrease. During the period 2000–2010, the eastern littoral area at northern Dongting Lake experienced a significant land transition. This transformation can be attributed to the implementation of policies related to the return of farmland to the lake and forests in 2002, which reduced the human occupation of land in the lake area. Subsequently, there was an expansion of land for urban construction, aligning with China's high rate of development during this decade, characterized by rapid growth in urban, rural, and city areas. In the functional spatial layout of ESs, the high-value areas of WY, CS, SC, and HQ were mainly in the mountainous hills at the edge of the study area, and the spatial pattern of the distribution of the high-value areas of FS was mainly in the plains around the Dongting Lake watershed. In the 2000–2020 changes, the ESs showed changes in WY in Dongting Lake waters, a slow decrease in the mean value of HQ, an overall increase in SC, an overall slow decrease in CS, and a gradual increase in FS. The land use overuse pattern is mainly policy-oriented, with obvious changes in DLA unutilized land and high LUD values clustered in the lake area related to the land policy of returning farmland to the lake at that time.

LUT has an impact not only on human life and socioeconomic characteristics but also on the regional spatial environment (Dong et al., 2021). This research used a micro-grid scale to explore the fact that ecosystem services in neighboring regions are strongly correlated. The spillover effect makes land use transitions affect ecosystem services not only within the same region but also in neighboring regions (Feng et al., 2023). This study explores the effects of spatial spillovers on ecosystem service types at a grid scale, with different combinations of influencing factors that enhance the persuasive power of GWR. The results also showed that while sensible land use would enhance ESs in nearby areas, socio-economic development would inevitably lead to an increase in transition intensity. Furthermore, the LUI exhibited a negative spatial correlation with the majority of ESs at the grid scale. After 2013, the area had a sharp increase in both urban and rural development, and as a result of the loss of forest land and the accumulation of rural dwelling land, SC services started to diminish. High-value areas of LUD are primarily concentrated in areas with infrequent human activities, primarily in areas with higher elevation and lower LUI and LUD. In contrast, the distribution pattern of high-value areas of SC is different. These areas, including LUD, have a negative correlation with SC and a more homogeneous land structure with more intact soil, primarily composed of forested land.

4.2 Implications for LUT

From 2000 to 2010, the central and northern parts of Dongting Lake witnessed dramatic areas of land-use transformation, mainly in the form of the transfer of arable land to construction land and forest land, leading to a decline in the regional capacity to supply ecosystem services. From 2010 to 2020, the transformation of the Dongting Lake region was reduced, with the spread of aggregation from urban areas to peri-urban areas. In the future, the land use transformation of the Dongting Lake area will take land consolidation, reclamation, development, and urban and rural construction land increase/decrease linkage as a platform to promote the comprehensive improvement of fields, water, mountains, forests, and villages; control the proportion of arable land and forest land transferring to construction land; and enhance the sustainability of the land use structure (Gomersall, 2021). How to enhance ecosystem services through effective land management is a key issue for the sustainable development of Dongting Lake (Griggs et al., 2013). Different ecosystem service types showed different trends of change, except for FS and WY, which showed a decreasing trend. Among them, in terms of carbon stock and

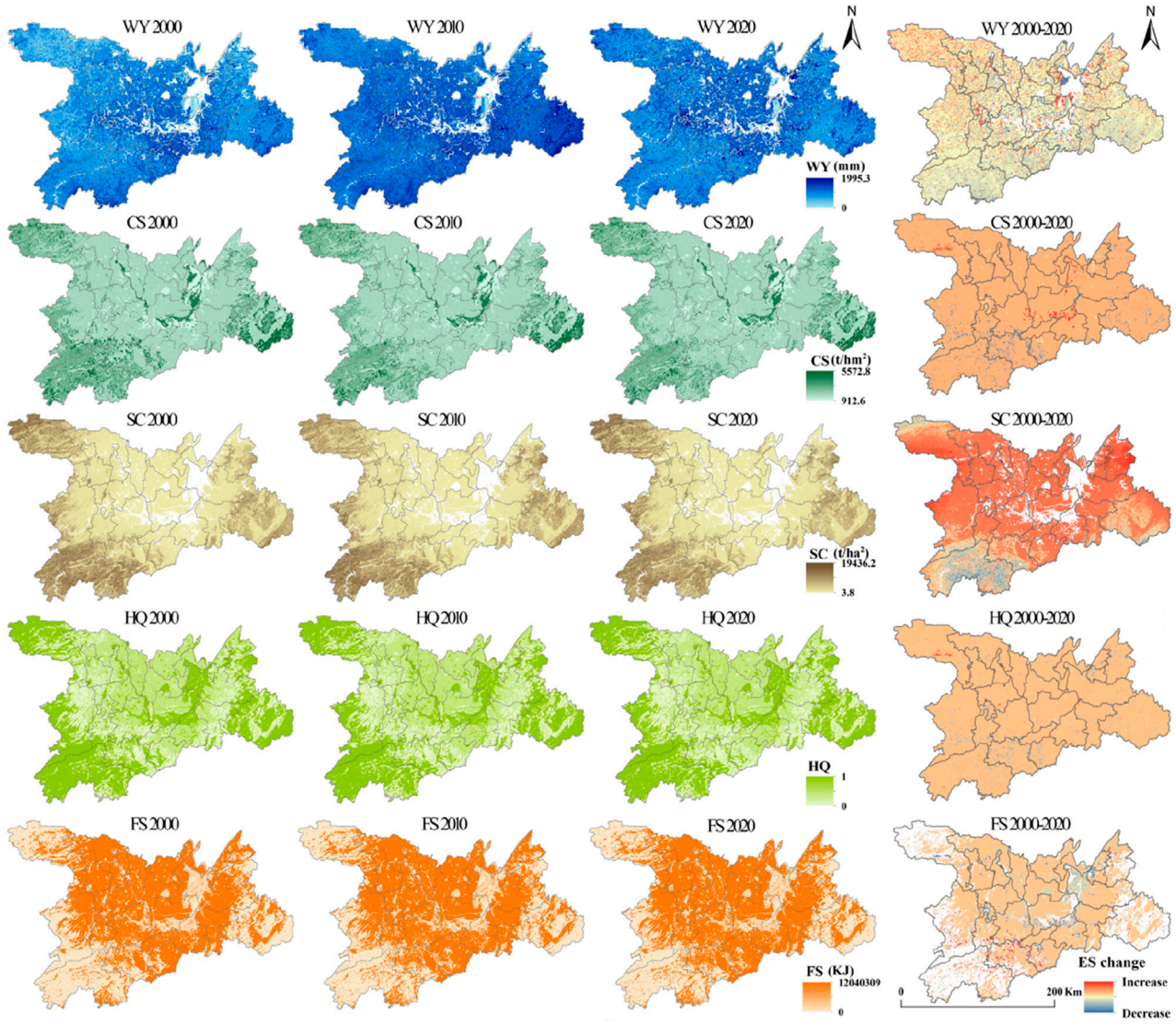

FIGURE 4
Changes in various types of ecosystem services, 2000–2020.

habitat quality, among different land use types, forest land was the main contributor to CS in the study area, while the expansion of construction land was the main reason for the decrease in CS. Therefore, the protection and restoration of forest ecosystems should be strengthened in the Dongting Lake area. For soil and water conservation, slope and vegetation cover in natural conditions determine the ability of soil and water conservation, and since the slope length is not easy to change, improving the vegetation cover on the ground surface can weaken the influence of slope length on soil erosion and reduce the spatial heterogeneity of soil erosion. When carrying out soil erosion control, corresponding soil erosion control measures can be formulated for the dominant factors of erosion differentiation in different regions. In terms of food production, arable land should be further protected, the scale of high-standard farmland should be expanded, and at the same time, agricultural production technology should be upgraded. In terms of water production, water ecology monitoring should be strengthened, wetland shrinkage and degradation should be controlled, and ecological restoration projects for wetland protection should be carried out. Overall, the Dongting Lake area needs to improve rural production, living conditions, and ecological environment and promote the development of large-scale agricultural management, centralized population living, and industrial agglomeration so as to mitigate the impacts of human activities and climate change on ecosystem services and improve the sustainability of the land space in the Dongting Lake area.

4.3 Shortcomings and future study

To explore the impact of LUT on the spatial and temporal changes in ecosystem services, this paper selected GWR to reflect the partial spatial characteristics. Among them, mountainous areas and waters are intuitively more sensitive than built-up areas, causing variations in ecosystem services related to carbon sequestration and water yield services different from other areas. This, in turn, affects

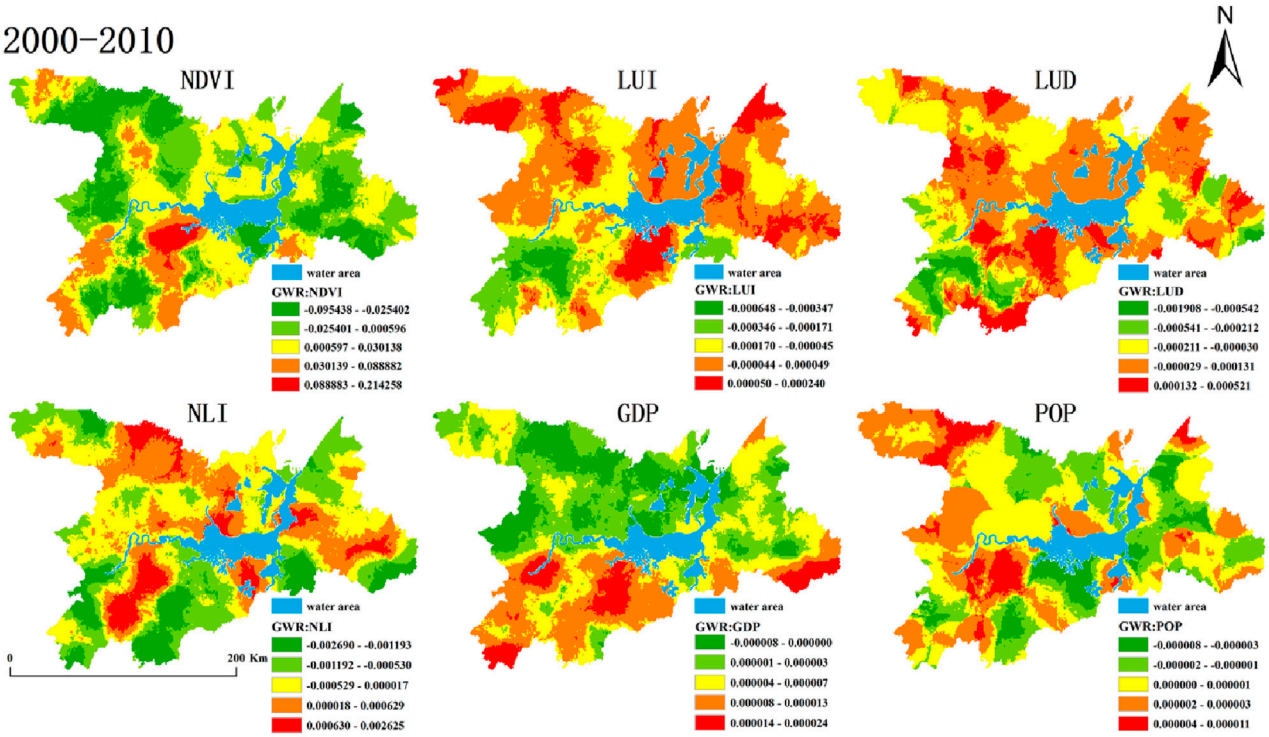

FIGURE 5
Changes in the coefficients of the role of different influencing factors, 2000–2010.

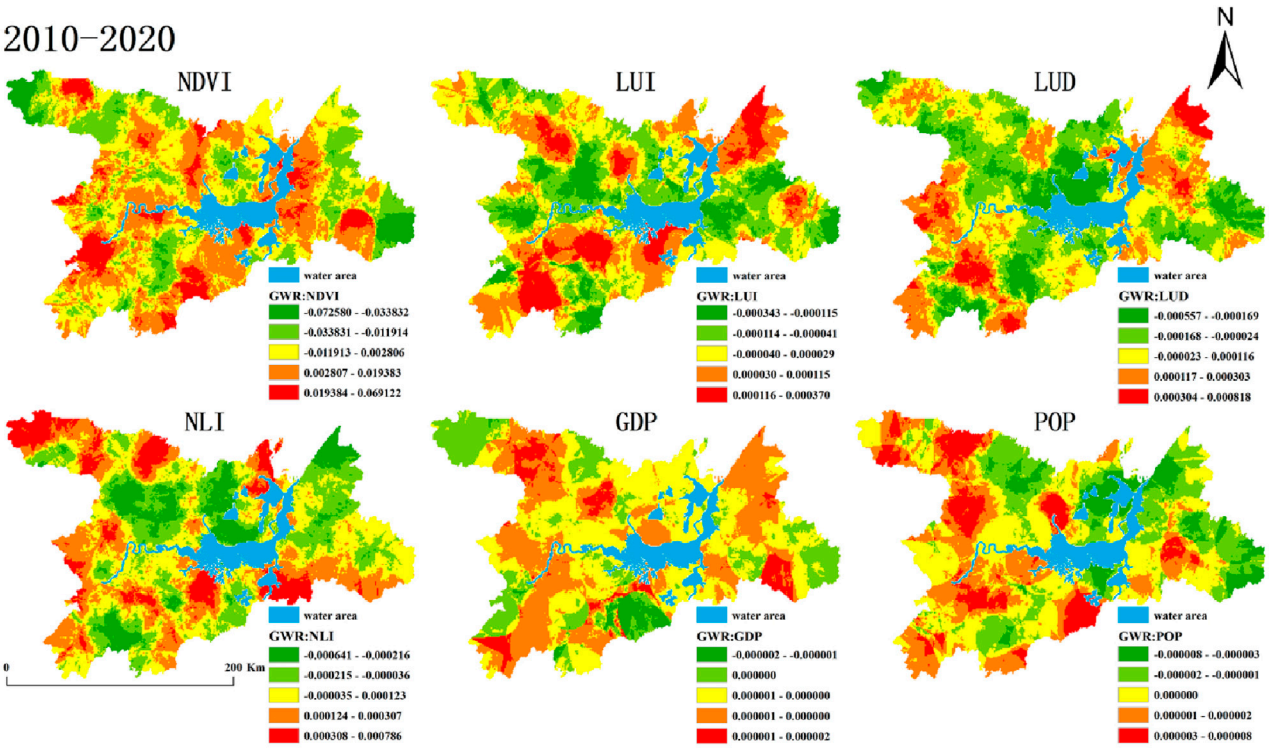

FIGURE 6
Changes in the coefficients of the role of different influencing factors, 2010–2020.

the median values of the corresponding coefficients of variation, which are usually used to characterize the overall GWR results (Chen et al., 2019). Future studies should refine the limitations to quantitative methods, owing to data accuracy. For example, this study measured five types of ecosystem services, which cannot fully reflect the regional ecosystem pattern. In addition, factors such as ecological protection policies should be considered in the future to improve the mechanism of ecosystem service changes.

5 Conclusion

In this paper, the Dongting Lake Ecological and Economic Zone serves as the focal point of our investigation, utilizing remote sensing images from 2000, 2010, and 2020 as primary data sources. Employing grid analysis alongside InVEST and GWR models, we examine the repercussions of LUT on ESs within the study area, spanning from 2000 to 2020. The principal conclusions are outlined as follows:

During the period 2000–2020, the rapid expansion of construction land in the study area led to a significant LUT. The result demonstrates that the mean value of intensity changed from 237.99 in 2000 to 238.92 in 2020. In particular, the high intensity of LUT is mainly distributed around the Dongting Lake Basin, while the low intensity is mainly distributed in the mountainous areas at the edge of the area. Additionally, the dynamics of LUT changed from 5.58 in 2000–2010 to 5.62 in 2010–2020. Among them, the high dynamics in 2000–2010 were mainly distributed in the coastal areas in the northeastern part of Dongting Lake and urban construction areas. On the other hand, the high dynamics in 2010–2020 were mainly located on the outskirts of cities and rural areas.

Different types of ecosystem services displayed spatial and temporal heterogeneity. To be specific, carbon sequestration services, habitat quality services, and soil conservation have similar spatial characteristics, and the high values are primarily distributed in high-elevation mountain areas. In contrast, food production services presented the opposite features, with high values mainly distributed in plain areas. Soil conservation declined first and then ascended. The low value of water services is related to the distribution of watersheds.

There are differences in the factors that influence ecosystem services in different periods. Compared with 2010–2020, NDVI coefficients had the largest value of change in 2000–2010 and the strongest impact on ecosystem services. Notably, the high values in 2000–2010 converge on the west side of Dongting Lake, while the high-value areas in 2010–2020 are scattered all over the research area. Furthermore, LUI and LUD had more grids with high values in 2000–2010, but the number of grids with high values decreased in 2010–2020. The NLI has a higher impact coefficient in the high-value range of 2000–2010 compared to 2010–2020. However, GDP and POP have the smallest coefficients, implying that they have the lowest explanatory validity compared to other impact factors. The findings have significant implications for understanding the relationship and evolutionary processes between land use transition and ecosystem services.

Data availability statement

The original contributions presented in the study are included in the article/Supplementary Material; further inquiries can be directed to the corresponding author.

Author contributions

XS: conceptualization, methodology, software, supervision, validation, and writing–original draft. QN: funding acquisition, project administration, validation, and writing–original draft. ZL: software, supervision, validation, visualization, and writing–original draft.

Funding

The author(s) declare that financial support was received for the research, authorship, and/or publication of this article. This research was funded by the “Hunan Provincial Natural Science Foundation Project” (No. 2022JJ50271).

Conflict of interest

The authors declare that the research was conducted in the absence of any commercial or financial relationships that could be construed as a potential conflict of interest.

Publisher’s note

References

Bai, Y., Chen, Y., Alatalo, J. M., Yang, Z., and Jiang, B. (2020). Scale effects on the relationships between land characteristics and ecosystem services - a case study in Taihu Lake Basin. China. *Sci. Total Environ.* 716, 137083. doi:10.1016/j.scitotenv.2020.137083

Banks-Leite, C., Ewers, R. M., Folkard-Tapp, H., and Fraser, A. (2020). Countering the effects of habitat loss, fragmentation, and degradation through habitat restoration. *One Earth* 3, 672–676. doi:10.1016/j.oneear.2020.11.016

Buckley Biggs, N. (2022). Drivers and constraints of land use transitions on Western grasslands: insights from a California mountain ranching community. *Landsc. Ecol.* 37, 1185–1205. doi:10.1007/s10980-021-01385-6

Burton, M. L., Samuelson, L. J., and Mackenzie, M. D. (2009). Riparian woody plant traits across an urban–rural land use gradient and implications for watershed function with urbanization. *Landsc. And Urban Plan.* 90, 42–55. doi:10.1016/j.landurbplan.2008.10.005

Cao, S., Liu, Z., Li, W., and Xian, J. (2021a). Balancing ecological conservation with socioeconomic development. *Ambio* 50, 1117–1122. doi:10.1007/s13280-020-01448-z

Cao, Y., Kong, L., Zhang, L., and Ouyang, Z. (2021b). The balance between economic development and ecosystem service value in the process of land urbanization: a case study of China's land urbanization from 2000 to 2015. *Land Use Policy* 108, 105536. doi:10.1016/j.landusepol.2021.105536

Chen, W., Chi, G., and Li, J. (2019). The spatial association of ecosystem services with land use and land cover change at the county level in China, 1995–2015. *Sci. Total Environ.* 669, 459–470. doi:10.1016/j.scitotenv.2019.03.139

Cong, W., Sun, X., Guo, H., and Shan, R. (2020). Comparison of the SWAT and InVEST models to determine hydrological ecosystem service spatial patterns, priorities and trade-offs in a complex basin. *Ecol. Indic.* 112, 106089. doi:10.1016/j.ecolind.2020.106089

de Groot, R. (2006). Function-analysis and valuation as a tool to assess land use conflicts in planning for sustainable, multi-functional landscapes. *Landsc. And Urban Plan.* 75, 175–186. doi:10.1016/j.landurbplan.2005.02.016

Dong, J. H., Zhang, Z. B., Da, X. J., Zhang, W. B., and Feng, X. L. (2021). Eco-environmental effects of land use transformation and its driving forces from the perspective of "production-living-ecological" spaces: a case study of Gansu Province. *Acta Ecol. Sin.* 41 (15), 5919–5928. doi:10.5846/stxb201909201969

El-Naggar, A., Zhou, R., Tang, R., Hur, J., Cai, Y., and Chang, S. X. (2022). Rice husk and its biochar have contrasting effects on water-soluble organic matter and the microbial community in a bamboo forest soil. *Land* 11, 2265. doi:10.3390/land11122265

Feng, X., Li, Y., Wang, X., Yang, J., Yu, E., Wang, S., et al. (2023). Impacts of land use transitions on ecosystem services: a research framework coupled with structure, function, and dynamics. *Sci. Total Environ.* 901, 166366. doi:10.1016/j.scitotenv.2023.166366

Gomersall, K. (2021). Governance of resettlement compensation and the cultural fix in rural China. *Environ. Plan. A* 53, 150–167. doi:10.1177/0308518x20926523

Griggs, D., Stafford-Smith, M., Gaffney, O., Rockström, J., Öhman, M. C., Shyamsundar, P., et al. (2013). Sustainable development goals for people and planet. *Nature* 495, 305–307. doi:10.1038/495305a

Hasan, S. S., Zhen, L., Miah, M. G., Ahamed, T., and Samie, A. (2020). Impact of land use change on ecosystem services: a review. *Environ. Dev.* 34, 100527. doi:10.1016/j.envdev.2020.100527

Jiang, L., and Zeng, Z. (2024). Analysis of flood water level variation in the yichang–chenglingji reach of the Yangtze River after three gorges project operation. *Water* 16, 841. doi:10.3390/w16060841

Jie, N., Cao, X., Chen, J., and Chen, X. (2023). A new method for identifying the central business districts with nighttime light radiance and angular effects. *Remote Sens.* 15, 239. doi:10.3390/rs15010239

Keyes, A. A., McLaughlin, J. P., Barner, A. K., and Dee, L. E. (2021). An ecological network approach to predict ecosystem service vulnerability to species losses. *Nat. Commun.* 12, 1586–1611. doi:10.1038/s41467-021-21824-x

Kleijn, D., Kohler, F., B´ aldi, A., Bat´ ary, P., Concepci´on, E. D., Clough, Y., et al. (2009). On the relationship between farmland biodiversity and land-use intensity in Europe. *Proc. R. Soc. B* 276, 903–909. doi:10.1098/rspb.2008.1509

Li, P., Zuo, D., Xu, Z., Zhang, R., Han, Y., Sun, W., et al. (2021). Dynamic changes of land use/cover and landscape pattern in a typical alpine river basin of the Qinghai-Tibet Plateau, China. *Land Degrad. Dev.* 32, 4327–4339. doi:10.1002/ldr.4039

Li, S., Jiang, C., Ma, Y., and Li, C. (2023). Spatiotemporal analysis of hydrometeorological factors in the source region of the dongting Lake Basin, China. *Atmosphere* 14, 1793. doi:10.3390/atmos14121793

Liu, C., Deng, C., Li, Z., and Liu, Y. (2022). Response characteristics of soil erosion to spatial conflict in the production-living-ecological space and their DrivingMechanism: a case study of dongting Lake Basin in China. *Land* 11, 1794. doi:10.3390/land11101794

Liu, C., Liu, Y., Giannetti, B. F., Almeida, C. M. V. B., Sevegnani, F., and Li, R. (2023). Spatiotemporal differentiation and mechanism of anthropogenic factors affecting ecosystem service value in the Urban Agglomeration around Poyang Lake, China. *Ecol. Indic.* 154, 110733. doi:10.1016/j.ecolind.2023.110733

Liu, J. Y. (1996). *The macro investigation and dynamic research of the resource and environment*. Beijing: China Science and Technology Press.

Long, H., and Chen, K. (2021). Urban-rural integrated development and land use transitions: a perspective of land system science. *Acta Geogr. Sin.* 76 (2), 295–309. doi:10.11821/dlxb202102004

Ma, L., Liu, H., Peng, J., and Wu, J. (2017). A review of ecosystem services supply and demand. *Acta Geogr. Sin.* 72 (7), 1277–1289. doi:10.11821/dlxb201707012

Ning, Q., and Ouyang, X. (2023). Spatio-temporal characteristics and mechanism of ecological degradation in a hilly southern area—a case study of Dong ting Lake Basin. *Environ. Sci. Pollut. Res.* 30, 45274–45284. doi:10.1007/s11356-023-25514-7

Ouyang, X., Wang, K., and Wei, X. (2022). The impact of the correlation between urban and rural construction land on ecosystem services: a case study of Dong ting Lake area. *J. Acta Ecol. Sin.* (21), 8713–8722. doi:10.5846/stxb202110182937

Qi, Y., Wang, R., Shen, P., Ren, S., and Hu, Y. (2023). Impacts of land use intensity on ecosystem services: a case study in harbin city, China. *Sustainability* 15, 14877. doi:10.3390/su152014877

Sancho Santos, M. E., Eva, Š., Pavel, H., and Christoph, S. (2021). Comment on "Diluted concentrations of methamphetamine in surface water induce behavior disorder, transgenerational toxicity, and ecosystem-level consequences of fish" by Wang et al. [Water Research 184 (2020) 116-164]. *Water Res.* 197, 117007. doi:10.1016/j.watres.2021.117007

Shi, Y., Feng, C.-C., Yu, Q., and Guo, L. (2021). Integrating supply and demand factors for estimating ecosystem services scarcity value and its response to urbanization in typical mountainous and hilly regions of south China. *Sci. Total Environ.* 796, 149032. doi:10.1016/j.scitotenv.2021.149032

Song, X. (2017). Research framework of land use transition. *Acta Geogr. Sin.* 72 (03), 471–487.

Song, X., Liu, Y., Zhu, X., Cao, G., Chen, Y., Zhang, Z., et al. (2022). The impacts of urban land expansion on ecosystem services in Wuhan, China. *Environ. Sci. Pollut. Res.* 29, 10635–10648. doi:10.1007/s11356-021-16419-4

Terrado, M., Sabater, S., Chaplin-Kramer, B., Mandle, L., Ziv, G., and Acuña, V. (2016). Model development for the assessment of terrestrial and aquatic habitat quality in conservation planning. *Sci. Total Environ.* 540, 63–70. doi:10.1016/j.scitotenv.2015.03.064

Wang, Y., Dai, E., Yin, L., and Ma, L. (2018). Land use/land cover change and the effects on ecosystem services in the Hengduan Mountain region, China. *Ecosyst. Serv.* 34, 55–67. doi:10.1016/j.ecoser.2018.09.008

Wang, Z., Fu, H., Liu, H., and Liao, C. (2023a). Urban development sustainability, industrial structure adjustment, and land use efficiency in China. *Sustain. Cities Soc.* 89, 104338. doi:10.1016/j.scs.2022.104338

Wang, Z., Wan, D., Liao, J., Lv, J., Wu, F., and Wang, L. (2023b). Ecological environment effect and driving factors of transformation of"Production-Living-Ecological Space"in Dong ting Lake eco-economic zone. *J. Sci. Technol. Eng.* 23 (9), 3876–3888. doi:10.12404/j.issn.1671-1815.2023.23.09.03876

Wei, P., Chen, S., Wu, M., Deng, Y., Xu, H., Jia, Y., et al. (2021). Using the InVEST model to assess the impacts of climate and land use changes on water yield in the upstream regions of the shule River Basin. *Water* 13, 1250. doi:10.3390/w13091250

Wen, L., Chatalova, L., Butsic, V., Hu, F. Z., and Zhang, A. (2020). Capitalization of land development rights in rural China: a choice experiment on individuals' preferences in peri-urban Shanghai. *Land Use Policy* 97, 104803. doi:10.1016/j.landusepol.2020.104803

Wentland, S. A., Ancona, Z. H., Bagstad, K. J., Boyd, J., Hass, J. L., Gindelsky, M., et al. (2020). Accounting for land in the United States: integrating physical land cover, land use, and monetary valuation. *Ecosyst. Serv.* 46, 101178. doi:10.1016/j.ecoser.2020.101178

Williams, J. R., Jones, C. A., and Dyke, P. T. (1984). A modeling approach to determining the relationship between erosion and soil productivity. *Trans. ASAE.* 27, 129–144.doi:10.13031/2013.32748

Xiang, H., Zhang, J., Mao, D., Wang, Z., Qiu, Z., and Yan, H. (2022). Identifying spatial similarities and mismatches between supply and demand of ecosystem services for sustainable Northeast China. *Ecol.Indic.* 134, 108501. doi:10.1016/j.ecolind.2021.108501

Xu, D. X., Wu, F., He, L. H., Liu, H. J., and Jiang, Y. (2019). Impact of land use change on ecosystem services: case study of the Zhangjiakou-Chengde area. *Acta Ecol. Sin.* 39 (20), 7493–7501. doi:10.5846/stxb201810072163

Yang, J., Zeng, C., and Cheng, Y. (2020). Spatial influence of ecological networks on land use intensity. *Sci. Total Environ.* 717, 137151. doi:10.1016/j.scitotenv.2020.137151

Yang, Q., Duan, X., Wang, L., and Jin, Z. (2018). Land use transformation and ecological environment effect based on "Three-life space": a case study of the core area of the Yangtze River Delta. *Sci. Geogr. Sin.* 38 (01), 97–106. doi:10.13249/j.cnki.sgs.2018.01.011

Yu, C., Zhang, Z., Jeppesen, E., Gao, Y., Liu, Y., Liu, Y., et al. (2024). Assessment of the effectiveness of China's protected areas in enhancing ecosystem services. *Ecosyst. Serv.* 65, 101588. doi:10.1016/j.ecoser.2023.101588

Zhao, Y., Luo, J., Li, T., Chen, J., Mi, Y., and Wang, K. (2023). A framework to identify priority areas for restoration: integrating human demand and ecosystem services in Dongting Lake eco-economic zone, China. *Land* 12, 965. doi:10.3390/land12050965

Zhou, Y., Li, X., and Liu, Y. (2020). Land use change and driving factors in rural China during the period 1995-2015. *Land Use Policy* 99, 105048. doi:10.1016/j.landusepol.2020.105048

Zou, Y., Meng, J., Zhu, L., Han, Z., and Ma, Y. (2024). Characterizing land use transition in China by accounting for the conflicts underlying land use structure and function. *J. Environ. Manag.* 349, 119311. doi:10.1016/j.jenvman.2023.119311

frontiers | Frontiers in Environmental Science

TYPE Original Research
PUBLISHED 30 July 2024
DOI 10.3389/fenvs.2024.1428197

OPEN ACCESS

EDITED BY
Xiao Ouyang,
Hunan University of Finance and Economics, China

REVIEWED BY
Siyun Chen,
Hunan University of Finance and Economics, China
Lijuan Cui,
Chinese Academy of Forestry, China

*CORRESPONDENCE
Yi Jin,
378568113@qq.com

RECEIVED 05 May 2024
ACCEPTED 15 July 2024
PUBLISHED 30 July 2024

CITATION
Wei J, Jin Y, Tan Q, Liu F, Ding C, Li T, Luo J, Hu C, Cui X, Liu Y, Zheng X and Zhang G (2024), Trend analysis of long-time series habitat quality in Beijing based on multiple models. *Front. Environ. Sci.* 12:1428197. doi: 10.3389/fenvs.2024.1428197

Trend analysis of long-time series habitat quality in Beijing based on multiple models

Jiaming Wei[1], Yi Jin[1]*, Qilin Tan[1], Fei Liu[1], Chi Ding[1], Tiantian Li[1], Ji Luo[2], Chen Hu[3], Xiaohong Cui[1], Yuheng Liu[1], Xiaoyi Zheng[1] and Guiwei Zhang[1]

[1]PowerChina Beijing Engineering Corporation Limited, Beijing, China, [2]Anhui Province Jing County Niu Ling Reservoir Project Construction Management Division, Xuancheng, Anhui, China, [3]Jing County Water Conservancy Bureau, Xuancheng, Anhui, China

This study selects Beijing from 1980 to 2020 as the research area, utilizing high temporal resolution land use data to analyze through the habitat quality module of the InVEST model. Unlike previous research, this study employs the Theil-Sen Median method and Mann-Kendall test to analyze the trend changes in habitat quality more accurately. This method has significant advantages in dealing with non-linear and non-normally distributed data over long time series, providing a more accurate and reliable analysis of habitat quality trends. Methodologically, the study first collects and organizes the land use type data of Beijing from 1980 to 2020, then uses the habitat quality module of the InVEST model to process and analyze the data of each year, assessing the impact of different land use types on habitat quality. Subsequently, the Theil-Sen Median method and Mann-Kendall test are used to analyze the time series trend of habitat quality, to identify and quantify the trend and significance of habitat quality changes. The results show that over the past 40 years, the area of construction land in Beijing has significantly expanded, leading to a compression of other types of land. The spatial distribution of habitat quality shows a clear difference between the two sides divided by a line connecting the northeast and southwest, with the west side being the area of good habitat quality and the east side being poorer. In the past 10 years, the overall habitat quality has improved, but most areas still show a decreasing trend, especially in the western and northern mountainous areas where habitat quality has significantly declined. Based on these findings, it is recommended that future urban planning and land management should pay more attention to the protection and improvement of habitat quality, especially the restoration work for areas with poor habitat quality.

KEYWORDS

Beijing, long time series, habitat quality, InVEST, Theil-Sen median

1 Introduction

As the process of urbanization accelerates, human activities increasingly impact natural habitats. Megacities, due to their unique agglomeration effect, exert tremendous pressure on the surrounding natural environment, posing a serious threat to biodiversity. Numerous studies have pointed out that urban expansion is one of the main drivers of biodiversity loss (Sala et al., 2000; Falcucci et al., 2007).

TABLE 1 Threat factors of habitat quality measurement of InVEST model.

Threat source	Maximum influence distance/km	Weight	Decline type
Plough	Eight	0.6	Linear
Village	Five	0.8	Index
Cities and towns	10	One	Index
Traffic	Three	0.6	Linear

TABLE 2 Sensitivity coefficient of habitat quality measurement of InVEST model.

Land type		Habitat suitability	Plough	Village	Cities and towns	Traffic
Plough	Paddy field	0.6	0.3	0.35	0.5	0.1
	Dry land	0.4	0.3	0.35	0.5	0.1
Woodland	Woodland	one	0.8	0.85	one	0.6
	Spinney	one	0.4	0.45	0.6	0.2
	Sparse wood land	one	0.85	0.9	one	0.65
	Other woodlands	one	0.9	0.95	one	0.7
Lawn	High coverage grassland	0.8	0.4	0.45	0.6	0.2
	Middle covered grassland	0.75	0.45	0.5	0.65	0.25
	Low-covered grassland	0.7	0.5	0.55	0.7	0.3
Waters	Rivers and canals	one	0.65	0.7	0.85	0.45
	Shuiku kengtang	one	0.7	0.75	0.9	0.5
	Beachland	0.6	0.75	0.8	0.95	0.55
Land for construction	Urban land use	0	0	0	0	0
	Rural residential land	0	0	0	0	0
	Other construction land	0	0	0	0	0
Unusually	Unused land 1	0	0	0	0	0
	Unused land 2	0	0	0	0	0

The process of urbanization is often accompanied by the loss of natural habitat and the degradation of ecosystem functions, which poses a serious threat to biodiversity. At the same time, the service functions provided by the ecosystem, such as water conservation, soil conservation and air purification, are directly related to human survival and health, and their loss will have a far-reaching impact on human wellbeing. First of all, rapid urbanization leads to fragmentation, islanding and artificialization of the natural environment, which not only limits the migration and reproduction of species, but also makes the ecosystem fragile and unstable. Coupled with environmental pollution and over-utilization of resources caused by human activities, many rare species are facing survival crisis, and the speed of biodiversity loss is accelerating day by day. Secondly, the loss of ecosystem services will have a serious impact on human life. For example, the decline of water conservation function will directly affect the safety of urban water supply; The loss of soil conservation function will aggravate soil erosion and land degradation; The weakening of air purification function will make urban air quality decline and threaten residents' health. The loss of these ecosystem services will seriously restrict the sustainable development of cities. Therefore, under the background of rapid urbanization, it is particularly urgent to protect biodiversity and ecosystem services.

Currently, methods for assessing biodiversity loss or habitat quality mainly include model prediction methods and landscape analysis methods. Model prediction methods forecast the range and quality of habitats based on changes in habitat conditions or land use types, such as species distribution prediction based on the Maximum Entropy model (MaxEnt) (Phillips et al., 2013), and habitat quality assessment using the InVEST (Integrated Valuation of Environmental Services and Tradeoffs) model (Tallis et al., 2012). As an integrated evaluation tool, the InVEST model can assess habitat quality and analyze multiple ecosystem services such as water retention and water supply calculation. Due to its relatively low data requirements and strong result visualization, it has been widely applied in habitat and ecosystem service research (Wang et al., 2023).

Although there has been a lot of habitat quality analysis using the InVEST model, most studies focus on assessments in specific areas or over short time scales. For example, one study used the InVEST model combined with the topographic distribution index and Mann-Kendall test to analyze the impact of topographic gradients on habitat quality, proposing ecological management suggestions for different altitude areas (Xiang et al., 2023); another study focused on the changes in habitat quality in the Wuyi Mountain reserve over 40 years, highlighting the close connection between population density and habitat quality (Zhang et al., 2023a). These studies provide valuable insights into understanding the impact of specific factors on habitat quality, but there is still a research gap in how to comprehensively assess and manage habitat quality in urban and surrounding areas against the backdrop of rapid urbanization.

In terms of coupling different models (Tang et al., 2023), scholars have used the InVEST (SWESMI) toolkit, HQR, and HRA models for ecosystem service modeling at the sub-basin scale to perform ecological quality, rarity, and risk assessment analysis, emphasizing the importance of land conservation and protected areas in maintaining habitat quality and reducing risks related to habitat degradation and biodiversity (Wu et al., 2023).

Habitat quality is an important indicator, which is used to evaluate the ability to maintain biodiversity and ecological carrying capacity in a region (Gao et al., 2017). At present, the research on spatial pattern of land use mainly focuses on land use efficiency, land use structure and land use function. Studies have shown that with the increase of residential and industrial land, the habitat quality in coastal urban areas has decreased significantly (Zhang et al., 2020). Scholars have studied the correlation and influence of compact urban development on the habitat quality in ecosystem services, providing a basis for urban ecological landscape construction (Yu et al., 2023). Zhao et al. (2022) used InVEST model to evaluate the impact of land use change on the habitat quality of Xiaolangdi reservoir area in China for more than 30 years. Taking Fuzhou natural wetland as an example, quantitatively analyzed the temporal and spatial changes of ecosystem service value caused by urban land activities, and showed that the ecosystem service function decreased significantly due to large-scale urban land expansion (Cai et al., 2013). Hu et al. analyzed the factors such as habitat quality, biodiversity and landscape diversity in Pan 'an Lake area of Xuzhou by using InVEST model, thus clarifying the ecological environment quality in this area (Hu and Xu, 2018). Jia et al.(2013) analyzed the land use and ecological changes in Xuzhou coal mining area, and found that the habitat quality in the study area continued to decline due to the increase of coal mining and urbanization.

In terms of characteristics and significance, this study adopts new technical means or integrates various methods to analyze habitat quality, such as combining remote sensing technology with ground survey data, which improves the accuracy and reliability of data; Compared with similar studies, this study may pay more attention to the collection and integration of long-time series data, and reveal the deep-seated laws and trends of habitat quality changes through big data analysis technology; The research area selected in this study may have special geographical, climatic or ecological characteristics, which makes the research results more targeted and practical for ecological protection and management in this area and even in a wider range. Compared with other research areas at home and abroad, this research area may face more unique habitat threats or protection challenges, so the research results are of great significance for formulating targeted ecological protection policies. This study may comprehensively evaluate the habitat quality from multiple dimensions, not only considering the traditional indicators such as biodiversity and habitat connectivity, but also including factors such as ecosystem services and human activities, making the evaluation results more comprehensive and closer to reality. At the same time, this study may pay more attention to the interaction and correlation between different habitat types, so as to reveal the complexity and comprehensiveness of habitat quality change more accurately. On the basis of revealing the trend of habitat quality change, it may further put forward operable policy suggestions and practical guidance, which provide scientific basis for ecological protection and management, and pay more attention to transforming research results into practical applications, and promote the continuous improvement of habitat quality through policy suggestions and specific practices.

As the capital of China and a megacity, the change of its habitat quality not only affects the quality of life of urban residents, but also directly affects the sustainable development of the city. With the rapid development of economy and the acceleration of urbanization, Beijing is facing many ecological and environmental problems, such as air pollution, water shortage and biodiversity reduction. Therefore, a long-time series trend analysis of Beijing's habitat quality is helpful to reveal the development law and evolution trend of these problems and provide scientific basis for formulating effective ecological protection and management policies. Beijing also has a relatively complete ecological environment monitoring system and rich data resources. Over the years, the government and all walks of life have continuously paid attention to and monitored the ecological environment in Beijing, and accumulated a lot of data. These data not only cover air quality, water resources quality, biodiversity and other aspects, but also include data of different time scales, which enables us to comprehensively analyze habitat quality from the perspective of long time series. In addition, Beijing has made a series of remarkable achievements and experiences in ecological environment protection. In recent years, Beijing Municipal Government has attached great importance to ecological environment protection, increased investment and implemented a series of effective policies and measures. How to reflect the implementation effect of these measures on a long time scale is also a problem worthy of in-depth study. By analyzing the long-term trend of Beijing's habitat quality, we can evaluate the effectiveness of these policies and measures, and provide experience and enlightenment for other cities. As an international metropolis, the change of habitat quality in Beijing is also of international significance. By analyzing the long-term trend of Beijing's habitat quality, we can compare and communicate with similar research in the world and jointly promote the development of global ecological environmental protection. In 2022, Beijing's population reached 21.843 million (Gao et al., 2017), and the city's rapid expansion and development have led to a shortage of construction land, with human impact reaching the development of overall habitat quality. However, the

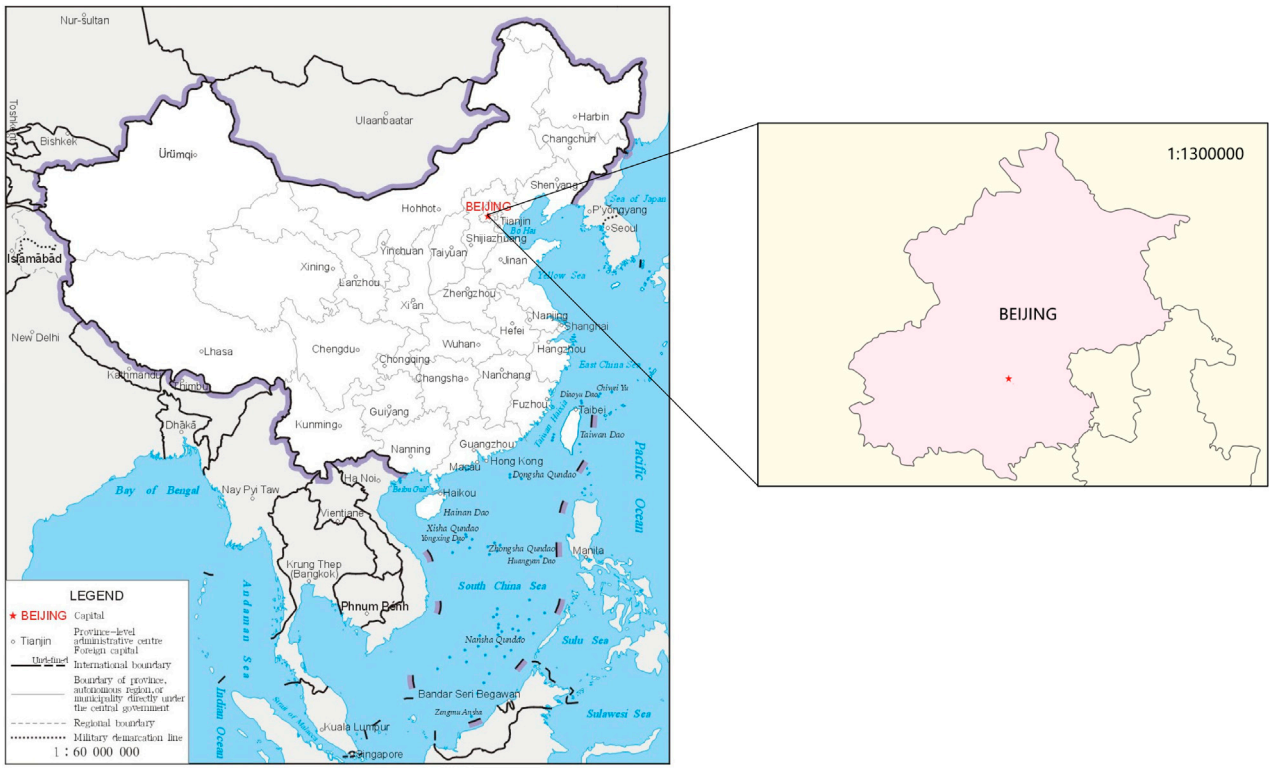

FIGURE 1
Regional location.

long-term impact and its distribution are not yet clear. In light of this, this study aims to conduct an in-depth analysis of the long-term trend of habitat quality in Beijing from 1980 to 2020 by analyzing changes in land use types and utilizing the habitat quality module of the InVEST model, combined with the Theil-Sen Median method and Mann-Kendall test. Specifically, this study seeks to reveal how human activities affect the trend of habitat quality changes during the rapid urbanization process and how these changes further impact biodiversity. Through a comprehensive analysis of long time series, this study hopes to provide more accurate data support and scientific policy recommendations for urban planning and ecological protection. Especially for megacities like Beijing, the findings of this study will contribute to achieving a sustainable balance between urban development and ecological conservation.

2 Research area and research methods

2.1 Overview of the study area

Beijing is the capital of People's Republic of China (PRC), a municipality directly under the Central Government, a national central city and a mega-city Figure 1. The State Council has approved China's political center, cultural center, international exchange center and scientific and technological innovation center. By 2020, Beijing has 16 districts with a total area of 16,410.54 square kilometers. By the end of 2022, the permanent population of Beijing was 21.843 million. Located in the north of China and the north of North China Plain, Beijing is adjacent to Tianjin in the east and Hebei Province in the rest. Its center is located at 116 20′ east longitude and 39 56′ north latitude. It is a world-famous ancient capital and a modern international city.

Beijing is high in the northwest and low in the southeast. The west, north and northeast are surrounded by mountains on three sides, and the southeast is a plain that slowly inclines to the Bohai Sea. The main rivers flowing through the territory are Yongding River, Chaobai River, North Canal, Juma River, etc. The climate of Beijing is warm temperate semi-humid semi-arid monsoon climate, with high temperature and rainy summer, cold and dry winter and short spring and autumn. Beijing was rated as the first-tier city in the world by the world urban research institute GaWC, and the United Nations report pointed out that Beijing ranked second in China in terms of human development index (Zhang et al., 2020).

2.2 Data sources and quality control

The high-precision land type classification map from 1980 to 2020 is selected as the research basis of habitat quality change, which comes from the 30 m data of Beijing, Institute of Geographical Sciences and Resources and Environment, China Academy of Sciences (Zhang et al., 2020).

The data that support the findings of this study are available from Resources and environment science data registration and publishing system but restrictions apply to the availability of

these data, which were used under license for the current study, and so are not publicly available. Data are however available from the authors upon reasonable request and with permission of Resources and environment science data registration and publishing system. The maps in the text are from the official maps on the Chinese government website and can be used freely without involving copyright issues. For more details, visit the website: http://bzdt.ch.mnr.gov.cn/.

In order to ensure the accuracy and reliability of remote sensing data, and then affect the application and research effect of remote sensing images, this study preprocesses remote sensing data, including geometric correction, image fusion, image mosaic, image cropping, cloud removal and shadow processing, and atmospheric correction. The purpose of these steps is to remove the noise and interference information in the original data and improve the data quality. In quality control, data verification evaluates the reliability and consistency of data by comparing with ground observation data; Data accuracy evaluation determines the accuracy of data through error analysis and verification test.

2.3 Research methods

2.3.1 Land use transfer matrix

Land use transfer matrix shows the quantitative relationship between land cover types in two different periods in the form of matrix, which can fully reflect the value and transfer direction of a regional land cover type (Yu et al., 2023). Land use transfer matrix is the application of Markov model in land use change. Markov model can not only quantitatively show the transformation between different land use types, but also reveal the transfer rate between different land use types. The land use transfer matrix comes from the quantitative description of system state and state transfer in system analysis. In the usual land use transfer matrix, the row indicates the land use type at time T1, and the column indicates the land use type at time T2.

2.3.2 Habitat quality measurement of invest model

Habitat quality means that the ecological environment can provide the ability to adapt to natural ecological conditions, which has strong regionality (Zhao et al., 2022). InVEST model is a comprehensive evaluation tool of ecosystem services, which can simulate the changes of the quality and value of ecosystem services under different land cover scenarios and provide comprehensive information of ecosystem services for decision makers. Compared with the traditional literal abstract expression, InVEST model can provide a visual expression of the evaluation results, which makes the results more intuitive and easy to understand, and helps decision makers to better understand and use the evaluation results. The model is robust to the changes and abnormal values of input data, and its flexible parameter setting also enables it to adapt to different research scenarios.

The quality of habitat can reflect the fragmentation degree of regional habitat and its anti-interference ability to habitat degradation. The range of calculation results is 0–1, and the larger the value, the stronger the anti-interference ability of the study area to habitat degradation. The calculation formula is:

$$Q_{xj} = H_j\left(1 - \left(\frac{D_{xj}^z}{D_{xj}^z - k^z}\right)\right)$$

Where Qxj represents the habitat quality of grid X in land use type J; Hj represents the habitat suitability of land use type J; Dxj indicates the stress level of grid X in land use type J; Z represents a normalized constant; K is the scaling constant. Where Dxj is calculated as follows:

$$D_{xj} = \sum_{r=1}^{R}\sum_{y=1}^{Y_r}\left(\frac{W_r}{\sum_{r=1}^{R} W_r}\right) r_j i_{rxy} \beta_x S_{jr}$$

Where r is the number of stress factors; R is a stress factor; Y is the grid number of stress factor r; Yr is the number of grids occupied by stress factors; Wr is the weight of stress factor, with the range of 0–1; Irxy is the influence (exponential or linear) of stress factor R on each grid of habitat; βx is the anti-interference level of habitat; Sjr is the relative sensitivity of different habitats to each stress factor (Tallis et al., 2012).

The determination of threat factor and sensitivity coefficient in this paper comes from the recommendation of model instruction, related literature (Cai et al., 2013; Hu and Xu, 2018; Wang et al., 2023; Liu et al., 2021; Ying et al., 2022; Zhang et al., 2023b; Tables 1, 2).

2.3.3 Trend analysis based on Theil-Sen Median method and Mann-Kendall test

Theil-Sen Median method, also known as Sen slope estimation, is a robust nonparametric trend calculation method. This method has high calculation efficiency, is insensitive to measurement error and interest group data, and is suitable for trend analysis of long-time series data (Jia et al., 2013). Theil Sen Median method is a nonparametric statistical method, and there is no strict assumption for data distribution, so it is suitable for all kinds of data sets, including non-normal distribution or abnormal values (Vannest et al., 2012). This method has high calculation efficiency and is insensitive to measurement errors and outliers, especially suitable for trend analysis of long-time series data. By considering all possible point pairs in the data set and calculating the median slope, Theil Sen Median method can provide robust estimation of data trends, reduce the influence of outliers on the results, and the calculated slope can directly reflect the changing trend of data with time, which is helpful for researchers to quickly understand the dynamic characteristics of data. Its calculation formula is:

$$\beta = \text{Median}\left(\frac{x_j - x_j}{j - i}\right) \quad \forall j > i$$

Where Median () stands for median, if $\beta > 0$, it indicates that habitat change is an increasing trend, and *vice versa*.

Mann-Kendall (MK) test is a nonparametric time series trend test method, which does not need the measured values to obey normal distribution and is not affected by missing values and abnormal values, and is suitable for the trend significance test of long time series data (Ban et al., 2023). Mann Kendall test is a nonparametric test method, which does not need to assume the data distribution and is not disturbed by a few abnormal values, so it has great flexibility and applicability for trend and catastrophe point analysis (Hamed and Rao, 1998). This method is especially suitable

for analyzing the trend and catastrophe point of time series of precipitation, runoff, temperature and water quality, and is helpful to reveal the long-term change characteristics of ecosystems. By calculating the z value and carrying out significance test, Mann Kendall test can judge the significance level of the trend and provide reliable decision-making basis for researchers. The process is as follows: for the sequence XT = X1, X2, XN, first determine the size relationship between xi and xj in all dual values (xi, xj, j > i) (set as S). Make the following assumptions: H0, the data in the sequence are randomly arranged, that is, there is no significant trend; H1, the sequence has an upward or downward trend. The formula for calculating the test statistic S is (in the formula for calculating Z, when S > 0, the molecule is S-1)

$$S = \sum_{i=1}^{n-1} \sum_{j=i+1}^{n} sgn\left(x_j - x_i\right)$$

Where sgn () is a symbolic function, and the calculation formula is:

$$sgn\left(x_j - x_i\right) = \begin{cases} 1 & x_j - x_i > 0 \\ 0 & x_j - x_i = 0 \\ -1 & x_j - x_i < 0 \end{cases}$$

Use the test statistic z for trend test, and the calculation method of z value is:

$$Z = \begin{cases} \dfrac{S}{\sqrt{Var\,(S)}} & (S > 0) \\ 0 & (S = 0) \\ \dfrac{S+1}{\sqrt{Var\,(S)}} & (S < 0) \end{cases}$$

Among them, the calculation formula of Var is:

$$\mathrm{Var}\,(S) = \frac{n(n-1)(2n+5) - \sum_{i=1}^{m}(t_i - 1)(2t_i + 5)}{18}$$

Where n is the number of data in the sequence, m is the number of repeated data groups, and ti is the number of repeated data in the I-th repeated data group.

The critical value Z1-α/2 is found in the normal distribution table under a given significance level by using the bilateral trend test. When | z | ≤ Z1-α/2, the original hypothesis is accepted, that is, the trend is not significant; If | z | > Z1-α/2, the original hypothesis is rejected, that is, the trend is significant.

Given the significance level α = 0.05, the critical value Z1-α/2 = 1.96. When the absolute value of Z is greater than 1.65, 1.96 and 2.58, it means that the trend has passed the significance test with 90%, 95% and 99% reliability respectively. Judgement method of trend significance.

When β > 0, the trend is characterized by an increasing trend; when Z > 2.58, it is characterized by an extremely significant increase; when 1.96 < Z ≤ 2.58, it is a significant increase; when 1.65 < Z ≤ 1.96, it is a slightly significant increase; when Z ≤ 1.65, it is a general increase.

When β = 0, the trend is characterized by no change.

When β < 0, the trend is characterized by decreasing trend; when Z > 2.58, it is characterized by extremely significant decrease; when 1.96 < Z ≤ 2.58, it is significantly decreased; when 1.65 < Z ≤ 1.96, it is slightly decreased; when Z ≤ 1.65, it is generally decreased.

Tread(i) = 3 was significantly increased; Slightly increased tread(i) = 2; Generally increase tread(i) = 1; Significantly reduce tread(i) = −3; Slightly decreased tread(i) = −2; Generally decreased tread(i) = −1; No change tread(i) = 0.

3 Results

3.1 Analysis of changes in land use types

With the development of urban and rural areas, the change of land use types also presents a certain spatial and temporal change. The change map of land use types is shown in Figure 2. In addition to the obvious expansion of construction land in the central city, there is also a certain expansion of construction land in the northern mountainous areas. The area of paddy fields is decreasing year by year, but the land use such as reservoirs and ponds has changed little. Specific to the area change, as shown in Figure 3. Among them, cultivated land, woodland, grassland, water area and other areas have all been compressed to a certain extent, in which the area of cultivated land has the largest reduction rate, while the area of woodland has a certain decline, but it still has a high quantity. During 1990–2010, the slope of the image was the largest, and the change rate was the largest. After 2010, it tended to develop steadily, on the contrary, the area of construction land expanded. During 1990–2010, the average and standard deviation of different land use types in Beijing from 1980 to 2020 are analyzed. As shown in Figure 4, the area of cultivated land and forest land has been in a large proportion in the past 40 years, of which the proportion of forest land is the largest, and its standard deviation is also small, indicating that the range of change is not large, but the standard deviation of cultivated land and construction land is the largest, indicating that they have changed in the past 40 years.

This paper analyzes the transfer of different land use types in Beijing from 1980 to 2020. As shown in Table 3, the land use transfer rate is 30.5%, with a total area of 499,982.98 hectares, of which the top five outflows are dry land, shrub land, high-coverage grassland, beach land and rural residential land. About 77% of dry land is converted into construction land (urban land, rural residential land and other construction land), about 83% of shrub land is converted into forested land, about 34% of high-coverage grassland is converted into forested land, about 72% of beach land flows out into natural land such as rivers, pits, grasslands and wooded land, 17% is converted into agricultural land such as dry land, and about 53% is used by rural residents.

Rural residential land, urban land, dry land, forested land and other construction land with the largest inflow. Among them, the main sources of urban land are dry land (73%) and rural residential land (15%); The main source of land for rural residents is dry land (81%); The main sources of dry land are other forest land (24%) and comprehensive improvement of rural residential land (21%); The main sources of forested land are dry land (16%), shrubbery (62%) and grassland (13%). The main source of other construction land is dry land (64%). There is a certain phenomenon of mutual conversion among dry land,

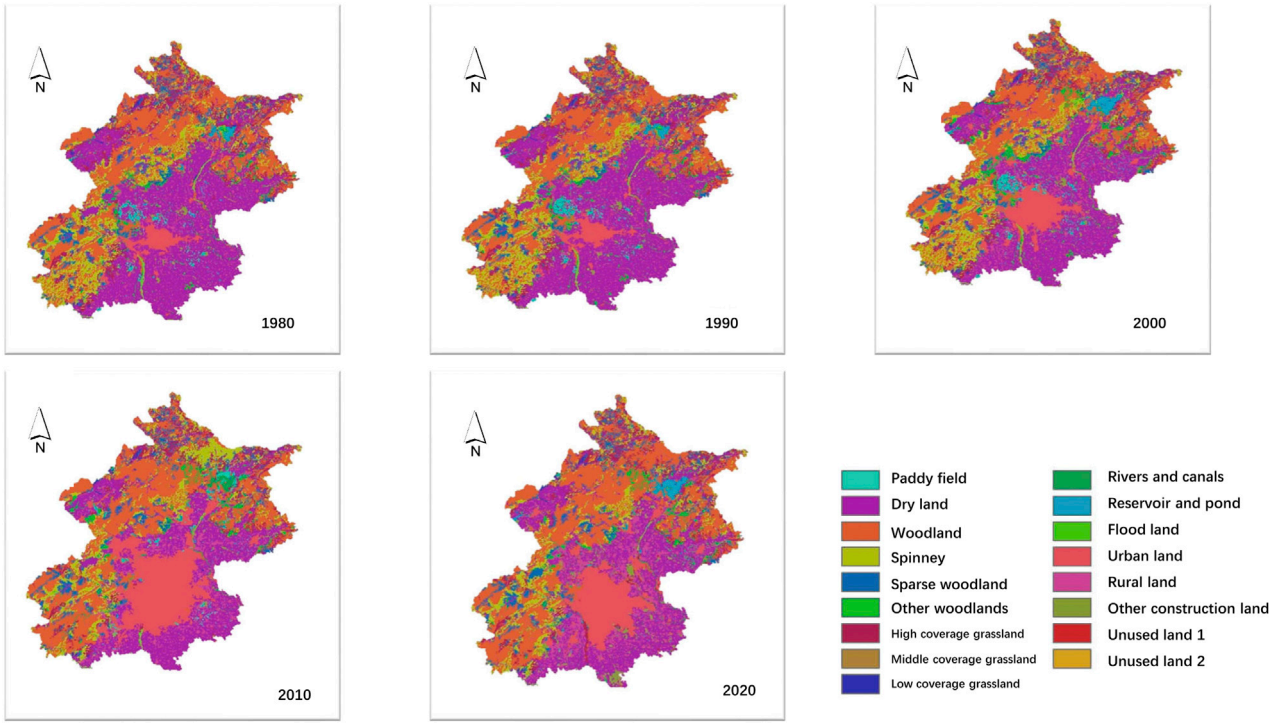

FIGURE 2
Distribution of land use types in Beijing in different periods.

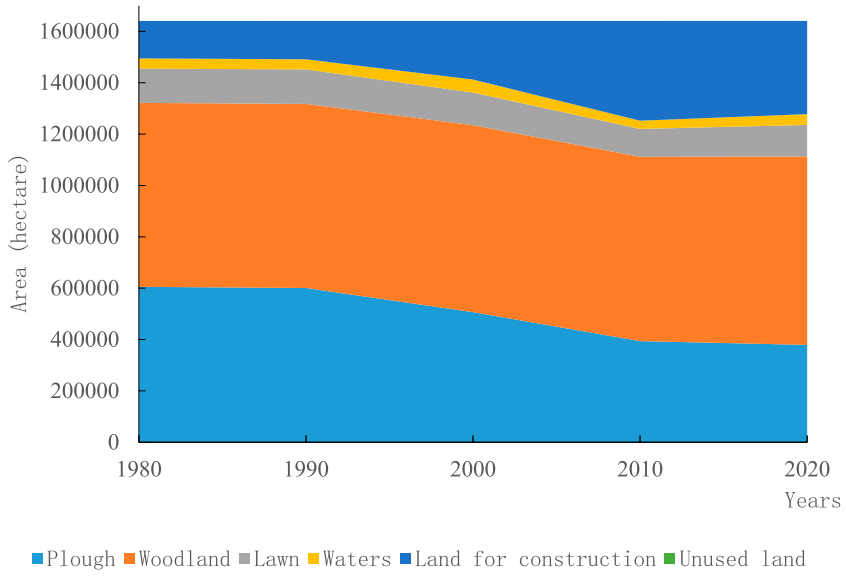

FIGURE 3
Area of land use types in Beijing in different periods.

woodland and grassland, and the conversion rate is high, while the change between reservoir pit and beach is small, and the sum of them only accounts for 4.5% of the total land transfer area.

This phenomenon reflects the emphasis on water resources and wetland conservation in the process of urbanization, as well as the recognition of the ecosystem services and biodiversity protection they offer. It also suggests the existence of natural, technical, and economic constraints that may be encountered in the process of land use planning and management.

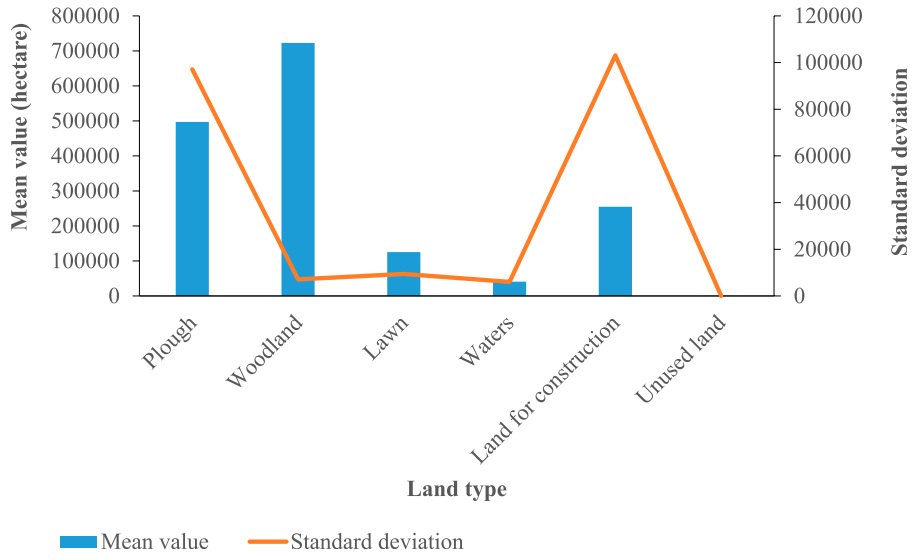

FIGURE 4
Analysis of mean and standard deviation of land use types in Beijing in different periods.

3.2 Change of habitat quality based on InVEST model

The distribution of habitat quality during 1980–2020 is shown in Figure 5, which is generally divided by the connecting line between northeast and southwest, with good habitat quality areas on the west side and poor habitat quality areas on the east side of the dividing line. Similar to the type of land use, the low habitat quality in the central city is expanding rapidly and seriously, approaching zero, and its radiation range is gradually expanding. The habitat quality in most areas in the northern and western mountainous areas is approaching one from a high level. With the development of the northwest city, the habitat quality in this area is gradually decreasing in the area with good habitat quality, and it is also producing certain negative radiation effects.

The trend analysis chart of habitat quality based on long time series is shown in Figure 6. Although the habitat quality has improved in the past 10 years, from a long-term perspective, most areas are still in a trend of relatively low habitat quality, and the areas with more serious decline and better increase are all in the western and northern mountainous areas. Because of the strong human interference, the strong radiation effect of the central city makes the trend analysis of this area unchanged. With the outward development of the city, urbanization is more serious, and the original northwest mountain habitat quality is excellent, which is easily affected by human activities in urban development. Combined with the distribution of habitat quality from 2010 to 2020, the red spots in the northwest are gradually fading, indicating that the trend of habitat quality is gradually getting better, and the red spots in the central city are also shrinking, indicating that the impact of urbanization is gradually narrowing.

4 Discussion

With the advancement of reform and opening up in 1980s, Beijing has also entered a stage of rapid development. The internal road network of the Second Ring Road has been established. In 1990s, the permanent population of Beijing reached 10 million. In the process of promoting the regulatory detailed planning, a large number of construction land has been transformed from the original land types in an orderly manner. Until 2000, Beijing entered a stage of rapid expansion. The construction of the Fifth Ring Road and the gathering of a large number of migrants forced the construction land in northern Beijing to expand again, and almost all other types of land were compressed to supply construction land. In 2010, the city's permanent population was 19.612 million, and the southern part of Beijing's urban area gradually developed, and the scale of the urban area also formed a trend of maximization. In recent years, with the promotion of national land space planning, Beijing's land planning and urban planning have been coordinated and unified, and Beijing's cities have entered the stage of repair, upgrading and perfection. The state has gradually attached importance to environmental protection, and the northern mountainous areas and western mountainous areas have become ecological conservation areas in Beijing, which have undergone ecological protection-oriented restrictive development, and finally formed a large land-use type division with the northeast and southwest connecting lines as the division.

Land use types refer to the different ways and purposes of human use of land resources. Common land use types include agricultural land, urban land, industrial land, woodland and grassland. Each land use type will have different specific impacts on habitat quality, and these impact mechanisms are complex and diverse, which are not only related to the balance of natural ecosystems, but also closely related to the sustainable development of human society. First of all, as the main source of food for human beings, the expansion of agricultural land often means cutting down a large number of natural vegetation and destroying the ecosystem. In agricultural activities, the extensive use of chemical fertilizers and pesticides will lead to soil pollution and water pollution, which will further affect the health and stability

TABLE 3 Beijing land use transfer matrix.

	Paddy field	dry land	Woodland	Spinney	Sparse wood land	Other woodlands	High coverage grassland	Middle covered grassland	Low-covered grassland	Rivers and canals	Shuiku kengtang	Beachland	Urban land use	Rural residential land	Other construction land	Unused land 1	Unused land 2	Amount to	Discharge
Paddy field	52.08	5058.06	686.36	51.09	0.00	75.50	271.66	0.00	0.00	80.83	90.60	0.00	4972.65	2580.35	390.90	0.00	0.00	14310.08	14258.00
Dry land	7.40	333110.14	14139.61	3310.94	6318.89	10241.91	10167.50	2225.79	641.28	3311.43	6577.52	737.74	79919.93	97933.17	21214.42	991.23	20.65	590869.53	257759.39
Woodland	0.00	2880.37	393280.99	2118.83	3671.57	2310.90	3379.06	182.28	19.31	350.35	461.33	276.47	867.54	1494.76	1289.42	0.00	0.19	412583.39	19302.40
Spinney	0.00	1059.85	55720.95	119869.46	1777.40	2885.94	1044.60	72.92	20.29	127.67	135.60	944.76	219.48	1438.70	1604.25	17.22	0.15	186939.24	67069.79
Sparse Wood land	0.00	1190.26	3494.26	664.84	68968.77	2631.87	1613.63	121.61	28.61	76.72	132.12	144.62	111.99	1253.96	568.11	0.00	0.25	81001.63	12032.86
Other woodlands	0.00	10683.94	1533.22	665.88	222.67	14099.11	1139.69	264.59	1.55	171.72	40.67	8.47	1639.20	3919.16	1048.97	4.02	0.00	35442.87	21343.76
High coverage grassland	0.00	5537.61	11470.46	3973.70	2506.63	926.54	78385.04	964.33	83.13	244.03	2740.97	99.80	122.90	2072.37	2254.34	277.67	0.85	111660.37	33275.33
Middle covered grassland	0.00	783.20	394.87	106.08	71.52	190.18	201.94	11877.28	8.11	81.94	24.77	0.03	44.76	383.00	743.35	0.00	0.00	14911.03	3033.75
Low-covered grassland	0.00	524.71	63.00	165.86	282.70	10.44	278.51	30.86	4497.62	8.27	308.32	0.22	19.86	386.79	349.24	7.40	0.00	6933.80	2436.19
Rivers and canals	1.08	878.46	425.24	33.49	33.58	9.24	221.82	0.55	16.51	4851.78	145.01	5.10	241.94	402.89	95.16	15.22	0.00	7377.06	2525.28
Shuiku kengtang	0.00	2346.62	344.09	16.15	16.78	64.67	301.27	0.95	1.02	104.79	9768.76	30.76	943.10	1361.87	377.88	66.54	0.00	15745.24	5976.48
Beachland	0.00	2434.53	1038.19	99.52	38.23	225.22	2452.12	58.65	61.09	2266.30	4327.03	2469.64	77.67	633.52	308.04	131.74	12.21	16633.71	14164.07
Urban land use	0.00	461.02	74.75	23.18	19.49	66.32	596.97	1.64	0.00	121.85	219.49	0.01	42354.26	2721.20	99.78	0.00	0.00	46759.96	4405.71
Rural residential land	6.40	9345.35	767.23	232.02	79.75	259.10	897.58	38.66	5.14	247.92	281.04	27.71	16678.43	53706.94	2583.65	33.03	0.00	85189.94	31483.00
Other construction land	0.00	1120.23	406.51	98.11	205.01	78.56	485.37	67.79	8.11	64.80	146.35	1.65	3644.50	4524.44	2964.27	0.27	0.00	13815.98	10851.71
Unused land 1	0.00	1.07	0.00	6.27	0.00	0.00	4.01	0.00	0.00	0.00	1.15	0.00	7.53	0.78	11.97	0.00	0.00	32.78	32.78
Unused land 2	0.00	0.00	0.00	1.03	0.24	1.51	0.00	0.00	0.00	0.00	0.00	0.00	0.00	7.74	21.97	0.00	7.87	40.36	32.49
Amount to	66.95	377415.44	483839.74	131436.48	84213.22	34077.02	101440.76	15907.92	5391.76	12110.41	25400.71	4746.97	151865.72	174821.64	35925.71	1544.33	42.18		0.00
Influx	14.88	44305.30	90558.75	11567.02	15244.45	19977.91	23055.73	4030.64	894.15	7258.63	15631.95	2277.33	109511.46	121114.70	32961.44	1544.33	34.31	0.00	499982.98

10.3389/fenvs.2024.1428197

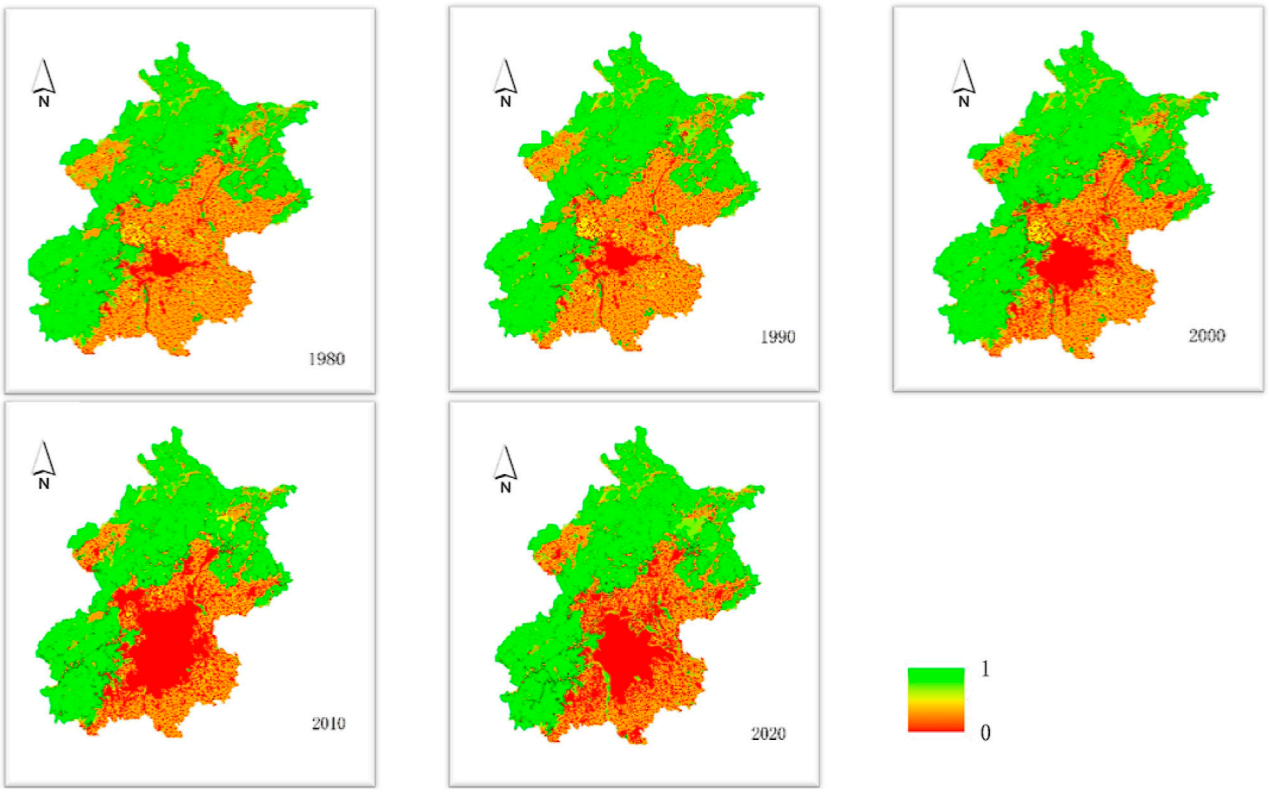

FIGURE 5
Habitat quality distribution.

of the ecosystem. In addition, over-exploitation and unreasonable utilization of agricultural land will also reduce biodiversity and reduce the service functions of ecosystems, such as soil conservation and water conservation. Urban land use is another important land use type. With the acceleration of urbanization, the area of urban land is expanding, which leads to the replacement of the original natural habitat by a large number of buildings. Urbanization not only changes the land cover, but also changes the structure and function of the ecosystem. For example, the heat island effect of urbanization will change the local climate and affect the survival and reproduction of animals and plants; Urban noise and light pollution can also cause interference and harm to living things. In addition, urban expansion is often accompanied by the fragmentation of biological habitats, which leads to the obstruction of species migration and gene exchange and further affects biodiversity. Industrial land is usually accompanied by emphasis on industrial activities and pollutant discharge, which has a particularly significant impact on the ecological environment. Waste gas, waste water and solid waste produced by industrial activities will directly or indirectly pollute soil, water and atmosphere, and cause serious damage to the quality of habitats. At the same time, the construction and operation of industrial land may also destroy the structure and function of ecosystem, such as destroying surface vegetation and changing hydrological cycle. These impacts not only damage the health of the ecosystem, but also pose a potential threat to human health and social well-being. In contrast, natural land use types such as woodland and grassland have positive effects on the maintenance of habitat quality. Woodland can provide rich biological habitats and maintain high biodiversity; At the same time, the forest also has the functions of regulating climate, conserving water and maintaining soil, which is very important for the stability of ecosystem and human survival. Grassland is also an important ecological barrier, which can slow down wind speed, prevent soil erosion and provide biological resources such as pasture. However, the protection and rational utilization of woodland and grassland also face many challenges. With the population growth and economic development, the demand for land resources is increasing, which leads to the continuous reduction of the area of woodland and grassland. In addition, unreasonable development and utilization will also destroy the structure and function of these natural ecosystems and reduce the quality of habitats.

For the transformation of land use types, the land use transfer rate in Beijing reached 30.5% from 1980 to 2020. In the 1980s and 1990s, the expansion of urban areas crowded out the original village cultivated land and transformed it into construction land and rural residential land. However, with the strengthening of urban planning and ecological attention, some shrubs and grasslands have become forested land due to manual intervention and natural succession, and about 30% of rural residential land has returned to cultivated land due to the national land comprehensive improvement policy. There is a certain phenomenon of mutual conversion among dry land, forest land and grassland, and the conversion rate is high, which shows that the conversion between natural land types is

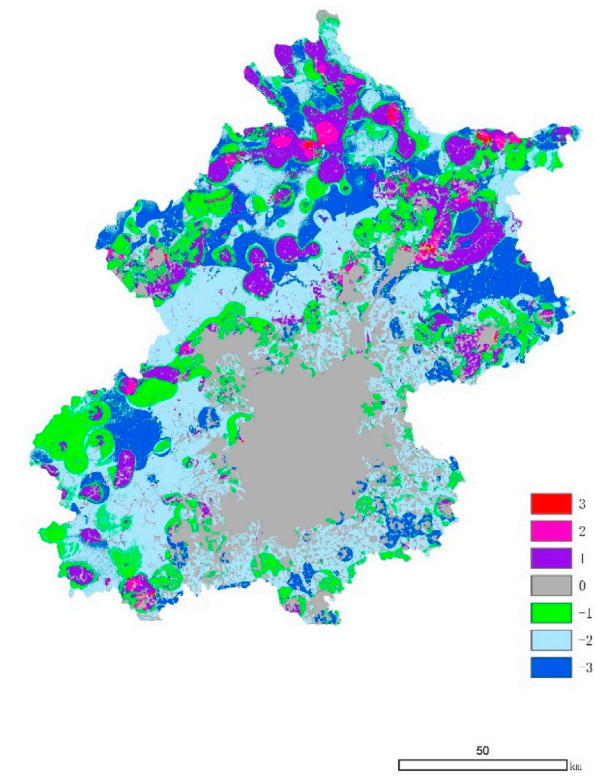

FIGURE 6
Trend analysis chart of habitat quality based on long time series.

convenient and simple, with low cost and easy realization, and is suitable for comprehensive land improvement. In addition, Beijing, as an extremely water-deficient city, has been making great efforts to protect the reservoirs, ponds and beaches within its jurisdiction before the implementation of the South-to-North Water Transfer Project, so the changes of the two land types are small, and the sum of them only accounts for 4.5% of the total land transfer area.

InVEST model is based on the simulation and analysis of land use types, so there is a strong correlation between habitat quality and land use types, and it also shows the distribution of habitat quality divided by the connecting line between northeast and southwest, which is similar to the previous study of Beijing ecological pattern by Dr. Yu Kongjian (Kongjian et al., 2010; Xinliang et al., 2018). In addition, the annual expansion of low habitat quality in the urban area reflects the negative expansion of habitat quality, and the influence of human activities will cause the radiation change of habitat quality reduction, and its strong radiation effect makes the region unchanged in the trend analysis year by year. With the outward development of the city, urbanization is more serious, and the original northwest mountain habitat quality is excellent, which is easily affected by human activities in urban development. Combined with the distribution of habitat quality from 2010 to 2020, the red spots in the northwest are gradually fading, indicating that the trend of habitat quality is gradually getting better, and the red spots in the central city are also shrinking, indicating that the impact of urbanization is gradually narrowing. Therefore, in the process of urban construction, it is particularly important to build a certain isolation buffer zone. On the one hand, it can block the negative habitat radiation of urban development and reduce the negative impact on the construction of ecological conservation areas in northern and western mountainous areas. On the other hand, with the development of urban re-wilderness, a certain urban country ecosystem will be gradually established in the urban area. Together with the natural ecosystem in mountainous areas, the isolation zone will become a certain ecological ecotone, which can provide a different ecosystem with higher ecological quality for the response zone.

Compared with previous research on the ecological pattern of Beijing by Dr. Yu Kongjian and others, this study utilizes the InVEST model to provide a more specific and quantified perspective, confirming the spatial distribution characteristics of habitat quality in Beijing and its correlation with the urbanization process. Although similar in macro trends to previous research, this study specifically demonstrates the changes in habitat quality over time through quantitative analysis, as well as the details of the impact of different land use types on habitat quality, thereby offering more concrete guidance and basis for urban planning and ecological protection.

Studying the long-time series trend of habitat quality in Beijing is helpful to fully understand the evolution law of urban ecological environment. By collecting and analyzing the data for many years, we can reveal the changing trend and influencing factors of Beijing's habitat quality in different periods, and then provide the basis for formulating scientific ecological protection policies and measures. At the same time, the study also helps to reveal the mechanism and path of urbanization affecting habitat quality, and provide scientific basis for urban planning and construction. In recent years, the Beijing Municipal Government has issued a series of ecological protection policies and measures, such as greening and beautification projects, wetland protection and ecological compensation, aiming at improving the quality of urban habitats. By evaluating the implementation effects of these policies and measures in a long time series, we can understand the improvement degree and existing problems of urban habitat quality, and then provide decision support for the optimization and perfection of policies. In addition, studying the long-term trend of habitat quality in Beijing is also helpful to improve the public's understanding and participation in ecological environment protection. By revealing the changing trend and potential risks of urban ecological environment, we can guide the public to pay more attention to the ecological environment problems around them, actively participate in ecological protection actions, and form a good atmosphere of common concern and common protection for the whole society.

From the perspective of application value, studying the long-term trend of habitat quality in Beijing can provide scientific basis for ecological restoration and environmental governance. By analyzing the causes and mechanisms of the decline of habitat quality, we can formulate corresponding ecological restoration and environmental governance programs to improve the quality of urban habitats. At the same time, the study can also provide a basis for the division and management of ecological functional areas, and promote the healthy and sustainable development of urban

ecosystems. In addition, studying the long-term trend of habitat quality in Beijing can also provide support and guidance for eco-tourism and green development. With people's increasing attention to the ecological environment and healthy life, eco-tourism has become a new way of tourism. Through the research and evaluation of urban habitat quality, we can explore and popularize the eco-tourism resources in Beijing and promote the green and sustainable development of tourism. At the same time, the research can also provide decision support and direction guidance for the development of green industries, and promote the green transformation and upgrading of Beijing's economy and society.

However, this study also faces certain limitations and challenges. Firstly, due to data constraints, the analysis in this paper mainly relies on macro data of land use conversion, lacking direct measurement of specific biodiversity indicators. This means that our assessment of habitat quality may not fully consider all dimensions of biodiversity. Secondly, although the InVEST model provides an effective tool for assessing habitat quality, the assumptions and parameter selections of the model itself may also affect the accuracy of the results. Moreover, urban development is a complex socio-economic process involving many factors and interventions, and the interactions of these factors may have complex effects on habitat quality, which this study did not fully cover.

Despite these challenges, the contributions of this paper to the knowledge field are still significant. This study not only provides a quantitative analysis of land use conversion and changes in habitat quality in Beijing over 40 years but also offers a new perspective on understanding the impact of urban development on habitat quality by linking it with the urbanization process. In particular, this study emphasizes the importance of establishing isolation buffer zones in urban planning to reduce the negative impact of urbanization on ecological conservation areas, while promoting urban rewilding, providing valuable insights for improving the quality of ecosystem services (Xiao et al., 2023).

Future research needs to further refine the relationship between land use types and biodiversity indicators, and explore more effective strategies for controlling the impact of urban development on the ecological environment, thereby providing more comprehensive and in-depth scientific support for achieving sustainable urban development.

5 Conclusion

Over the past few decades, the types and areas of land use in urban and rural areas have undergone significant changes. From 1990 to 2010, the expansion of construction land was the most noticeable, and this change was almost achieved by compressing other types of land, among which cultivated land and construction land have experienced certain changes in nearly 40 years. In Beijing, between 1980 and 2020, the land use type transfer rate reached 30.5%, involving a total area of 499,982.98 ha. During this process, the top five outflows were dry land, shrubland, high-cover grassland, beach land, and rural residential land, while the largest inflows were rural residential land, urban land, dry land, forested land, and other construction lands. In terms of habitat quality, the overall trend from 1980 to 2020 shows that the area west of the line connecting the northeast and southwest has good habitat quality, while the east side has poorer habitat quality. In the last decade, although the overall habitat quality has improved, most areas are still in a trend of declining habitat quality, especially in some areas of the western and northern mountains, where the decrease in habitat quality is more severe, and the areas with better improvement are also located in these mountains. Facing the ecological pressure brought by urban construction, it is recommended to introduce the concept of isolation buffer zones in urban construction. Such buffer zones can effectively block the negative impact of urban development on the surrounding habitat, while providing higher ecological quality and ecosystem services for the city. Through such measures, a balance can be found between urban development and ecological protection, thus promoting the realization of sustainable development.

Data availability statement

The original contributions presented in the study are included in the article/Supplementary material, further inquiries can be directed to the corresponding author.

Author contributions

JW: Conceptualization, Data curation, Formal Analysis, Funding acquisition, Investigation, Methodology, Project administration, Resources, Software, Supervision, Validation, Visualization, Writing–original draft, Writing–review and editing. YJ: Conceptualization, Writing–original draft, Writing–review and editing. QT: Conceptualization, Writing–original draft, Writing–review and editing. FL: Conceptualization, Writing–original draft, Writing–review and editing. CD: Writing–original draft, Writing–review and editing. TL: Conceptualization, Writing–original draft, Writing–review and editing. JL: Supervision, Writing–original draft. CH: Supervision, Writing–review and editing. XC: Conceptualization, Writing–original draft, Writing–review and editing. YL: Conceptualization, Writing–original draft, Writing–review and editing. XZ: Conceptualization, Writing–original draft, Writing–review and editing. GZ: Conceptualization, Writing–original draft, Writing–review and editing.

Funding

The author(s) declare that no financial support was received for the research, authorship, and/or publication of this article.

Conflict of interest

Authors JW, YJ, QT, FL, CD, TL, XC, YL, XZ, and GZ were employed by PowerChina Beijing Engineering Corporation Limited. Author JL was employed by Anhui Province Jing County Niu Ling Reservoir Project Construction Management Division. Author CH was employed by Jing County Water Conservancy Bureau.

Publisher's note

References

Ban, Y., Liu, X., Yin, Z., Li, X., Yin, L., and Zheng, W. (2023). Effect of urbanization on aerosol optical depth over Beijing: Land use and surface temperature analysis. *Urban Clim.* 51, 101655. doi:10.1016/j.uclim.2023.101655

Cai, Y. B., Zhang, H., Pan, W. B., Chen, Y. H., and Wang, X. R. (2013). Land use pattern, socio-economic development, and assessment of their impacts on ecosystem service value: study on natural wetlands distribution area (NWDA) in Fuzhou city, southeastern China. *Environ. Monit. Assess.* 185, 5111–5123. doi:10.1007/s10661-012-2929-x

Falcucci, A., Maiorano, L., and Boitani, L. (2007). Changes in land-use/land-cover patterns in Italy and their implications for biodiversity conservation. *Landsc. Ecol.* 22 (4), 617–631. doi:10.1007/s10980-006-9056-4

Gao, Y., Ma, L., Liu, J., Zhuang, Z., and Huang, Q. (2017). Constructing ecological networks based on habitat quality assessment: a case study of Changzhou, China. *Sci. Rep.* 7 (1), 46073. doi:10.1038/srep46073

Hamed, K. H., and Rao, A. R. (1998). A modified Mann-Kendall trend test for autocorrelated data. *J. hydrology* 204 (1). doi:10.1016/s0022-1694(97)00125-x

Hu, X., and Xu, H. (2018). A new remote sensing index for assessing the spatial heterogeneity in urban ecological quality: a case from Fuzhou City, China. *Ecol. Indic.* 89, 11–21. doi:10.1016/j.ecolind.2018.02.006

Jia, X., Li, G., and Zhao, H. (2013). Study on the change of landscape ecological quality based on land use: a case study in resource-exhausted mining area. *Prog. Environ. Prot. Process. Resour. Pts* 1–4 (295–298), 2679–2683.

Kongjian, Y., Sisi, W., Dihua, L., et al. (2010). The ecological bottom line of Beijing's urban expansion-basic ecosystem services and its security pattern. *Urban Plan.* (2), 19–24.

Liu, M., Zhang, H., Wang, Y., et al. (2021). Study on habitat quality of farming-pastoral ecotone in northern China based on land use. *Res. Soil Water Conservation* 28 (3), 156–162.

Phillips, S. J., Anderson, R. P., Schapire, R. E., Phillips, S. J., Anderson, R. P., and Schapire, R. E. (2013). Maximum entropy modeling of species geographic distributions. *Ecol. Model.* 190, 231–259. doi:10.1016/j.ecolmodel.2005.03.026

Sala, O. E., Iii, F. S. C., Armesto, J. J., Berlow, E., Bloomfield, J., et al. (2000). Biodiversity: global biodiversity scenarios for the year 2100. *Science* 287 (5459), 1770–1774. doi:10.1126/science.287.5459.1770

Tallis, H. T., Ricketts, T., Guerry, A. D., et al. (2012). InVEST 2.4.4 user's guide [EB/OL]. Available at: http://ncp-dev.stanford.edu/~dataportal/invest-releasesfdocumentation/InVEST_2.4.4_Documentation.pdf.

Tang, J., Zhou, L., Dang, X., Hu, F., Yuan, B., Yuan, Z., et al. (2023). Impacts and predictions of urban expansion on habitat quality in the densely populated areas: a case study of the Yellow River Basin, China. *Ecol. Indic.* 151, 110320. doi:10.1016/j.ecolind.2023.110320

Vannest, K. J., Parker, R. I., Davis, J. L., Soares, D. A., and Smith, S. L. (2012). The Theil–Sen slope for high-stakes decisions from progress monitoring. *Behav. Disord.* 37 (4), 271–280. doi:10.1177/019874291203700406

Wang, A., Zhang, M., Kafy, A. A., Tong, B., Hao, D., and Feng, Y. (2023). Predicting the impacts of urban land change on LST and carbon storage using InVEST, CA-ANN and WOA-LSTM models in Guangzhou, China. *Earth Sci. Inf.* 16.1, 437–454. doi:10.1007/s12145-022-00875-8

Wu, W., Xu, L., Zheng, H., and Zhang, X. (2023). How much carbon storage will the ecological space leave in a rapid urbanization area? Scenario analysis from Beijing-Tianjin-Hebei Urban Agglomeration. *Resour. Conservation Recycl.* 189, 106774. doi:10.1016/j.resconrec.2022.106774

Xiang, Q., Kan, A., Yu, X., Liu, F., Huang, H., Li, W., et al. (2023). Assessment of topographic effect on habitat quality in mountainous area using InVEST model. *Land* 12 (1), 186. doi:10.3390/land12010186

Xiao, P., Zhou, Y., Li, M., and Xu, J. (2023). Spatiotemporal patterns of habitat quality and its topographic gradient effects of Hubei Province based on the InVEST model. *Environ. Dev. Sustain.* 25, 6419–6448. doi:10.1007/s10668-022-02310-w

Xinliang, X., Liu, J., Shuwen, Z., Rendong, L., Changzhen, Y., and Wu, S. (2018). Multi-period remote sensing monitoring data set of land use in China (CNLUCC). *Resour. Environ. Sci. data registration Publ. Syst.* doi:10.12078/2018

Ying, X., Zhang, Y., and Enhua, L. (2022). Temporal and spatial evolution and prediction of habitat quality in the four-lake basin of Jianghan Plain. *Resour. Environ. Yangtze River Basin* 31 (7), 1616–1626.

Yu, P., Zhang, S., Yung, E. H. K., Chan, E. H., Luan, B., and Chen, Y. (2023). On the urban compactness to ecosystem services in a rapidly urbanising metropolitan area: highlighting scale effects and spatial non–stationary. *Environ. Impact Assess. Rev.* 98, 106975. doi:10.1016/j.eiar.2022.106975

Zhang, M., Wang, J., Zhang, Y., and Wang, J. (2023b). Ecological response of land use change in a large opencast coal mine area of China. *Resour. Policy* 82, 103551. doi:10.1016/j.resourpol.2023.103551

Zhang, X., Liao, L., Huang, Y., Fang, Q., and Lan, S. (2023a). Conservation outcome assessment of Wuyishan protected areas based on InVEST and propensity score matching. *Glob. Ecol. Conservation* 45, e02516. doi:10.1016/j.gecco.2023.e02516

Zhang, X., Song, W., Lang, Y., Feng, X., Yuan, Q., and Wang, J. (2020). Land use changes in the coastal zone of China's Hebei Province and the corresponding impacts on habitat quality. *Land use policy* 99, 104957. doi:10.1016/j.landusepol.2020.104957

Zhao, L., Yu, W., Meng, P., Zhang, J., and Zhang, J. (2022). InVEST model analysis of the impacts of land use change on landscape pattern and habitat quality in the xiaolangdi Reservoir area of the Yellow River basin, China. *Land Degrad. Dev.* 33 (15), 2870–2884. doi:10.1002/ldr.4361

frontiers | Frontiers in Environmental Science

TYPE Original Research
PUBLISHED 23 October 2024
DOI 10.3389/fenvs.2024.1427728

OPEN ACCESS

EDITED BY
Juergen Pilz,
University of Klagenfurt, Austria

REVIEWED BY
Huiping Jiang,
Chinese Academy of Sciences, China
Xiwei Guo,
The Pennsylvania State University (PSU), United States
Subhanil Guha,
National Institute of Technology Raipur, India

*CORRESPONDENCE
Yuning Cheng,
18069112618@163.com

RECEIVED 04 May 2024
ACCEPTED 30 September 2024
PUBLISHED 23 October 2024

CITATION
Wang X and Cheng Y (2024) From Sangbo to urban landscape: morphological and hydrological transformations of Xuanwu Lake through integrating historical interpretation and geographic analysis.
Front. Environ. Sci. 12:1427728.
doi: 10.3389/fenvs.2024.1427728

From Sangbo to urban landscape: morphological and hydrological transformations of Xuanwu Lake through integrating historical interpretation and geographic analysis

Xueyuan Wang and Yuning Cheng*

School of Architecture, Southeast University, Nanjing, China

Introduction: Xuanwu Lake in Nanjing has undergone a rich history, evolving from native Sangbo to a naval training ground, from an imperial garden to farmland, and finally to a vibrant urban landscape. The lake's legacy can be attributed to its unique geographical and hydrological conditions. Exploring historical transformations of the lake and surrounding landscape patterns provides insights for optimizing urban water space in contemporary China.

Methods: Traditional analyses of lake changes based solely on historical records may lack precision due to deviations and artistic interpretations found in ancient maps. However, considering the reciprocal compatibility between local geomorphology, undulating terrains, and water bodies allows for accurate reduction of the lake's morphology by inferring and validating its geographical features. This research combines historical interpretation and geographical analysis to reconstruct the historical shape of Xuanwu Lake, uncover the intrinsic mechanisms driving spatial changes over time, and analyze the morphological changes and connectivity patterns of its hydrological system.

Results: The morphology and hydrological dynamics of Xuanwu Lake are deeply intertwined with the policies prevailing in different eras. In antiquity, Xuanwu Lake, as a natural body of water, sustained the surrounding ecosystem and the livelihoods of local inhabitants. During the imperial period, it was integrated into the royal gardens, with its utilization and configuration modified by political directives, including the establishment of a naval training facility and its conversion into a royal recreational venue. Subsequently, in response to economic imperatives, Xuanwu Lake was transformed into agricultural land, which led to challenges such as flooding and drought. Ultimately, due to ecological security and recreational needs under urbanization, it was restored to lake form.

Discussion: By interpreting the bidirectional adaptation between the lake's ecosystem functions and city development activities, this research provides insights for water space management and ecological restoration in contemporary Xuanwu Lake. The findings provide guidance for the sustainable development of city-lake relationships to enhance the resilience of urban ecological spaces.

KEYWORDS

historical interpretation, geographic analysis, morphological reduction, city-water relationships, urban lakes

1 Introduction: the morphological reduction of Nanjing Xuanwu Lake

The harmonious coexistence of cities and water in the historical context of China is a distinctive cultural phenomenon within the development process of Chinese urbanization[1]. It represents a unique symbiotic relationship where cities have flourished alongside the presence of water throughout history[2], imparting a profound cultural legacy. The names of famous lakes like West Lake in Hangzhou and East Lake in Wuhan[3], which are derived from their geographical locations, vividly demonstrate the close association between water systems and urban orientations[4]. Located outside the ancient city walls (Jiang et al., 1986) of Nanjing[5], in the northeastern corner of the old town (Haiming, 2019), lies Xuanwu Lake[7]. This urban lake seamlessly blends natural beauty with cultural landscapes, making it a captivating sight with its expansive water surface and five lush islands (Hu, 2017). The original name of Xuanwu Lake was "Sangbo" (Wei, 2012), which was called "Jiang Lake" during the period of the Eastern Wu Dynasty, also known as "Hou Lake"[8]. (Geng, 2019). In the Eastern Jin Dynasty, it was called "North Lake," (Siqian, 2022) and during the Liu Song period of the Southern Dynasties, it was named "Xuanwu Lake (Hu, 2017)." (Chen, 2016) The name "Xuanwu" is derived from the Chinese concept of the Five Elements[9], representing the direction of North. (Xu and Xu, 2011). As one of the Four Symbols, Xuanwu represents the northern direction. (Yinghe, 2008)[10]. Xuanwu is often depicted as a divine creature with the form of a black tortoise combined with a snake. It has a black tortoise shell on one-half and a snake body on

1 The Ming City Wall of Nanjing is one of the best-preserved and largest Ming Dynasty city walls in China. Constructed during the Hongwu period of the Ming Dynasty (1,368–1,398), the Ming City Wall is about 35.2 km long. The city wall boasts several gate towers and corner towers, as well as defensive facilities such as moats and trenches. The Ming City Walls were constructed with many rebuilds and expansions, and played an important role in military defense and administration throughout history. The moats surrounding the walls also provided an additional line of defense for Nanjing.

2 Nanjing was once one of the important ancient capitals of China, and was particularly prosperous during the Ming and Qing dynasties. After moving the capital to Nanjing, Zhu Di, the first Ming emperor, embarked on a massive construction and restoration project, which included the construction of defenses such as city walls and gates. Over time, Nanjing gradually developed into a bustling urban center, and ancient streets, buildings and cultural relics accumulated to form the Nanjing Old Town.

3 There are five existing islands in Xuanwu Lake, including Liang Island, Ying Island, Huan Island, Cui Island and Ling Island.

4 Before the Qin Dynasty, Xuanwu Lake was called "Sangbo", meaning natural lake.

5 The founder of the Eastern Wu Dynasty (222–280 AD) was Sun Quan. His grandfather's name was Zhong, so he renamed Zhongshan to Jiangshan to avoid the taboo, and at the same time changed the name of Moling Lake to "Jiangling Lake" and "Jiang Lake". Because the lake is located in the north of Zhongshan (now Zijin Mountain), and in the southern foot of Zhongshan there is another Yanque Lake called "front lake", so Xuanwu Lake is also called "back lake".

7 The name of Xuanwu Lake of Xuanwu began in the Liu Song period of the Southern Dynasty, and it is written in the Taiping Huan Yu Ji: "At the end of the Yuanjia period of the Song Dynasty, a black dragon was seen in the lake, so the name of the lake was changed to Xuanwu." Emperor Wen of the Song Dynasty built the northern dike and established Xuanwu Lake in the 23rd year of Yuanjia (446).

8 The Five Elements theory is a unique concept in ancient Chinese philosophy, dividing the natural and human world into five fundamental elements: wood, fire, earth, metal, and water. Each element is associated with directions, seasons, colors, organs, emotions, and more.

9 The Five Elements is an important concept in ancient Chinese philosophy that divides the natural and human world into five basic elements: wood, fire, soil, gold and water. Each element is associated with direction, seasons, colors, organs, and emotions. Water is one of these basic elements in the Five Elements theory, and the north is considered to be closely associated with the element of water. This is mainly due to the geographic features of China, where the northern regions are usually colder and have large expanses of water, such as the Yangtze River, Yellow River and other important rivers. There are also many lakes and oceans in the north, such as the East China Sea and the Bohai Sea.

10 Feng Shui is an ancient traditional Chinese theory that aims to create a harmonious, balanced and prosperous living atmosphere through environmental and spatial layout. It combines many aspects of geography, astronomy, meteorology, philosophy, religion and culture, and is widely used in the fields of architectural design, urban planning, home furnishing and feng shui counseling.

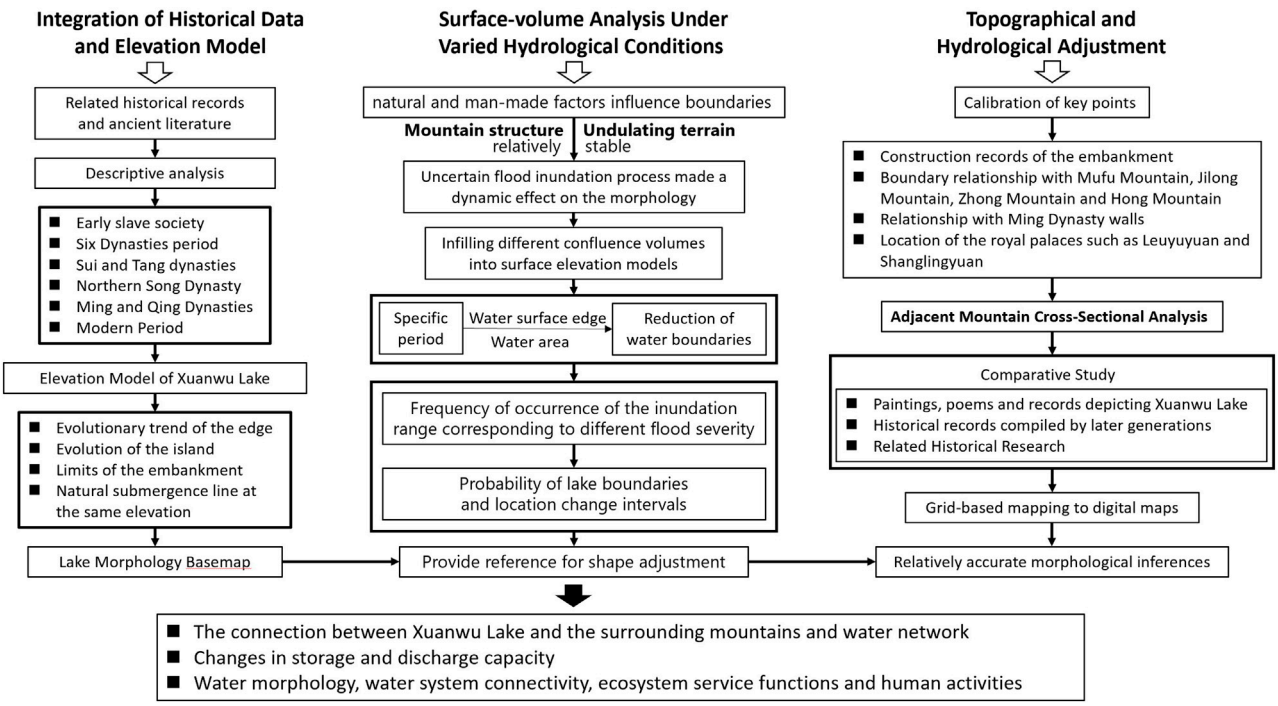

FIGURE 1
The framework for reducting the historical shape of Xuanwu Lake through the combination of historical interpretation and geographical analysis.

the other half[11]. In traditional Feng Shui (Yanshou et al., 1975-06), placing Xuanwu in the north is believed to balance the energy of the land and protect homes. However, in the case of Xuanwu Lake, the name "North Lake" is more symbolic of the relationship between the lake and the city. Xuanwu Lake has been preserved and inherited until today not solely based on Feng Shui beliefs, but rather due to the local topography, the natural conditions of convergence for water, and the maintenance of the lake, shaping a harmonious relationship between the city and the lake. From this perspective, the wisdom of ancient Chinese people emphasized the ecological principle of adapting to local conditions, rather than simply relying on Feng Shui remnants.

As a witness to the shift of power and urban development, Xuanwu Lake holds research value in terms of its historical development, morphological changes, and the evolution of its ecosystem services. The spatial transformations of Xuanwu Lake have been directly influenced by ancient political decisions and production activities. Simultaneously, the lake's ecological functions and morphological manifestations have also imposed limitations and guided social activities. This intricate interplay has shaped a historically rich chronicle of the mutual development between society and the aquatic environment.

The ancient history of Xuanwu Lake dates back as far as 2,300 years ago, yet the documentation and pictorial records fail to provide a comprehensive portrayal of its evolving shape. Previous research on Xuanwu Lake has primarily focused on its historical events, water quality, and lake landscapes. However, these historical records often exhibit ambiguity in spatial descriptions, making it difficult to accurately depict the true geographical details. For instance, "Jinling Map" in "Di Li Ren Zi Xu Zhi" (Wenbao, 2010) tends to reflect the cognitive intentions and conceptual understanding of the drafter, leading to deviations in terms of orientation, scale, and shape (Xu and Xu, 2011). Furthermore, subsequent cartography and speculative maps produced during the early stages of immature techniques such as distance measurement and positioning also suffer from varying degrees of positional drift. With the establishment and development of disciplines such as urban morphology, cultural landscapes, and landscape history, research on the interpretation of historical records has delved deeper. To overcome these limitations, the research has employed a method integrating historical interpretation and geographical analysis, utilizing modern vector maps to precisely reorganize spatial information and trace the historical morphological transformations of Xuanwu Lake.

The research aims to comprehensively analyze the evolvement of Xuanwu Lake, offering a historical assessment of its morphological characteristics, water connectivity, landscape pattern and city dynamics, serving as a valuable reference for contemporary water environment management and ecological restoration of Xuanwu Lake. By meticulously examining the transformations of Xuanwu Lake, this research establishes a framework that transcends boundaries, contributing to the broader discourse on sustainable urban-water development in China and the international context.

11 The book "Di Li Ren Zi Xu Zhi", written by Xu Shanji and Xu Shanshu in the Ming Dynasty, is a landmark work in the history of Chinese geomancy, and is regarded as the bible of geomancy by later generations of geomancers. The title of the book means what a geographer needs to know. The Xu brothers compiled and organized their years of study and practice in this book, which not only contains the classic assertions of geomancy masters from different dynasties, but also extremely detailed and real feng shui cases.

2 Methods: the framework for restoring the historical shape of Xuanwu Lake through the combination of historical interpretation and geographical analysis

This approach hinges on the temporal and spatial extrapolations derived from combined historical and geographical information. It utilizes significant spatial transformations of Xuanwu Lake as pivotal reference points, emphasizing the structural role of geographic information. The innovative aspect of this methodology lies in the inference of the lake's historical existence and transformations based on stable and realistic physical geographical data[12]. It is important to note that the shoreline of Xuanwu Lake exhibits certain variations. The southern shoreline was stabilized after renovations during the Ming Dynasty, which coincided with the construction of the city wall. Similarly, the western shoreline was also solidified. In contrast, the northern and eastern shorelines have undergone significant changes, and the historical evolution of their forms still shows certain deviations.

The method is delineated into three principal components. (1) Integration and Interpretation of Historical Data and Elevation Model: This involves the systematic review and interpretation of textual historical records and maps to establish an accurate spatial framework[13]. A surface elevation model is constructed to identify stable topographical features and hill structures, serving as geographic references. These features are instrumental in correcting the baseline morphology of the lake, ensuring historical accuracy[14]. (2) Surface-volume Analysis Under Varied Hydrological Conditions: Utilizing a volumetric filling approach, this component identifies potential inundation areas under different rainfall and flood scenarios[15]. The methodology assesses the uncertainty of the lake's morphology through probability density evaluations, providing a statistically robust framework for understanding morphological variations[16]. (3) Topographical and Hydrological Adjustment: Based on the analysis of nearby mountain profiles, this step involves the precise adjustment of the lake's morphological boundaries. It considers the interconnected relationships among mountains, rivers, and the lake, alongside the variations in their storage and detention capacities. This adjustment facilitates a comprehensive analysis of changes in lake morphology, connectivity, and the urban-water interface. These components collectively enhance the understanding of Xuanwu Lake's historical landscape, contributing valuable insights into the interplay between natural formations and historical developments. Specific technical pathways are shown in Figure 1.

2.1 Formation of lake morphology basemap based on historical material interpretation and elevation calibration

The foundational spatial reference for lake morphology was developed through a rigorous interpretation of historical texts and maps, resulting in the creation of a comprehensive basemap delineating the lake's shape. This process was followed by the construction of a surface model to identify relatively stable surface undulations and ridge structures, which served as geographical references for calibrating the lake's morphology.

Initially, a descriptive analysis and systematic review of primary historical documents and cartographic materials provided a foundational spatial location of Xuanwu Lake's morphology and boundaries over various historical periods. This analysis offered a generalized depiction of the lake's spatial structure at specific times. Given that landforms, terrains, and mountain patterns change more gradually compared to built structures such as palaces, buildings, and roads, the study utilized relatively stable spatial elements—such as actual terrain and mountain configurations—as reference points. By refining roughness and resampling, a surface elevation model reflecting the overall topographic variations were developed (Cheng and Wang, 2021), as Figure 2. Natural inundation lines at elevations matching key reference points were employed to calibrate the lake's morphology, as Figure 3.

The research traced the historical evolution of Xuanwu Lake from the earliest identifiable period, using structural changes as indicators to delineate different phases. Morphological features from various periods were digitized into maps using ArcGIS, based on historical records, local gazetteers, and related literature. By integrating urban development and historical events, the study inferred the lake's evolution, changes in its area, and the conditions of its islands and embankments.

12 An oxbow lake is used to describe a bow-shaped lake. It refers to the river flowing in the plains area with the flow of water on the surface of the river scouring and erosion, the river more and more curved, and finally led to the river naturally cut off straight. The river flows straight from the straightened part, and the original curved channel is abandoned, forming a lake, which is called an ox yoke lake because of its shape resembling an ox yoke.

13 In the "Preliminary Study on the Age of the Ancient Qinhuai River and Sediments in Nanjing" by Jiang Sishun, Ang Chaohai, and Yang Huicheng, it is hypothesized that Xuanwu Lake is a sedimentary lake left over from the ancient Qinhuai River.

14 Geological theory deduces that the formation of Xuanwu Lake is due to the four major fracture phenomena of the nearby Zhongshan Reverse Bunker Fault, Tianbao City Fault, Fugui Mountain Fault, and Taipingmen Fault, which led to the formation of the Xuanwu Lake lowland. After millions of years of erosion by wind and rain, it gradually dissolved into a low-lying waterlogged place.

15 The Pre-Qin Period (Paleolithic Period to 221 BC) refers to the historical era before the establishment of the Qin Dynasty. Broadly speaking, the pre-Qin period refers to all historical periods before the establishment of the Qin Dynasty.

16 The Six Dynasties (222 AD - 589 AD), generally refers to the six dynasties in the south of Chinese history from the Three Kingdoms period to the Sui Dynasty. The six dynasties are Sun Wu, Eastern Jin, Southern Song (or Liu Song), Southern Qi (or Xiao Qi), Southern Liang (or Xiao Liang), and Southern Chen.

2.2 Assessing uncertainty in lake morphology based on probability density

In historical studies, the uncertainty associated with water body morphology stems from a myriad of complex factors. Both natural and anthropogenic environmental changes impact the boundaries of these water bodies. For Xuanwu Lake in a relatively natural environment, uncertain flood events exerted dynamic influences on its morphology throughout different periods. Positioned between Red Mountain to the north, Zhong Mountain to the east, Jilong Mountain and Fuzhou Mountain to the south, the lake's mountainous and topographical features have remained relatively stable over time. Consequently, the floodplain dynamics of this natural lake have had a pronounced effect on its edges.

To address this complexity, the study utilizes probability density assessments to quantify the uncertainty in lake morphology. Building upon historical material interpretation and elevation calibration, the research computes runoff volumes under various storm recurrence intervals and applies the surface volume method to map the water extent across different flood scenarios. Probability density evaluations of the lake's boundaries are conducted based on the frequency of inundation events, as Figure 4. The surface volume method, an approximation algorithm, uses surface elevation data to progressively fill the model with varying runoff volumes, refining calculations to approximate the water surface extent. By employing inversion techniques of surface volume filling, the study reconstructs the water body boundaries that align with specific historical periods. Based on the frequency of inundation areas corresponding to different storm recurrence intervals, the research assesses the variability in lake boundary positions and their likelihood, thus enhancing boundary accuracy and providing a basis for subsequent morphological refinements.

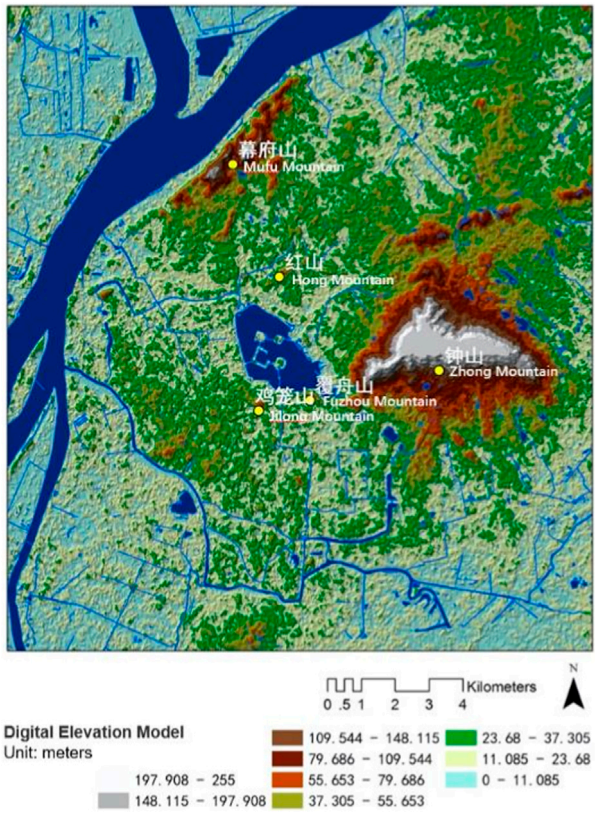

FIGURE 2
The elevation model that expresses the overall undulation pattern around Xuanwu lake.

2.3 Adjusting lake morphology boundaries based on adjacent mountain cross-sectional analysis

To delineate the boundaries of Xuanwu Lake in relation to nearby topographical features such as Mufu Mountain, Zhong Mountain, Hong Mountain, and Shijing Mountain, this study employs cross-sectional analysis of these adjacent mountain ranges. This approach deepens the understanding of the interactions between the lake and its surrounding environment. Using interpolation methods based on relatively accurate landmark positions (Cheng and Wang, 2021), the study adjusts the lake's morphological boundaries, as Figure 5. By integrating historical elements such as the Ming city walls, Xuanwu Lake's embankments, Leyou Garden, and Shanglin Garden, the study contrasts vector information from various historical periods to verify consistency with textual descriptions, thereby achieving a more accurate morphological reconstruction. The study performs a comparative analysis of multiple historical sources, including later compilations and research literature, overlaying historical information to refine and correct the boundaries based on the ratio of spatial element changes. Building upon this morphological reconstruction, the research explores the lake-mountain relationship, river-lake interactions, and the evolution of inflow and storage capabilities of Xuanwu Lake. It also examines the lake's water body transformation and its structural connections with the urban water network, further investigating the dynamic relationships between the lake's water morphology, connectivity of water systems, and urban water relationships.

Overall, by vectorizing information and reconstructing spatial elements, this approach provides a historically accurate representation of Xuanwu Lake's morphology. It enhances the accuracy of morphological representations, mitigates conflicts between historical data and actual terrain, and compensates for historical inaccuracies. This method offers a clearer, more detailed depiction of the lake's evolutionary process, facilitating both visual representation and in-depth analysis.

3 Results: inferring the spatial pattern changes of Nanjing Xuanwu Lake based on geographical information

Through the interpretation and reorganization of historical records and geomorphological information, the evolution of the spatial pattern of Xuanwu Lake is traced to restore and rectify its lake morphology, reflecting the spatiotemporal changes in the relationship between the city and water.

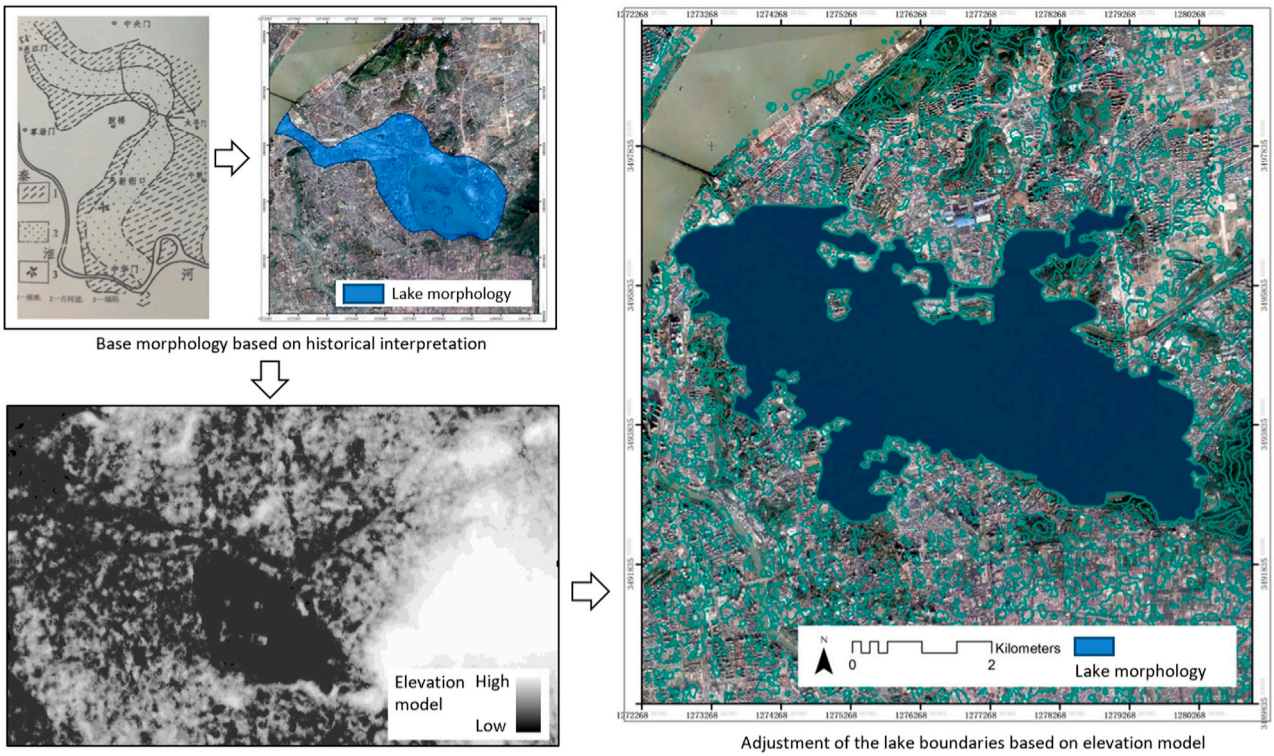

FIGURE 3
Lake morphology basemap based on historical material interpretation and elevation calibration.

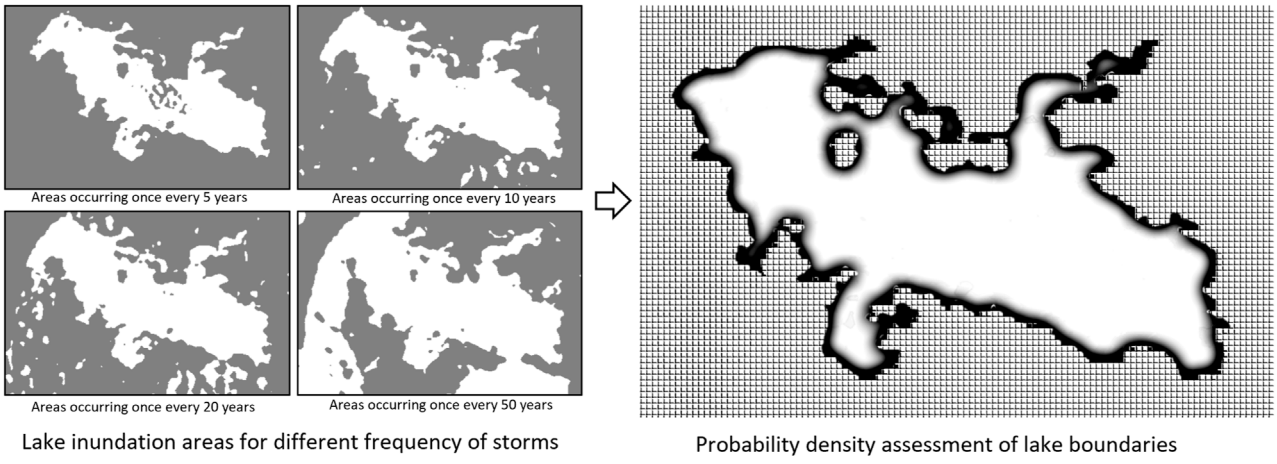

FIGURE 4
Probability density assessment of lake boundaries based on inundation areas for different frequency of storms.

3.1 The early period of slave society: lakes formed by mountain runoff under natural processes

The exact formation time and hydrological conditions of Xuanwu Lake are difficult to ascertain. Whether it originated as the ancient Oxbow Lake (Zongyi and Yihua, 2011) in the old course of the Yangtze River, as a sedimentary lake left by the ancient Qinhuai River, (Nai and Yanzhao, 2011), or as a tectonic lake formed by the Daxing Mountain fault (Le, 2014), it eventually became known as a "Sangbo Lake" according to historical records (Jiang et al., 1986), indicating a natural water area. (Figures 6, 7). During the pre-Qin period (Xu, 2020), the geographic location of Xuanwu Lake was relatively consistent with that of the Six Dynasties (Yuli and Song, 2022-0). It extended south to Fuzhou Mountain and Jiming Mountain and east to Zhong Mountain (Wei, 2012). Morphological reduction of Xuanwu Lake in early slave societies based on the integration of historical interpretation and geographic analysis is shown in Figure 5.

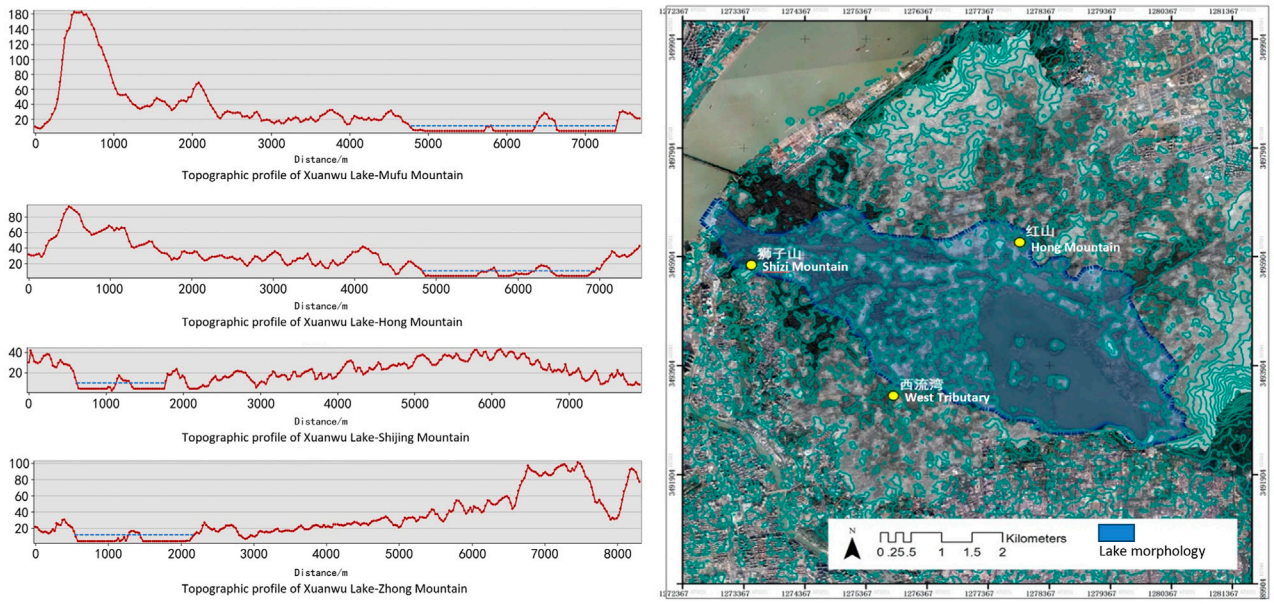

FIGURE 5
Adjustment of lake morphology boundaries based on analysis of neighboring mountain profiles.

Emperor Qin Shi Huang started the excavation of Fang Mountain in 210 BC to release the "royal air," allowing the Huai River to flow through Jinling City. Jinling City was subsequently renamed "Moling City", while the "Sangbo Lake" was renamed Moling Lake.[17] At that time, the hydrological processes within the Xuanwu Lake basin area were minimally influenced by human activities, maintaining the natural runoff characteristics and connectivity with the Yangtze River. The lake area had abundant water resources, receiving rainwater runoff from the northern foothills of Zhong Mountain. The dynamics balance between the inflow and outflow of the small watershed endowed the lake with certain storage and discharge capacity. The surrounding residents simply enjoyed the water ecosystem services provided by the lake.

3.2 The six dynasties period: xuanwu lake under the influence of the sacred mountain and immortal island theory

During the Six Dynasties period, Nanjing was established as the capital city (Figure 8). With the development of agricultural civilization and the increase in urban population, the hydrological condition and water functions of Xuanwu Lake underwent certain changes due to small-scale utilization, transitioning from a natural lake to an increasingly urban lake influenced by human activities. At this time, Xuanwu Lake extended eastward to the northwest foothills of Zhong Mountain, northward to Gulou Hill, and westward to the present-day Xiliuwan Park (Li, 2022). The Morphological Reduction of Lake Xuanwu in the Six Dynasties is shown in Figure 9.

In 229 AD, Sun Quan relocated the capital to Jianye, marking the beginning of Nanjing's foundation as a capital city.[18] During this period, various embankments were constructed and maintained. Xuanwu Lake served purposes such as military reviews and martial arts training, providing water for the urban water system and imperial gardens. In the second year of Emperor Wu's reign[19], known as Chih-Wu Era, a Chao Channel[20] was excavated to divert water from Xuanwu Lake into the palace complex (Lu, 2019). From then on, Xuanwu Lake was connected to the

17 In 210 B.C., Emperor Qin came to Jinling during his fifth eastern tour. The Taoist priest beside Qin said that this place had the spirit of the emperor. Qin was so shocked that he ordered the excavation of Fangshan Mountain and the diversion of Huai River to flow through Jinling City in order to release the king's spirit, and renamed "Jinling" as "Moling". The name "Moling" is the fodder for horses, which is the meaning of changing Golden Mountain into Grass Mountain.

18 In the 17th year of Jian'an of the Eastern Han Dynasty, Sun Quan moved his seat from Jingkou to Moling, built a city on Stone Mountain as a place for storing food and equipment, and changed the name from Moling to Jianye, which means "Establishing the Great Cause of the Emperor."

19 The Great Emperor of Wu, Sun Quan (182–252), courtesy name Zhongmou, born in Fuchun County, Wu County (now Fuyang District, Hangzhou City, Zhejiang Province), was the founding emperor of Wu during the Three Kingdoms period (reigned 229–252), a statesman and military commander-in-chief.

20 Chaogou, also known as Chengbei Ditch, is named for its northern connection to Xuanwu Lake, which brings the river tide to Nanjing City. It is connected to Yundu in the west, Pearl River in the south and Qingxi in the east, connecting the two major water systems in Nanjing - the Qinhuai River system and the Jinchuan River along the Yangtze River.

FIGURE 6
Map of Jinling, depicting the landscape relationship between the Yangtze River, Zijinshan Mountain and Xuanwu Lake. Source: Shanji Xu, Shanshu Xu, What a Geographer Needs to Know, World Knowledge Publishing House, 2011, available on open source website Chinese Repository Library.

Yangtze River, ensuring abundant water supply for both the city and the Qingxi River outside the city. Xuanwu Lake maintained the water balance of the capital city of Jianye through its own hydrological cycle.

The "Jingding Jiankang Zhi[21]" records, "In the fourth year of Chih-Wu era in Wu Dynasty, the Qingxi canal was dug, releasing water from the back lake. In the second year of Emperor Sun Hao's Baoding era, a northern canal was built, redirecting water from the back lake into the new palace, encircling the palaces, and thus gaining its name (Zhou, 2008)." Both the urban water system of Jianye and the new palace relied on Xuanwu Lake. In the third year of the Daxing period of the Eastern Jin Dynasty[22], Emperor Yuan[23] began constructing North Lake and built a six-li (approximately 3 km) long embankment. Historical records state, "The long embankment was built to dam the waters from the northern mountains. It extended from Fuzhou Mountain in the east to Mufu Mountain in the west, a distance of over six li." The southwest shore of Xuanwu Lake was enclosed by the embankment, altering the natural hydrological processes along the shoreline.

Later, Emperor Wen[24] of the Song Dynasty established three divine mountains[25] in the lake (457 AD) and four pavilions, integrating Xuanwu Lake into the imperial gardens. During this period, the theories of divine mountains and immortal islands, as well as the beliefs in immortals and adepts, flourished. In this cultural context, Xuanwu Lake was developed through hydraulic dredging, resulting in islands within the water. Xuanwu Lake can be regarded as 'One Pool and Three Mountains' of Nanjing. The "Nan Shi (Southern History)[26]" states, "In the 20th year of Yuanjia, a northern embankment was built, establishing Zhenwu Lake in the Leyou Garden to the north, with four pavilions within the lake." The construction of the northern embankment was primarily aimed at preventing water leakage from Xuanwu Lake and raising the water level, resulting in an area reduction. At this time, both the southern and northern shores of Xuanwu Lake had embankments, gradually shaping the natural hydrological processes of the lake through human intervention.

Xuanwu Lake has served as a battlefield for military conflicts and a training ground for naval forces on multiple occasions (Chen, 2016). During the Liu Song dynasty, when Xiao Daocheng held the position of Minister, he stationed troops at Xuanwu Lake and defeated Prince Jianping, Liu Jingsu.[27] In the 11th year of the Taijian era of Emperor Xuan of the Chen dynasty, he ordered the

21 The Jingding Jiankang Zhi is the first surviving official governmental record in the history of Nanjing square records, which was repaired by Ma Guangzu and compiled by Zhou Yinghe in the Southern Song Dynasty. The Zhi preserves a great deal of original information concerning national and local history.

22 The Eastern Jin Dynasty (317–420 AD) was a dynasty established after Sima Rui, a descendant of the Western Jin imperial family, moved the capital south.

23 Sima Rui, Emperor Yuan of the Jin Dynasty (276–323 AD), courtesy name Jingwen, born in Wenxian County, Hanoi County (present-day Wenxian County, Henan Province). He was the founding emperor of the Eastern Jin Dynasty.

24 Liu Yilong, Emperor of Song (407–453), was the third emperor of the Southern Song Dynasty. Liu Yilong's reign was the most powerful period of the Eastern Jin Dynasty and the Northern and Southern Dynasties, known as the " the reign of Yuanjia".

25 The name "Three Gods Mountain" comes from the "Records of the Grand Historian" (史记). Emperor Wen of Song Dynasty piled up five small islands from the dredged mud of the lake, and named three of them according to their sizes as "Penglai", "Fangzhang" and "Yingzhou", collectively known as the "Three Divine Mountains", which are the predecessors of Liang island, Huan island and Ying island in today's Xuanwu Lake.

26 Nan Shi (Southern History) is one of the twenty-four histories, a chronicle of Chinese history, consisting of eighty volumes, including ten volumes of the main chronicle and seventy volumes of biographies. The history starts from the first year of Song Emperor Liu Yu's Yongchu (420 AD), and ends at the third year of Chen Shubao's Zhenming (589 AD). The Southern History and the Northern History are sister works, which were compiled by Master Li and his son Li Yanshou in two generations.

27 The historical background of this battle was the political struggle and military conflict during the Liu Song period. The emperor Liu Yu governed inappropriately and the dynasty was in disorder. Xiao Daocheng, who was stationed at the lake, led a naval force that played an important role in the eventual victory.

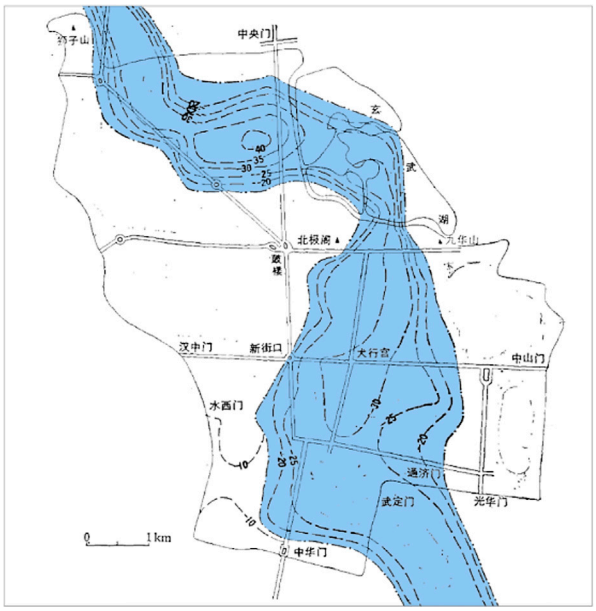

FIGURE 7
Relationship between the ancient Qinhuai River and the present-day Xuanwu Lake, redrawn from the bedrock isobath map of ancient river channels in Nanjing, China. Jiang Si Shan, Ang Chao Hai, Yang Huicheng, et al. A preliminary study on the paleochannels and the age of sediments in the Qinhuai River, Nanjing. Journal of Geology, 1986(01):91-103.

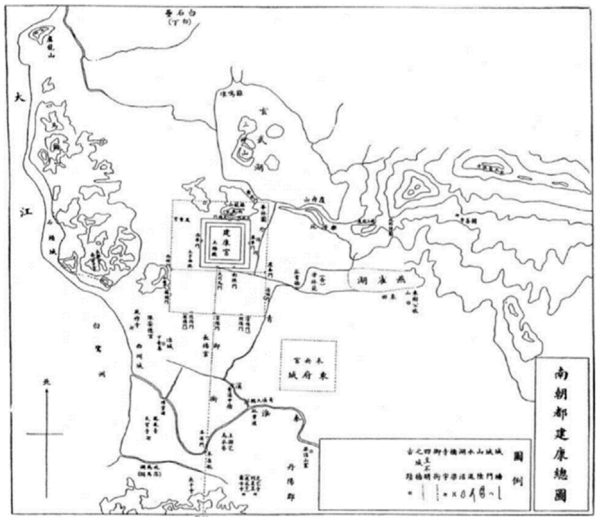

FIGURE 8
General map of Jiankang, the capital of south China, depicting the city's relationship with Xuanwu Lake and the surrounding landscape. Source: Zhu Qian, Jinling Ancient Monuments Map Kao, China Bookstore, 2006, available on open source website Chinese Repository Library.

commander Ren Zhong to lead an army of a hundred thousand infantry and cavalry to form a grand martial display on the surface of Zhenwu Lake.[28] Towards the end of the Liang dynasty, during the prolonged siege of Tai City by Hou Jing, who failed to capture the city, it was decided to take advantage of the water level difference between Xuanwu Lake and Tai City.[29] The decision was made to breach Xuanwu Lake's embankment and flood Tai City with the rushing waters. The majestic waves of the lake surged towards Tai City, causing water levels to rise both inside and outside the city, transforming the palace and royal avenues into torrents under the impact of Xuanwu Lake's forceful assault.

3.3 Sui and tang dynasties: low interference evolution of Xuanwu Lake as a far countryside natural place

After the unification of the Sui Dynasty[30], Jiankang City, adorned with numerous palaces, was reduced to rubble in order to completely eradicate the royal aura of Jinling. Buildings were demolished and the land was reclaimed as fields, a process known as "Pingdang Gengken" or "leveling and cultivation." As the capital cities of the Six Dynasties fell into silence, Xuanwu Lake also became desolate and deserted. In the fourth year of the Tianxi era of the Song Dynasty[31], it was renamed as the "Fangsheng Pond," symbolizing the emperor's benevolent virtue of showing compassion towards plants and animals, thereby manifesting the imperial reverence for the spirits of nature. "The moon shines over the vacant rear lake, waves rippling towards Yingzhou Island.[32]" Consequently, Xuanwu Lake underwent more than three

28 In the 11th year of Emperor Xuan Chen's Taijian reign, he ordered Governor Ren Zhong to lead 100,000 infantry and cavalry troops in a large-scale military manoeuvre in formation on Zhenwu Lake. The purpose of this martial act was to demonstrate the military strength and determination of the imperial court, as well as a demonstration and deterrent to internal and external hostile forces.

29 At the end of the Liang Dynasty, Hou Jing led an army to besiege the city of Taicheng in an attempt to capture the regime of the Liang Dynasty. However, due to the strong defence of Taicheng, Hou Jing's army was unable to attack it for a long time. In order to break the deadlock, Hou Jing took advantage of the water level of Xuanwu Lake and adopted the strategy of flooding Taicheng with drowning water.

30 The term "Sui defeats Chen" refers to the war of unification of China by the Sui Dynasty, in which Yang Jian, the Emperor of the Sui Dynasty, sent his army to pacify the Chen Dynasty of the southern part of the country. The war took place between 588 and 589 AD and was a key battle between the Sui and Chen dynasties.

31 The Tianxi was the year number used during the reign of Emperor Zhenzong of Song, and it lasted for about 4 years, from 1,017 to 1021 AD.

32 "The moon over the lake is still shining over the Yingzhou Island" is from the Tang Dynasty poet Li Bai's "Recitation under the Moon at the West Tower of Jinling City", meaning that the moon over the lake, which has remained unchanged for ages, still shines on the desolate and cold Yingzhou Island on the waves of the lake. This cold and hazy scenery is a combination of the poet's deep sadness about the old country's depression and the changes in personnel.

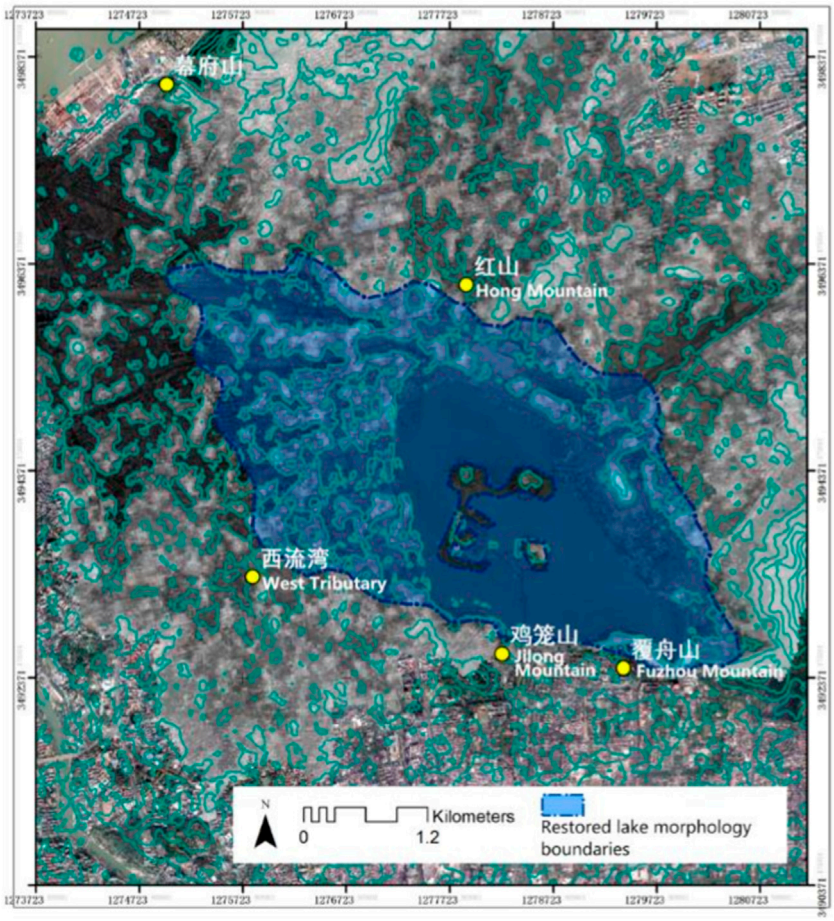

FIGURE 9
Morphological reduction of lake Xuanwu in the six dynasties based on the integration of historical interpretation and geographic analysis.

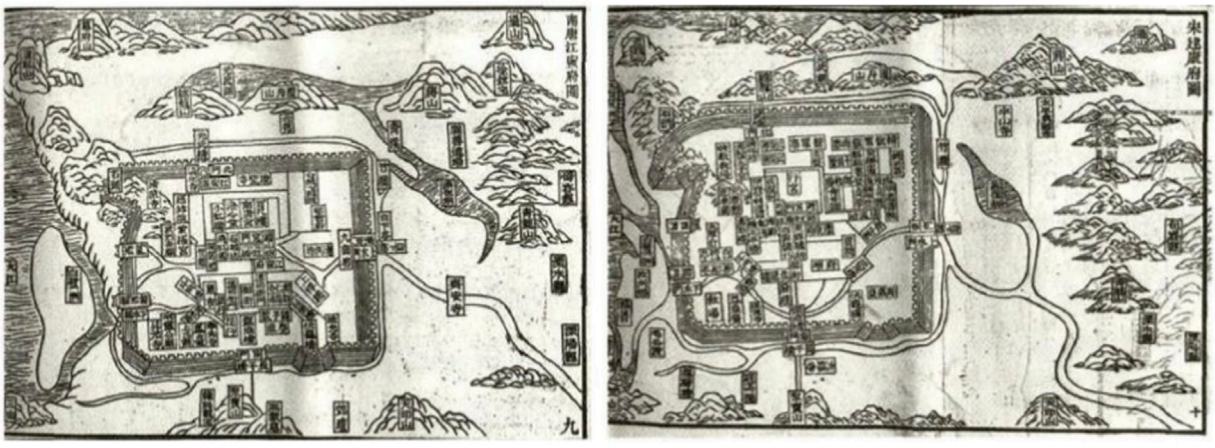

FIGURE 10
"Map of Jiangning Prefecture in Nankang" and "Map of Jiankang Prefecture in Song", comparing the changes of Jiankang City from the Southern Tang Dynasty to the Song Dynasty period. Source: Chen Yi, Ancient and Modern Map of Jinling, Nanjing Publishing House, 2017. Available in the Chinese Library of the School of Diagram and Architecture, Southeast University.

hundred years of natural evolution, eventually becoming a suburban lake during the Five Dynasties period[33]. It harmoniously blended with the surrounding landscape, including Jiang Mountain, Jilong Mountain, and Mufu Mountain (Zhen, 2010). "To the north of Jinling lies a lake, stretching for dozens of miles. Mufu and Jilong Mountains encircle it from the west, while Zhongfu and Jiang Mountains proudly stand on its left. These renowned mountains and grand rivers form a picturesque panorama.[34]"

3.4 Northern song dynasty: the abandonment of lakes and agricultural reclamation resulting in the conversion of lake water release into farmland

Due to the development of agrarian economy during Northern Song Dynasty[35], Xuanwu Lake was frequently filled and its hydrological processes were greatly disrupted. The primary function of the water system was irrigation for agricultural purposes, with the water level fluctuating between seven to four feet annually[36]. As the agrarian economy continued to grow, the demand for irrigation increased, prompting further landfilling of Xuanwu Lake. Unable to maintain its own water balance, the lake started experiencing siltation and water depletion, eventually transforming into arable land. Subsequently, the area of Xuanwu Lake gradually shrank, but remnants of the water body remained. (Figure 10).

However, the lake suffered the most substantial anthropogenic disturbance in history – "Xie Hu Wei Tian"or "Draining the lake as farmland". In the eighth year of Xining[37] during the Northern Song Dynasty, Wang Anshi, the magistrate of Jiangning Prefecture, obtained permission from Emperor Shenzong to convert Xuanwu Lake into farmland.[38] Two hundred hectares of land were distributed among the impoverished and famished people for cultivation (Jun and Zhao, 2022). The waters of Xuanwu Lake were drained, leaving only a cross-shaped canal for irrigation purposes. Morphological Reduction of Lake Xuanwu in the Northern Song Dynasty is shown in Figure 11. Consequently, Xuanwu Lake completely disappeared for over two hundred years. This drastic human intervention severely damaged the aquatic ecosystem of Xuanwu Lake, causing a discontinuity in the hydrological processes within the basin and the inability to sustain rainwater-harvesting functions.

Originally interconnected with numerous water networks inside Nanjing City, Xuanwu Lake continuously supplied water to the city, mitigating river tides and mountainous runoff during heavy rainfall. This ensured the city's safety against floods and provided a reservoir for water storage. However, after being converted into agricultural land, the disruption of this beneficial water regulation process resulted in frequent siltation of the city's waterways due to water scarcity during dry seasons and led to waterlogging during rainy periods. The loss of Xuanwu Lake's aquatic ecosystem services dealt a heavy blow to Nanjing's urban safety barriers.

3.5 Ming and Qing dynasties: restoration of Xuanwu Lake and its isolation as a royal sanctuary

After being turned into farmland, the waterways in Nanjing frequently silted up, prompting two major dredging efforts by the Yuan dynasty[39] to restore the channels of Xuanwu Lake.[40] Historical records in the third year of the Zheng dynasty, stating that "the Dushui Yongtian Bureau opened and dredged the waterways of the lake extending from Zhong Mountain's Pearl Bridge to Jinling Longwan River, spanning seventeen li." This dredging allowed the waterways to extend all the way to the present-day Qinhuai River[41]. Xuanwu Lake

33 The Five Dynasties period refers to the period from the destruction of the Tang by Zhu Wen in 907 AD to the establishment of the Northern Song Dynasty in 960 AD. In the short span of 54 years, the Central Plains saw the successive dynasties of Liang, Tang, Jin, Han, and Friday, historically known as the Later Liang, Later Tang, Later Jin, Later Han, and Later Zhou.

34 This record is from Zheng Wenbao's "Recent Affairs of the Southern Tang Dynasty" from the Northern Song Dynasty, depicting Xuanwu Lake and its landscape pattern. Although the city of Jiankang was destroyed, the area is still surrounded by beautiful mountains and glistening lakes, with remnants of the Six Dynasties hidden among them. Literati who came here were prone to a sense of prosperity and decline, they either remembered the pain of the deceased country, or expressed the sadness of their own sorrow, or issued the question of heaven's will, and looked at the world through the eyes of poets, giving birth to many famous pieces of ancient Jinling nostalgia.

35 The Northern Song period was the dynasty that followed the Five Dynasties and Ten Kingdoms of China and lasted from 960 to 1127 AD. The Northern Song period was an era of economic prosperity, cultural flourishing, technological advancement, and relative political enlightenment.

36 Seven feet to four feet means about 2.3 m–1.3 m. One foot is one of the units of length commonly used in China, and one foot is equal to about one-third of a metre.

37 Xining, was a year name of Emperor Zhao Xu, Emperor Shenzong, during the Northern Song Dynasty, for a total of 10 years, from 1,068 to 1077 AD.

38 Wang Anshi, the prefect of Jiangning, proposed to Emperor Shenzong of Song to convert the lake into a field to solve the livelihood problem of the poor people. He planned to create a cross river within the lake to drain away the excess water so that the poor could have access to abundant aquatic products. This idea was approved by Emperor Shenzong of Song, thus helping the poor and increasing the state's revenue.

39 The Yuan Dynasty (1,271–1368 AD) was the first major unified dynasty in China founded by an ethnic minority.

40 During the Yuan Dynasty, local officials in Nanjing dredged Xuanwu Lake twice, and it was not until the fifth year of the Yuan Dynasty's Dade (1301 A.D.) and the third year of the Zhizheng Dynasty (1343 A.D.) that the city's situation, which was plagued by rain, was ameliorated.

41 Qinhuai River is the largest regional river in Nanjing. Its role in navigation and irrigation has nurtured Nanjing's ancient civilisation, and it is known as the mother river of Nanjing.

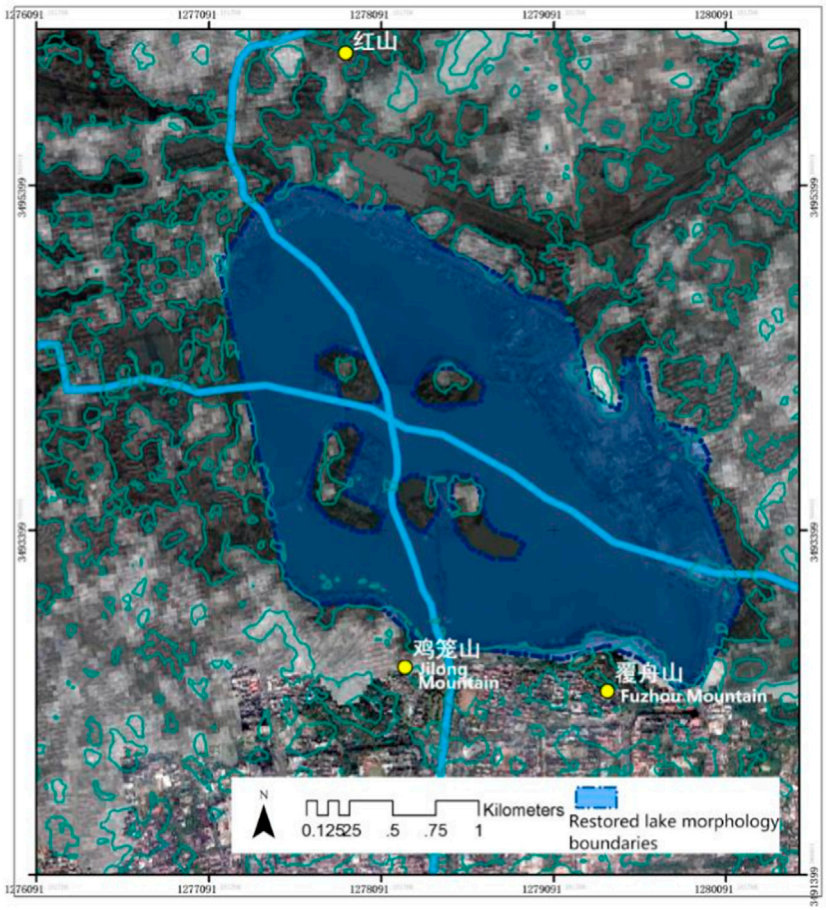

FIGURE 11
Morphological reduction of Lake Xuanwu in the northern song dynasty based on the integration of historical interpretation and geographic analysis.

reappeared on the map of Nanjing, providing some relief from the problems of flooding and drought.

It was during the Ming dynasty[42] that Xuanwu Lake truly regained its former glory, serving as the repository of the national household registrations and records of tribute and taxes for the Ming government—an esteemed place known as the Huangce Ku, or the Yellow Registry Warehouse[43]. (Figure 12). The Ming Dynasty Annals of Ying Tianfu[44] recorded, "Under the rule of Zhao and Song, it was turned into farmland, and during the Yuan dynasty, it became a small pond. In the Ming dynasty, it was restored to become a lake, storing the maps and records of the whole country (Wang and Wang, 2002)." With dedicated personnel guarding the Huangce Ku house within Xuanwu Lake, it became an inaccessible forbidden lake. "Few have set foot in this treasury of maps, with only towers and pavilions against the setting sun.[45]" Xuanwu Lake once again evolved into a naturally balanced ecosystem, forming a harmonious relationship with the surrounding mountains of Mufu, Zhong, Fuzhou, and Jiming. (Figure 13). During the Zhengde era[46], Ji Zongdao[47], a junior official of the Ministry of

42 The Ming Dynasty (1,368–1,644) was founded by Zhu Yuanzhang, the first Ming emperor. The capital was initially established at Nanjing, and was moved to Beijing during the reign of Emperor Chengzu of the Ming Dynasty.

43 Hongwu 14th year, Zhu Yuanzhang personally planned in Nanjing Xuanwu Lake in the centre of the island to build China's largest archive of feudal society - yellow book library, special storage of national service records of the central archives. During the two hundred years from 1,391 to 1,642, all the land and household records were hidden here.

44 Wanli yingtianfu zhi is a square journal of Nanjing in the Ming Dynasty. The record of the Ming dynasty rules and regulations and Jinling past events quite consistent with the historical tradition.

45 This line of the poem was used by people at that time to express their yearning for the beautiful scenery of Xuanwu Lake and their helplessness in not being able to enter it.

46 Zhengde was the year name of the 10th emperor of the Ming Dynasty, Ming Wuzong Zhu Houzhao (1,506–1521 AD), and was used by Ming Shizong, who assumed the throne in the 16th year of Zhengde.

47 Ji Zongdao was the first Xieyuan in the history of Liuzhou, who was the first place in the countryside examination in the imperial examination system. He was a man of great ability, broad-minded and opinionated, and in times of disasters and failures, he would plead for the people and fight for the reduction of taxes.

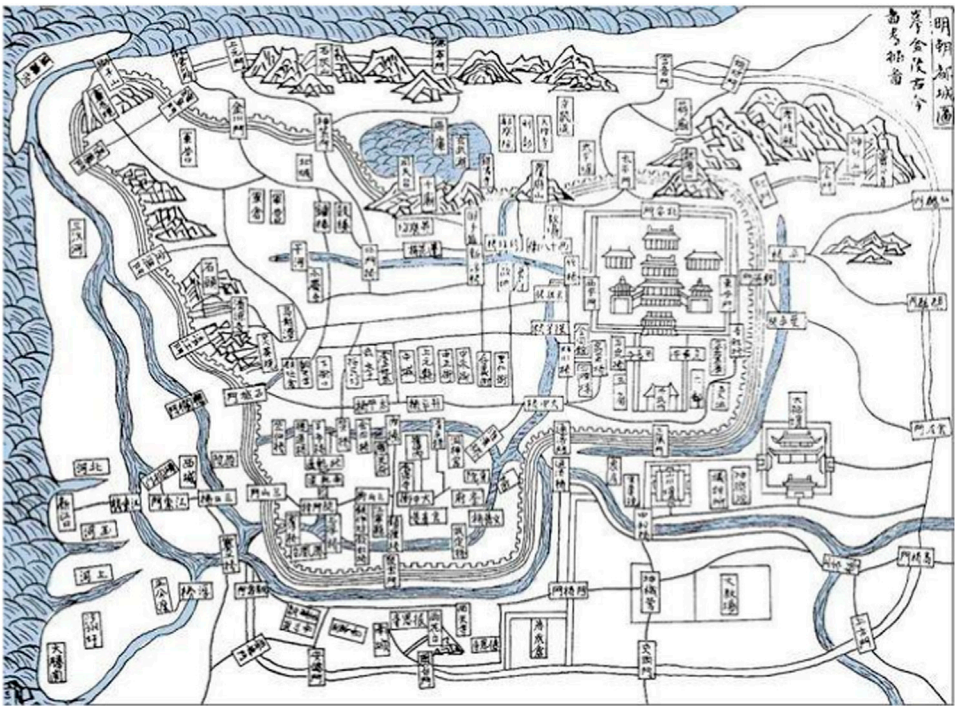

FIGURE 12
Back River map, depicting the distribution of islands and the relationship between the layout of depots on the islands when Xuanwu Lake was used as a yellow volume storehouse during the Ming dynasty. Source: Wang Qi, Wang Siyi, San Cai Tu Hui, Shanghai Ancient Books Publishing House, 1988.

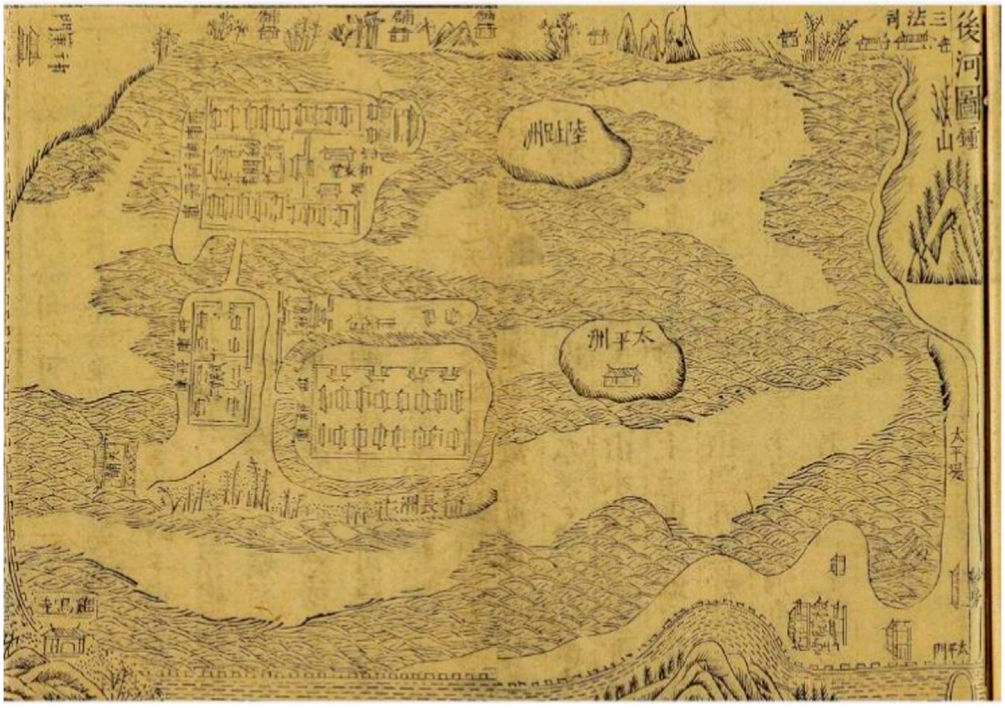

FIGURE 13
Map of the capital city of the Ming dynasty, depicting the relationship between Xuanwu Lake and the layout of the capital city and the structure of the landscape. Source: Written and revised by the Ministry of Rites of the Ming Dynasty, Hongwu Capital City Map, Nanjing Publishing House, 2006. Available in the Chinese Library of the School of Figure Architecture, Southeast University.

Revenue, wrote in his "Passing Through Hou Lake[48]": "I stood at the bow of the boat, gazing in all directions. To the southeast, there stood the towering Zhongshan Mountain, veiled in celestial majesty; to the northwest, mountain peaks rose like screens and curtains—Mount Mufu; the undulating ridges lay prostrated on the ground, covered with thick pine forests—Mount Fuzhou; and jutting out above the city walls, palaces and pavilions stood in disarray, with pagodas soaring into the sky—Mount Jiming Islands emerged from the water, their presence subtle amidst the fog and water." After its natural restoration, Xuanwu Lake shimmered with lush vitality, showcasing the beauty of nature.

During the reign of Emperor Qianlong[49] in the Qing Dynasty[50], Xuanwu Lake became one of the "Forty-eight Scenes of Jinling,[51]" earning the name "North Lake Veiled in Mist and Willow.[52]" Emperor Qianlong established his palace[53] on the northern shore of Xuanwu Lake, leaving behind numerous poetic works that extolled the pristine waters and natural splendor of this scenic landscape. One verse reads, "Here I stand, marveling at the vast expanse, where Xuanwu's clarity reveals its depths,[54]" while another paints a vivid picture, stating, "The mirror-like surface embraces the depth of spring waters, with white aromatic plants and green cattails adorning the azure banks.[55]"

In the late Qing Dynasty[56], notable figures like Zeng Guofan[57] undertook the construction of various facilities around Xuanwu Lake. The renowned Zeng's Embankment[58] was built between Guqi Slope and Liang island, while the Fengrun Gate[59] was erected atop the Ming city wall. Additionally, a new embankment was constructed, accompanied by an expansion of the lake's green spaces. Lu Shi Xue Tang Newly Measured Complete Map of Jinling Provincial Capital comprehensively reflects the layout of streets and alleys of Nanjing city. (Figure 14). These efforts marked the transformation of Xuanwu Lake into a modern-day park, providing the city with a plethora of invaluable ecological services owing to its favorable landscape conditions.

3.6 Period since modern times: urban garden relying on artificial maintenance of water quantity and quality

In modern times[60], with China's opening up, Xuanwu Lake has been referred to as 'Wuzhou Park,' which is distinctly different from the concept of immortals. The term 'Wuzhou' not only denotes the five islands of Xuanwu Lake but also embodies the idea of 'five continents and four oceans' on a global scale. During this period, Xuanwu Lake became a highly popular urban park in Nanjing. However, as urban construction in Nanjing expanded, many lakes were filled in, leading to siltation and a reduction in size, with Xuanwu Lake being no exception (Geng, 2019). To restore the vitality of Xuanwu Lake, extensive dredging was carried out in the 1950s. However, the sediment from the dredging encroached upon a portion of the lake's surface, resulting in its compression to the west of Zeng's Embankment and further reduction in size. In 1960, to improve connectivity within Xuanwu Lake, long embankments were constructed on the north side of the lake, connecting Cui island and the lake shore, Huan island and Ling island, as well as Ling island and the lake shore. These embankments

48 The Record of Crossing the Back Lake was written by Ji Zongdao in the seventh year of Zhengde of Emperor Wuzong of the Ming Dynasty (1512 AD). At that time, he was serving in the Ministry of Revenue in Nanjing. The Ministry of Revenue was in charge of the national population, taxes and other matters, and such books and archives since the beginning of the Ming Dynasty, that is, stored in the Xuanwu Lake Liangzhou.

49 Emperor Qianlong was the sixth emperor of the Qing Dynasty and the fourth emperor after the Qing army entered the country. The Qianlong Emperor was a refined and elegant man who wrote and recited poems throughout his life, with more than 42,000 poems.

50 The Qing Dynasty (1,616–1912 AD) was the last feudal dynasty in Chinese history. The first part of the Qing Dynasty was characterised by agricultural and commercial development, with the emergence of dense commercial cities in the south of the Yangtze River, during which the authoritarianism of ancient China also reached its highest peak.

51 The Forty-eight Scenic Spots of Jinling refers to the representative spots of the ancient capital Nanjing, representing the cultural heritage of Nanjing in various periods.

52 North Lake Smoke and Willow is one of the forty-eight scenic spots in Jinling, famous for the willow trees and fog around the lake, expressing the mood of calmness and calmness and vigorous growth.

53 Xinggong refers to the palace where the ancient emperors lived when they travelled, and also refers to the official offices or residences where the emperors temporarily resided after leaving the capital.

54 This poem is from Qianlong's old five-character poem "Questions on Jiming Mountain."

55 This line is from Qianlong's seven-character poem "Miscellaneous Rhapsody on the Immediate Scene of Yuanwu Lake".

56 The Late Qing Dynasty (1840–1912) was the late period of the Qing Dynasty's rule, the beginning of China's modern history, and the formation of a semi-colonial and semi-feudal society in modern China.

57 Zeng Guofan, Xiangqi in Hunan Province, was a Chinese politician, strategist, rationalist, and man of letters in the late Qing Dynasty, and the leader of the Xiang Army, an armed force of Han landlords in the late Qing Dynasty.

58 Zuo Zongtang in order to fulfill the long-cherished wish of Zeng Guofan, built a new dike connecting Liangzhou from Cuizhou, directly connected to the ten-mile long dike, and named this dike "Zeng Gong dike".

59 Opened in 1908, Fengrun Gate is located between Shenzemun and Jiefangmen and Taipingmen, and was renamed Xuanwumen after its proximity to Xuanwu Lake.

60 Modern China refers to the period from the Opium War in 1840 to the founding of the People's Republic of China in 1949, which was also the period of China's semi-colonial and semi-feudal society.

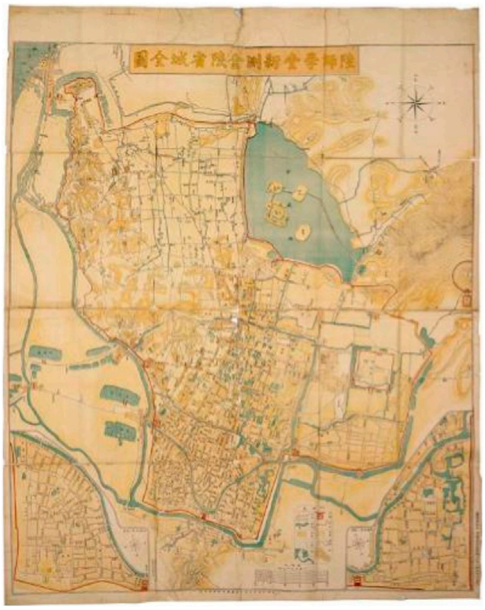

FIGURE 14
Lu Shi Xue Tang Newly Measured Complete Map of Jinling Provincial Capital, a map comprehensively reflecting the layout of streets and alleys of Nanjing city, drawn by Zhong Bingxi and Li Delin, graduates of Jiangnan Lu Shi Xue Tang, under the order of Liu Kunyi, the Governor of the Two Rivers. Source: "Old Maps, Old Shadows of Nanjing: 1903 Newly Surveyed Complete Map of Jinling Provincial City by the Land Division School", Nanjing Publishing House, 2014.

facilitated transportation between the various islands of Xuanwu Lake. Morphological Reduction of Lake Xuanwu in the Qing Dynasty (A) and the 1960s (B) is shown in Figure 15. In the 1990s, Xuanwu Lake lost an area of nearly 50,000 square meters due to urban development, which displayed a strong tendency to encroach upon the lake. This led to a decrease in the effective convergence space of the watersheds, the interruption of runoff pathways, and a gradual weakening of the connection between Xuanwu Lake and its surrounding water systems. As a result, the lake's water storage capacity diminished, leading to frequent occurrence of urban waterlogging.

The discharge of domestic and industrial wastewater from urban activities has also significantly impacted the ecological balance and self-purification capacity of Xuanwu Lake. By the mid-1980s, the lake water began exhibiting signs of organic pollution and eutrophication. In the 1990s, eutrophication worsened, resulting in extensive fish mortality. In 1998, the Comprehensive Remediation Project of Xuanwu Lake was initiated, which included a water diversion project with an annual total water intake exceeding 70 million tons, averaging approximately 220,000 tons per day.

Today, Xuanwu Lake relies on the Comprehensive Remediation Project to replenish water volume and improve water quality. It maintains a relatively stable ecosystem and satisfies the aesthetic and recreational needs through a large amount of water flushing from the Yangtze River and periodic sediment dredging. However, Xuanwu Lake is still in a "sub-healthy" state, with its water often experiencing mild to moderate eutrophication.

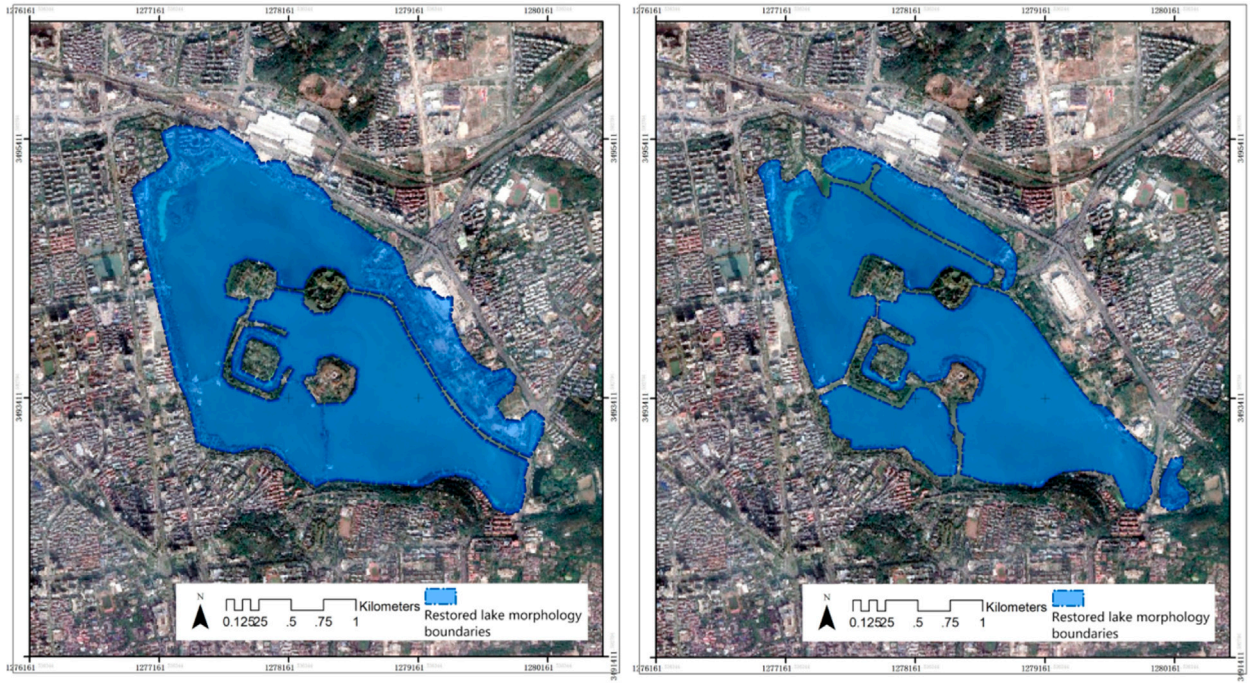

FIGURE 15
Morphological reduction of lake xuanwu in the qing Dynasty **(A)** and the 1960s **(B)** based on the integration of historical interpretation and geographic analysis.

4 Discussion: evolution of the spatial pattern of Xuanwu Lake and the relationship between city and water

The ancient cities, palaces, and water systems of China were intricately tied to the culture of feng shui. As a renowned and mysterious Chinese tradition, feng shui encompasses a conceptual and practical system based on geographic environment, energy flow, and aura. Its main focus is on how the arrangement and adjustment of surroundings can positively influence human life and the development of various entities. However, when examining Xuanwu Lake, it becomes evident that historical Chinese urban water layouts were more pragmatic, emphasizing adaptation to the local conditions.

China has a large number of famous historical and cultural cities, each embodying diverse synergies between urban landscapes and water systems, facilitating sustainable development. The functions of these water systems have evolved in tandem with urban development. With the widespread implementation of modern municipal infrastructure and diversified transportation methods, the once prominent roles of waterways for transportation and agricultural irrigation have gradually diminished, shining a greater spotlight on the ecological role of urban water networks. In the case of present-day Xuanwu Lake, its original functions in military training, transportation, agricultural irrigation, and water supply for daily use have faded away, leaving behind its ecological significance as maintenance of landscape connectivity. This indicates the shift from productivity-oriented purposes to prioritizing the hydrological regime and water ecological safety, whilst emphasizing the nurturing effects of water on the surrounding environment and its ecological service functions. This perspective provides valuable insights into the changing dynamics of urban water relationships in Xuanwu Lake from a historical standpoint.

4.1 Changes in the spatial pattern of Xuanwu Lake

The development and utilization of Xuanwu Lake by humans have led to numerous alterations, disappearances, and reappearances, driving the contraction and expansion of the lake's edge in different periods. Originally, when carefully shaped by humanity, Xuanwu Lake existed as a natural and complete body of water, unobstructed by dams or islands, with a pristine shoreline. Historical records indicate that the lake's area was once four times its current size. Subsequently, two river embankments were constructed, and three islands were created within the lake, enhancing the complexity of the water's morphology and resulting in a more meandering shoreline.

After experiencing transformations such as turning the lake into farmland and expanding it through land reclamation, the lake's area was reduced by two-thirds. During this process, bridges and embankments were introduced to partition the water surface, and the number of islands increased. Following the Republican period[61], significant contraction of Xuanwu Lake's shape became evident. In the 1980s, there were frequent incidents of encroachment and artificial landscaping along the lake by various establishments, such as the occupation of the lake by water sports schools, filling of the lake for golf courses, and encroachment by Xuanwu Gate Square and Lotus Square. As a result, the lake's circumference decreased from 12 to 9.5 km. In modern times, the shape of the lake's shoreline has been further influenced by urban development, causing Xuanwu Lake to gradually diminish due to dredging and land utilization.

Initially, the water morphology of Xuanwu Lake represented a primary expanse with winding contours. Subsequently, the water surface became more diverse, featuring sporadic bridges, embankments, and islets, without dominating the overall water area. In the later stage, the water surface exhibited greater diversity, with larger areas occupied by islets and embankments in the central region. Finally, the lake contracted along its edge, increasing the island area within, elevating the overall marginality of the lake's shoreline while reducing its centrality and aggregation. The general form of the lake tended toward regularity, with the most notable changes occurring adjacent to the western side of the Ming City Wall.

4.2 Changes in the connectivity of Xuanwu Lake and Nanjing's water system

According to historical records, Xuanwu Lake was originally connected to the Jinchuan River system[62] to the south and the Yangtze River to the west. The "Jiaqing Jiangning Prefecture Chronicles[63]" states: "Zhidu River, now known as Guanyin Gate, flows into the Yangtze River. South of Maigao Bridge, water flows through Santa Temple into Back Lake, where it meets the waters of the mountains northeast of Zhong Mountain and flows westward through Dashuiguan and Fu Family Bridge (which should be located east of today's Mufu Mountain) into the Yangtze River (Yao and Lv, 2001)." In the depression between Lion Hill and Mufu Mountain, there was a gap approximately four to 5 km wide, through which the rising tide of the Yangtze River surged into Xuanwu Lake. Emperor Chen Xuan[64], sitting atop the North Gate, reviewed a procession of 100,000 soldiers and cavalry advancing toward the foot of Zhongshan *via* Jimingdai, while 500 warships sailed in various formations into the Yangtze River. This grand spectacle demonstrates the wide passage between the

61 The Republican Period (1912–1949) refers to the period from the fall of the Qing Dynasty to the establishment of the People's Republic of China.

62 Jinchuan River is a tributary of the Yangtze River flowing through the northern part of the main city of Nanjing, with a watershed area of nearly 60 square kilometers.

63 The jiaqing jiangningshi is jiaqing 16 years into the book of jiangningshi, weather, maps, boundaries, history, chronology, landscapes, monuments, customs and products, establishment, service, science and tribute, people, gold and stone, art and literature and other twenty-one categories.

64 Chen Xu, Emperor Xuan of Chen (530–582), during the reign of Emperor Xuan of Chen, the country was relatively stable and politically clear. He built water conservancies, reclaimed wasteland and encouraged farmers to produce, which led to some socio-economic recovery and development.

Yangtze River and Xuanwu Lake at that time, with expansive water surfaces and navigable channels.

In the early days, the connectivity of Xuanwu Lake's water system was excellent, as the water from Zhongshan continuously flowed into the lake. It converged through Chaogou, joining the Pearl River[65] and Yangwu Yundu before entering the Qinhuai River on the eastern side of Jilong Mountain. The "Tai Ping Huan Yu Ji[66]" accurately locates Qingxi: "Qingxi is located six miles north of the county to drain the water from Xuanwu Lake and flow south into the Qinhuai River (Le, 2014)." The "Annals of Jiankang[67]" provides a clear position on the relationship between Qingxi, Yundu and Chao channels: "Qingxi flows eastward connects with Yundu, entering the Qinhuai River. Another canal is opened, leading north to Houhu, to direct the lake water. The eastern outlet to Qingxi is a tidal channel (Xu, 2020)." Xuanwu Lake, through the influx of the Yangtze River, the connection with Yundu, the communication with Qingxi, and its arrival at the Qinhuai River, also provided various water sources for the surrounding areas, including the imperial gardens such as Leyou Park and Hualin Garden, forming an interconnected water network that constitutes the main urban area of Nanjing.

When Zhu Yuanzhang[68] established his capital in Nanjing, he built the city walls on the southern and western shores of Xuanwu Lake. Xuanwu Lake, serving as a natural "protective moat," separated the lake from the city walls and effectively cut off its previous connection to the Yangtze River. Moreover, at the junction of Zhongshan Mountain and Xuanwu Lake, the "Taiping Embankment" was constructed. This embankment divided a section of the lake that was adjacent to the western slope of Zhongshan Mountain, creating what is now known as Baima Lake. As a result, the direct hydrological connection between Xuanwu Lake and the western slope of Zhongshan Mountain was severed. The establishment of Huangceku further limited the connectivity between Xuanwu Lake and the surrounding water systems. To ensure the safety of Huangceku, the water flow and level of Xuanwu Lake were tightly controlled. At that time, there was a water gate called Dashugen[69] on the west side of Xuanwu Lake, which connected to Jinchuan River, and the Jinchuan River flowed into the Yangtze River. The protective moat outside the northwest and Shence Gates[70] formed a connection, while to the south, through Wumiao Gate[71], Chao channels were introduced, linking to Qingxi and later flowing into Qinhuai River. The lake water served as a protective barrier for Huangceku. The opening and closing of the gates were strictly regulated to maintain a balanced water level and appropriate water volume in Xuanwu Lake.

With the development of modern construction, pollution sources, including domestic pollution around Xuanwu Lake and the discharge of agricultural and industrial wastewater along the lake, have increased. Surface runoff quality has declined, and the interconnected water systems have transferred pollution from the city to Xuanwu Lake. In order to control external pollution of the lake water, the existing Tangjia mountain and Zijin mountain diversion channels have been blocked, preventing the runoff from the northern foot of Zijinshan and the northeast watershed from replenishing Xuanwu Lake. Overall, Xuanwu Lake has no self-sustaining water sources. It is completely dependent on the pumping of water from the Yangtze River, and water discharge is regulated through the gates.

In history, Xuanwu Lake used to rise and fall with the Yangtze Rive. In different periods, Xuanwu Lake provided water for various internal and external water systems, such as Yundu River, Qingxi River, Chengbei River[72], Qianbei Ditch, Tidal Channel, and Pearl River. However, nowadays, the tidal channel and Xuanwu Lake are separated, and the network of water systems within the watershed appears obstructed and fragmented when observed from satellite

65 Pearl River is an important river in Nanjing city area, with a total length of about 23 km, flowing through the central area of Nanjing, which is one of the mother rivers of Nanjing.

66 Taiping Huan Yu Ji was written by Le Shi, a geographer during the Song Dynasty, and its content includes dozens of items such as mountains, rivers, scenic spots, cities, towns, bridges, temples, and products of each continent, which was one of the more comprehensive geographic journals at that time, and it can be used to understand the establishment of the prefectures in the beginning of the Song Dynasty and their geographic history.

67 The Jiankang Shilu, written by Wei Diayi during the Tang Dynasty, is a chronological account of the historical development of the Jiankang region during the Southern Dynasties in terms of politics, economy, culture, society and military affairs.

68 Zhu Yuanzhang was the founding emperor of the Ming Dynasty. During his reign, politically, he strengthened the centralization of power, abolished the prime minister and the Central Committee, set up three divisions to divide local power, and severely punished the corrupt officials and lawless dignitaries; militarily, he implemented the system of guards; economically, he engaged in the immigrants and the military, constructed water conservancy, reduced taxes, measured the land of the whole country, and checked the household accounts; culturally, he tightly grasped the education, greatly promoted the imperial examinations, and set up a state academy for the cultivation of talents; and in foreign relations, he established the "no-conquest state". In terms of culture, he emphasized education, promoted the imperial examinations, and established the Guozijian to cultivate talents. Under his rule, social production gradually recovered and developed, known as the " reign of Hongwu".

69 Dashugen Sluice Gate is a sluice gate built during the Ming Dynasty, located above the Xuanwu Lake Tunnel in Nanjing, starting from Xuanwumen in the south and leading to Central Road in the north.

70 Shenze Gate is one of the thirteen Ming Dynasty capital city gates on the Ming City Wall of Nanjing, located east of the Central Gate of Nanjing, west of Nanjing Railway Station and north of Xuanwu Lake.

71 Located near the Jiefang Gate of Xuanwu Lake in Nanjing, Wumiao Lock is the outlet of Xuanwu Lake in Nanjing and the earliest water gate in Nanjing. The Wumiao Lock was designed in the Ming Dynasty, and at that time its water conservancy construction and building were world-class.

72 Chengbei River originates from Gangnan, southeast of Ma'an Township, Liuhe District, Nanjing, and is a branch of Chu River, with a total length of 19.8 km and a watershed area of 138.9 square kilometers.

images. Multiple branches of the interconnected water systems have been converted from surface runoff to underground pipelines. As a result, the connectivity of Xuanwu Lake's water system has significantly decreased in modern times.

4.3 Evolution of city-water relations and human activities

The ancient Xuanwu Lake provides high-quality ecosystem services: pleasant climate, clean water resources, abundant shoreline vegetation, and diverse aquatic animals. People have settled around the lake, benefiting from Xuanwu Lake's provision of high-quality living materials and a livable environment. Furthermore, the expansive water surface of Xuanwu Lake serves as a training ground for the navy, leading to human interventions to improve its edges, increase connectivity with the water system, and change the landscape—primarily driven by political reasons.

After being incorporated into the Royal Gardens, the Shanglin Garden, Leyou Garden, Hualin Garden, and the "Three Gods Mountain" in the middle of the lake, all relying on Xuanwu Lake, became places for daily royal recreation and hosting large-scale events, providing diverse cultural services. The lake and mountain pattern surrounding Xuanwu Lake, along with the water network, collectively serve as excellent barriers for defending Jiankang City in times of war.

However, with the onset of economic development, the ecological services provided by Xuanwu Lake were not fully recognized, leading to the lake being used for agriculture through drainage, disregarding its role as a reservoir and undermining its functionality.[73] This practice has subsequently resulted in numerous flood and drought problems. "Jinling's land is high on the outside but low in the middle. Xuanwu Lake, though it receives water from the various streams of Beishan, suffers from storage loss, rendering it useless in times of drought or flood.[74]" The reasons behind this lie in the fact that although Xuanwu Lake has been transformed into farmland under human control, it still remains in a low-lying terrain. Water from Zijin Mountain and Mufu Mountain continues to flow into the area, and the gap leading to the Yangtze River has been filled, causing poor drainage and making it prone to waterlogging. After the construction of city walls, water from Xuanwu Lake could directly protect the northeast of Nanjing City, while the west and north sides of the city were adjacent to the Yangtze River, providing natural defense. The imbalances within the aquatic ecosystem of Xuanwu Lake resulted in the breach of the city's safety barrier, leading to both drought and flood disasters. Thus, these urban calamities have prompted efforts to restore Xuanwu Lake once again.

During the Ming Dynasty, Xuanwu Lake, as part of the imperial Yellow Registry, served as a secluded royal sanctuary, cut off from the outside world. The primary function of Xuanwu Lake during this period was spatial isolation. The location of the Yellow Registry on the central island of Xuanwu Lake was chosen for several reasons. Firstly, its proximity to the capital city facilitated easy transportation. Secondly, its enclosed surroundings made it convenient for administration. Lastly, the three islands surrounding the water provided natural protection against fires.

After its reopening, Xuanwu Lake's recreational and cultural value was fully realized, leading to a new phase of development and refurbishment. In 1872, Zeng Guofan oversaw the restoration of the Lake Temple in Liangzhou and the construction of landmarks such as Hu Xin Pavilion and Da Xian Tower. To address the issue of difficult access to Taiping Gate, Zuo Zongtang[75] constructed a long embankment connecting Guqi Geng to Liangzhou. Zhang Zhidong[76] erected the "Chu Ri Fu Rong" archway along this embankment. Duan Fang[77] expanded the green spaces within the lake, opened Fengrun Gate, and built new embankments. These initiatives significantly enhanced the recreational services of Xuanwu Lake.In 1946, Chiang Kai-shek returned the capital to Nanjing[78], and Xuanwu Lake became the political and cultural epicenter of the city. It served as a gateway for international cultural exhibitions and various diplomatic exchanges.

Following the era of reform and opening up, Xuanwu Lake transformed into an urban landscape. Its high-quality recreational services led to the addition of facilities and the renovation of buildings. However, simultaneous development of surrounding construction sites had a disruptive impact on the ecological system of Xuanwu Lake. Over the past 3 decades, the water quality of Xuanwu Lake has declined, and its aquatic ecosystem has deteriorated. Contemporary efforts are being made to explore sustainable ways to enhance the water environment of Xuanwu Lake and its surrounding water system, aiming to strengthen its ecological resilience. The relationship between the city and Xuanwu Lake has

73 In the eighth year of Xining (1,075), Wang Anshi gave the emperor a report on the "Hutian Shuo", arguing that the Xuanwu Lake had been regarded as a place of amusement in former times, but now it was vacant and useless, and that the minister (referring to Wang Anshi) wanted to open up the source of the Cross River internally for a while, and that draining off the excess water would allow the poor and hungry people to have access to the rich resources of snails, mussels, fish and shrimps, and thus improve their living conditions. The emperor's consent was obtained.

74 The history is from "Song Shi - River and Drainage Records", meaning that the topography of Nanjing was high on the outside but low on the inside, and that Xuanwu Lake was actually influenced by all the water from the northern mountains. As Xuanwu Lake could not store these waters effectively, it resulted in either droughts or floods.

75 Zuo Zongtang (1812–1885), a native of Xiangyin, Hunan Province, was a minister of the Qing Dynasty and a famous Xiangjun general.

76 Zhang Zhidong (1837–1909), who was appointed governor of Shanxi during the Sino-French War, offered insights into war preparations, gambling cessation, military training, and defense.

77 Duanfang (1861–1911), a native of the Zhengbai Banner in Manchuria, served as Governor-General of Zhili and Minister of the Northern Ocean.

78 On 18 April 1927, the Chinese Nationalist Party formally held a ceremony for the establishment of the Nationalist Government's capital at the Jiangsu Provincial Assembly in Dingjiaqiao, Nanjing (present-day No. 10, Hunan Road), and issued the Declaration on the Establishment of the Capital of Nanjing.

been closely intertwined with political and economic changes, exerting mutual influence over the long term.

4.4 Comparative analysis of historical evolution and city-water relationships between Xuanwu Lake and Hangzhou's West Lake

Xuanwu Lake and Hangzhou's West Lake provide a rich comparative framework for examining their historical development and the evolution of urban-lake relationships. This analysis seeks to explore the complex interplay between lakes and urban environments, contributing to reflections on sustainable urban development.

In contemporary settings, Xuanwu Lake and West Lake reveal striking contrasts in their urban water relationships and social service functions. These differences primarily arise from the positional relationship of Xuanwu Lake relative to Nanjing and the structural variations within the city. Originally serving as a water source and defensive moat, Xuanwu Lake, situated as the "back lake," was isolated beyond the city walls. Initially conceived as a defensive barrier, it gradually transformed into a royal garden and eventually emerged as a significant public open space. Prior to Nanjing's rapid land development, Xuanwu Lake resembled a garden for the city. In contrast, West Lake serves as a quintessential "inner lake," deeply integrated into the daily life of Hangzhou's inhabitants. Its spatial relationship with the city embodies a "city-water synergy," with both commercial and residential developments clustering around it. This arrangement has substantially enhanced the quality of urban spaces in its vicinity.

In history, Xuanwu Lake and West Lake have experienced markedly different trajectories. As previously discussed, Wang Anshi's reforms during the Song Dynasty drastically altered Xuanwu Lake by transforming it into arable land. Similarly, West Lake underwent significant intervention during the ancient period, by the Northern Song scholar Su Shi. In 1,090, as Governor of Hangzhou, Su noticed the lake's deteriorated state, which had become overrun with weeds and silted from years of neglect. Su petitioned Emperor Zhezong with a proposal for the lake's revitalization, stating, "The success or failure of water management appears to be governed by natural and human principles. However, a discerning ruler who understands the times and invests in water projects to benefit the populace and mitigate disasters ensures that such measures yield visible results and are difficult to reverse." Utilizing imperial permits for tax exemption, Su secured funding for the lake's restoration. He organized manpower and resources to remove silt and vegetation, thus restoring the lake's original expanse. Additionally, he constructed the "Su Causeway" using the removed silt and vegetation, which featured six bridges to facilitate transportation and enhance the lake's aesthetics. Furthermore, Su established a dedicated agency for the lake's dredging and maintenance, ensuring the long-term effectiveness of the restoration efforts. His initiatives not only resolved practical issues but also imbued West Lake with distinctive cultural significance.

Wang Anshi and Su Shi exhibited marked differences in their approaches, methodologies, and outcomes regarding lake management, resulting in the distinct historical trajectories of Xuanwu Lake and West Lake. Wang's governance philosophy tended towards pragmatism with a focus on immediate gains. In managing Xuanwu Lake, he adopted a strategy of "draining the lake to create farmland," aimed at expanding agricultural land. However, this approach neglected the lake's ecological significance and its long-term impact on the city, leading to Xuanwu Lake's disappearance for over two centuries and exacerbating severe flooding and drought issues. In contrast, Su prioritized ecological balance and cultural sensitivity in his management of West Lake. He advocated for a harmonious integration of water management and ecology, sought extensive public input, conducted thorough field surveys, and developed a practical and sustainable management plan. This approach not only preserved West Lake's ecological integrity but also enhanced its role as a significant cultural and tourist resource, thereby fostering urban economic development.

A deeper examination of these differences reveals that they stem from the individual backgrounds and values of the administrators. Wang Anshi, the initiator of the "Xining Reform" (1,069–1,085), aimed to rectify the impoverished state of the Northern Song Dynasty through a series of reformative policies and measures. Facing substantial political pressure, Wang was urgent in seeking immediate results. Conversely, Su Shi operated within a relatively stable environment, allowing him to consider long-term benefits more thoroughly.

Overall, Xuanwu Lake, with its distinctive geographical location and historical context, became a crucial element of Nanjing's urban spatial structure, while West Lake, with its integration into Hangzhou's cityscape and rich cultural heritage, stands as a symbol of the city's cultural identity. These cases reflect a profound interaction between urban spaces and water bodies with unique characteristics. Historical evolution underscores that successful management requires not only scientific decision-making and effective methods but also a deep understanding of ecological environment, alongside essential public participation and feedback mechanisms.

5 Contemporary insights into the management and optimization of the Xuanwu Lake water environment

The study takes a long view of the historical process, and restores the historical shape of Xuanwu Lake through information vectorization and spatial reconstruction based on the interpretation of historical materials, and visually expresses the edge characteristics of Xuanwu Lake, the connectivity of the water system, and the evolution pattern of its landscape pattern. Xuanwu Lake was a pristine pond in the early days, used as a training ground for the royal navy during the Six Dynasties, then as a royal garden, then filled in as a field during the Northern Song Dynasty, restored as a royal forbidden lake during the Ming and Qing Dynasties, and became a popular urban landscape in modern times.

Reflecting on history, over the past approximately 2,300 years for which records are available, Xuanwu Lake has maintained its long-term hydrological balance by collecting surface runoff from the surrounding areas and connecting with the water network. Ancient people engaged in a prolonged dialogue with the environment, fully exploring the various external benefits of Xuanwu Lake. However, when it comes to the contemporary water environment issues facing

Xuanwu Lake, relying solely on engineering measures to address the problems of declining water quality and insufficient water quantity is merely a surface approach to restoration. The underlying causes of the decline in water environmental quality in Xuanwu Lake lie in the city's development patterns and changes in ecological processes.

Generally speaking, the restoration of the hydrological processes of Xuanwu Lake remains fundamental to water environmental management. The synchronicity between the self-sustaining capacity of Xuanwu Lake's water system, the changes in hydrological processes and connectivity of the water network is relatively favorable. To a certain extent, this indicates that the density of the water system in the Xuanwu Lake watershed, the effective connectivity of river channels, and the land use development of smaller watershed catchments should be key points of intervention for water environmental management in Xuanwu Lake. Therefore, the sustainable recovery of Xuanwu Lake requires attention to the underlying process mechanisms and causes of the issues, aiming to restore hydrological processes and reconstruct the spatial network of the water system through natural or quasi-natural methods. This will allow the basin's water network to nurture the vitality of the lake, thus reviving the natural spirit of Xuanwu Lake.

Data availability statement

The original contributions presented in the study are included in the article/supplementary material, further inquiries can be directed to the corresponding author.

Author contributions

XW: Conceptualization, Data curation, Formal Analysis, Methodology, Software, Validation, Visualization, Writing–original draft, Writing–review and editing. YC: Conceptualization, Funding acquisition, Supervision, Writing–review and editing.

Funding

The author(s) declare that financial support was received for the research, authorship, and/or publication of this article. Supported by the National Natural Science Foundation of China under the "Theory and Methods of Urban Green Space Planning under Low Impact Development" (No. 51838003).

Acknowledgments

During the preparation of this work the authors used ChatGPT 4o mini in order to improve language and readability.

Conflict of interest

The authors declare that the research was conducted in the absence of any commercial or financial relationships that could be construed as a potential conflict of interest.

Publisher's note

References

Chen, V. (2016). Comply with the development, scenery and situation: Xuanwu Lake and Nanjing. *Architect* (1), 11.

Cheng, Y., and Wang, X. (2021). Pseudo-naturalization: ecological wisdom and approaches for urban lake water environment management - taking Nanjing Xuanwu Lake as an example. *Chin. Gard.* 37 (07), 19–24. doi:10.19775/j.cla.2021.07.0019

Haiming, Lu (2019). *Canals of nanjing through the ages*. Nanjing Press.

Hu, Y. (2017). From royal court pond to modern city park - historical changes of Xuanwu Lake in nanjing. *Guangdong Gard.* 39 (01), 4–8. doi:10.3969/j.issn.1671-2641.2017.01.001

Jiang, S., Ang, C., Yang, H., and Fei, X. (1986). A preliminary study on the paleochannels and the age of sediments in the Qinhuai River, Nanjing. *J. Geol.* (01), 91–103.

Geng, J. (2019). Exploration of the causes of ecological function degradation of Xuanwu Lake under the perspective of historical change of water system. *Urban Constr. Theory Res. Electron. Ed.* 311 (29), 8–9. doi:10.19569/j.cnki.cn119313/tu.201929004

Lu, H. (2019). *Canals of Nanjing through the ages*. Nanjing: Nanjing Press.

Yao, N., and Lv, Y. (2011). *Jiaqing jiangningfu zhi*. Nanjing: Nanjing Press.

Le, S. (2014). *Taiping Huanyu Ji*. Beijing: Zhonghua shuju.

Li, S (2022). *The spatial pattern of Jiankang city in the six dynasties and nanjing city in the ming dynasty and its comparison*. Nanjing: Chongqing University. doi:10.27670/d.cnki.gcqdu.2022.002417

Xu, S. (2020). *Jiangkang Shilu*. Nanjing: Nanjing Press.

Wei, Y. (2012). *Environmental ethics review of Xuanwu Lake development and governance*. Nanjing: Nanjing Forestry University.

Zhen, W. (2010). *Recent affairs of the southern Tang dynasty*. Beijing: The Commercial Press.

Xu, S., and Xu, S. (2011). *What a geographer needs to know*. Beijing: World Knowledge Publishing House–10.

Yanshou, Li (1975). *Nan Shi*. Beijing: Zhonghua shuju.

Zhou, Y. (2008). *Jingding Jiankang zhi*. Nanjing: Nanjing Publishing House.

Jun, Y., and Zhao, S. (2022). *The history of song-river drainage*. Zhejiang: Zhejiang Gongshang University Press.

Wang, Z., and Wang, Y. (2011). *Wanli yingtianfu zhi*. Nanjing: Nanjing Press–06.

frontiers | Frontiers in Environmental Science

TYPE Original Research
PUBLISHED 19 November 2024
DOI 10.3389/fenvs.2024.1500045

OPEN ACCESS

EDITED BY
Salvador García-Ayllón Veintimilla,
Polytechnic University of Cartagena, Spain

REVIEWED BY
Cai Yongli,
Shanghai Jiao Tong University, China
Chen Wanxu,
China University of Geosciences Wuhan, China

*CORRESPONDENCE
Wei Chen,
chenwei19@tju.edu.cn

RECEIVED 22 September 2024
ACCEPTED 01 November 2024
PUBLISHED 19 November 2024

CITATION
Liu J, Chen W, Ding H, Liu Z, Xu M, Singh RP and Liu C (2024) Changing characteristics of land cover, landscape pattern and ecosystem services in the Bohai Rim region of China. *Front. Environ. Sci.* 12:1500045. doi: 10.3389/fenvs.2024.1500045

Changing characteristics of land cover, landscape pattern and ecosystem services in the Bohai Rim region of China

Jiaqi Liu[1,2,3,4], Wei Chen[1,2,3,4]*, Hu Ding[1,2,3,4], Zhanhang Liu[1,2,3,4], Min Xu[5], Ramesh P. Singh[6] and Congqiang Liu[1,2,3,4]

[1]Institute of Surface-Earth System Science, School of Earth System Science, Tianjin University, Tianjin, China, [2]Tianjin Key Laboratory of Earth's Critical Zone Science and Sustainable Development in Bohai Rim, Tianjin University, Tianjin, China, [3]Tianjin Bohai Rim Coastal Earth Critical Zone National Observation and Research Station (Bohai National CZO), Tianjin University, Tianjin, China, [4]Haihe Laboratory of Sustainable Chemical Transformations, Tianjin, China, [5]State Key Laboratory of Remote Sensing Science, Aerospace Information Research Institute, Chinese Academy of Sciences, Beijing, China, [6]School of Life and Environmental Sciences, Schmid College of Science and Technology, Chapman University, Orange, CA, United States

Since the Anthropocene, ecosystems have been continuously deteriorating due to global climate change and human intervention. Exploring the changing characteristics of land use/land cover (LULC), landscape pattern and ecosystem service (ES) and their drivers is crucial for regional ecosystem management and sustainable development. Taking the Bohai Rim region of China as an example, we used the land use transfer matrix, landscape pattern index and InVEST model to analyze the changing characteristics of LULC, landscape pattern and six key ESs [crop production (CP), water yield (WY), carbon storage (CS), soil conservation (SC), habitat quality (HQ), landscape aesthetics (LA)] during 2000–2020. Detailed analysis of the natural and anthropogenic factors affecting the landscape pattern and ES changes has been considered in this study. The results show that the areas of forest, water and impervious land increased, while those of cropland, shrubs, grassland and barren land decreased during 2000–2020. The landscape was fragmented, complex and decentralized during 2000–2015, while the three trends eased during 2015–2020. From 2000 to 2020, CP, WY, and SC capacity show an increasing trend, while CS, HQ, and LA capacity tend to a decline. Natural factors (e.g., precipitation, temperature, altitude) and human factors (e.g., technological progress, policy changes, and LULC forms) are the main factors affecting landscape pattern and ESs. The present study can provide theoretical basis for ecological restoration, ecological product value realization, and land planning in the typical developed urban area.

KEYWORDS

land use/land cover, landscape pattern, ecosystem service, Bohai Rim region, InVEST model

1 Introduction

Land is dynamic, its monitoring provides information about the human impacts on natural ecosystems environment, socio-economics and policies. Land use/Land cover (LULC) change is related to many ecological problems, such as soil erosion, land desertification and biodiversity loss (Zhang et al., 2020). It changes the supply of ecosystem products and services by affecting ecosystem structure and processes (e.g., vegetation cover, carbon sources and sinks), and has become the most important driving force affecting landscape pattern and ecosystem service (ES) (Assesment, 2005). Human estimated that LULC change has affected almost a third (32%) of the global land area in just 6 decades (1960–2019) and the area affected by global LULC change is nearly four times greater than previously thought (Winkler et al., 2021). A finite land area implies that fulfilling sustainable development goals requires increasing land-use efficiency of both storing carbon and producing food (Searchinger et al., 2018). Quantifying the dynamics of LULC change is critical in tackling global societal challenges such as food security, climate change, and biodiversity loss.

Landscape pattern refers to the structural composition and spatial configuration of landscape elements (forests, cropland, cities, etc.) (Wang et al., 2022), which is used to describe how landscape elements are spatially distributed and interconnected (Fu et al., 2022). Landscape pattern is influenced by human activities and climate change, its changes at the regional scale can directly affect energy flow and material circulation of ecosystem (Teutschbein et al., 2018), thus influencing the effects of ESs (Shao et al., 2023). The knowledge of the landscape pattern changes is the basis for comprehensively understanding regional ecological and environment changes, identifying ecological risks (Jiang et al., 2023), and rational planning LULC policies reasonably (van der Plas et al., 2019). Therefore, a comprehensive quantification of global landscape fragmentation is urgently required to guide landscape protection and restoration policies (Ma et al., 2023).

ESs refer to the benefits that humans obtain from ecosystems, typically divided into provisioning, supporting, regulating and cultural services (Assesment, 2005). ESs are considered as a bridge between natural ecosystems and human societies. The strategic planning for ESs could reduce tradeoffs between environmental quality and development (Bai et al., 2018). However, ESs have been continuously degraded since the Anthropocene as a result of global climate change and human intervention (Liu et al., 2024a). The Millennium Ecosystem Assessment (MA) report points out more than 60% of the world's ecosystems are currently or have already degraded (Assesment, 2005). The Intergovernmental Science-Policy Platform on Biodiversity and Ecosystem Services (IPBES) found that 14 of 18 ecosystem components have declined since 1970 (Liu et al., 2022a). Therefore, it is necessary to accurately assess the spatiotemporal distribution of ESs and identify their potential drivers. This is the basis for avoiding the continuous degradation of ESs and the prerequisite for optimizing land use policies and delineating ecological red lines (Jiang et al., 2019; Ouyang et al., 2016).

The study of landscape heterogeneity is the focus of landscape pattern analysis and the landscape pattern indices are usually used to quantitatively evaluate regional landscape patterns, describe the spatial morphology, structure and heterogeneity of regional landscapes (Li et al., 2017). Currently, the research on landscape pattern has expanded to the fields of landscape ecological risk, ecological security pattern, ecological restoration, and has become the core of landscape ecology research. After the discussion of concepts, connotations and classification methods (Costanza et al., 1997; Fisher et al., 2009), the research on ESs has mainly focused on trade-offs and synergies, ecosystem service bundles (ESB). There are two main types of evaluation methods for ESs, namely, the value and the material quality methods. The material quantity method can objectively reflect the formation mechanism of ESs. The evaluation results are objective, stable, highly reliable, and do not change dramatically with the scarcity of ES. In particular, assessments using satellite remote sensing data have the advantages of finer spatial resolution, more comprehensive coverage and better temporal monitoring capabilities compared to traditional administrative unit-scale assessments. They avoid the locality and partiality that may exist in ground surveys and can more effectively identify the spatial distribution and changing patterns of ESs. The InVEST model can evaluate a wide range of ESs and can be combined with multi-source data, which has been widely used globally. However, existing studies on landscape patterns and ESs are mostly single-type studies, lacking systematic studies combining the two. At the same time, most studies are concentrated at a single city scale, with fewer studies at the city cluster scale, and they mostly concentrated in metropolitan areas such as the Yangtze River Delta and the Pearl River Delta, lacking studies on a broader scale of urban agglomerations. In addition, most studies focus on terrestrial ESs, with fewer studies on coastal and offshore ESs (Liu et al., 2020).

The Bohai Rim region is a key area in the Beijing-Tianjin-Hebei coordinated economic development strategy, and is rich in coastal ecological resources, with numerous types of estuarine deltas and coastal wetland reserves. However, it is also an ecologically fragile area. Since the area is a natural semi-enclosed bay surrounded by land on three sides, it has inherent characteristics such as insufficient hydrodynamics and weak water exchange capacity. In recent years, with the dual impact of global climate change and rapid urbanization, a series of ecological and environmental problems have emerged, including increased land pollution emissions, serious industrial and agricultural pollution (Zhao et al., 2021), fragmentation and isolation of coastal key belt landscapes, decreased ecological connectivity (Liu et al., 2020), and a significant reduction in natural wetland area (Wang et al., 2021). At present, it is urgent to conduct in-depth research on the landscape pattern and ESs in the Bohai Rim region.

In this study, we quantitatively assessed six landscape pattern indices and six ESs in the Bohai Rim region based on the analysis of LULC changes from 2000 to 2020 using Fragstats software, InVEST model, statistical data and landscape indicator assessment. Here, we focused to (1) clarify the changing characteristics of LULC, landscape patterns and ESs in the Bohai Rim region, (2) analyze the possible drivers affecting their spatial and temporal distributions, (3) propose detailed ecological management recommendations for different key zones in the Bohai Rim region.

2 Materials and methods

2.1 Study area

The Bohai Rim region is an important industrial and agricultural base in China, with rich agricultural, mineral, oil and gas and tourism resources. This region, centered on Beijing and Tianjin, is an important economic zone in eastern China with a concentrated population and increasingly concentrated industries. With a variety of ecosystems, including estuarine delta wetlands, cropland, breeding ponds, salt flats, forests, coastal mudflats and towns, the Bohai Rim region is an important part of the ecosystems in northern China and provides a wide range of ESs (Ning et al., 2011). With the rapid development of urbanization and industrialization in the Bohai Rim region, coastal development activities have become increasingly frequent, and LULC patterns have changed significantly. In addition, the Bohai Sea is surrounded by land on three sides, and there are problems such as innate hydrodynamic insufficiency and weak exchange capacity of water bodies. Global climate change and human activities have exposed the ecological environment in the Bohai Rim region to multiple risks such as coastal wetland shrinkage, nearshore soil salinization, biodiversity reduction, and water environment deterioration. The Bohai Rim region studied in this article includes 15 coastal cities, including Tianjin, Hebei Province (Qinhuangdao, Tangshan, Cangzhou), Shandong Province (Yantai, Weihai, Dongying, Qingdao, Binzhou, Weifang), and Liaoning Province (Dalian, Yingkou, Panjin, Jinzhou, and Huludao) (Figure 1).

2.2 Data sources and processing

The main data of this study includes two categories: spatial data and statistical data. All spatial data were uniformly converted to the WGS_1984_UTM_50N coordinate system, and specific data information is shown in Table 1. Based on current situation of study area, we reclassified the snow land in the original LULC data into barren land and the wetland into water, which is divided into 7 types: cropland, forest, shrub, grassland, water, barren land, and impervious land. The MOD16A2GF product has a temporal resolution of 8 days, and the MOD13A3 product is monthly NDVI raster data. The two are batch projected by MRT (MODIS Reprojection Tools) software, and the Maximum Value Composites method was used to form the PET and NDVI datasets of each year. DEM data was filled in ArcGIS software. The final assessment results of each ES are at a resolution of 30 m.

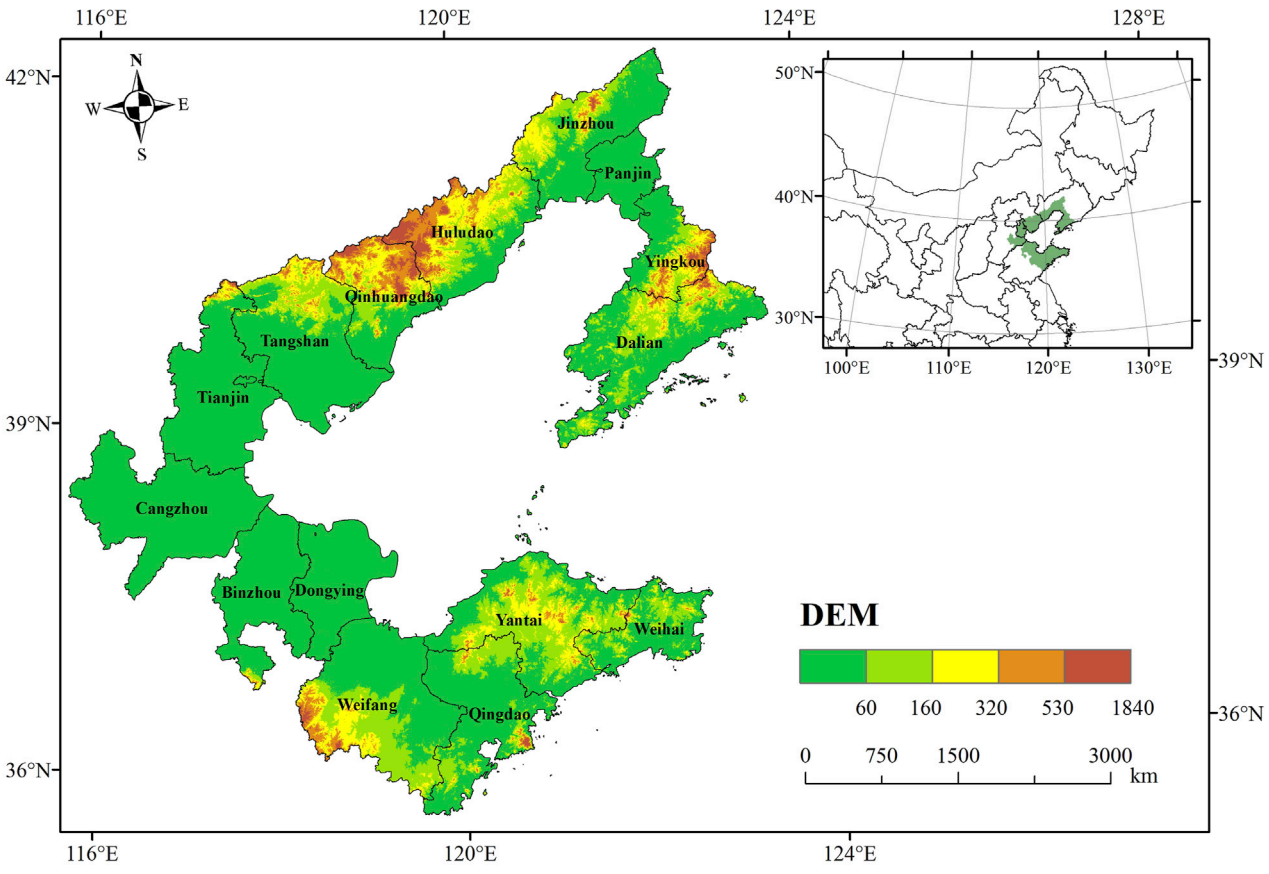

FIGURE 1
Location map of the Bohai Rim Region.

TABLE 1 Data sources and descriptions.

Data types	Application	Format	Data sources	Resolution
LULC	WY, CS, SC, HQ, LA	Raster	CLCD Land Use Dataset (https://zenodo.org/records/5816591#.ZAWM3BVBy5c)	30 m
Average annual rainfall	WY, SC	Raster	National Earth System Science Data Center (https://www.geodata.cn/)	1 km
Potential evapotranspiration	WY	Raster	MODIS Global Land Evapotranspiration Product MOD16A2GF (https://ladsweb.modaps.eosdis.nasa.gov/search/)	500 m
DEM	SC	Raster	Geospatial Data Cloud (https://www.gscloud.cn/)	30 m
Soil data	WY, SC	Raster	World Soil Database (HWSD) (https://www.fao.org/soils-portal/data-hub/soil-maps-and-databases/harmonized-world-soil-database-v12/en/)	1 km
NDVI	CP	Raster	MODIS Normalized Difference Vegetation Index MOD13A3 (https://ladsweb.modaps.eosdis.nasa.gov/search/)	1 km
Root restriction layer depth	WY	Raster	Data of "Bedrock Depth Map of China with a Spatial Resolution of 100 m" (https://doi.org/10.1038/s41597-019-0345-6)	1 km
Administrative boundaries	CP, WY, CS、SC, HQ, LA	Vector	Resources and Environmental Science and Data Center, Chinese Academy of Sciences (https://www.resdc.cn/)	——
Basin boundaries	WY, SC	Vector	HydroBASINS (http://hydrosheds.org/)	——
Road data	HQ	Vector	Peking University School of Urban and Environmental Sciences Geographic Data Platform (http://geodata.pku.edu.cn)	——
Crop production	CP	Statistical data	Statistical Yearbook	——

TABLE 2 Landscape pattern index and its ecological significance.

Indicator name	Indicator type	Meaning of indicators	Application scale
Patch density (PD)	Fragmentation	The number of patches per unit area is an important indicator for describing landscape fragmentation. The larger the PD, the greater the degree of fragmentation	Patch, Landscape
Edge Density (ED)	Complexity	It refers to the edge length between patches of heterogeneous landscape elements per unit area of the overall landscape, which can reflect the complexity of the landscape to a certain extent	Patch, Landscape
Landscape shape index (LSI)	Complexity	It is used to reflect the complexity of the landscape. The larger the LSI value, the greater the complexity of the landscape	Patch, Landscape
Aggregation index (AI)	Aggregation	It indicates the degree of patch agglomeration within a landscape area. The larger the AI value, the greater the degree of aggregation of different types of patches in the landscape	Patch, Landscape
Contagion (CONTAG)	Aggregation	It describes the aggregation degree or extension trend of different patch types in the landscape. The larger the CONTAG value, the greater the aggregation degree of different types of patches in the landscape	Landscape
Shannon Diversity Index (SHDI)	Fragmentation	It reflects the fragmentation of the landscape and is particularly sensitive to the uneven distribution of patch types in the landscape. The higher the degree of fragmentation, the greater the information content of its uncertainty, and the higher the calculated SHDI	Landscape

2.3 Research methods

2.3.1 LULC change analysis

The method of LULC transfer matrix is used to study LULC change, and the application of its results can clearly represent the specific structural characteristics of LULC and the changes of functional types of LULC. The expression is shown in Equation 1:

$$S_{ij} = \begin{bmatrix} S_{\mathrm{ij}} & \cdots & S_{in} \\ \vdots & \ddots & \vdots \\ S_{nj} & \cdots & S_{nn} \end{bmatrix}, \quad (i, j = 1, 2 \ldots, n) \tag{1}$$

In the formula, S represents the area (km^2), S_{ij} represents the area transfer matrix, n represents the LULC type, i and j represent different LULC types during the study period. If i = j represents the area of LULC type that has not changed (Lai et al., 2016).

2.3.2 Landscape pattern index selection

This study selected patch density (PD), edge density (ED), landscape shape index (LSI), aggregation index (AI), contagion (CONTAG), and Shannon's diversity index (SHDI) from two aspects: patch metrics and landscape metrics. They were used to reflect landscape fragmentation, complexity, and aggregation. Detailed information of each index is shown in Table 2. All landscape pattern indices were calculated in Fragstats 4.2 software.

TABLE 3 Overview of ecosystem services assessed in this study.

Level 1 classification	Level 2 classification	Abbreviation	Assessment methods
Provisioning services	Crop production	CP	Statistical Methods
	Water yield	WY	InVEST
Regulating services	Carbon storage	CS	InVEST
	Soil conservation	SC	InVEST
Supporting services	Habitat quality	HQ	InVEST
Cultural services	Landscape aesthetics	LA	Landscape indicator assessment

2.3.3 Ecosystem services assessment

Based on the ES classification system proposed by The Millennium Ecosystem Assessment (MA), and according to the actual situation and research foundation of the Bohai Rim region, six important ESs were selected: crop production (CP), water yield (WY), carbon storage (CS), soil conservation (SC), habitat quality (HQ), and landscape aesthetics (LA) (Table 3).

CP and WY are Provisioning services. In the past 20 years, cropland in the Bohai Rim region has been continuously decreasing, the coastal land has been salinized, and extreme droughts and floods disasters have occurred frequently, which has a great impact on CP. Therefore, evaluating CP and WY is of great significance to ensuring the wellbeing of the people's lives. The coastal wetlands in the Bohai Rim region have been seriously degraded, resulting in a decrease in CS capacity and weakened flood control capacity. Deforestation and inappropriate construction activities have increased the risk of soil erosion and caused the loss of fertile topsoil. Therefore, CS and SC were selected as the research objects of regulating services. The coastal zone around the Bohai Rim region has been seriously eroded and faces multiple ecological risks such as eutrophication and biodiversity degradation. Therefore, HQ was selected as the research object of supporting services. The Bohai Rim region has a wide variety of landforms, covering mountains, plains, estuaries, coasts, islands, wetlands, etc., which is a microcosm of China's landform diversity. Therefore, LA were selected to represent the cultural services of the region.

2.3.3.1 CP

The CP data obtained from the statistical yearbooks of provinces and cities in the Bohai Rim region includes grains, beans, and potatoes, all of which are produced on cropland. Previous studies have shown that there is a significant linear relationship between CP and NDVI, therefore CP is allocated to cropland grids according to the NDVI value (Equation 2).

$$G_i = G_{sum} \times \frac{NDVI_i}{NDVI_{sum}} \tag{2}$$

In the formula: G_i is the crop production in the i-grid (kg); G_{sum} is the total crop production in the study area (kg); $NDVI_i$ is the normalized vegetation index of the i-grid; $NDVI_{sum}$ is the sum of NDVI values for cropland in the study area.

2.3.3.2 WY

WY affects human production and life in various ways. This study uses the Annual Water Yield module in the InVEST model to estimate WY services, the specific model parameters are presented in the Supplementary Table S1. This module is based on the principle of water balance and uses the difference between regional rainfall and evapotranspiration to determine WY (Equation 3) (Hu et al., 2019).

$$Y(x) = P(x)\text{-}AET(x) = \left(1\text{-}\frac{AET(x)}{P(x)}\right) \times P(x) \tag{3}$$

In the formula: Y(x) is the annual water yield of regional unit x (mm), P(x) and AET(x) are the annual rainfall and actual evapotranspiration of grid x (mm), respectively.

2.3.3.3 CS

The widely distributed wetland ecosystems in the Bohai Rim region are particularly important carbon sinks that can store a large amount of organic carbon. The Carbon Storage module of the InVEST has been widely used to evaluate CS. It divides the CS of each LULC type into four basic carbon pools: aboveground biomass carbon (C_{above}), belowground biomass carbon (C_{below}), soil organic carbon (C_{soil}), dead organic matter carbon (C_{dead}) (Zhu et al., 2020), The calculation formula is as follows (Equations 4, 5):

$$C_i = C_{i\text{-}above} + C_{i\text{-}below} + C_{i\text{-}soil} + C_{i\text{-}dead} \tag{4}$$

$$C_{tot} = \sum_{i=1}^{n} C_i \times S_i \tag{5}$$

In the formula: i represents a certain LULC type; $C_{i\text{-}above}$ is the aboveground biomass carbon density (t/km^2) of LULC type i; $C_{i\text{-}below}$ is the underground biomass carbon density (t/km^2) of LULC type i; $C_{i\text{-}soil}$ is the soil carbon density (t/km^2) of LULC type i; $C_{i\text{-}dead}$ is the dead organic carbon density (t/km^2) of LULC type i; C_{tot} is the total carbon storage(t) of the ecosystem, S_i is the area (km^2) of LULC type i, n is the number of LULC types, which is 7 in this study. Carbon density data was obtained by consulting relevant literature (Li et al., 2020; Xia et al., 2023a; Zhu et al., 2022) (Supplementary Table S2).

2.3.3.4 SC

The InVEST model Sediment Delivery Ratio module (SDR) was used to simulate and evaluate SC. This module is a spatial display model for raster calculation. Based on the modified general soil loss equation, it uses LULC data, DEM data, soil property data,

TABLE 4 Area of LULC types in the Bohai Rim Area (km²).

LULC types	2000	2005	2010	2015	2020
Cropland	102,143.46	100,083.76	97,087.70	94,048.48	92,258.73
Forest	16,965.44	16,742.20	17,205.35	17,842.78	17,731.20
Shrub	1.14	0.59	0.64	1.96	1.18
Grassland	3,993.77	3,657.58	3,426.04	3,043.73	2684.97
Water	5,238.98	5,990.00	6,005.28	5,959.92	6,150.36
Barren	2,227.22	2,059.85	1,796.64	1,396.36	320.19
Impervious	21,400.04	23,436.06	26,448.39	29,676.83	32,823.41
Total	151,970.05	151,970.05	151,970.05	151,970.05	151,970.05

precipitation data, vegetation cover factors, soil and water conservation measures factors to calculate the annual soil erosion and sediment transport rate of the grid, and then simulates the raster soil erosion and sediment transport process (Liu et al., 2023), The calculation formula is as follows (Equations 6–8):

$$S_x = RKLS_x\text{-}USLE_x \quad (6)$$

$$RKLS_x = R_x \times K_x \times L_n \times S_x \quad (7)$$

$$USLE_x = R_x \times K_x \times L_n \times S_x \times C_x \times P_x \quad (8)$$

In the formula: S_x is the SC capacity(t); $RKLS_x$ is the potential soil erosion capacity(t); $USLE_x$ is the actual soil erosion capacity(t); R_x is the precipitation erosion rate; L_n is the slope length gradient factor; S_x is the slope gradient factor; K_x is the soil erodibility factor. Among them, R_x factor is calculated based on the R value calculation model established by Zhang Wenbo (Zhang and Fu, 2003) and the annual average precipitation. K_x factor is calculated using the soil erodibility K value calculation model established by Wischmeier (Wischmeier et al., 1971) combined with soil data. C_x、 P_x values are determined with reference to the InVEST Chinese manual and relevant literature (Liu et al., 2024b) (Supplementary Table S3).

2.3.3.5 HQ

The maintenance of biodiversity is closely related to HQ. Use the Habitat Quality module of the InVEST to evaluate the HQ index, with a range of values from 0 to 1. The larger the value, the higher the HQ. The formula is as follows (Equation 9):

$$Q_{xj} = H_j\left(1\text{-}\frac{D_{xj}^z}{D_{xj}^z + k^z}\right) \quad (9)$$

In the formula, Q_{xj} is the habitat quality of grid x in LULC type j; H_j is the habitat suitability of LULC type j; D_{xj} is the habitat stress level of grid x in LULC type j, k is a semi saturation constant; z is a normalized constant. This study determined the parameters based on relevant literature (Deng et al., 2018) (Supplementary Tables S4, S5).

2.3.3.6 LA

LA refers to the benefits and comfort that individuals gain from interacting with visually pleasing natural landscapes, and is an intangible cultural service (Langemeyer et al., 2018). The evaluation of LA is often based on two criteria: naturalness and landscape diversity. Naturalness refers to the degree of human interference, while landscape diversity reflects the diversity of landscape structure (Frank et al., 2013). Naturalness is quantified using the chlorophyll index from 1 (natural) to 7 (artificial) (Xia et al., 2023b). Landscape diversity was quantified using the Shannon's diversity index (SHDI) in Fragstats 4.2 software. The final LA index was obtained by adding the normalized values of naturalness and landscape diversity (Equation 10).

$$LA_i = (NT_i + LD_i)/2 \quad (10)$$

In the formula: LA_i is the landscape aesthetics value of the i grid; NT_i is the normalized naturalness value of the i grid; LD_i is the normalized SHDI value of the i grid. All three indicators are standardized to 1–100.

3 Results

3.1 LULC distribution characteristics

The LULC types in the Bohai Rim region are mainly cropland land, impervious land and forest, among which cropland accounts for the largest proportion, exceeding 60% at all stages of the study period. Impervious land and forest account for more than 14% and 11%. Shrubs account for the smallest proportion, with an average area of only 1.1 km² over 20 years (Table 4).

From the perspective of the spatial distribution (Figure 2), cropland is widely distributed, covering most of the Bohai Rim region; forest is mainly distributed in the north and northwest, shrubs and grasslands are mainly distributed in the northwest of the study area and the northern area of Shandong Peninsula; water is mainly distributed on the edge of the Bohai Bay; barren land is mainly distributed in the edge of Laizhou Bay and Bohai Bay, as well as the Yellow River Delta; impervious land are mainly distributed in the marginal areas of the coast and the city centers.

From the perspective of the temporal distribution, the proportions of forest, water and impervious land have expanded from 11.16%, 3.45%, 14.08% in 2000 to 11.67%, 4.05%, 21.60% in 2020; while the area proportions of cropland, grassland and barren land decreased from 67.21%, 2.63%, 1.47%–60.71%, 1.77% and 0.21%. From 2000 to 2020,

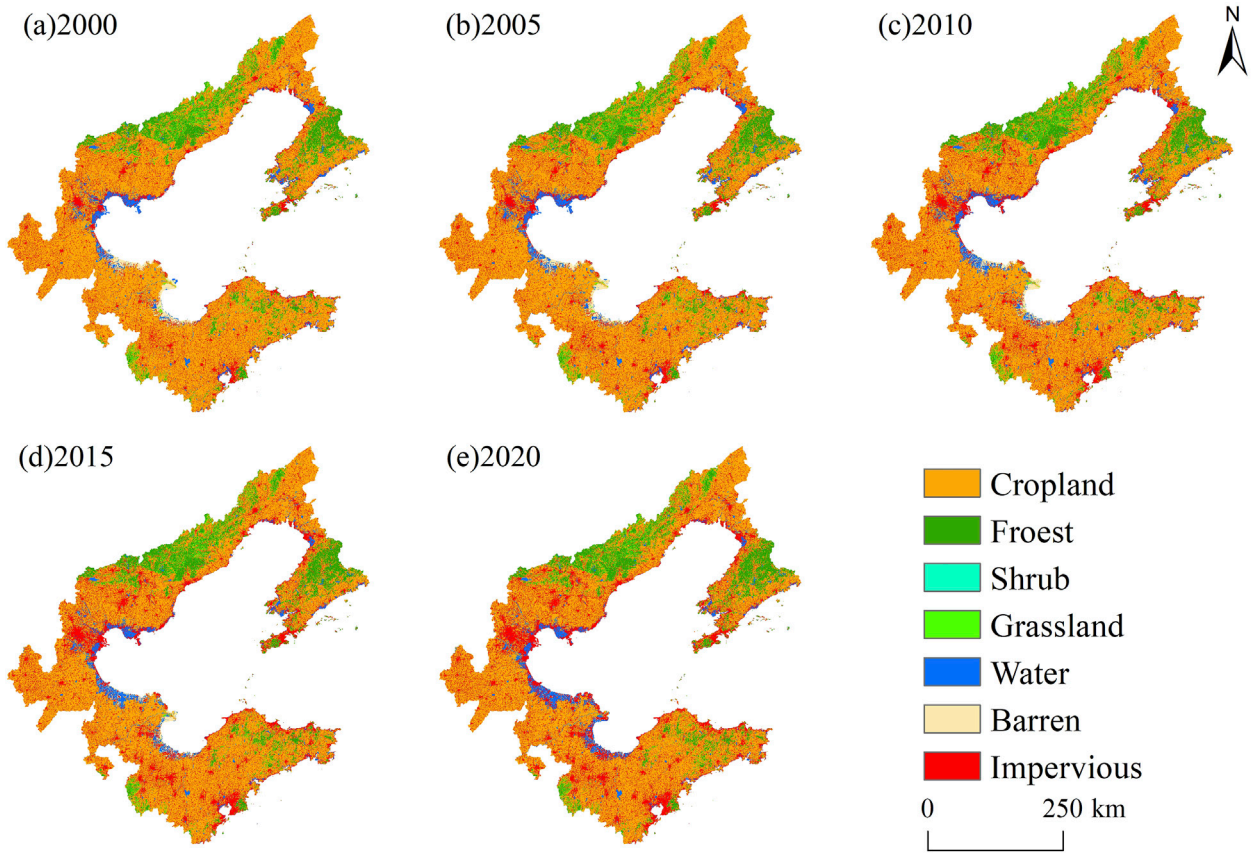

FIGURE 2
LULC change map of the Bohai Rim region.

TABLE 5 LULC change transfer matrix during 2000-2020 (km²).

2000/2020	Cropland	Forest	Shrub	Grassland	Water	Barren	Impervious	Initial area
Cropland	89,301.68	1,490.55	0.00	541.89	1,360.23	24.21	9,424.89	102,143.46
Forest	1,322.72	15,409.10	0.69	79.13	1.92	0.14	151.74	16,965.44
Shrub	0.02	0.23	0.20	0.68	0.00	0.00	0.00	1.14
Grassland	882.84	826.52	0.28	2,060.70	36.42	18.89	168.11	3,993.77
Water	509.56	4.30	0.00	0.62	3,126.99	28.52	1,568.98	5,238.98
Barren	113.10	0.01	0.00	1.70	1,002.22	239.17	871.02	2,227.22
Impervious	128.80	0.50	0.00	0.25	622.57	9.26	20,638.67	21,400.04
Final area	92,258.73	17,731.20	1.18	2,684.97	6,150.36	320.19	32,823.41	151,970.05

the area of forest and shrub showed a trend of first decreasing and then expanding. This study further calculated the LULC transfer matrix (Table 5) and drew the LULC transfer Sankey diagram (Figure 3). During the study period, 12,841.78 km² of cropland was transferred out and 2,957.05 km² was transferred in, mainly transforming into impervious land, forest and water; 761.37 km² of impervious land was transferred out and 12,184.74 km² was transferred in, mainly from cropland and water. 1,556.34 km² of forest was transferred out and 2,322.11 km² was transferred in, mainly from cropland and water; 2,111.99 km² of water was transferred out and 3,023.37 km² were transferred in, mainly from cropland and barren land. Overall, the LULC types in the Bohai Rim region changed drastically, mainly among cropland, impervious land, forest, and water.

3.2 Landscape pattern index characteristics

At the landscape metrics (Figure 4), PD and SHDI both increased from 2000 to 2015 and decreased from 2015 to 2020,

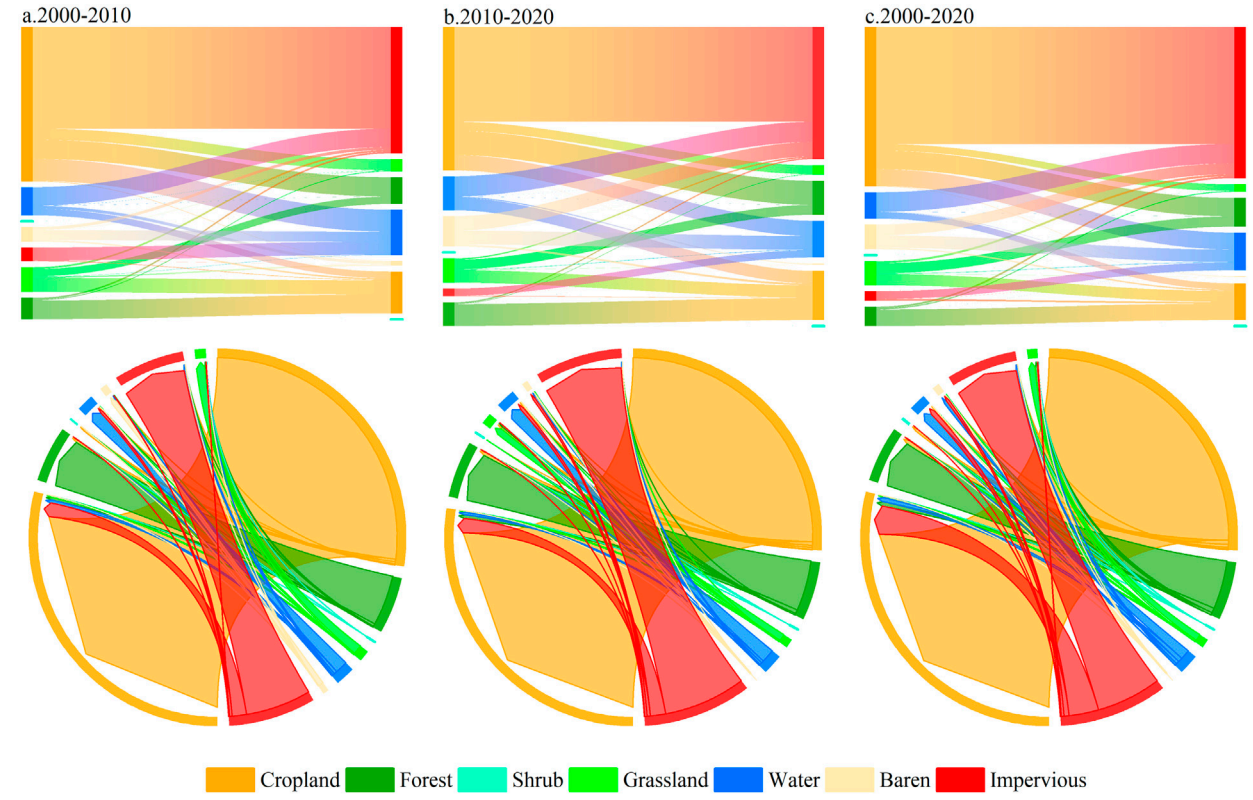

FIGURE 3
Sankey diagram of LULC changes in the Bohai Rim region.

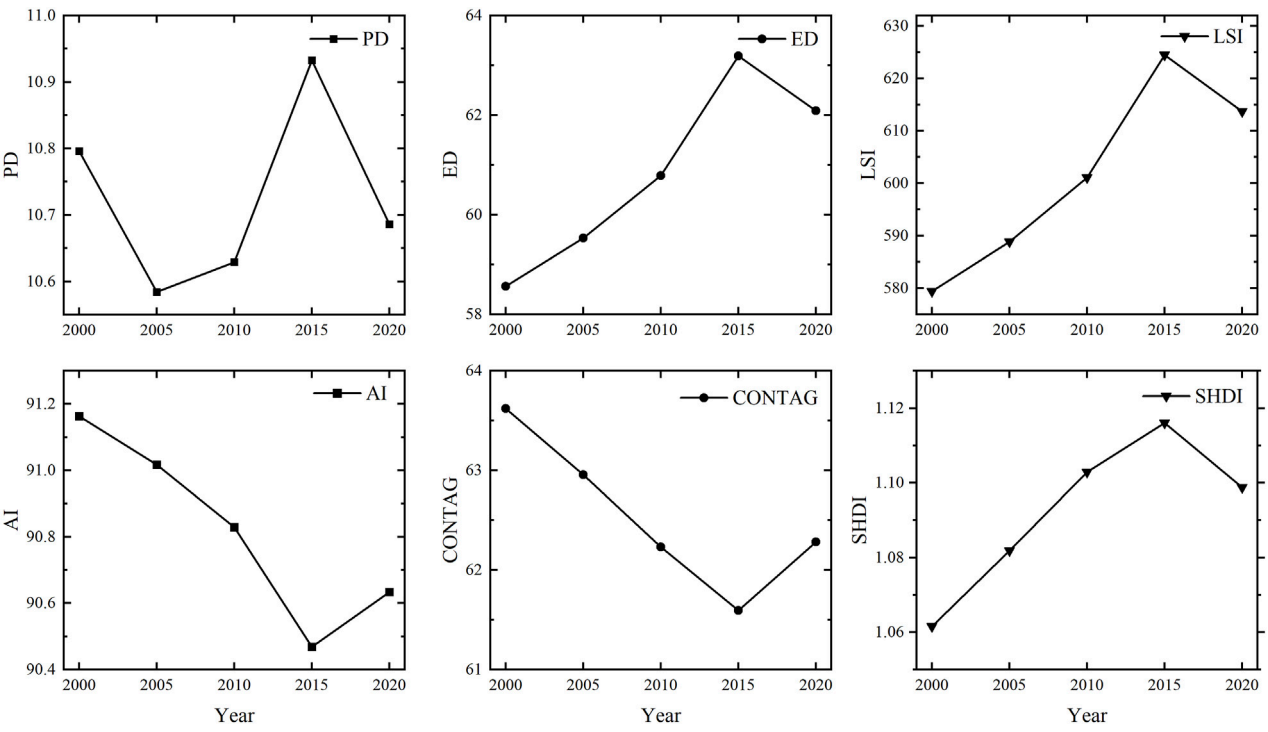

FIGURE 4
Landscape pattern index changes at the landscape level in the Bohai Rim region.

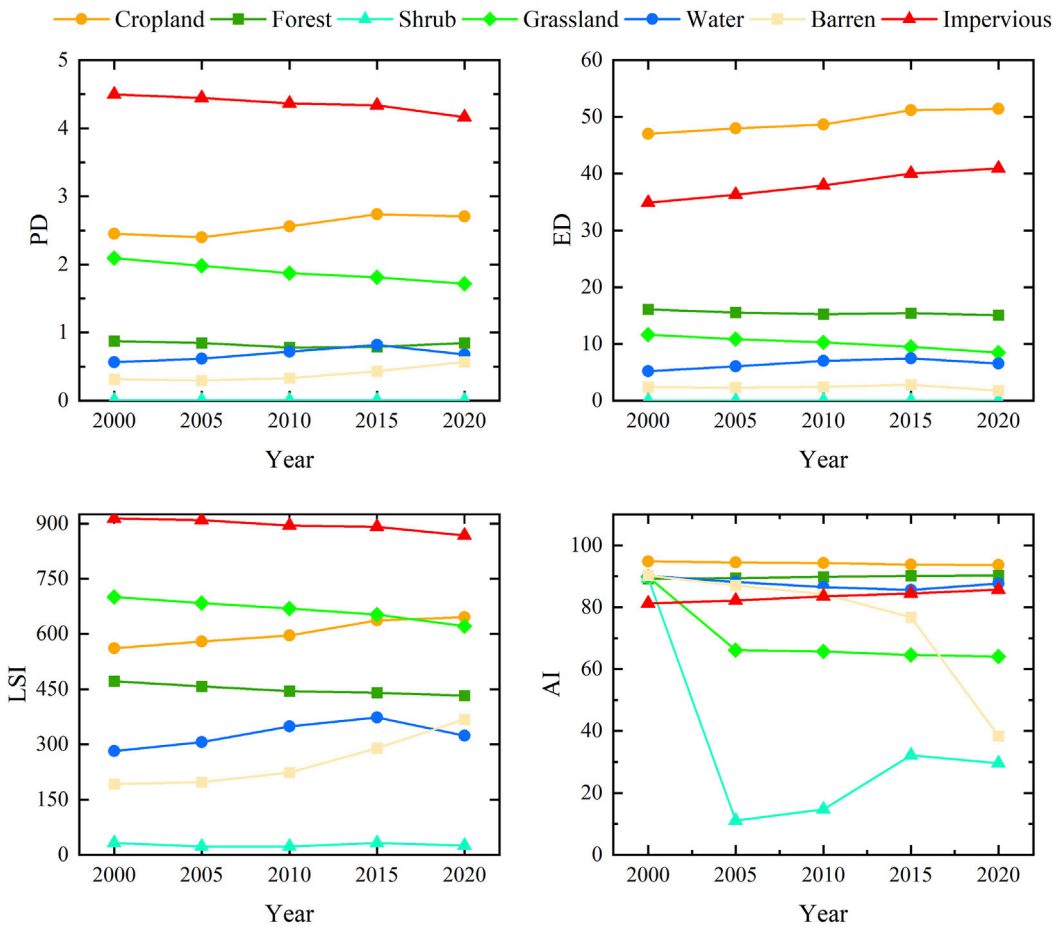

FIGURE 5
Landscape pattern index changes at the patch level in the Bohai Rim region.

indicating that the degree of regional landscape fragmentation first increased and then decreased. ED and LSI increased rapidly from 2000 to 2015 and decreased from 2015 to 2020, indicating that the landscape shape first became complex and then tended to be simplified. AI and CONTAG both decreased significantly from 2000 to 2015 and increased from 2015 to 2020, indicating that the connectivity between landscape patches weakened and the separation increased in the early stage, which was alleviated in the later stage.

At the patch metrics (Figure 5), PD, ED and LSI of cropland increased, while AI decreased, indicating that cropland landscape has an obvious trend of fragmentation, complexity and dispersion. PD of forest decreased from 2000 to 2010 and increased from 2010 to 2020, its ED and LSI continued to decrease, and AI continued to increase, indicating that the degree of fragmentation in forest first decreased and then increased, with a process of simplified shape and aggregation of patches. Shrubs have fewer patches, are easily affected by external conditions, and change erratically. PD, ED, LSI and AI of grassland continued to decrease. PD, ED and LSI of water increased from 2000 to 2015, then decreased slightly from 2015 to 2020, but were still higher than the level of 2000; its AI decreased during 2000–2015 and increased significantly from 2015 to 2020. PD and LSI of barren land increased, AI decreased, ED increased during 2000–2015 and decreased to a level lower than that in 2000 during 2015–2020. PD and LSI of the impervious land continued to decrease, while ED and AI continued to increase.

3.3 Distribution characteristics of ESs

3.3.1 Provisioning services

3.3.1.1 CP

In general, CP shows an increasing trend from 2000 to 2020 (Figure 6A). The total crop production in 2000, 2005, 2010, 2015 and 2020 was 2365.12wt, 2802.27wt, 3,265.03wt, 3,049.83wt, 3,139.67wt, and the yield per unit area was 1,526.20 kg/hm^2, 1808.29 kg/hm^2, 2106.91 kg/hm^2, 1968.04 kg/hm^2, 2026.01 kg/hm^2 respectively. CP continued to increase from 2000 to 2010, increasing by 38% in 2010 compared with 2000, and decreased slightly from 2010 to 2020.

3.3.1.2 WY

WY has generally shown an increasing trend (Figure 6B). The total water yield in 2000, 2005, 2010, 2015 and 2020 was 10.07 billion m^3, 23.56 billion m^3, 25.73 billion m^3, 12.86 billion m^3

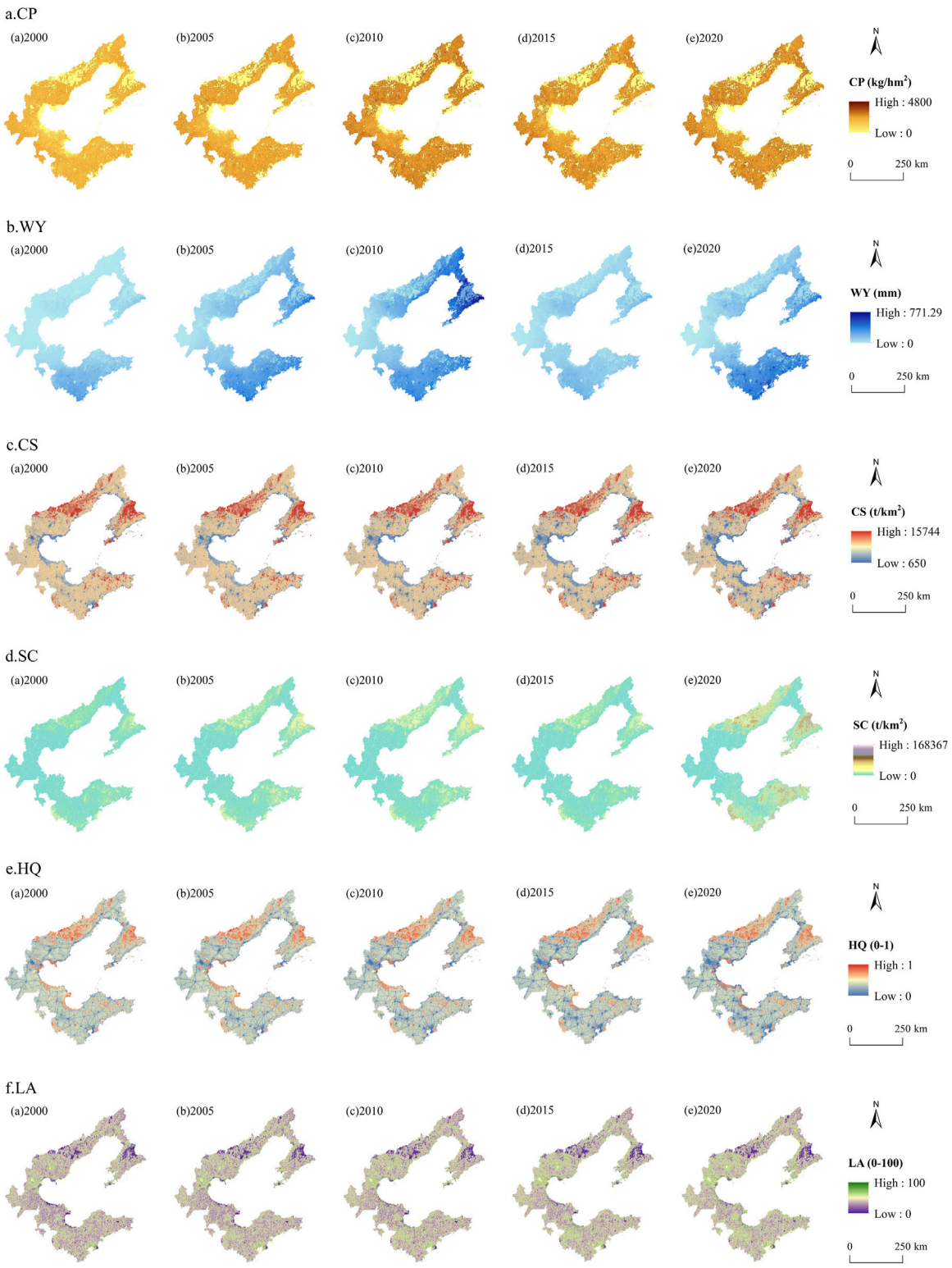

FIGURE 6
Spatial distribution of ecosystem services in the Bohai Rim region of China during 2000–2020.

and 26.35 billion m^3. In 2015, WY decreased by 12.863 billion m^3 compared with 2010. The spatial distribution of WY in the Bohai Rim region is high in the north and south and low in the center. The high-value areas are mainly distributed in the Shandong Peninsula, the coast of Liaodong Bay and the Liaodong Peninsula, while the low-value areas are mainly distributed in Tianjin, Cangzhou, the northern part of Qinhuangdao and Huludao, and the central and northern part of Dalian.

3.3.2 Regulating services

3.3.2.1 CS

From a temporal perspective, carbon storage shows a decreasing trend (Figure 6C). The total carbon storage in 2000, 2005, 2010, 2015 and 2020 was 134.87 × 10^7t, 132.50 × 10^7t, 130.20 × 10^7t, 127.96 × 10^7t, 125.51 × 10^7t. In the past 20 years, 9.37 × 10^7t carbon has been lost, with soil carbon storage losing the most, at 9.10 × 10^7t. Aboveground biomass carbon storage has increased by 0.03 × 10^7t over the past 20 years, which is due to the fact that the aboveground biomass carbon density of forest is large, and the forest area increased between 2000 and 2020. From a spatial perspective, CS distribution pattern in the Bohai Rim region was relatively consistent from 2000 to 2020, with no obvious spatial changes. Areas with higher CS are mainly distributed in the northern mountainous areas of Qinhuangdao and Huludao, as well as the central and northern areas of Dalian, with the highest value of 15,744 t/km^2. The LULC types in these areas are mainly forest, shrubs and grassland. The areas with lower CS are mainly distributed in the Bohai Bay, Laizhou Bay, Liaodong Bay coast and the central areas of various provinces and cities. The LULC types in these areas are mainly water and impervious land, with the lowest value of 650 t/km^2.

3.3.2.2 SC

(2) SC: From a temporal perspective, soil conservation generally showed an increasing trend (Figure 6D). The SC level in 2000, 2005, 2010, 2015 and 2020 were 3,579.86 t/km^2, 5,853.93 t/km^2, 6,463.65 t/km^2, 4,236.31 t/km^2 and 7,071.22 t/km^2. In 2015, SC significantly decreased, with a decrease of 33,848.90wt compared to 2010. From a spatial perspective, SC was generally low but locally high. Liaoning Province has the strongest SC capacity at 8,302.31 t/km^2, which is 1.53 times the average value of the Bohai Rim region. Yingkou has the highest average SC capacity at 13,866.25 t/km^2. Tianjin has the lowest SC capacity, which is 1,363.94 t/km^2, only 25% of the average value.

3.3.3 Supporting services

3.3.3.1 HQ

From a temporal perspective, HQ index has been declining (Figure 6E). The average HQ index in the study area in 2000, 2005, 2010, 2015 and 2020 was 0.39, 0.38, 0.37, 0.36 and 0.35. In the past 20 years, the HQ index has decreased by 10.26%, indicating that the overall HQ of the ecosystem in the Bohai Rim region has been deteriorating. From a spatial perspective, the HQ in the Bohai Rim region has significant spatial heterogeneity, with high values mainly distributed in Qinhuangdao, Dalian, Yingkou, Huludao, Bohai Bay and the coast of Laizhou Bay. Low values are mainly distributed in Qingdao, Tianjin, Cangzhou and Weifang. These areas have large populations, high human activity intensity, large demand for infrastructure construction, and rapid economic development, which drives the gradual expansion of non-habitat areas.

3.3.4 Cultural services

3.3.4.1 LA

From a temporal perspective, LA index in the Bohai Rim region has been continuously increasing (Figure 6F). The average LA index of the study area in 2000, 2005, 2010, 2015, and 2020 were 40.07, 40.81, 41.70, 42.70, and 43.56. From 2000 to 2020, the LA index increased by 8.71%, indicating that the quality of LA has continued to deteriorate. From a spatial perspective, Yingkou, Qinhuangdao, and Huludao have the lowest LA values, indicating that residents can gain more benefits and comfort from the interaction with the natural landscape in these areas. The higher cultural services in these areas can help realize the value of cultural ecological products, such as developing ecotourism, promoting cultural tourism consumption and creating characteristic tourism brands. Tianjin, Tangshan and Qingdao have the highest LA values. This means that the natural landscapes in these areas provide residents with lower spiritual comfort, which is not conducive to the realization of ecological product value and regional sustainable development.

4 Discussion

4.1 InVEST model results accuracy verification

The verification of the WY is based on the data from the Water Resources Bulletin. The actual water resources in the study area in 2000, 2005, 2010, 2015, and 2020 were 10.423 billion m^3, 23.135 billion m^3, 23.267 billion m^3, 14.07 billion m^3 and 23.54 billion m^3 respectively. The error between the model simulation results and the actual water resources is controlled at around 10%, so the results are reliable.

The carbon density data of CS were considered in accordance with the following principles: the four basic carbon pool data were considered from published data obtained from field investigations. The missing data were used from neighboring regions. This approach and criteria ensured the credibility of the results to the greatest extent.

The assessment results obtained from the SC module were verified with reference to relevant research (Feng et al., 2022; Wang et al., 2022). Since the Bohai Rim region spans multiple watershed divisions, the results are also within the overall range. Therefore, it has a reasonable value.

The evaluation results of the HQ by province are basically consistent with the findings of Tianjin (Li et al., 2022b) and Dongying (Ding et al., 2021), with a difference of about 10%. In addition, the HQ change rate of Dongying from 2000 to 2020 is found to be consistent with the trends in the Yellow River Delta (Liu et al., 2022b), with a change rate of about 15.8%, this provides a good confidence.

4.2 Analysis of factors influencing landscape pattern and ESs

4.2.1 Analysis of factors influencing landscape patterns

In general, before 2015, landscape fragmentation increased, and the patch shapes tended to be complex and dispersed. This situation improved after 2015. The reasons for the landscape fragmentation, complexity, and dispersion from 2000 to 2015 include two aspects. First, intense human activities such

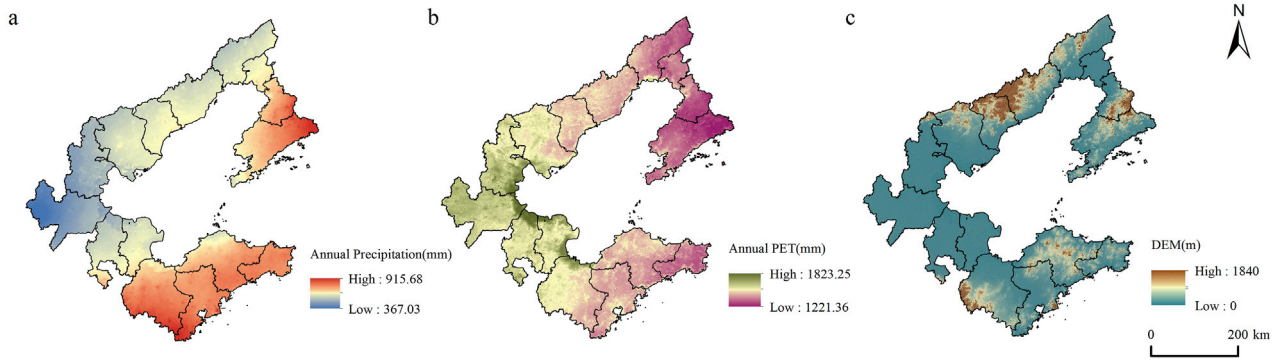

FIGURE 7
Schematic diagram of natural environment in the Bohai Rim region of China.

as cropland occupation, urban construction, and rail transit construction divided the originally coherent natural patches into discrete small patches. Second, returning cropland to forests and lakes, various reclamation activities have led to a significant transformation in LULC patterns, exacerbating the degree of regional landscape fragmentation, complexity and decentralization. In 2015, China issued the "Opinions on Accelerating the Construction of Ecological Civilization", to increase the forest, grassland and wetland coverage rate by 2020. The "National Land Planning Outline (2016–2030)" and the "National Agricultural Sustainable Development Plan (2015–2030)" followed strategies at the same time, both requiring strict ecological protection system. The fragmented patches cropland areas have been integrated; the main landscape types are considered as a large area. Highly urbanized areas continued to expand, and small built-up areas are integrated with large landscapes, making the landscape homogenized. The degree of patch aggregation was high, and the fragmentation and complexity of the landscape were alleviated.

The continuous policy of returning cropland to forest and the occupation of cropland have increased the fragmentation and complexity of the cropland landscape and reduced its aggregation. The policy of returning cropland to forest requires converting eligible sloping cropland with a degree of 25 or above into forests and grasslands, which has formed a larger area of fragmented forest in the later period (Hao et al., 2017), making the degree of forest fragmentation increased during 2010–2020. It can be seen from the LULC transfer matrix that the area of grassland transferred out is larger than the area transferred in, and the fragmented patches are converted into cropland and forest, which are integrated with the larger landscape. Therefore, the degree of landscape fragmentation of grassland continues to decrease, and patches become more simplified and dispersed. From 2000 to 2015, various human activities such as land reclamation, aquaculture, and reservoir construction, as well as the policy of returning cropland to lakes, have made the regional water landscape fragmented, complex, and decentralized. In 2015, China further increased its support for wetland protection, and the central government allocated $223.2 million in wetland subsidies, covering wetland protection and restoration, returning cropland to wetlands, and ecological compensation. With the new relevant policies, the area and quantity of wetlands increased significantly from 2015 to 2020, expanding the connectivity between wetlands and making their shapes simpler. As a result, the fragmentation, complexity, and dispersion of water landscape patches were reduced. The area of barren land decreased while the impervious land expands year by year. Therefore, the landscape pattern of the two is opposite. In the process of barren land converting into impervious land, although the landscape pattern is fragmented, complex, and dispersed. The expansion of the impervious land increases the uniformity of its patches, reducing the degree of fragmentation and the complexity of the landscape, increasing the aggregation of patches.

4.2.2 Analysis of factors influencing ESs

The natural factors, precipitation, temperature and altitude are the main factors affecting ESs (Figure 7). In 2015, the average precipitation in the study area was only 562 mm, about 83% of that in 2010 (Figure 8), resulting in a decrease of 215.2wt in CP in 2015 compared with 2010, a decline of about 6.6%; WY decreased by 12.862 billion m^3 compared with 2010, a decline of about 50%; the decline in precipitation directly changed the precipitation runoff erosion rate (Zhang et al., 2022), that contributed decline of 2,227.34 t/km^2 in SC intensity in the Bohai Rim region, which is consistent with the Luan River Basin (Liu et al., 2023). The temperature mainly affects ESs through its influence on regional evapotranspiration. In 2015, the average temperature in the study area was 12.51°C, which was 0.81°C higher than in 2010 (Figure 8). This increased the potential evaporation of vegetation and significantly reduced the WY. The northern parts of Dalian and Huludao, the southern part of Yingkou in Liaoning Province are located at higher altitudes, with less urbanization and human activities. Vegetation coverage, soil thickness and biodiversity all increase with altitude, and the SC capacity is the strongest. Similarly, Yantai and the southwestern part of Weifang in Shandong Province are at higher altitudes, coupled with higher annual precipitation throughout the province, so the SC capacity is relatively strong. However, most areas of Hebei province and Tianjin are at a low altitude, with low vegetation coverage, few artificial protection

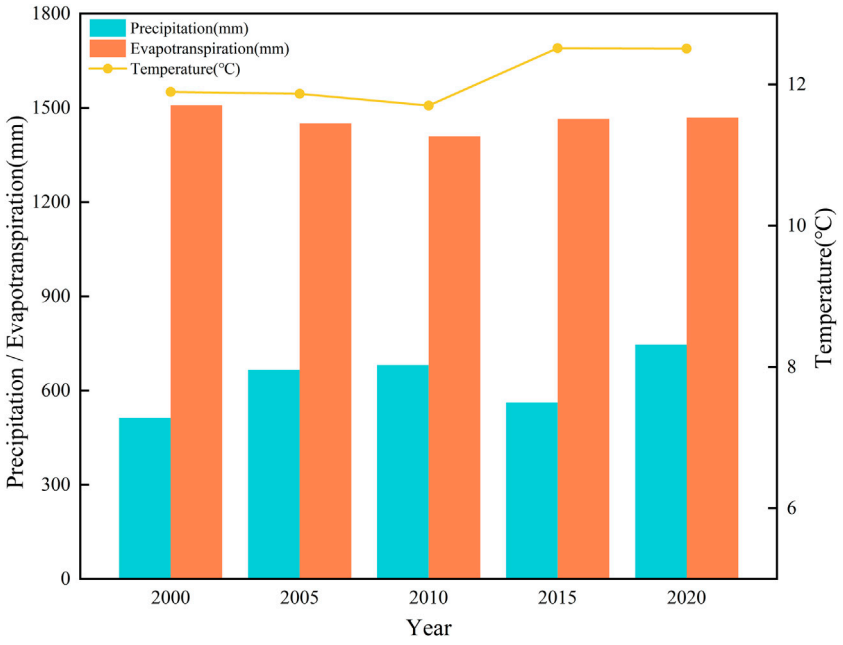

FIGURE 8
Changes in average temperature, precipitation and evapotranspiration in the Bohai Rim region during 2000–2020.

measures, and high intensity of urban construction, resulting in low SC function.

The human factors such as, development of technology, policy changes and LULC patterns are the main factors affecting ESs. From 2000 to 2010, crop varieties and planting technologies developed rapidly, and CP increased rapidly. In 2020, the Bohai Rim region faced multiple threats such as severe floods and COVID-19 epidemic, and the total CP declined. However, the government increased its support for crop production, implemented various policies to support agriculture and benefit farmers, actively responded to epidemics and disasters. So the impact of agricultural disasters on CP was limited. The LULC form is an important factor affecting regional ESs. Shandong Province is in the eastern coastal area and the middle and lower reaches of the Yellow River. It has superior geographical conditions and rich natural resources, with a small proportion of mountains, a vast area of cropland, and the CP level is high. Hebei and Liaoning provinces have widespread forest distribution and a large proportion of aquaculture. The effective cropland planting area is relatively small, and the degree of nearshore soil salinization is serious, resulting in low regional CP. Different LULC have different supply capacities for ESs due to differences in vegetation coverage, vegetation canopy height, canopy interception, soil moisture content, evapotranspiration capacity, and litter water holding capacity. The vegetation coverage of cropland and impervious land is low, the soil has a weak ability to absorb water, making it easy to form runoff (Guo et al., 2023), so the WY is relatively high. At the same time, these areas are either typical areas of urban expansion or key areas for agricultural planting. Urban construction and human activities have caused serious damage to HQ and LA. Due to the lack of artificial protection measures, SC and CS are also relatively low. Forests, shrubs and grasslands, due to their strong interception effect on precipitation and high evapotranspiration coefficients, are not conducive to water retention and have low WY level. However, due to its high vegetation coverage and less interference from human activities, the corresponding soil texture is less erodible, resulting in higher SC, HQ, and LA level.

4.3 Typical area analysis

The Bohai Rim region is vast, and due to differences in natural resource endowments and socio-economic factors among administrative, various ESs are highly heterogeneous and dynamic. For example, when comparing Qinhuangdao and Tianjin, the dominant ESs in Tianjin are provisioning services, while those in Qinhuangdao are regulating, supporting and cultural services (Table 6). The average CP in Qinhuangdao in the past 20 years is 80.28wt, accounting for 2.74% of the total area. While Tianjin has a greater advantage in CP, with an average of 166.95wt, accounting for 5.71%, about twice that of Qinhuangdao. However, the regulating service of Qinhuangdao is much higher than that of Tianjin, especially SC. The area of Tianjin is about 11,966.45 km^2 and the SC is 1632.15wt, while the area of Qinhuangdao is about 7750 km^2 and the SC is 7407.67wt, about 4.5 times those of Tianjin. In the past 20 years, the supporting and cultural service of Qinhuangdao have been much higher than the average level of the Bohai Rim region, while Tianjin is lower than it (Figure 9).

In the past 20 years, CP in Tianjin has continued to improve (Table 7). Compared with Qinhuangdao, the growth trend in Tianjin is stable, indicating that it has a stronger ability to resist natural risks and human interference, and is a key area for CP. WY

TABLE 6 Comparison of ESs between Tianjin and Qinhuangdao during 2000-2020.

ES	Tianjin		Qinhuangdao	
	Total	Proportion	Total	Proportion
CP	834.78 (wt)	5.71%	401.34 (wt)	2.74%
WY	2.51 (billion m^3)	2.55%	3.06 (billion m^3)	3.10%
CS	7,870.44 (wt)	6.04%	8,299.72 (wt)	6.37%
SC	1632.15 (wt)	1.87%	7407.67 (wt)	8.50%
HY	0.312	—	0.496	—
LA	47	—	36.09	—

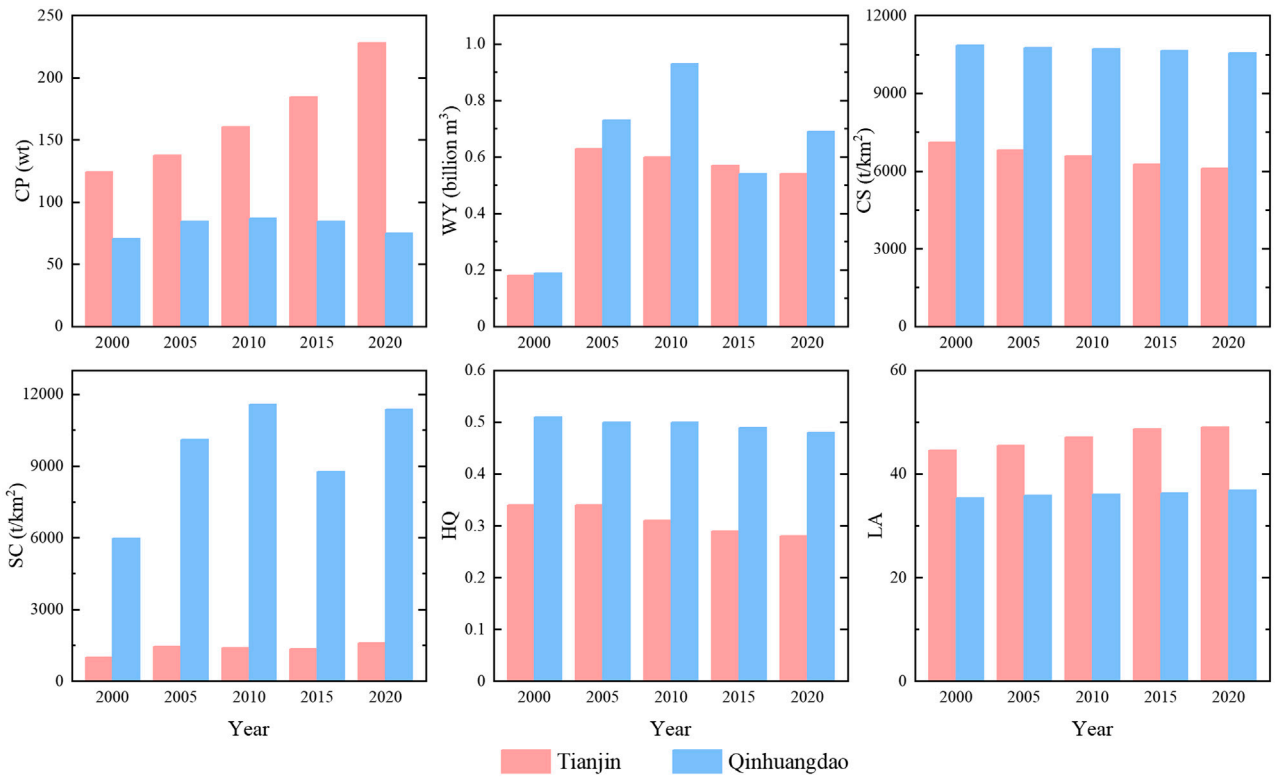

FIGURE 9
Schematic diagram of the comparison of ESs between Tianjin and Qinhuangdao.

in Tianjin has continued to decline since it increased to a maximum of 0.63 billion m^3 in 2005, while the overall precipitation has not changed much from 2005 to 2020. It indicates that the WY in Tianjin is highly related to human activities. Although the amount of WY increased due to the dramatic expansion of impervious land, this high value has been offset by the reduction in cropland with similarly high WY capacity. At the same time, with the implementation of policy documents such as returning cropland to the lake, "Tianjin Land Use Master Plan (2006–2020)," "Tianjin Wetland Protection Ordinance," "Tianjin Wetland Nature Reserve Plan (2017–2025)," Tianjin has established an eco-friendly land use pattern that coordinates rivers, beaches, bays, lakes and seas. The internal structure and spatial layout of ecological construction and wetland protection land have been optimized, and many artificial wetlands have been integrated to form a wetland ecological network with higher connectivity and better aggregation, making WY in Tianjin more balanced and reducing the risk of floods caused by urban construction.

Qinhuangdao has distinct regional characteristic and is a famous coastal touristic area, leisure and holiday resort in China. Tourism and port logistics are its traditional advantageous industries. Qinhuangdao has outstanding capabilities in regulating, supporting and cultural services, with CS, SC, HQ, and LA all at a leading level in the Bohai Rim region (Table 8). This is mainly due to the warm temperate semi-humid continental monsoon climate in this region, which is greatly

TABLE 7 Tianjin ecosystem services.

ES	2000	2005	2010	2015	2020
CP (wt)	124.05	137.50	160.56	184.48	228.18
WY (billion m^3)	0.18	0.63	0.60	0.57	0.54
CS (t/km^2)	7,115.47	6,807.73	6,588.12	6,259.78	6,114.36
SC (t/km^2)	1,006.15	1,448.69	1,410.78	1,361.04	1,593.04
HQ	0.34	0.34	0.31	0.29	0.28
LA	44.62	45.52	47.08	48.68	49.09

TABLE 8 Qinhuangdao ecosystem services.

ES	2000	2005	2010	2015	2020
CP (wt)	70.50	84.59	86.82	84.44	74.99
WY (billion m^3)	0.19	0.73	0.93	0.54	0.69
CS (t/km^2)	10,866.00	10,756.12	10,711.12	10,660.93	10,552.43
SC (t/km^2)	5,976.48	10,102.59	11,565.89	8,759.95	11,386.54
HQ	0.51	0.50	0.50	0.49	0.48
LA	35.37	35.88	36.06	36.28	36.85

affected by the ocean. The climate is mild, with little rain and dryness in spring, warm and no scorching heat in summer, cool and sunny in autumn, and long and no severe cold in winter. In addition, the northern part of Qinhuangdao is dominated by mountainous and low hills, with forests, shrubs and grasslands as its main LULC types, which have good CS, SC and HQ capabilities. However, in the past 20 years due to the development of large-scale construction projects such as Qinhuangdao Economic and Technological Development Zone, Qinhuangdao Seaport Economic Development Zone, and Qinhuangdao Port, the ESs have degraded to varying degrees, among which CS has declined by 243wt, HQ by 4.92% and LA index has increased by 4.18%. In the future, Qinhuangdao should continue to leverage its regional advantages. The southeastern coastal areas should promote the concentrated and contiguous protection of agricultural land, strictly control the occupation of cropland by new construction, and revitalize existing construction land. The northern areas should effectively protect water sources and ecologically fragile areas, conduct comprehensive management of soil erosion and land degradation to ensure the continuous supply of ESs.

4.4 Policy planning suggestions

The natural environmental conditions and human activities are important factors influencing the regional landscape patterns and ESs. No single development policy can improve all landscape patterns and ESs. How to resolve the contradiction between protection and development is the core issue of ecological civilization construction (Li et al., 2022a). Firstly, people should actively respond to the influence of natural factors. The Bohai Rim region has a temperate monsoon climate with uneven spatial distribution of rainfall, which is vulnerable to drought risks. Therefore, the provisioning service levels such as crop production and water yield in most areas fluctuate greatly. It is necessary to vigorously develop regional agricultural irrigation technologies and optimize agricultural irrigation strategies. The drip irrigation method will improve CP levels and save water resources (Wu, 2013). Water resources can be planned and managed to avoid waste through rainwater collection, wastewater recycling and freshwater protection. According to the characteristics of the ecosystem, sloping cropland and other cropland with low CP should be converted into forests and grasslands. In areas with heavy precipitation and strong soil erosion, forests should be considered priority, the areas with low precipitation and weak soil erosion, grasslands should be considered as priority basis. Selecting drought-resistant and water-saving species can also help alleviate water shortages. In addition, continuing to scientifically promote the implementation of water diversion projects is also one of the basic policies that local governments must adhere to, ensuring accurate and precise water diversion, refining water allocation plans, and strengthening precise scheduling from water sources to ecosystems.

Second, the irregular urban expansion should be restricted, and the urban landscape structure should be optimized. Correlativity study showed that rapid urbanization expansion and high-intensity land development are the main reasons for the ESs decline in the Yangtze River Delta urban agglomeration (Lu et al., 2024). Some scholars have compared the response of ESs in Shenzhen and Hong Kong to rural-urban transitions. And a persistent downward trend in the ESs was observed for both cities, although the decline in Shenzhen was much stronger than in Hong Kong. This was because as an island city, Hong Kong's urban expansion was much slower compared to Shenzhen's extremely rapid urbanization due to limitations in land availability (Xu et al., 2020). Therefore the results of ESs assessments should be incorporated into urban landscape planning. Adopting a green, low-carbon, and resource-saving urban development model. For example, when planning urban construction, attention should be paid to reducing the occupation of ecological land such as forests and grasslands, rationally constructing urban green spaces, integrating transportation networks, water networks, and ecological networks (Fu et al., 2022), configuring green infrastructure such as sponge cities to increase urban infiltration and reduce runoff (Yang et al., 2024), so as to improve WY levels, reduce land use intensity and ecological risks in urbanized areas. For urban parks and green spaces, it is necessary to arrange them in a hierarchical manner according to the spatial structure of population concentration, so as to form a complete park system, which can provide cultural services accurately while ensuring the fairness of green spaces, and ultimately promote the improvement of human wellbeing through ESs (Tu et al., 2019).

Third, people should strengthen the protection and restoration of key land types. Protect forests, shrubs, grasslands and wetlands with high regulating and supporting services, and maintain a sustainable supply of ESs by optimizing nature reserve

management strategies and implementing key ecosystem protection projects (Ma et al., 2021). At the same time, strengthening the landscape connectivity of key land types, aggregating small plots into larger patches can improve the supply level of ESs. To protect cropland resources, improve cropland quality, county-level people's governments should strengthen daily supervision of the conversion of cropland into construction land within the county area, and vigorously develop intensive cropland (Xing et al., 2020). When developing ecosystem optimization strategies, the resilience of different ecosystems should be considered (Zhao et al., 2019). For example, forest ecosystems tend to have stronger natural recovery capabilities and ecological resilience, while cropland, barren land, and wetland ecosystems are relatively fragile and less resilient (Liu et al., 2018; Seidl et al., 2014). Conducting refined design in this way will be more conducive to achieving sustainable management of regional ecosystems.

4.5 Limitations and prospects

This study uses InVEST model to evaluate ESs, the quality of evaluation depends on the accuracy of the LULC data classification. However, the accuracy of the Wuhan University CLCD dataset used in this paper is only 79.31%, and no more detailed secondary classification was performed when using it due to the difficulty in obtaining other parameters. In the future research, more detailed LULC classification and higher resolution, more accurate LULC datasets should be used.

In addition, this study only evaluated six key ESs that dominate the Bohai Rim region. Due to the large scope of study area, it cannot fully represent the overall ecological status of the region. In the future, scholars can add ESs that reflect regional characteristics, such as aquaculture and water purification. Moreover, the use of LA to characterize cultural services is usually limited to specific locations (Dou et al., 2022), and it is difficult to accurately reflect their overall situation. In the future, when conducting cultural service assessments, it is necessary to comprehensively select assessment indicators based on research needs and data availability. Finally, although the assessment results have been validated by other studies, the lack of measured data may still lead to certain uncertainties in the results. Future studies can support the assessment results by obtaining observational data from field surveys.

5 Conclusion

This study uses spatial and statistical data to quantify LULC, landscape pattern and ESs in the Bohai Rim region from 2000 to 2020 and analyses their change characteristics and influencing factors. The results show that from 2000 to 2020, the area of forest, water and impervious land increased, while the area of cropland, shrubs, grassland, and barren land decreased. From 2000 to 2015, the landscape in the Bohai Rim region were small and fragmented, complex and dispersed. Subsequently, during 2015–2020, landscape fragmentation weakened, the morphological structure was simplified, and the patches tended to aggregate. From 2000 to 2020, CP, WY and SC capacity show an increasing trend, while CS, HQ and LA capacity show a decline trend. This study suggests that natural factors such as precipitation, temperature and altitude, as well as human factors such as technological progress, policy changes and LULC types are the main factors affecting the changes in landscape pattern and ESs. In the future, ecological managers and policymakers should focus on optimizing regional irrigation strategies and the methods of returning farmland to forest and grassland to reduce the constraints of natural factors on the supply of ESs; adopt methods such as configuring sponge cities, developing urban green spaces to limit the irregular expansion of cities and optimize urban landscape structure; continue to strengthen the protection and restoration of key land types, and protect high-quality forests, grasslands and wetlands to maintain a sustainable supply of ESs. The present study helps us to fully understand the changing characteristics and influencing factors of LULC, landscape pattern and ESs in the Bohai Rim region, and provide a basis for regional ecological restoration, ecological product value realization and territorial spatial planning.

Data availability statement

The original contributions presented in the study are included in the article/Supplementary Material, further inquiries can be directed to the corresponding author.

Author contributions

JL: Conceptualization, Formal Analysis, Investigation, Methodology, Writing–original draft, Writing–review and editing. WC: Project administration, Supervision, Writing–review and editing. HD: Project administration, Supervision, Writing–review and editing. ZL: Data curation, Software, Writing–review and editing. MX: Writing–review and editing. RS: Writing–review and editing. CL: Funding acquisition, Project administration, Supervision, Writing–review and editing.

Funding

The author(s) declare that financial support was received for the research, authorship, and/or publication of this article. This research was funded by the National Key Research and Development Program of China (Grant No. 2022YFF130100202), the National Natural Science Foundation of China (Grant Nos 42293262 and 42271077) and the Science and Technology Innovation Leading Talent Cultivation Project (Climbing Plan) of Tianjin University (Grant No. 2023XPD-0021).

Acknowledgments

We appreciate reviewers and their valuable comments. Also, we thank Editors for the editing and comments. We also thank the Haihe Laboratory of Sustainable Chemical Transformations for financial support.

Conflict of interest

The authors declare that the research was conducted in the absence of any commercial or financial relationships that could be construed as a potential conflict of interest.

Publisher's note

All claims expressed in this article are solely those of the authors and do not necessarily represent those of their affiliated organizations, or those of the publisher, the editors and the reviewers. Any product that may be evaluated in this article, or claim that may be made by its manufacturer, is not guaranteed or endorsed by the publisher.

Supplementary material

The Supplementary Material for this article can be found online at: https://www.frontiersin.org/articles/10.3389/fenvs.2024.1500045/full#supplementary-material

References

Assesment, M. E. (2005). Ecosystems and human well-being: synthesis. *Phys. Teach.* 34, 534. Available at: unep.org/resources/report/ecosystem-and-human-well-being-synthesis.

Bai, Y., Wong, C. P., Jiang, B., Hughes, A. C., Wang, M., and Wang, Q. (2018). Developing China's Ecological Redline Policy using ecosystem services assessments for land use planning. *Nat. Commun.* 9, 3034. doi:10.1038/s41467-018-05306-1

Costanza, R., Arge, Groot, R. D., Farberk, S., Belt, M. V. D., Hannon, B., et al. (1997). The value of the world's ecosystem services and natural capital. *Nature* 387, 253–260. doi:10.1038/387253a0

Deng, Y., Jiang, W., Wang, W., Lu, J., and Chen, K. (2018). Urban expansion led to the degradation of habitat quality in the Beijing-Tianjin- Hebei Area. *Acta Ecol. Sin.* 38, 4516–4525. doi:10.5846/stxb201712062200

Ding, Q. L., Chen, Y., Bu, L. T., and Ye, Y. M. (2021). Multi-Scenario analysis of habitat quality in the Yellow River Delta by coupling FLUS with InVEST model. *Int. J. Environ. Res. Public Health.* 18, 2389. doi:10.3390/ijerph18052389

Dou, Y. A., Zhen, L., Bakker, M., Yu, X. B., Carsjens, G. J., Liu, J. G., et al. (2022). Investigating the potential impact of ecological restoration strategies on people-landscape interactions through cultural ecosystem services: a case study of Xilin Gol, China. *J. Environ. Manage.* 316, 115185. doi:10.1016/j.jenvman.2022.115185

Feng, X. R., Zhang, T., Feng, P., and Li, J. Z. (2022). Evaluation and tradeoff-synergy analysis of ecosystem services in Luanhe River Basin. *Ecohydrology* 15, 12. doi:10.1002/eco.2473

Fisher, B., Turner, R. K., and Morling, P. (2009). Defining and classifying ecosystem services for decision making. *Ecol. Econ.* 68, 643–653. doi:10.1016/j.ecolecon.2008.09.014

Frank, S., Fürst, C., Koschke, L., Witt, A., and Makeschin, F. (2013). Assessment of landscape aesthetics-Validation of a landscape metrics-based assessment by visual estimation of the scenic beauty. *Ecol. Indic.* 32, 222–231. doi:10.1016/j.ecolind.2013.03.026

Fu, F., Deng, S. M., Wu, D., Liu, W. W., and Bai, Z. H. (2022). Research on the spatiotemporal evolution of land use landscape pattern in a county area based on CA-Markov model. *Sust. Cities Soc.* 80, 103760. doi:10.1016/j.scs.2022.103760

Guo, Q., Yu, C. X., Xu, Z. H., Yang, Y., and Wang, X. (2023). Impacts of climate and land-use changes on water yields: similarities and differences among typical watersheds distributed throughout China. *J. Hydrol.-Reg. Stud.* 45, 101294. doi:10.1016/j.ejrh.2022.101294

Hao, R. F., Yu, D. Y., Liu, Y. P., Liu, Y., Qiao, J. M., Wang, X., et al. (2017). Impacts of changes in climate and landscape pattern on ecosystem services. *Sci. Total Environ.* 579, 718–728. doi:10.1016/j.scitotenv.2016.11.036

Hu, T., Wu, J. S., and Li, W. F. (2019). Assessing relationships of ecosystem services on multi-scale: a case study of soil erosion control and water yield in the Pearl River Delta. *Ecol. Indic.* 99, 193–202. doi:10.1016/j.ecolind.2018.11.066

Jiang, B., Bai, Y., Wong, C. P., Xu, X. B., and Alatalo, J. M. (2019). China's ecological civilization program-Implementing ecological redline policy. *Land Use Pol.* 81, 111–114. doi:10.1016/j.landusepol.2018.10.031

Jiang, B. H., Chen, W., Dai, X. A., Xu, M., Liu, L. F., Sakai, T., et al. (2023). Change of the spatial and temporal pattern of ecological vulnerability: a case study on Cheng-Yu urban agglomeration, Southwest China. *Ecol. Indic.* 149, 110161. doi:10.1016/j.ecolind.2023.110161

Lai, L., Huang, X. J., Yang, H., Chuai, X. W., Zhang, M., Zhong, T. Y., et al. (2016). Carbon emissions from land-use change and management in China between 1990 and 2010. *Sci. Adv.* 2, e1601063. doi:10.1126/sciadv.1601063

Langemeyer, J., Calcagni, F., and Baró, F. (2018). Mapping the intangible: using geolocated social media data to examine landscape aesthetics. *Land Use Pol.* 77, 542–552. doi:10.1016/j.landusepol.2018.05.049

Li, H. L., Peng, J., Liu, Y. X., and Hu, Y. N. (2017). Urbanization impact on landscape patterns in Beijing City, China: a spatial heterogeneity perspective. *Ecol. Indic.* 82, 50–60. doi:10.1016/j.ecolind.2017.06.032

Li, J., Xia, S., Yu, X., Li, S., Xu, C., Zhao, N., et al. (2020). Evaluation of carbon storage on terrestrial ecosystem in Hebei province based on InVEST model. *J. Ecol. Rural. Environ.* 36, 854–861. doi:10.19741/j.issn.1673-4831.2019.0918

Li, Q., Li, W. J., Wang, S., and Wang, J. F. (2022a). Assessing heterogeneity of trade-offs/synergies and values among ecosystem services in Beijing-Tianjin-Hebei urban agglomeration. *Ecol. Indic.* 140, 109026. doi:10.1016/j.ecolind.2022.109026

Li, X., Liu, Z. S., Li, S. J., and Li, Y. X. (2022b). Multi-Scenario simulation analysis of land use impacts on habitat quality in Tianjin based on the PLUS model coupled with the InVEST model. *Sustainability* 14, 6923. doi:10.3390/su14116923

Liu, C., Li, S., Liu, X., Wang, B., Lang, Y., Ding, H., et al. (2024a). Biogeochemical cycles in the Anthropocene and its significance. *Earth Sci. Front.* 31, 455–466. doi:10.13745/j.esf.sf.2024.1.26

Liu, C., Men, B., Shen, Y., and Pang, J. (2023). Soil conservation and water purification services and their trade-offs and synergies in Luanhe River Basin. *Acta Ecol. Sin.* 43, 5740–5752. doi:10.5846/stxb202207101963

Liu, H. X., Gao, C. Y., and Wang, G. P. (2018). Understand the resilience and regime shift of the wetland ecosystem after human disturbances. *Sci. Total Environ.* 643, 1031–1040. doi:10.1016/j.scitotenv.2018.06.276

Liu, Q., Qiao, J. J., Li, M. J., and Huang, M. J. (2024b). Spatiotemporal heterogeneity of ecosystem service interactions and their drivers at different spatial scales in the Yellow River Basin. *Sci. Total Environ.* 908, 168486. doi:10.1016/j.scitotenv.2023.168486

Liu, W., Zhan, J. Y., Zhao, F., Wang, C., Zhang, F., Teng, Y. M., et al. (2022a). Spatio-temporal variations of ecosystem services and their drivers in the Pearl River Delta, China. *J. Clean. Prod.* 337, 130466. doi:10.1016/j.jclepro.2022.130466

Liu, Y. B., Han, M., Wang, M., Fan, C., and Zhao, H. (2022b). Habitat quality assessment in the Yellow River Delta based on remote sensing and scenario analysis for land use/land cover. *Sustainability* 14, 15904. doi:10.3390/su142315904

Liu, Y. B., Hou, X. Y., Li, X. W., Song, B. Y., and Wang, C. (2020). Assessing and predicting changes in ecosystem service values based on land use/cover change in the Bohai Rim coastal zone. *Ecol. Indic.* 111, 106004. doi:10.1016/j.ecolind.2019.106004

Lu, Y. G., Wang, J. C., and Jiang, X. K. (2024). Spatial and temporal changes of ecosystem service value and its influencing mechanism in the Yangtze River Delta urban agglomeration. *Sci. Rep.* 14, 19476. doi:10.1038/s41598-024-70248-2

Ma, J., Li, J. W., Wu, W. B., and Liu, J. J. (2023). Global forest fragmentation change from 2000 to 2020. *Nat. Commun.* 14, 3752. doi:10.1038/s41467-023-39221-x

Ma, S., Qiao, Y. P., Wang, L. J., and Zhang, J. C. (2021). Terrain gradient variations in ecosystem services of different vegetation types in mountainous regions: vegetation resource conservation and sustainable development. *For. Ecol. Manage.* 482, 118856. doi:10.1016/j.foreco.2020.118856

Ning, S. A., Hai, Y. Y., and Nan, J. (2011). Response of ecosystem service value to land use change in coastal zone of Bohai Sea in last 30 years. *Adv. Mat. Res.*, 347–353. doi:10.4028/www.scientifc.net/AMR.347-353.3963

Ouyang, Z., Zheng, H., Xiao, Y., Polasky, S., Liu, J., Xu, W., et al. (2016). Improvements in ecosystem services from investments in natural capital. *Science* 352, 1455–1459. doi:10.1126/science.aaf2295

Searchinger, T. D., Wirsenius, S., Beringer, T., and Dumas, P. (2018). Assessing the efficiency of changes in land use for mitigating climate change. *Nature* 564, 249–253. doi:10.1038/s41586-018-0757-z

Seidl, R., Rammer, W., and Spies, T. A. (2014). Disturbance legacies increase the resilience of forest ecosystem structure, composition, and functioning. *Ecol. Appl.* 24, 2063–2077. doi:10.1890/14-0255.1

Shao, Y. J., Liu, Y. S., Li, Y. H., and Yuan, X. F. (2023). Regional ecosystem services relationships and their potential driving factors in the Yellow River Basin, China. *J. Geogr. Sci.* 33, 863–884. doi:10.1007/s11442-023-2110-1

Teutschbein, C., Grabs, T., Laudon, H., Karlsen, R. H., and Bishop, K. (2018). Simulating streamflow in ungauged basins under a changing climate: the importance of landscape characteristics. *J. Hydrol.* 561, 160–178. doi:10.1016/j.jhydrol.2018.03.060

Tu, X., Huang, G., and Wu, J. (2019). Review of the relationship between urban greenspace accessibility and human well-being. *Acta Ecol. Sin.* 39, 421–431. doi:10.5846/stxb201802030294

van der Plas, F., Allan, E., Fischer, M., Alt, F., Arndt, H., Binkenstein, J., et al. (2019). Towards the development of general rules describing landscape heterogeneity-multifunctionality relationships. *J. Appl. Ecol.* 56, 168–179. doi:10.1111/1365-2664.13260

Wang, H. R., Zhang, M. D., Wang, C. Y., Wang, K. Y., Wang, C., Li, Y., et al. (2022). Spatial and temporal changes of landscape patterns and their effects on ecosystem services in the huaihe River Basin, China. *Land* 11, 513. doi:10.3390/land11040513

Wang, X. X., Xiao, X. M., Xu, X., Zou, Z. H., Chen, B. Q., Qin, Y. W., et al. (2021). Rebound in China's coastal wetlands following conservation and restoration. *Nat. Sustain.* 4, 1076–1083. doi:10.1038/s41893-021-00793-5

Winkler, K., Fuchs, R., Rounsevell, M., and Herold, M. (2021). Global land use changes are four times greater than previously estimated. *Nat. Commun.* 12, 2501. doi:10.1038/s41467-021-22702-2

Wischmeier, W. H., Johnson, C. B., and Cross, B. V. (1971). A soil erodibility nomograph for farmland and construction sites. *J. Soil Water Conserv.* 26, 189–193. Available at: researchgate.net/publication/303183461_A_soil_erodibility_nomograph_for_farmland_and_construction_sites/citations.

Wu, J. G. (2013). Landscape sustainability science: ecosystem services and human well-being in changing landscapes. *Landsc. Ecol.* 28, 999–1023. doi:10.1007/s10980-013-9894-9

Xia, C., Guo, H., Zhao, J., Xue, F., Wang, C., Zhou, J., et al. (2023a). Dynamic responses of ecosystem services to urbanization at multi-spatial scales in the Beijing-Tianjin-Hebei region. *Acta Ecol. Sin.* 43, 2756–2769. doi:10.5846/stxb202204181049

Xia, H., Yuan, S. F., and Prishchepov, A. V. (2023b). Spatial-temporal heterogeneity of ecosystem service interactions and their social-ecological drivers: implications for spatial planning and management. *Resour. Conserv. Recycl.* 189, 106767. doi:10.1016/j.resconrec.2022.106767

Xing, L., Hu, M. S., and Wang, Y. (2020). Integrating ecosystem services value and uncertainty into regional ecological risk assessment: a case study of Hubei Province, Central China. *Sci. Total Environ.* 740, 140126. doi:10.1016/j.scitotenv.2020.140126

Xu, C., Jiang, W. Y., Huang, Q. Y., and Wang, Y. T. (2020). Ecosystem services response to rural-urban transitions in coastal and island cities: a comparison between Shenzhen and Hong Kong, China. *J. Clean. Prod.* 260, 121033. doi:10.1016/j.jclepro.2020.121033

Yang, K., Han, Q., and Vries, B. d. (2024). Urbanization effects on the food-water-energy nexus within ecosystem services: a case study of the Beijing-Tianjin-Hebei urban agglomeration in China. *Ecol. Indic.* 160, 111845. doi:10.1016/j.ecolind.2024.111845

Zhang, T. J., Zhang, S. P., Cao, Q., Wang, H. Y., and Li, Y. L. (2022). The spatiotemporal dynamics of ecosystem services bundles and the social-economic-ecological drivers in the Yellow River Delta region. *Ecol. Indic.* 135, 108573. doi:10.1016/j.ecolind.2022.108573

Zhang, W., Chang, W. J., Zhu, Z. C., and Hui, Z. (2020). Landscape ecological risk assessment of Chinese coastal cities based on land use change. *Appl. Geogr.* 117, 102174. doi:10.1016/j.apgeog.2020.102174

Zhang, W., and Fu, J. (2003). Rainfall erosivity estimation under different rainfall amount. *Resour. Sci.* 25, 35–41. doi:resci.cn/CN/Y2003/V25/I1/35

Zhao, W. Z., Han, Z. L., Yan, X. L., and Zhong, J. Q. (2019). Land use management based on multi-scenario allocation and trade-offs of ecosystem services in Wafangdian County, Liaoning Province, China. *PeerJ* 7, e7673. doi:10.7717/peerj.7673

Zhao, X., Zhang, Q., He, G. Z., Zhang, L., and Lu, Y. L. (2021). Delineating pollution threat intensity from onshore industries to coastal wetlands in the Bohai Rim, the Yangtze River Delta, and the Pearl River Delta, China. *J. Clean. Prod.* 320, 128880. doi:10.1016/j.jclepro.2021.128880

Zhu, L. Y., Song, R. X., Sun, S., Li, Y., and Hu, K. (2022). Land use/land cover change and its impact on ecosystem carbon storage in coastal areas of China from 1980 to 2050. *Ecol. Indic.* 142, 109178. doi:10.1016/j.ecolind.2022.109178

Zhu, W. B., Zhang, J. J., Cui, Y. P., and Zhu, L. Q. (2020). Ecosystem carbon storage under different scenarios of land use change in Qihe catchment, China. *J. Geogr. Sci.* 30, 1507–1522. doi:10.1007/s11442-020-1796-6

frontiers | Frontiers in Environmental Science

TYPE Original Research
PUBLISHED 10 March 2025
DOI 10.3389/fenvs.2025.1542002

OPEN ACCESS

EDITED BY
Salvador García-Ayllón Veintimilla,
Polytechnic University of Cartagena, Spain

REVIEWED BY
Jinman Wang,
China University of Geosciences, China
Peidong Han,
Northwest A&F University, China

*CORRESPONDENCE
Aman Fang,
fangaman@henau.edu.cn

RECEIVED 09 December 2024
ACCEPTED 19 February 2025
PUBLISHED 10 March 2025

CITATION
Fang A, Shi Y, Chen W, Shi L, Wang J and Ma Y (2025) Trade-off and synergy relationships and regional regulation of multifunctional cultivated land in the Yellow River Basin.
Front. Environ. Sci. 13:1542002.
doi: 10.3389/fenvs.2025.1542002

Trade-off and synergy relationships and regional regulation of multifunctional cultivated land in the Yellow River Basin

Aman Fang[1]*, Yuanqing Shi[1], Weiqiang Chen[1], Lingfei Shi[1], Jinlong Wang[2] and Yuehong Ma[1]

[1]College of Resources and Environmental Sciences, Henan Agricultural University, Zhengzhou, China, [2]Henan Province Fifth Geological Brigade Co., Ltd., Zhengzhou, China

Exploring the multifunctional trade-off and synergy relationship of cultivated land is of great significance for protecting cultivated land resources, ensuring food security, maintaining ecological security, and promoting high-quality development in the Yellow River Basin. Based on the selection of 379 counties with concentrated distribution of cultivated land, this study comprehensively evaluates the three-dimensional functional level of "production-society-ecology" of cultivated land from 2010 to 2020. The coupling coordination degree model, land system function trade-off degree model, and K-means clustering analysis method are used to analyze the trade-off and synergy relationship between cultivated land functions and divide the functional zones in the Yellow River Basin. 1) In the last 10 years, the levels of cultivated land production, social, and ecological functions in the Yellow River Basin are in the range of 0.01–0.47, 0.04 to 0.23, and 0.03 to 0.23, respectively. The production function is at a stable level, while the overall level of social and ecological functions has slightly improved. 2) The level of multifunctional coupling and coordination of cultivated land ranges from 0.22 to 0.65. Only 31.13% of counties have a high coupling degree between multiple functions. The production-ecological function in the upstream regions show a coordinated development trend. The social-ecological function in the midstream regions is well coordinated, and the production-social function and production-ecological function in downstream regions towards collaborative development. 3) According to the dominant functional types and the characteristics of multifunctional coupling and coordination, the cultivated land of Yellow River Basin is divided into 7 multifunctional zones, involving 149 with multifunctional advantage zones, 19 with P-S functional composite zones, 21 with P-E functional composite zones, 21 with S-E functional composite zones, 74 with social functional dominant zones, 29 with ecological functional dominant zones, 44 with grain functional dominant zones, and 22 with remediation key zones. The results can provide decision support for differentiated management of cultivated land in the Yellow River Basin and mutual promotion between functions.

KEYWORDS

trade-off and synergy, functional zones, cultivated land, land system function trade-off degree, Yellow River Basin

1 Introduction

As the fundamental resource and spatial carrier for human survival and development, the functional expansion of cultivated land is closely linked to social and economic reforms, as well as changes in human needs (Zhang et al., 2023; Zou et al., 2021). With China transitions from an agricultural to a modern industrial society and then progresses towards an ecological civilization, the multifunctionality of cultivated land has emerged as an inevitable trend in response to continuously rising human demands (Wu et al., 2024; Dong and Zhao, 2019; Qian et al., 2020). Cultivated land has gradually played a role in stabilizing food production, maintaining social stability, and ensuring ecological security, evolving from initially addressing the basic needs of food and clothing, to promoting industrialization and urbanization, and then to fostering rural revitalization and ecological civilization construction, all while striving to achieve the goal of sustainable development (Xiong et al., 2021; Zhu et al., 2020). However, the scarcity of cultivated land resources has led to increasingly fierce land conflicts and spatial competition between food security, ecological protection, and urban development, seriously affecting the potential of cultivated land production, diminishing its social contribution value, and causing ecosystem degradation, which violates the scientific concept of sustainable use of cultivated land (Lv et al., 2023). The current management model for cultivated land production functions struggles to accommodate the diverse practical demands of farmland utilization (Fang et al., 2018). Therefore, exploring the multifunctionality of cultivated land utilization and achieving coordinated multifunctional utilization of farmland has become an urgent practical issue in balancing the interests of multiple parties and enhancing the effectiveness of farmland protection.

The existing literature on the multifunctionality of cultivated land primarily focuses on conceptual explanations (Song and Li, 2019; Wei et al., 2022), functional classification and indicator system construction, influencing factors exploration (Zhang et al., 2021; Liu et al., 2023), analysis of coupling and coordination relationships, and spatial zoning optimization (Jiang et al., 2021; Niu et al., 2022; Luo et al., 2023). The methods have gradually evolved from initial qualitative explanations and analysis of concepts to functional interaction and driving mechanism analysis based on mathematical statistics, while using ArcGIS software to achieve spatial regulation of functional zoning (Fei et al., 2023; Wang et al., 2023; Sylla et al., 2020; Qian et al., 2022). Due to the fact that the various functions of cultivated land do not work independently, but rather have a competitive and mutually reinforcing relationship. Thus, trade-off collaborative analysis is applied to identify the interrelationships and mutual benefits between various dimensions of farmland functions, in order to propose targeted coordinated management measures. In view of the trade-off and synergy between the functions of cultivated land, some scholars have not only understood the relationships between the functions through the correlation coefficient, but also realized the spatial expression of this correlation, identified the spatial association of each partition in the region, and realized the function optimization partition of cultivated land (Qian et al., 2022; Gao et al., 2021).

The Yellow River Basin, as a region in northern China with abundant reserve resources of cultivated land, nurtures 12% of the country's population. Land use conflicts, such as agricultural non-point source pollution, soil degradation, and the "Non-grain" and "Non-agriculture" utilization of cultivated land, have posed a serious threat to the protection of cultivated land in river basins. The management of cultivated land in the Yellow River Basin from the perspective of multi-function has become an important means to ensure regional sustainable development. Analyzing the trade-off and synergy relationship of each function and putting forward targeted suggestions to reduce trade-offs and increasing synergy play important role in maximizing the multifunctional utilization benefits of cultivated land in the Yellow River Basin. At present, most scholars have always paid attention to the multifunctional evaluation of land use in the Yellow River Basin (Niu P. et al., 2022). Only a few of studies focus on the cultivated land. Meanwhile, the study areas involve a section of the Yellow River Basin, for instance, Henan Province and Gansu Province. How is the functional utilization of cultivated land in the entire Yellow River Basin? Can we improve the utilization efficiency of cultivated land in the Yellow River Basin through zoning management and control to achieve ecological protection in the basin? The objectives of this study were: (1) to assess the spatial and temporal differentiation characteristics of multifunction of cultivated land in the Yellow River Basin; (2) to obtained the trade-off and synergy relationship between the functions of each dimension; (3) to divide the functional division of cultivated land and put forward the corresponding control strategy.

2 Materials and methods

2.1 Study area

The Yellow River Basin covers 1,900 km^2 from east to west, and 1,100 km^2 from north to south. It flows through 9 provinces, involving 44 cities (prefectures, leagues) and 424 counties (banners), as shown in Figure 1. The terrain shows a three-step decline, high in the west and low in the east. There are significant spatial differences in climate conditions, with an annual precipitation of 116–1,038 mm and an annual temperature of −13°C–15°C. The temperature and precipitation are relatively high in the southeast region, while they are relatively low in the northeast and northwest regions. The cultivated land area in the Yellow River Basin was approximately 2.50×10^5 km^2 in 2020. A total of 379 counties were selected to study with considering the concentrated distribution of cultivated land, regional connectivity, and the convenience of zoning management. Among them, there were 54 in Gansu Province, 59 in Henan Province, 35 in Inner Mongolia Autonomous Region, 22 in Ningxia Hui Autonomous Region, 14 in Qinghai Province, 37 in Shandong Province, 84 in Shanxi Province, and 74 in Shaanxi Province. The specific counties are shown in Figure 1.

2.2 Data sources

The vector data for the Yellow River Basin and the administrative boundary, and the land use status data at 1 km

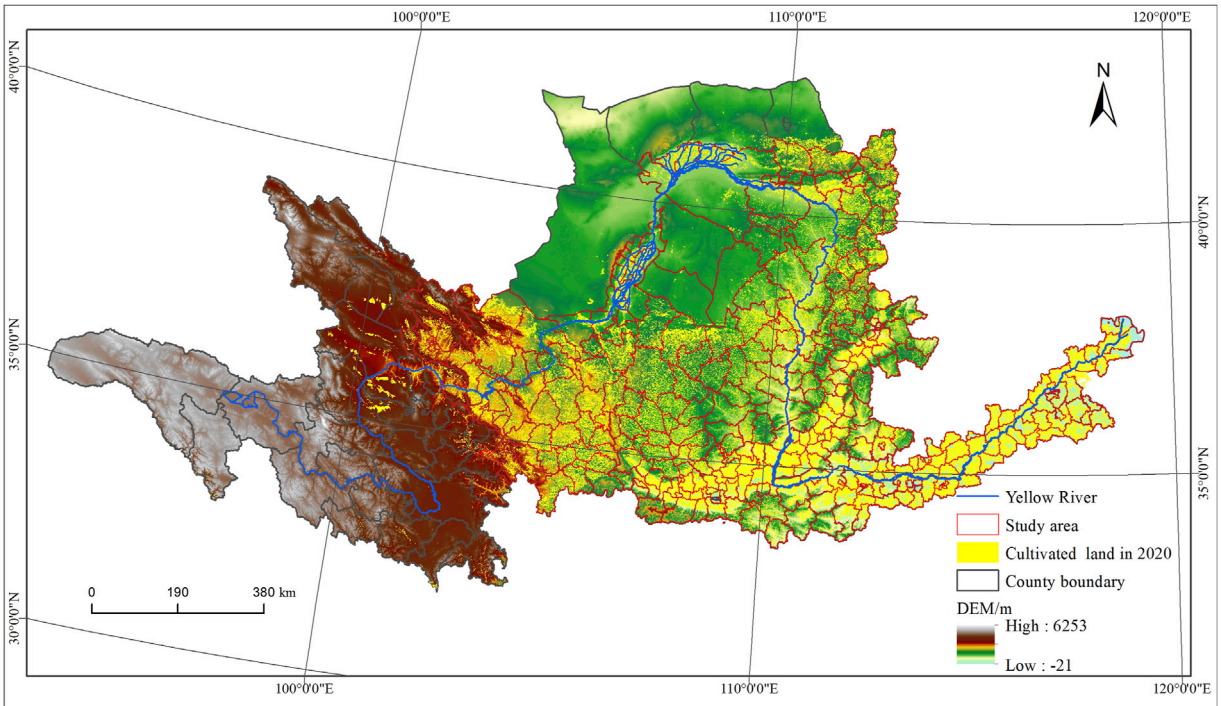

Gansu (Baiyin District, Huining County, Jingtai County, Jingyuan County, Pingchuan District, Anding District, Lintao County, Longxi County, Min County, Tongwei County, Weiyuan County, Zhang County, Lintan County, Anning District, Chengguan District, Gaolan County, Honggu District, Qilihe District, Xigu District, Yongdeng County, Yuzhong County, Dongxiang Autonomous County, Guanghe County, Hezheng County, Jishishan County, Kangle County, Linxia City, Linxia County, Yongjing County, Li County, Chongxin County, Huating City, Jingchuan County, Jingning County, Kongtong District,Lingtai County, Zhuanglang County, Heshui County, Huachi County, Huan County, Ning County, Qingcheng County, Xifeng District, Zhenyuan County, Zhengning County, Gangu County, Maiji District, Qin'an County, Qinzhou District, Qingshui County, Wushan County, Zhangjiachuan County, Gulang County, Tianzhu County)

Henan (Hua County,Xun County,Jiyuan City,Bo'ai County,Mengzhou City,Qinyang City,Wen County,Wuzhi County,Gulou District,Lankao County,Longting District,Xiangfu District, Shunhe Hui District,Yuwangtai District,Chanhe Hui District,Jili District,Jianxi District,Old Town,Luanchuan County,Luolong District,Luoning County,Mengjin County, Ruyang County,Song County,Xigong District,Xin'an County,Yanshi City,Yichuan County,Yiyang County,Fan County,Hualong District,Puyang County,Taiqian County, Hubin District,Lingbao City,Lushi County,Mianchi County,Shanzhou District,Yima City,Fengqiu County,Hongqi District,Huojia County,Weibin District,Weihui City, Xinxiang County,Yanjin County,Yuanyang County,Changyuan City,Dengfeng City,Erqi District,Gongyi City,Guancheng Hui District,Huiji District,Jinshui District, Shangjie District,Xinmi City,Xinzheng City,Xingyang City,Zhongmou County)

Inner Mongolia (Dengkou County, Hanggin Rear Banner, Linhe District, Urad Front Banner,Wuyuan County, Donghe District, Guyang County, Jiuyuan District, Kundulun District, Qingshan District, Shiguai District, Tumotetyou County, Dalad Banner, Dongsheng District, Otog Banner, Otog Front Banner, Hanggin Banner, Uxin Banner, Ejin Horo Banner, Zhungeer Banner, Helingeer County, Huimin District,Qingshuihe County,Saihan District, Tumotetyou County, Toketo County, Wuchuan County,New Town District, Yuquan District, Haibo Bay District, Hainan District,Uda District, Chahar Right Middle Banner,Liangcheng County,Zhuozi County)

Ningxia (Jingyuan County, Longde County, Pengyang County, Xiji County,Yuanzhou District,Dawukou District,Huinong District,Pingluo County,Hongsibao District,Litong District, Qingtongxia City,Tongxin County,Yanchi County,Jinfeng District,Lingwu City,Xixia District,Xingqing District,Yongning County,Haiyuan County,Shapotou District, Ledu District, Zhongning County)

Qinghai (Menyuan Hui Autonomous County,Mutuozu Autonomous County,Hualong Hui Autonomous County, Ping'an District,Minhe Huizu Tuzu Autonomous County, Huangzhong District,Xunhua Salar Autonomous County,Chengbei District,Chengdong District,Chengxi District,Chengzhong District, Datong Hui Tu Zu Autonomous County, Huangyuan County)

Shandong (Bincheng District,BoxingCounty,Huimin County,Qihe County,Dongying District,Hekou District,Kenli District,Lijin County,Dongming County,Juancheng County, Dudan District,Yuncheng County,Gangcheng District, Huaiyin District,Jiyang District,Laiwu District,Licheng District, Lixia District, Pingyin County, Shizhong District, Tianqiao District, Zhangqiu District,Changqing District,Liangshan County, Wenshang County, Dong'e County, Shen County, Yanggu County, Daiyue District, Dongping County, Feicheng City, Ningyang County,Taishan District,Xintai City,Boshan District,Gaoqing County,Yiyuan County)

Shanxi (Zuoyun County, Urban Areas,Gaoping City,Lingchuan County,Qinshui County,Yangcheng County,Zezhou County,Heshun County,Jiexiu City,Lingshi County,Pingyao County, Qi County,Shouyang County,Taigu District,Xiyang County,Yuci District,Yushe County,Anze County,Daning County,Fenxi County,Fushan District,Gu County,Hongdong County, Houma City,Huozhou City,Ji County,Pu County,Quwo County,Xi County,Xiangning County,Xiangfen County,Yaodu District,Yicheng County,Yonghe County,Fangshan County, Fenyang City,Jiaocheng County,Jiaokou County,Lan County,Lishi District,Lin County,Liulin County,Shilou County,Wenshui County,Xiaoyi City,Xing County,Zhongyang County, Pinglu District,Shuocheng District,Youyu County,Gujiao City,Jiancaoping District,Jinyuan District,Lou Fan County,Qingxu County,Wanbolin District,Xiaodian District, Xinghualing District,Yangqu County,Yingze District,Baode County,Hequ County,Jingle County,Kelan County,Ningwu County,Pianguan County,Shenchi County,Wuzhai County, Xinfu District,Yu County,Hejin City,Jishan County,Jiang County,Linyi County,Pinglu County,Ruicheng County,Wangrong County,Wenxi County,Xia County,Xinjiang County, Yanhu District,Yongji City,Yuanqu County,Qinyuan County)

Shaanxi (Chencang District,Fengxiang County,Fufeng County,Jintai District,Linyou County,Long County,Mei County,Qishan County,Qianyang County,Taibai County,Weibin District, Danfeng County,Lonan County,Shangzhou District,Wangyi District,Yaozhou District,Yijun County,Yintai District,Baishui County,Chengcheng County,Dali County,Fuping County, Hancheng City,Heyang County,Huayin City,Huazhou District,Linwei District,Pucheng County,Tongguan County,Baqiao District,Gaoling District,Huyi District,Lantian County, Lintong District,Yanliang District,Chang'an District,Zhouzhi County,Binzhou City,Chunhua County,Jingyang County,Liquan County,Qian County,Qindu District,Sanyuan County, Wugong County,Xingping City,Xunyi County,Yongshou County,Changwu County,Ansai District,Baota District,Fu County,Ganquan County,Huangling County,Huanglong County, Luochuan County,Wuqi County,Yanchuan County,Yanchang County,Yichuan County,Zhidan County,Zichang City,Dingbian County,Fugu County, Hengshan District,Jia County, Jingbian County,Mizhi County,Qingjian County,Shenmu City,Suide County,Wubao County,Yuyang District,Zizhou County)

FIGURE 1
Distribution of cultivated land in the Yellow River Basin.

resolution (2010, 2020) were obtained from the Resource and Environmental Science and Data Center of the Chinese Academy of Sciences (https://www.resdc.cn/). Land use types were reclassified into six categories using ArcGIS 10.8 software: cultivated land, forest land, grassland, water area, construction land, and unused land. All spatial data were processed into Albers projection. The socioeconomic statistics of counties and banners were obtained from statistical yearbook, economic and social survey yearbook, economic statistical yearbook and county statistical yearbook of the corresponding years, provinces and cities. The missing data was replaced by data from adjacent years.

TABLE 1 Multifunctional evaluation index system for cultivated land.

Function types	Specific index	Index description	Index attribute	Index weight	Functional weight
PF	Grain crop yield	Grain yield/cultivated land area	+	0.124	0.488
	Economic crop yield	Economic crop yield/cultivated land area	+	0.117	
	Average agricultural output value of cultivated land	Total agricultural output value/cultivated land area	+	0.169	
	Land reclamation rate	Cultivated land area/total land area	+	0.078	
SF	Agricultural practitioners proportion	Agricultural employed population/Total regional population	+	0.061	0.254
	Family agricultural income proportion	Family agricultural income/rural *per capita* net income	+	0.055	
	Agricultural mechanization level	Total power of agricultural machinery/agricultural employed population	-	0.079	
	The carrying capacity of rural labor force	Agricultural employed population/cultivated land area	-	0.059	
EF	Farmland ecosystem diversity	Total sown area of crops/cultivated land area	+	0.054	0.258
	Chemical load of cultivated land use	Chemical fertilizer application/cultivated land area	-	0.067	
	Carbon sequestration function	Natural carbon sequestration/cultivated land area	+	0.081	
	Ecological land proportion	Cultivated land area/the difference between the total land area and the construction land area	+	0.056	

2.3 Multi-functional evaluation of cultivated land

2.3.1 Construction of index system

According to both the previous studies and the national regional ecological protection and high-quality development requirements, the function of cultivated land was divided into three categories, namely, production, social security, and ecology (Wang et al., 2023). Considering the principles of science, systematic, operable, and objectivity, and combining the actual situation of cultivated land in the Yellow River Basin, a total of 12 indices were finally selected to construct the multifunctional evaluation index system of cultivated land, containing grain crop yield, land reclamation rate, and other indicators (Wang and Chen, 2022; Zhou et al., 2022) (Table 1).

The production function (PF) of cultivated land reflects the crop output capacity of cultivated land resources and makes a great contribution to ensuring food supply, which is the most basic function. The three aspects of crop yield, output value, and utilization status were the main basis for index selection. The yield per unit area of grain and economic crops reflects the physical production level of cultivated land. The average output value represents the economic production level of cultivated land. Land reclamation rate characterizes the degree of cultivated land development and renewal to reflect the utilization status. The social function (SF) states that cultivated land, as a production factor for farmers to survive, mainly plays a role in maintaining life and providing employment security. To indicate the function of cultivated land to carry rural surplus labor force and meet the needs of promoting rural social and economic development, this study selects the proportion of agricultural practitioners, the proportion of family agricultural income, the *per capita* level of agricultural mechanization, and the carrying capacity of rural labor force. The ecological function (EF) reveals the regional ecological security ability of cultivated land to regulate climate, water conservation, and soil and water conservation. It is determined by four factors: farmland ecosystem diversity, chemical load of cultivated land use, carbon sequestration function and proportion of ecological land. Considering the major crops of Yellow River Basin, the cultivation areas of wheat, corn, oilseed, and vegetable were used to calculate the diversity index of farmland ecosystem (Niu et al., 2022). The calculation formula is shown below to elaborated in Equations 1, 2:

$$H_q = -\sum_{i=1}^{4} P_q \cdot l_n P_q \tag{1}$$

$$P_q = \frac{S_q}{S} \tag{2}$$

where H_q is the diversity index of farmland ecosystem, P_q is the ratio of crop q to total sown area, S_q is the sown area of crop q, and S is the total sown area.

According to existing research, the natural carbon sequestration of cultivated land is obtained by the following formulas to by Equation 3:

$$A_c = \sum_{i=1}^{m} A_{c_i} = \sum_{i=1}^{m} \left[C_{pi} \times Y_i \times (1 - W_i) \times (1 + R_i) \right] \Big/ H_i \tag{3}$$

where A_c is the natural carbon sequestration of cultivated land, A_{c_i} is the carbon absorption capacity, C_{pi}, Y_i, W_i, R_i, and H_i respectively refer to carbon content rate, economic outputs, water coefficient, top-root ratio, and economic coefficient of crop i. The m value is 4, which means that wheat, corn, oilseed, and vegetable are selected to calculate the natural carbon sequestration. The related parameters of these crops were from Chen et al. (2016).

2.3.2 Index processing

To ensure the comparability between the various indices, the range normalization method was applied to convert the original data into dimensionless data. The specific calculation formula for the positive and negative indices are expressed as Equations 4, 5:

$$\text{Positive indices: } X_{ij} = \frac{x_{ij} - x_{jmin}}{x_{jmax} - x_{jmin}} \tag{4}$$

$$\text{Negative indices: } X_{ij} = \frac{x_{jmax} - x_{ij}}{x_{jmax} - x_{jmin}} \tag{5}$$

where X_{ij} means the standardized value, x_{ij} means the actual value of the jth index of the ith county, and x_{jmax} and x_{jmin} mean the maximum and minimum values of the jth index, respectively.

2.3.3 Weight determination

Entropy weight method and analytic hierarchy process were used to determine the index layer weight comprehensively and accurately (Fang et al., 2018). Among them, the determination of functional indicator weights using Analytic Hierarchy Process were from the relevant literature (Zhang et al., 2023; Luo et al., 2023), and obtained by Yaahp software. The entropy weight is calculated by Equations 6–11:

$$Y_{ij} = \frac{X_{ij}}{\sum_{i=1}^{m} X_{ij}} \tag{6}$$

$$e_j = -k\sum_{i=1}^{m}\left(Y_{ij} \cdot \ln Y_{ij}\right) \tag{7}$$

$$k = \frac{1}{\ln m} \tag{8}$$

$$d_j = 1 - e_j \tag{9}$$

$$W_{kj} = \frac{d_j}{\sum_{j=1}^{n} d_j} \tag{10}$$

$$W_j = \frac{\left(W_{aj} + W_{kj}\right)}{2} \tag{11}$$

where Y_{ij} is the percentage of the jth indicator for year i, e_j is index information entropy, d_j is the difference coefficient of index j, W_{aj} is the analytic hierarchy weight, W_{kj} is the entropy weight, W_j is the comprehensive weight of index j, and m is the number of samples. The results have been shown in Table 1.

2.3.4 Multi-functional value of cultivated land

The comprehensive weighting method was used to calculate the multi-functional scores of cultivated land in counties of the Yellow River Basin, with Equation 12:

$$F = \sum_{i=1}^{m}\sum_{j=1}^{n}\left(X_{ij} \cdot W_j\right) \tag{12}$$

where F is the multi-functional value of cultivated land.

2.4 Trade-off and synergy evaluation of cultivated land utilization function and partition

The multifunctional zoning ways of cultivated land are shown in Figure 2; Table 2. Firstly, the coupling and coordination relationship

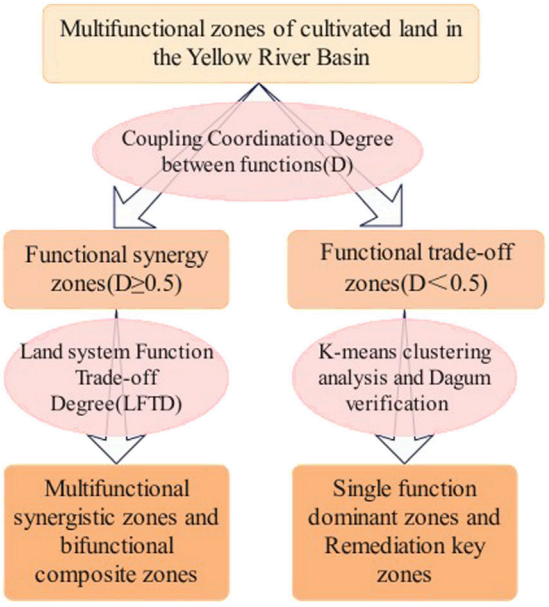

FIGURE 2
Multifunctional zoning ways of cultivated land.

is analyzed between the PF, SF, and EF of cultivated land in the Yellow River Basin. The functional synergy and trade-off zones are obtained on the basic of the coupling coordination degree. Then, the multifunctional synergy zones and the functional composite zones are distinguished combined with the Land system Function Trade-off Degree (LFTD). As shown in Table 2, the LFTD values of PF, SF, and EF are higher than 0 in the multifunctional synergy zones. For the composite zones of production-social (P-S) function, production-ecological (P-E) function, and social-ecological (S-E) function, their corresponding LFTD values are more than 0. In terms of the functional trade-off zones, it includes the single function dominant zones and remediation key zones and is realized by the K-means clustering analysis (Zhao et al., 2024) and Dagum verification (Zhang et al., 2019).

2.4.1 Coupling coordination degree

Coupling Coordination Degree model has been widely applied in the study of coupling and coordination relationship between three or more subsystems. Farmland is a complex system, with production, social security, and ecological functions. By coupling and coordinating the multifunctional evaluation of cultivated land based on its inherent coupling relationship, it is possible to comprehensively evaluate the quality of cultivated land from the perspective of overall development level (Wei et al., 2022). The specific formulas are expressed as Equations 13–15:

$$C = \sqrt[3]{\frac{F_P \times F_S \times F_E}{(F_P + F_S + F_E)^3}} \tag{13}$$

$$T = W_P F_P + W_S F_S + W_E F_E \tag{14}$$

$$D = \sqrt{C \times T} \tag{15}$$

where C, T and D mean coupling degree, coordination degree, and coupling coordination degree, F_P, F_S, and F_E are functional values of production, social, and ecology, and W_P, W_S, and W_E are 0.488,

TABLE 2 The multifunctional zoning foundation of cultivated land.

D	$LFTD_{PS}$	$LFTD_{PE}$	$LFTD_{SE}$	Zones
≥0.5	>0	>0	>0	Multifunctional advantage zones
	>0	<0	<0	P-S functional composite zones
	<0	>0	<0	P-E functional composite zones
	<0	<0	>0	S-E functional composite zones

0.254, and 0.258, respectively. The corresponding functional values in 2020 was selected to calculate the C and T. According to the existing research (Zhou et al., 2025), it expresses a coupling relationship with the D value at least 0.5, but an imbalance relationship with the D value lower 0.5.

2.4.2 Land system function trade-off degree

The trade-off synergy theory has been widely used in the study of ecosystem service relationships. Trade-off represents that different ecosystem services are negatively correlated in the same period of time, and the two are in a state of ups and downs. Synergy represents a positive correlation between different ecosystem services, with the same increase or decrease. As an integral part of the ecosystem, cultivated land is inevitable in the situation of multi-functional trade-off and coordination. The trade-off of cultivated land utilization indicates that there are opposite trends of change between different functions. However, the synergy means that there are similar trends. Land system Function Trade-off Degree (LFTD) originates from the ecosystem service balance model, which reflects the direction and degree of interaction between farmland use functions through data linear fitting, thus achieving its balance and collaborative analysis (Niu P. et al., 2022). The specific formula is as follows:

$$\mathrm{LFTD}_{XY} = \frac{LFC_{xa} - LFC_{xb}}{LFC_{ya} - LFC_{yb}} \tag{16}$$

where LFC_{xa} and LFC_{xb} mean the functional value of the xth type land system at time a and time b, and LFC_{ya} and LFC_{yb} mean the functional value of the yth type land system at time a and time b. There is a synergy relationship between xth type and yth type with the LFTD value greater than 0, but a trade-off relationship with the LFTD value lower than 0. The absolute value of LFTD reflects the level of trade-off/synergy.

3 Results

3.1 Spatio-temporal distribution of multifunctional cultivated land in the Yellow River Basin

The functional scores of cultivated land in 379 counties in the Yellow River Basin are shown in Figure 3. In terms of production capacity, the PF values were in the range of 0.01–0.47 from 2010 to 2020. The production capacity presented a stable trend of cultivated land in the Yellow River Basin, with the PF values lower than 0.2 in more than 73.88% of counties. There were higher PF values in the Ningxia Plain, Hetao Plain, and the middle and lower regions of the Yellow River Basin, which indicates that the yields of food crops and economic crops are relatively greater in these regions. A significant increasing trend of production capacity was found in Weihui City, Fengqiu County, Huojia County in Henan Province, Kundulun District, Qingshan District in Inner Mongolia Autonomous Region, and Qingtongxia City, Yongning County in Ningxia Hui Autonomous Region. In contrast, the production capacity tended to decrease in Wenshang County, Daiyue District, Shen County, Yanggu County and Feicheng County in Shandong Province in the last 10 years. For social function, the SF values were 0.04–0.23 from 2010 to 2020. There was an increasing trend of social function in 61.48% of counties, which is mainly attributed to the enhancement of mechanization levels and the increase in family agricultural incomes (He, 2021). Meanwhile, this means that the living standards of farmers who rely on cultivated land for survival have improved, and life and employment can be basically guaranteed in these counties. In particular, the upward trend was more obvious in Mei County, Jingyang County, and Tongguan County in Shaanxi Province, and Ruyang County, Yiyang County, and Hua County in Henan Province. However, the social security capacity exhibited a downward trend in Lingwu City in Ningxia Hui Autonomous Region, Xintai City and Qihe County in Shandong Province. As for ecological functions, the EF values ranged from 0.03 to 0.23 between 2010 and 2020. Cultivated land utilization in the Yellow River Basin had a positive impact on the ecology in 64.91% of counties with the rising PF values. The ecological function of cultivated land tended to increase in Wangyi District, Huayin City and Hancheng City in Shanxi Province, Hegong District and Shangjie District, but decrease in Qi County, Qingxu County and Taigu County in Shanxi Province, Yiyuan County, Liangshan County and Yanggu County in Shandong Province. On the whole, the multifunctional values of cultivated land in the Yellow River Basin was generally in the range of 0.17–0.85 during the study period, and a significant spatial differences were showed among the all counties. The change value of multi-function score of cultivated land in 233 counties was greater than 0, indicating that the production capacity, social security capacity and ecological protection capacity of cultivated land in the Yellow River Basin have gradually increased in the last 10 years. Due to the rich resources of agricultural and sideline products and good ecological environment in the downstream region of the Yellow River, it is an important agricultural planting area, a main producing area of high-quality agricultural products and a core area of grain in China (Chen et al., 2022). Meanwhile, agriculture is also the basis for the survival of regional farmers. Therefore, the multifunctional values of cultivated land in the downstream region was higher than that in the upstream region and midstream region.

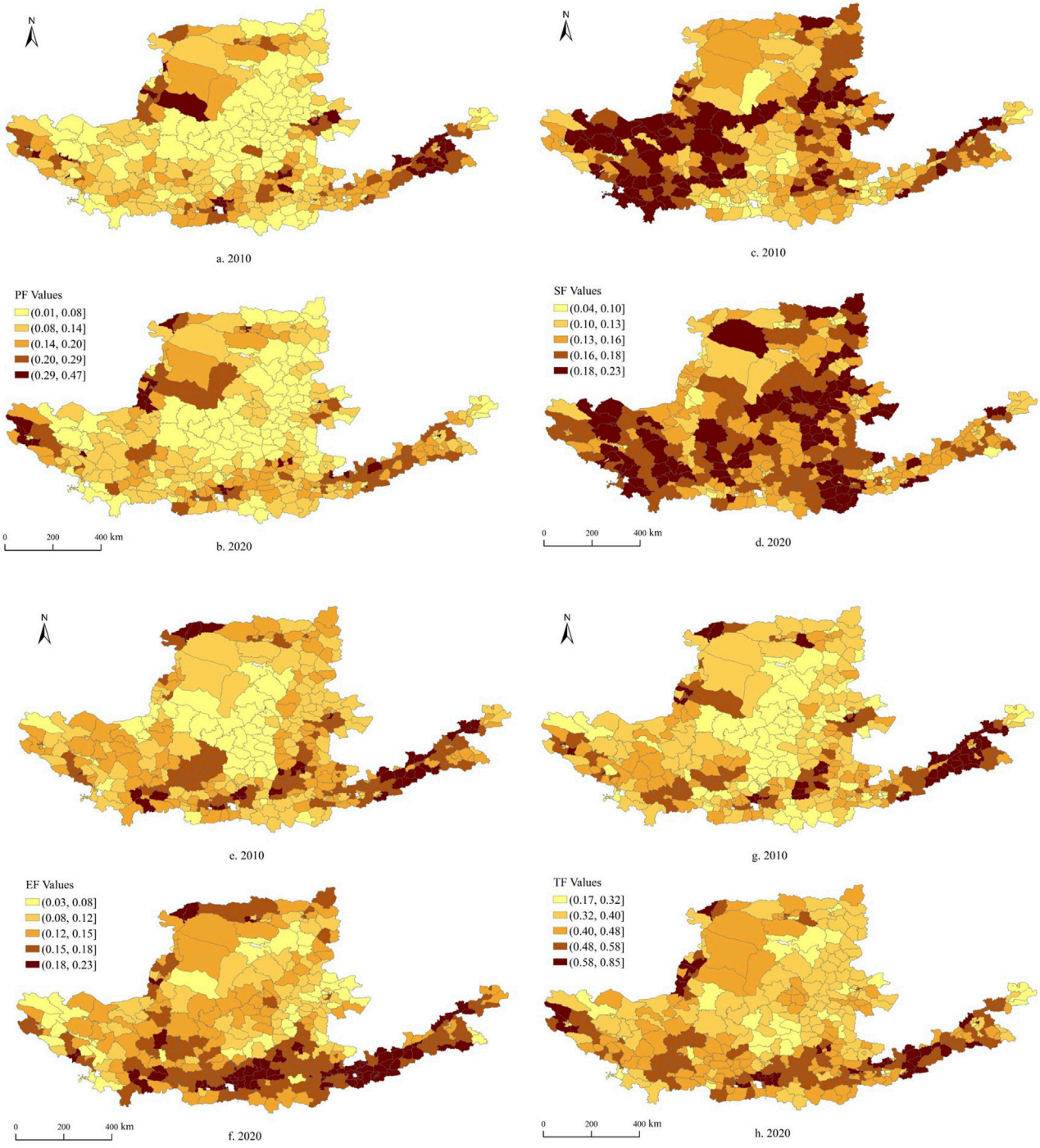

FIGURE 3
The functional values of cultivated land in the Yellow River Basin.

3.2 Trade-off and synergy analysis of multifunctional cultivated land in the Yellow River Basin

The trade-off and synergistic relationship between the functions of cultivated land in the Yellow River Basin is shown in Figure 4. Overall, the D values in 31.13% of counties were greater than or equal 0.5, which suggests that there is a coupling relationship between production function, social function, and ecological function in these regions. On the contrary, it expresses an imbalance relationship between these three functions in 68.87% of counties with the D values lower than 0.5. It means that the multifunctionality of cultivated land in the Yellow River Basin has not been fully utilized during the research period. From 2010 to 2020, the number of counties with the LFTD values greater than 0 between the production-ecological function, social-ecological

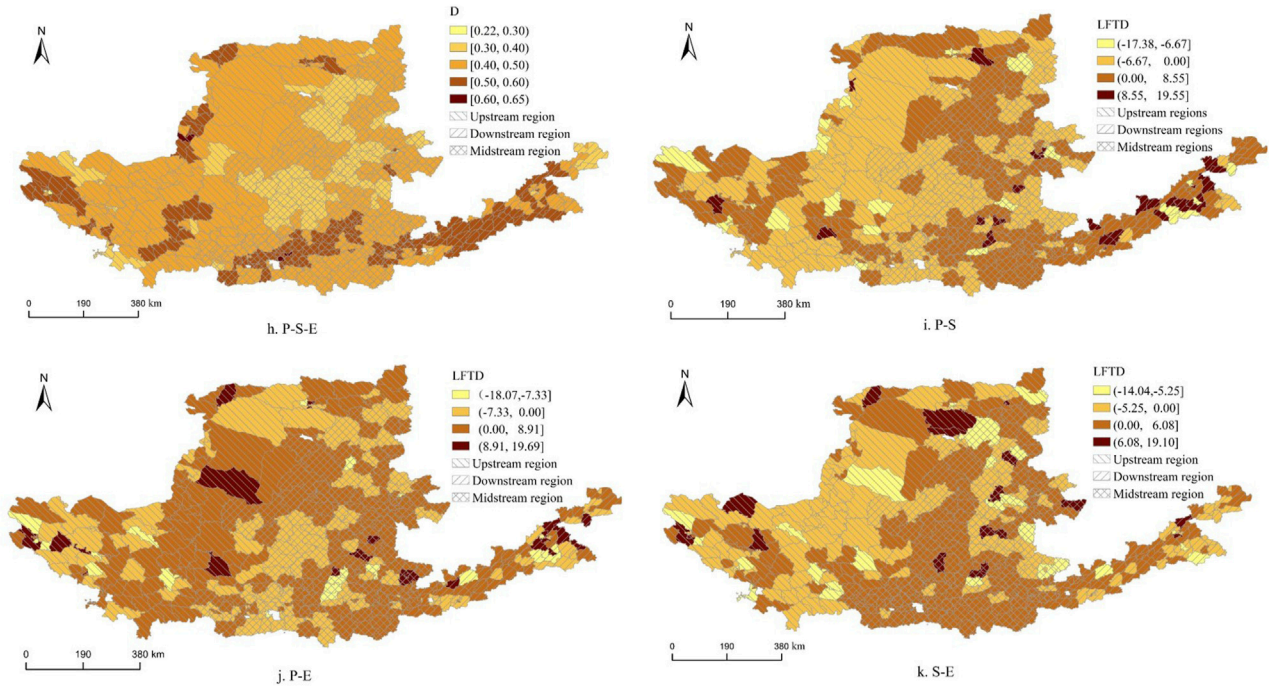

FIGURE 4
The collaborative and trade-off degree between the functions of cultivated land in the Yellow River Basin.

function and production-social function of cultivated land in the Yellow River Basin accounted for 63.06%, 62.27%, and 53.30% of the total number of study area, respectively. It is proved that there is a better synergistic change trend between the functions. The upstream regions of the Yellow River are dominated by mountains, and the distribution of cultivated land is relatively small. The LFTD values were higher than 0 in 63.03% of the upstream counties. It shows that the good maintenance of cultivated land ecosystem service function has a mutual gain effect on cultivated land production capacity and product quality in the upstream regions during 2010–2020. It is inseparable from the national commitment to the protection of the water supply areas and ecological security barriers in the upstream regions of the Yellow River (Pang et al., 2024). However, for the production-social function and social-ecological function, a trade-off relationship was appeared in 57.98% of the upstream counties with the corresponding LFTD values less than 0. This was due to the fact that the income, employment opportunities and other social security benefits obtained by cultivated land use are relatively small for the livestock-based farmers. The cultivated land in the midstream regions of the Yellow River is mainly distributed in Shaanxi Province, Shanxi Province and Henan Province. There is a mutual gain relationship between the two functions in counties over 53.4% of midstream regions with the corresponding LFTD values greater than 0. Reasonable agricultural production structure and high output capacity not only enhance the diversity of cultivated land ecosystem, but also increase the farmers' income.

The terrain of the lower Yellow River is mainly plain, which results in the better natural conditions and convenient agricultural mechanization. Therefore, the LFTD values between the two functions was higher than 0 in counties over 62.32% of downstream regions. In particular, the synergetic relationship of production-ecological function was the most intense with the counties proportion more than 72.46%. In these regions, regional farmers mainly used cultivated land to grow traditional food crops.

3.3 Preliminary zoning and verification of cultivated land functions in the Yellow River Basin

According to the multifunctional zoning ways, multifunctional advantage zones, P-S functional composite zones, P-E functional composite zones, and S-E functional composite zones were obtained on the basic of the coupling coordination degree and the land system function trade-off degree. For the functional trade-off zones, the optimal classification number of multi-functional clustering algorithm for cultivated land is 4 categories referring to the elbow method (Figure 5) (Li, 2023). Based on the K-means clustering results of cultivated land functions in 2020, the functional trade-off zones were divided into grain function dominant zones, social function dominant zones, ecological function dominant zones, and remediation key zones (Figure 6), and its corresponding PF values, SF values, and EF values were relatively high in these function dominant zones. All the function values were low in the remediation key zones. The rationality of the clustering partition scheme was tested in accordance with the Gini coefficient (Table 3) of the multi-functional type partition of cultivated land. From the perspective of the source and contribution rate of the overall regional gap of the cultivated land function index, the three functions that contribute the most to the overall regional disparities were the interregional disparities, and their contribution rates were all greater than 50%. The

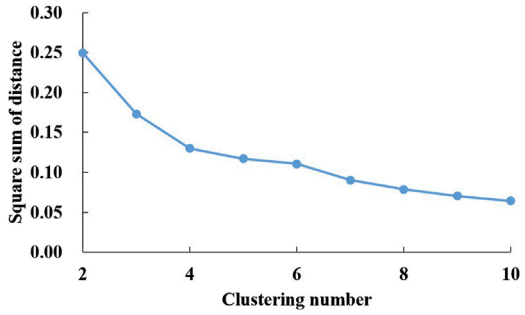

FIGURE 5
Square sum of distance under different numbers of clusters.

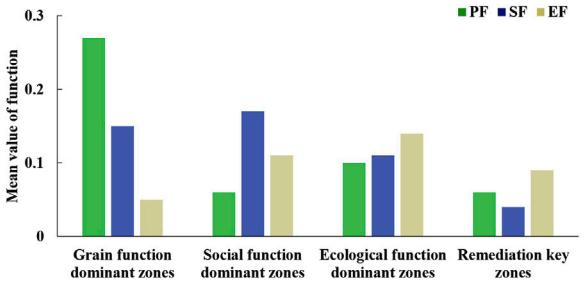

FIGURE 6
Clustering results of cultivated land functional trade-off zones in 2020.

interregional contribution rate of PF was as high as 74.64%. Therefore, the K-means clustering zoning scheme had a small gap in the functional zones of cultivated land, and the interregional gap is the main reason for the overall regional differences in the functions of cultivated land.

3.4 Multi-functional zoning of cultivated land in the Yellow River Basin

There were 7 categories of cultivated land functional zones in the Yellow River Basin and the specific distribution was shown in Figure 7.

A total of 149 counties, accounting for 39.31% of the selected counties, were in the multifunction advantage zones. Among them, 81.21% of counties were in the midstream and downstream regions of the Yellow River Basin. On one hand, for the counties around the city center, in virtue of the higher level of urbanization and denser population, human beings have a strong demand for the production quality, economic benefits, ecological maintenance and other functions of cultivated land in these regions. Meanwhile, because of better economic benefits and output, stable agricultural population and sufficient agricultural subsidies can maintain the good social effect of cultivated land, so multiple functions can be coordinated development. However, the fragmentation of cultivated land is serious with the impact of rapid urbanization. How to integrate cultivated land into the urban ecosystem is an important direction for the adjustment of cultivated land use in these regions. Some approaches, such as urban agriculture or green infrastructure construction, can help achieve the coordinated development of cultivated land production functions and urban ecological functions. On the other hand, in the counties far away from large cities, cultivation and management are relatively convenient owing to its high contiguity. Due to being a traditional grain producing area, agricultural technology has been effectively promoted, and the utilization efficiency of cultivated land is high. The input of high-yielding materials has been controlled and shown a downward trend, and the overall efficiency of cultivated land is high. In addition, because of their distance from cities, these regions have a better ecological environment and cultivated land can maintain a certain ecological maintenance function. The development of ecological agriculture and the application of sustainable farming techniques can ensure food production while enhancing ecological functions.

The composite zones involved 61 counties, including 19 with P-S function, 21 with P-E function, and 21 with S-E function. The P-S function composite zones were mainly in the upstream and downstream regions. The agricultural population in these zones has a high degree of dependence on cultivated land. High value-added crops and characteristic agriculture are planted, and ecological compensation policies are applied to protect regional ecology. Most of the P-E function composite zones were located in the upstream regions, especially in the Ningxia Plain. Water-saving irrigation technology can be promoted and ecological agricultural models such as crop rotation, intercropping, and organic agriculture are being applied in these zones. The S-E function composite zones were mainly distributed in the midstream regions. These regions are far away from the economic development center, the urbanization degree is relatively low and the overall economic level is relatively backward. Ecotourism projects are developed based on the favorable ecological environment and agricultural landscape, aiming to enhance the regional economic level.

There were 147 counties of dominant zones, containing 74 with social function, 29 with ecological function and 44 with grain function in Yellow River Basin. For the social functional dominant zones, the fragile ecological environment of the Loess Plateau is a restrictive factor for regional ecology and agricultural development. The relevant departments should focus on the combination of ecological compensation and cultivated land protection compensation policies, mobilize local subjective enthusiasm for environmental protection and cultivated land protection, and compensate for the loss of opportunity cost of land use conversion in specific areas. The ecological functional dominant zones were in the upstream. Dry land is the main type and it is difficult to realize agricultural modernization. The utilization efficiency and comprehensive benefits are far lower than other regions. Measures such as ecological restoration and returning farmland to forests and grasslands should be taken to enhance regional ecological functions, while exploring local characteristic agricultural models. As for the grain function dominant zones in the upstream, the degree of intensive utilization of cultivated land is very high, and there is even a trend of excessive intensification. Excessive input of pesticides

TABLE 3 Gini coefficient and contribution rate of cultivated land functional trade-off zones.

Function	Gini coefficient				Contribution rate		
	Total	Intraregional Gini coefficient G_W	Interregional gini coefficient G_b	Super variable density gini coefficient G_t	Intraregional contribution rate G_w	Interregional contribution rate G_t	Super variable density contribution rate G_t
PF	0.138	0.020	0.103	0.015	14.49%	74.64%	10.87%
SF	0.124	0.021	0.086	0.017	16.94%	69.35%	13.71%
EF	0.126	0.028	0.067	0.031	22.22%	53.17%	24.60%

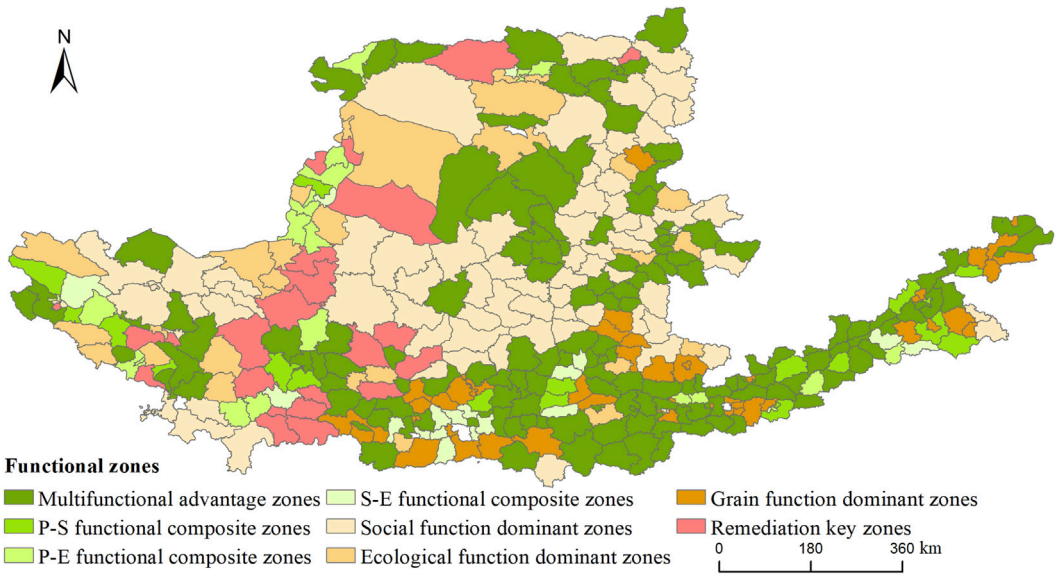

FIGURE 7
Multifunctional zones of cultivated land in the Yellow River Basin.

and fertilizers has a significant impact on cultivated land and its surrounding ecological environment. Therefore, the food security and ecological maintenance functions in these regions are often strongly imbalanced. It can be solved through precision agriculture technology and green production methods. In addition, there were 22 counties with the low functional values. A poor utilization condition of cultivated land and scarce resources were found in these regions, and the development path is limited because of the geographical and geomorphic features. Thus, a worse multifunctional synergy was present. With the rise of agricultural production costs and the gradual weakening of regional agriculture in the national economic system, many young and middle-aged rural laborers have shifted to urban areas and the secondary and tertiary industries. The continuous loss of agricultural population has led to the long-term inefficient utilization of cultivated land resources, resulting in relatively weak regional cultivated land production functions and limited paths for functional improvement. The government can increase financial subsidies and technical support to improve the utilization conditions of cultivated land and enhance production functions.

4 Discussions

Due to the increasing demand for diversified food by humans, cultivated land needs to play multiple functions in addition to maintaining food security. Promoting the coordinated development of multifunctional cultivated land is an important way to advance regional cultivated land protection and utilization, and achieve sustainable agricultural development. The dynamic changes in the trade-off and synergy of multifunctional utilization of cultivated land through system analysis are beneficial for improving the comprehensive utilization efficiency of cultivated land in Yellow River Basin. The evolution trend of cultivated land functions and the balance and synergy between them in the downstream region of the Yellow River are basically consistent with the research of Niu H. P. et al. (2022). For the Gansu Province located upstream region, the cultivated land functions in Lanzhou city, Dingxi city, and Baiyin city are in an imbalance relationship, which is in accord with the research of Wang and Yang (2024). Compared with other regions in China,

such as the Yangtze River Basin and the Pearl River Delta, the Yellow River Basin faces more significant challenges in balancing ecological protection and agricultural production due to its fragile ecosystem and lower average income levels. For the Yangtze River Basin, it has achieved a higher level of multifunctional synergy in cultivated land utilization, largely due to its advanced agricultural infrastructure and higher economic development level (Li, 2023). Similarly, the Pearl River Delta region has focused on integrating urban development with agricultural modernization, resulting in a more balanced development of production, social, and ecological functions of cultivated land (Zhang et al., 2024). Globally, the multifunctional utilization of cultivated land in the Yellow River Basin shares similarities with regions like the Nile River Basin in Africa, where water scarcity and soil degradation are critical issues. However, the Yellow River Basin has made significant progress in ecological restoration and sustainable agricultural practices, which sets it apart from other regions facing similar challenges (Jones and Thornton, 2015).

Compared with existing research, the cultivated land protection zones of the entire Yellow River Basin and differentiated management measures based on the trade-off and synergy relationship were obtained by this study. In general, more than half of the counties have good collaborative development relationships between functions, which suggesting that there is a relatively good utilization condition of cultivated land in the Yellow River Basin. Meanwhile, it can meet the needs of the transformation of human dietary structure. As for the cultivated land in the dominant zones, on the premise of exerting its dominant function, other functions can be improved by improving the relatively weak production, social, and ecological conditions in the zones. These zones can be used as dynamic control zones for cultivated land utilization, timely supplementing the demand for corresponding functional farmland based on the needs of food security, social development, and ecological protection. For the remediation key zones, the production function of cultivated land has not been fully valued, and efforts should be made to improve the quality of regional cultivated land, promote the development of modern agriculture, and achieve the coordinated development of multiple functions.

The multifunctionality of cultivated land is constrained by various factors, and currently there is no unified standard for the multifunctionality connotation of cultivated land. Due to subjective factors and the difficulty of obtaining data, the evaluation index system for multifunctionality of cultivated land constructed is not comprehensive enough in this study. Furthermore, the comparison with other regions in China and globally highlights the need for a more standardized and universally applicable framework for evaluating cultivated land multifunctionality. Therefore, the subsequent research should pay attention to start from a smaller scale, refine the multifunctional categories of cultivated land, and construct a more suitable evaluation index system. In the future, key factors affecting the balance and coordination of multifunctional cultivated land can be further identified, and more precise and detailed countermeasures can be proposed for the actual utilization of cultivated land in different regions.

5 Conclusion

Based on the indicator system constructed from three aspects of production, society and ecology, this study analyzed the spatial evolution trend of cultivated land functional level and the trade-off and synergy relationship between functions from 2010 to 2020, divided the functional zones, and proposed management measures of cultivated land in the Yellow River Basin. The main conclusions were as follows:

1) In the past 10 years, 61.47% of counties in the Yellow River Basin have shown a slight increase in the multifunctional level of cultivated land. Among them, the production function of cultivated land was strong and basically in a stable state. The social and ecological functions of cultivated land were showing an increasing trend, particularly in the midstream and downstream regions.
2) Overall, the coupling and synergy between the production, social, and ecological functions of cultivated land in the Yellow River Basin was relatively low. The production and ecological functions of cultivated land in the upstream region showed a trend of coordinated development. The social and ecological functions of cultivated land in the midstream region were well coordinated, while the production, social, and ecological functions of cultivated land in the downstream region were well coordinated.
3) The cultivated land in the Yellow River Basin was divided into 7 functional zones, including 149 with multifunctional advantage zones, 19 with P-S functional composite zones, 21 with P-E functional composite zones, 21with S-E functional composite zones, 74 with social functional dominant zones, 29 with ecological functional dominant zones, 44 with grain functional dominant zones, and 22 with remediation key zones. The existing favorable conditions of agricultural production can be maintained in the future utilization of cultivated land for the advantage zones and composite zones. As for the dominant zones and remediation zones, improving the corresponding production conditions and ecological environment to meet the demand for farmland utilization in social development is the main remediation path.

Data availability statement

The raw data supporting the conclusions of this article will be made available by the authors, without undue reservation. Requests to access these datasets should be directed to Aman Fang fangaman@henau.edu.cn

Author contributions

AF: Writing–original draft, Writing–review and editing, Formal Analysis, Funding acquisition, Methodology. YS: Investigation, Writing–review and editing. WC: Funding acquisition, Methodology, Writing–review and editing. LS: Funding acquisition, Supervision, Writing–review and editing. JW:

Investigation, Writing–review and editing. YM: Investigation, Resources, Writing–review and editing.

Funding

The author(s) declare that financial support was received for the research, authorship, and/or publication of this article. This research was funded the Henan Philosophy and Social Science Planning Project (No. 2023CJJ153), Natural Science Foundation project of Henan Province (Grant No. 242300420602), and National Key R&D Program of China (2021YFD1700900).

Conflict of interest

Author JW was employed by Henan Province Fifth Geological Brigade Co., Ltd.

The remaining authors declare that the research was conducted in the absence of any commercial or financial relationships that could be construed as a potential conflict of interest.

Generative AI statement

The author(s) declare that no Generative AI was used in the creation of this manuscript.

Publisher's note

All claims expressed in this article are solely those of the authors and do not necessarily represent those of their affiliated organizations, or those of the publisher, the editors and the reviewers. Any product that may be evaluated in this article, or claim that may be made by its manufacturer, is not guaranteed or endorsed by the publisher.

References

Chen, L., Hao, J. M., Wang, F., Yin, Y. Y., Gao, Y., Duan, W. K., et al. (2016). Carbon sequestration function of cultivated land use system based on the carbon cycle for the Huang-Huai-Hai Plain. *Resour. Sci.* 38 (6), 1039–1053. doi:10.18402/resci.2016.06.04

Chen, S., Hou, M. Y., Li, Y. Y., Deng, Y. J., and Yao, S. B. (2022). Spatial-temporal matching patterns for grain production using water and energy resources and damping effect in the Yellow River Basin. *Trans. Chin. Soc. Agric. Eng.* 38 (18), 246–254. doi:10.11975/j.issn.1002-6819.2022.18.027

Dong, P. Y., and Zhao, H. F. (2019). Study on trade-off and synergy relationship of cultivated land multifunction: a case of Qingpu District, Shanghai. *Resour. Environ. Yangtze Basin* 28 (2), 368–375. doi:10.11870/cjlyzyyhj201902013

Fang, Y., Wang, J., Kong, X. S., Wu, R. T., Li, B. L., and Liu, L. L. (2018). Trade-off relation measurement and zoning optimization of multi-functionality of cultivated land use: a case study of Henan province. *Chin. Land Sci.* 32 (11), 57–64. doi:10.11994/zgtdkx.20181019.151512

Fei, X., Shao, Y. P., Xu, B. G., Huan, L., Xie, X. F., Xu, Y., et al. (2023). Evaluation and zoning of cultivated land quality based on a space–function–environment. *Land* 12 (1), 174. doi:10.3390/land12010174

Gao, X., Song, Z. Y., Li, C. X., Cha, L. S., Liang, S. Y., and Tang, H. Z. (2021). Spatial differentiation characteristics of cultivated land multifunctional value under urban-rural gradient. *Trans. Chin. Soc. Agric. Eng.* 37 (16), 251–259. doi:10.11975/j.issn.1002-6819.2021.16.031

He, B. (2021). "Research on the coupling and coordinated development of agricultural economy and ecological environment in the middle and lower reaches of the Yellow River,". Master' Thesis (Taiyuan, China: Shanxi Normal University).

Jiang, Y., Yang, C. M., Nie, Y., Wang, R., and Wu, Y. E. (2021). Spatio-temporal evolution and coupling coordination analysis of farmland multi functions in county regions of Hubei province, China. *Mountain Research* 39 (6), 891–900. doi:10.16089/j.cnki.1008-2786.000647

Jones, P. G., and Thornton, P. K. (2015). Representative soil profiles for the Harmonized World Soil Database at different spatial resolutions for agricultural modelling applications. *Agric. Syst.* 139, 93–99. doi:10.1016/j.agsy.2015.07.003

Li, Y. (2023). "Multifunctional evaluation and zoning of cultivated land on the perspective of demand and supply: a case study of the Yangtze River middle reaches urban agglomeration,". Master' Thesis (Nanchang, China: Jiangxi Normal University).

Liu, Y., Wan, C. Y., Xu, G. L., Chen, L. T., and Yang, C. (2023). Exploring the relationship and influencing factors of cultivated land multifunction in China from the perspective of trade-off/synergy. *Ecol. Indic.* 149, 110171. doi:10.1016/j.ecolind.2023.110171

Luo, S. D., Lai, Q. B., Wang, X. D., Wang, Y. P., and Zhao, Y. F. (2023). Control and management of Cropland regionalization in Fujian Province of China using multi-functional evaluation and trade-off/synergy relationships. *Trans. Chin. Soc. Agric. Eng.* 39 (13), 271–280. doi:10.11975/j.issn.1002-6819.202302160

Lv, L. G., Han, X., Long, H. L., Zhou, B. B., Zang, Y. Z., Wang, J., et al. (2023). Research progress and prospects on supply and demand matching of farmland multifunctions. *Resour. Sci.* 45 (7), 1351–1365. doi:10.18402/resci.2023.07.06

Niu, H. P., Zhao, X. M., Xiao, D. Y., An, R., and Liu, M. M. (2022). Spatial-temporal pattern evolution and trade-off relationship of cultivated land multifunction in the Yellow River Basin (Henan Section). *Trans. Chin. Soc. Agric. Eng.* 38 (23), 223–236. doi:10.11975/j.issn.1002-6819.2022.23.024

Niu, P., Zhou, J. X., Yang, Y. F., and Xia, Y. T. (2022). Evolution and trade-off in the multifunctional cultivated land system in henan province, China: from the perspective of the social-ecological system. *Front. Ecol. Evol.* 10. doi:10.3389/fevo.2022.822807

Pang, C. Y., Wen, Q., Ding, J. M., Wu, X. Y., and Shi, L. N. (2024). Ecosystem services and their trade-offs and synergies in the upper reaches of the Yellow River basin. *Acta Ecol. Sin.* 44 (12), 5003–5013. doi:10.20103/j.stxb.202306281376

Qian, F. K., Chi, Y. R., and Lal, R. (2020). Spatiotemporal characteristics analysis of multifunctional cultivated land: a case-study in Shenyang, Northeast China. *Land Degrad. and Dev.* 31 (14), 1812–1822. doi:10.1002/ldr.3576

Qian, F. K., Chi, Y. R., Xu, H., Pang, R. R., Wang, S. Z., Li, H. X., et al. (2022). Study on evolution of trade-off and synergy relationship of multifunctional cultivated land from 2006 to 2020: a case of shenyang city. *China Land Sci.* 36 (10), 31–39. doi:10.11994/zgtdkx.20220919.110225

Song, X. Q., and Li, X. Y. (2019). Theoretical explanation and case study of regional cultivated land use function transition. *Acta Geogr. Sin.* 74 (5), 992–1010. doi:10.11821/dlxb201905012

Sylla, M., Hagemann, N., and Szewrański, S. (2020). Mapping trade-offs and synergies among peri-urban ecosystem services to address spatial policy. *Environ. Sci. Policy* 112, 79–90. doi:10.1016/j.envsci.2020.06.002

Wang, L. L., Hu, Q. Y., Liu, L. M., and Yuan, C. C. (2023). Land use multifunctions in metropolis fringe: spatiotemporal identification and trade-off analysis. *Land* 12 (1), 87. doi:10.3390/land12010087

Wang, X. W., and Chen, H. (2022). Dynamic changes of cultivated land use and grain production in the lower reaches of the Yellow River based on GlobeLand30. *Front. Environ. Sci.* 10, 974812. doi:10.3389/fenvs.2022.974812

Wang, Y. T., and Yang, Q. (2024). Analysis of temporal and spatial evolution characteristics of coupling coordination of cultivated land" production-living-ecological "space in upper reaches of Yellow River-A case study of Gansu province. *J. Agric. Sci. Technol.* doi:10.13304/j.nykjdb.2024.0282

Wang, Z. J., Yang, H., Hu, Y. M., Peng, Y. P., Liu, L., Su, S. Q., et al. (2023). Multifunctional trade-off/synergy relationship of cultivated land in Guangdong: a long time series analysis from 2010 to 2030. *Ecol. Indic.* 154, 110700. doi:10.1016/j.ecolind.2023.110700

Wei, X. D., Lin, L. G., Luo, P. P., Wang, S. N., Yang, J., and Guan, J. (2022). Spatiotemporal pattern and driving force analysis of multi-functional coupling coordinated development of cultivated land. *Trans. Chin. Soc. Agric. Eng.* 38 (4), 260–269. doi:10.11975/j.issn.1002-6819.2022.04.030

Wu, Z. H., Hao, J. M., Chen, H., and Tan, Y. Z. (2024). Multifunctional evaluation and key tradeoffs and synergy relationships of cultivatedland in Hebei province of China. *Trans. Chin. Soc. Agric. Eng.* 40 (14), 199–209. doi:10.11975/j.issn.1002-6819.202403052

Xiong, C. S., Zhang, Y. L., Wang, Y. J., Luan, Q. L., and Liu, X. (2021). Multi-function evaluation and zoning control of cultivated land in China. *Chin. Land Sci.* 35 (10), 104–114. doi:10.11994/zgtdkx.20210916.155106

Zhang, L. G., Lu, R. C., Ma, G. B., and Ma, D. Y. (2024). Multifunctional utilization and optimization strategy of cultivated land in guangxi section of Pearl River-xijiang river economic belt. *Res. Soil Water Conservation* 31 (3), 276–286.

Zhang, L. G., Wang, Z. Q., Chai, J., and Li, B. Q. (2019). Multifunction spatial differentiation and comprehensive zoning of cultivated land in hubei province. *Areal Res. Dev.* 38 (5), 125–130. doi:10.3969/j.issn.1003-2363.2019.05.024

Zhang, S. Y., Hu, W. Y., Li, M. R., Guo, Z. X., Wang, L. Y., and Wu, L. H. (2021). Multiscale research on spatial supply-demand mismatches and synergic strategies of multifunctional cultivated land. *J. Environ. Manag.* 299, 113605. doi:10.1016/j.jenvman.2021.113605

Zhang, Y., Dai, Y. Q., Chen, Y. Y., and Ke, X. L. (2023). Spatial-temporal evolution and driving factors of cultivated land multifunctional coupling coordination development in China. *Trans. Chin. Soc. Agric. Eng.* 39 (7), 244–255. doi:10.11975/j.issn.1002-6819.202209185

Zhao, S. X., Li, Z. Z., and Wang, B. (2024). Trade-off and synergy relationships and regional regulation of multifunctional cultivated land in Henan province. *Transactions of the Chinese Society for Agricultural Machinery*55 (11), 363–374. doi:10.6041/j.issn.1000-1298.2024.11.036

Zhou, X., Wu, D., Li, J. F., Liang, J. L., Zhang, D., and Chen, W. X. (2022). Cultivated land use efficiency and its driving factors in the Yellow River Basin, China. *Ecol. Indic.* 144, 109411. doi:10.1016/j.ecolind.2022.109411

Zhou, Y., Yu, S. J., and Yu, Z. Y. (2025). Spatiotemporal coupling of grain production, economic development, and ecological protection in China′s major grain-producing areas. *Acta Ecol. Sin.* 45 (4), 1–15. doi:10.20103/j.stxb.202311302615

Zhu, C. M., Li, W. Y., Du, Y. Y., Xu, H. W., and Wang, K. (2020). Spatial-temporal change, trade-off and synergy relationships of cropland multifunctional value in Zhejiang Province, China. *Trans. Chin. Soc. Agric. Eng.* 36 (14), 263–272. doi:10.11975/j.issn.1002-6819.2020.14.032

Zou, L. L., Li, Y. R., Liu, Y. S., and Wang, J. Y. (2021). Theory building and empirical research of production-living-ecological function of cultivated land based on the elements. *Geogr. Res.* 40 (3), 839–855. doi:10.11821/dlyj020200400

Frontiers in Environmental Science

Explores the anthropogenic impact on our natural world

An innovative journal that advances knowledge of the natural world and its intersections with human society. It supports the formulation of policies that lead to a more inhabitable and sustainable world.

Discover the latest Research Topics

See more →

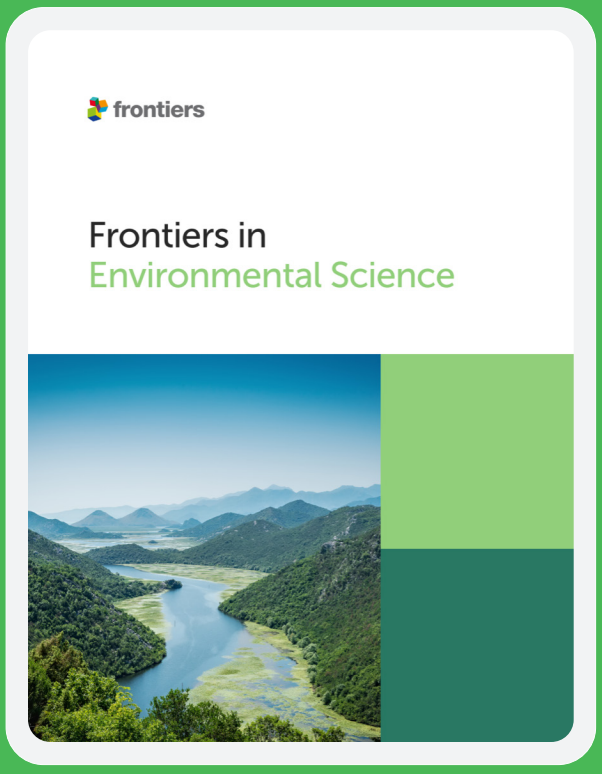

Frontiers

Avenue du Tribunal-Fédéral 34
1005 Lausanne, Switzerland
frontiersin.org

Contact us

+41 (0)21 510 17 00
frontiersin.org/about/contact